EFFECT OF COAL BOTTOM ASH ON STRENGTH AND DURABILITY PROPERTIES OF CONCRETE

A Thesis
Submitted in fulfilment of the requirement
for the award of the degree of

DOCTOR OF PHILOSOPHY
IN
CIVIL ENGINEERING

MALKIT SINGH
Registration No. 951002002

DEPARTMENT OF CIVIL ENGINEERING
THAPAR UNIVERSITY, PATIALA-147004
PUNJAB (INDIA)
2015

CERTIFICATE

Certify that the thesis entitled **"Effect of coal bottom ash on strength and durability properties of concrete"** which is submitted by Malkit Singh, in fulfilment of the requirements for the award of degree of Doctor of Philosophy in the Department of Civil Engineering, Thapar University, Patiala, is a record of candidate's own original and independent research work carried out by him under my supervision and guidance. The matter embodied in this thesis has not been submitted in part or full to any other University or Institute for the award of any degree.

(Dr. Rafat Siddique)
Senior Professor
Department of Civil Engineering
Thapar University, Patiala
Punjab, India.

DECLARATION

I hereby declare that the research work presented in this thesis entitled **"Effect of coal bottom ash on strength and durability properties of concrete"** submitted for the award of the degree of Doctor of Philosophy in the department of Civil Engineering, Thapar University, Patiala is an authenticated record of my own research work carried out under the supervision of Dr. Rafat Siddique Sr. Professor, Department of Civil Engineering and refers other researcher's work are duly listed in reference section.

The matter presented in this thesis has not previously been submitted in part or full to any other University or Institution for award of any degree in India or Abroad.

(Malkit Singh)

ACKNOWLEDGEMENT

- *First of all I thank the almighty whose blessings have enabled me to accomplish this research work.*
- *I would like to express my gratitude to my supervisor Dr. Rafat siddique Sr. professor, Department of Civil Engineering, Thapar university, Patiala for his invaluable guidance, moral support and encouragement during the entire period of this research which cannot adequately be expressed in words in this acknowledgement.*
- *I would like to extend my acknowledgement to my advisory committee members Dr. Naveen Kawatra, Dr. P.P. Bansal and Dr. Rajiv Mehta for their valuable suggestions and feedbacks. The inputs provided by Dr. Naveen Kawatra, Head Department of Civil Engineering, his interest and critical appraisal during the early stages of this research are invaluable.*
- *The help and support provided by technical staff Er. Varinder Kumar Sharma and Shri Ram Sumiran during the entire research period are greatly appreciated. I am grateful to Er. Ravinder Singh Bedi Assistant Executive Engineer, Er. Charankanwal Singh Assistant Engineer; Er. Bhan Singh Assistant Engineer; Er. Puran Singh Assistant Engineer; Er R. K. Parbhakar Assistant Engineer; and Sh. Bal Chand contractor for their help and support.*
- *I am also grateful to Sh Kunal fellow research scholar, Col. BJS Randhawa and Er. Jaideep Aggarwal Sr. Executive Engineer for their help and encouragement during the entire research period.*
- *I also acknowledge the support of Central Research Facility IIT Ropar and SAI labs Thapar University for SEM and XRD analysis.*
- *Special thanks to my wife Harmanpreet Kaur and daughter Harsimarjot Kaur for their patience, understanding and constant support during the whole research program.*

(Malkit Singh)

LIST OF PUBLICATIONS

1. Singh M. and Siddique R., "Effect of low-calcium coal bottom ash as fine aggregate on microstructure and properties of concrete." ***ACI Materials Journal*** **(IF: 1.12) (Accepted)**
2. Singh M. and Siddique R., "Effect of coal bottom ash as partial replacement of sand on workability and strength properties of concrete" ***Journal of Cleaner Productions****,* (2015) doi:10.1016/j.jclepro.2015.08.001 **(IF: 3.844)**
3. Singh M. and Siddique R., "Properties of concrete containing high volumes of coal bottom ash as fine aggregate." ***Journal of Cleaner Productions****,* 91(2015) 269-278 **(IF: 3.844)**
4. Singh M. and Siddique R., "Strength properties and micro structural properties of concrete containing coal bottom ash as partial replacement of fine aggregate." ***Construction and Building Material****,* 50 (2014): 246-25 (IF: 2.265)
5. Singh M. and Siddique R., "Compressive strength, drying shrinkage and chemical resistance of concrete incorporating coal bottom ash as partial or total replacement of sand." ***Construction and Building Material****,* 68 (2014): 39-48 **(IF: 2.265)**
6. Singh M. and Siddique R., "Effect of coal bottom ash as partial replacement of sand on properties of concrete." ***Resources, Conservation and Recycling****,* 72 (2013): 20-32 **(IF: 2.692)**
7. Siddique R., Singh M. Ait-Mokhtar , K. and Belarbi, R., "Durability properties of concrete made with high volumes of low-calcium coal bottom ash as replacement of two types of sand" ***Materials in Civil Engineering, ASCE***, ***(Accepted)***

ABSTRACT

In India, about 35 million tons of coal bottom ash is produced annually. It is dumped on land adjoining sites of thermal power plants and is becoming environmental hazard to surrounding community. The productive use of coal bottom ash is the best way to alleviate the problems associated with its disposal.

The present research work has been carried out to evaluate the feasibility of utilization of coal bottom ash as fine aggregate in concrete. Concrete 'A' made with sands having fineness modulus of 1.97 and concrete 'B' made with sands having fineness modulus of 2.58 were designed to achieve 28-day compressive strength of 38 and 34 N/mm^2, respectively. In both concretes, river sand was replaced with coal bottom ash at 20, 30, 40, 50, 75 and 100% levels. Properties such as workability, bleeding and air content of fresh concrete were evaluated. Tests for compressive strength, splitting tensile strength, modulus of elasticity, water absorption and water absorption, pulse velocity, chloride permeability, abrasion resistance, sulphate resistance, acid resistance and drying shrinkage were performed up to the age of 365 days.

Test results show that workability and water loss through bleeding decreased whereas entrained air content increased on inclusion of coal bottom ash as replacement of sand in both concretes tested. For concrete 'A' and 'B', unit density decreased almost linearly with increase in coal bottom ash content. At early curing age of 7 days, bottom ash concrete mixtures achieved lower compressive strength. 28-day compressive strength of bottom ash concrete mixtures varied between 35.0 and 37.5 N/mm^2 for concrete 'A' and between 26.7 and 32.2 N/mm^2 for concrete 'B' as compared to 38.20 and 34.0 N/mm^2, respectively, of control concrete mixtures. With age, compressive strength of bottom ash concrete mixtures increased at a faster rate than that of control concrete mixtures. For both concretes 'A' and 'B', after 180 days, compressive strength of bottom ash concrete mixtures was approximately equal to that of control concrete mixtures.

28-day splitting tensile strength of bottom ash concrete mixtures varied between 2.72 and 2.96 N/mm^2 for concrete 'A' and between 2.16 and 2.52 N/mm^2 for concrete 'B'. However, 28-day splitting tensile strength of control concrete was 2.67 N/mm^2 for concrete 'A' and 2.57 N/mm^2 for concrete 'B'. For both concretes 'A' and 'B', after 90 days, splitting tensile strength of bottom ash concrete mixtures was either equal or more than that

of respective control concrete mixture. Modulus of elasticity of bottom ash concrete mixtures was in the range of 27.6 - 23.1 GPa for concrete 'A' and 25.4 - 21.3 GPa for concrete 'B' against 29.2 and 25.4 GPa, respectively, of control concrete mixtures. Inclusion of coal bottom ash in concrete resulted in better dimensional stability. The effect of coal bottom ash on pulse velocity values of concrete was not significant.

Sorptivity of bottom ash concrete mixtures increased with increase in coal bottom ash content. However, the chloride permeability of bottom ash mixtures was comparable to that of control concrete mixtures. It is evident from the test results that after 28-day of curing age, compressive strength, resistance to chloride ion penetration and resistance to abrasion increased significantly due to pozzolanic action of coal bottom ash. Abrasion resistance of bottom ash concrete mixtures was lower than that of control concrete mixtures.

Bottom ash concretes of both grades of concrete experienced higher expansion strains than control concretes under external sulfate attack but the total strains were much less than 0.1% at which compressive strength starts decreasing. As such, no loss in 28-day compressive strength was observed. The performance of bottom ash concrete mixtures under external sulphuric acid attack was identical to that of control concrete mixtures.

Micro-structural analysis (scanning electron micrograph) reveals that pozzolanic activity of coal bottom ash in bottom ash concrete mixtures started after 28-day of curing age. XRD spectrums indicate that the phase composition of powder concrete paste was not changed qualitatively, however, the change in phase proportions was observed on use of coal bottom ash in concrete.

TABLE OF CONTENTS

LIST OF TABLES

LIST OF FIGURES

ABBREVIATIONS

Abbreviations		**Word(s)**
ACI	-	American Concrete Institute
ASTM	-	American Society for Testing and Materials
Bag	-	Baggase fly ash
BIS	-	Bureau of Indian Standards
CASH	-	Calcium Aluminum Silicate Hydrate
CBA	-	Coal Bottom Ash
CH	-	Calcium Hydroxide
CS	-	Calcium silicate
CSH	-	Calcium Silicate Hydrate
CTM	-	Compression Testing Machine
E	-	Ettringite
EDS	-	Energy Dispersive X-ray spectroscopy
FA	-	Fly Ash
GGBFS	-	Ground Granulated Blast Furnace Slag
HRWRA	-	High Range Water Reducing Admixtures
ICDD	-	International Center for Diffraction Data
ITZ	-	Inter Transition Zone
JCPDS	-	Joint Committee on Powder Diffraction Standards
MBM	-	Meat and bone meal
MK	-	Metakaolin
MSWI	-	Municipal Solid Waste Incinerator
OPC	-	Ordinary Portland Cement
P	-	Portlandite

PFA	-	Pulverized Fuel Ash
Q	-	Quartz
RCPT	-	Rapid Chloride Permeability Test
RHA	-	Rice husk ash
SCC	-	Self Compacting concrete
SCM	-	Supplementary Cementitious Material
SEM	-	Scanning Electron Microscopy
SF	-	Silica Fume
SSA	-	Sewage Sludge Ash
TF	-	Titanium Fume
UHP	-	Ultra High Performance
UPV	-	Ultrasonic Pulse Velocity
UTM	-	Universal Testing Machine
w/c	-	Water to cement ratio
w/b	-	Water to binder ratio
XRD	-	X- Ray Diffraction

LIST OF UNITS

Units		Word(s)
kg	-	Kilogram
g	-	Gram
mg	-	Milligram
lb	-	Pound
°C	-	Degree Celsius
%	-	Percent
rpm	-	Revolutions per minute
m	-	Meter
yd	-	Yard
cm	-	Centimeter
mm	-	Millimeter
µm	-	Micrometer
cm^2/g	-	Centimeter square per gram
N	-	Newton
MPa	-	Mega Pascal
GPa	-	Gega Pascal
kg/m^3	-	Kilogram per cubic meter
lb/yd^3	-	Pound per cubic yard
N/mm^2	-	Newton per square millimeter
kN	-	Kilo Newton
hr	-	Hour
min	-	Minute
sec	-	Second

l	-	Liter
ml	-	Milliliter
V	-	Volts
C	-	Coulomb
kV	-	Kilovolt
m/s	-	Meter per second
km/s	-	Kilometer per second
θ	-	Theta

CHAPTER-1

INTRODUCTION

This chapter presents introduction to production of coal bottom ash and its physical and chemical properties. It also includes impact of coal bottom ash on environment, its various uses and objective of the present research work.

1.1 PREAMBLE

Various industries produce numerous solid waste materials. The disposal of these solid waste materials is an environment hazard for the surrounding living beings. Cachim et al. (2014) observed that because of increasing environmental concerns and sustainable issues, the utilization of solid waste materials is the need of the hour. The productive use of solid waste materials is the best way to alleviate the problems associated with their disposal. The construction industry has enormous potential for the use of solid waste materials as construction material. Based upon their properties, the solid waste materials can either be used as supplementary cementitious materials or as replacement of fine/coarse aggregate in concrete or mortars. Based on the research reports some solid waste materials such as fly ash, silica fume, grounded blast furnace slag etc have been put in use in manufacturing of either cement or concrete.

In India, about 67% of electricity requirements are fulfilled by the coal fired thermal power plants (CEA, 2012). Electricity demand in the country is increasing every year. At present, the country is facing average energy shortage of 6.7% at national level but the southern part of the country experience 26.7% energy shortage (CEA, 2012). To fill up the exiting gap between demand and supply of power and to meet the increasing energy requirements, coal fired thermal power plants are being set up in large number in the country. Coal fired thermal power plants produce large volumes of coal bottom ash. Till now, it is treated as solid waste material and is disposed off on open land.

As per Central Electricity Authority, India, report (2014), about 57.63% of coal ash produced by coal fired thermal power plants is used in cement production and in manufacturing of bricks and tiles, construction of ash dykes and reclamation of low lying areas. Fly ash is used as raw material in manufacturing of cement and bricks. However, coal bottom ash is not used in any form. The enormous quantity of coal bottom ash is getting accumulated near the power plant sites. The dumped coal bottom ash on open land is posing environmental hazards to the surrounding community and ecosystem.

On the other hand, large volumes of river sand are extracted for use as a construction material as there is a boom in infrastructure development in the country. River sand is the prime raw material used as fine aggregate in the production of concrete. The rate at which mining of river sand is taking place, the natural resources of river sand cannot sustain indefinitely. The natural resources are dwindling gradually. Moreover, exploitation of natural resources results in unbalancing the ecological system. In Punjab (India) for protection of environment, mining of river sand is banned in most of the area. As such, the price of river sand has sky rocketed and surpassed that of coarse aggregate. Consequently the construction industry is badly affected due to the scarcity of river sand. In the present scenario, therefore it becomes essential and significant to find the substitute material of river sand and save the non renewable natural resources.

The present research work was aimed to explore the possibility of use of low-calcium coal bottom ash as a construction material in place of the river sand. The appearance and particle size of coal bottom ash is similar to that of river sand. The physical properties of coal bottom ash attract it to be used in concrete as fine aggregate either in partial or total replacement of river sand. In the literature published during the last decade, coal bottom ash has been targeted as fine aggregate in concrete. The published research data which is confined to strength properties only indicate that coal bottom ash is a viable material as sand replacement in concrete. The present research study was motivated by the ecological concerns over the disposal of coal bottom ash and scarcity of natural sources of river sand in the country. The ultimate objective of the present research study was to explore the feasibility of use of low-calcium coal bottom ash either in partial or total replacement of natural river sand in manufacturing of concrete.

1.2 COAL BOTTOM ASH

Coal bottom ash is the by-product of coal combustion. The rock detritus filled in the fissures of coal become separated from the coal during pulverization. In the furnace, carbon, other combustible matter burns, and the non-combustible matter result in coal ash. Swirling air carries the ash particles out of hot zone where it cools down. The boiler flue gas carries away the finer and lighter particles of coal ash. The boiler flue gases pass through the electrostatic precipitators before reaching the environment. In the electrostatic precipitators, coal ash particles are extracted from the boiler flue gases. The coal ash collected from the electrostatic precipitators is called fly ash. Fly ash constitutes about 80%

of coal ash. During the combustion process some particles of the coal ash accumulate on the furnace walls and steam pipes in the furnace and form clinkers. These clinkers build up and fall to the bottom of furnace. In addition, the coarser particles, which are too heavy to remain in suspension with the flue gases, settle down at the base of the furnace. The ash collected at the bottom of furnace is called coal bottom ash. Coal bottom ash constitutes about 20% of coal ash and the rest is fly ash.

At present, India is the third largest consumer of coal. About 524 million tons of coal is burnt in coal fired thermal power annually (CEA, 2014). They are the main source of production of coal ash. Indian coals have higher ash content up to 45% depending upon the source of the coal and result in large volumes of coal ash (CEA, 2014). As per Central Electricity Authority, India, report (CEA, 2014), 143 no coal fired thermal power plants with installed capacity of 133381 MW produced about 173 million tons of coal ash annually. With the capacity addition of 22282 MW by the end of 2017, the production of coal ash is estimated to about 220 million tons per year. Fig. 1.1 shows the production of coal ash at coal fired thermal power plant.

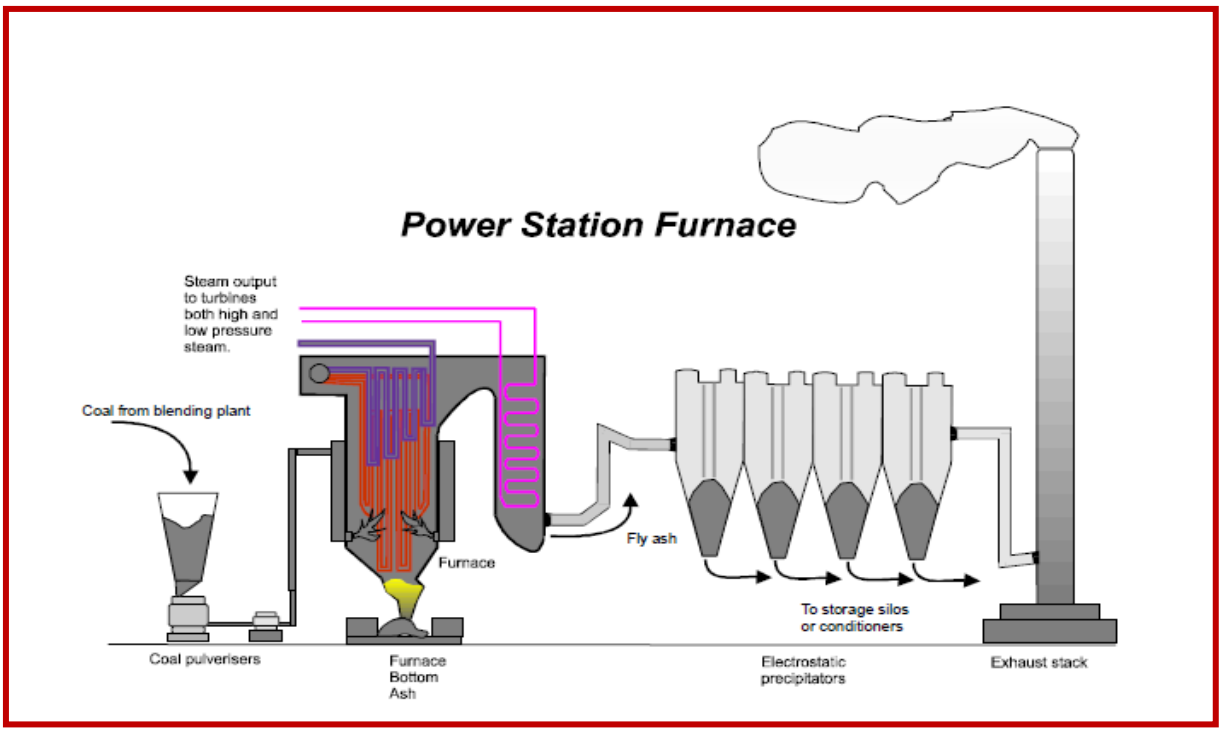

Fig. 1.1: Production of coal bottom ash (Barnes and Sear, 2004)

1.2.1 Physical Properties of Coal Bottom Ash

The coal bottom ash is mainly due to the presence of rock detritus in the fissures of the coal seams. The variability in the rock detritus from one source to another therefore causes variation in the properties of coal bottom ash as well. The factors that affect the properties of coal bottom ash are:-

- Degree of pulverization of coal
- Firing temperature in the furnace
- Type of furnace

Coal bottom ash has angular, irregular, porous and rough surface textured particles. The particles of coal bottom ash range from fine sand to fine gravel. Coal bottom ash has appearance and particle size distribution similar to that of river sand. Coal bottom ash is usually a well-graded material although variations in particle size distribution can be encountered from the same power plant. Particles of coal bottom ash have interlocking characteristics. Coal bottom ash is lighter and more brittle as compared to natural river sand. The specific gravity of coal bottom ash varies from 1.2 to 2.47 depending upon the source and type of coal. Coal bottom ash with low specific gravity has a porous texture that readily degrades under loading or compaction. Coal bottom ash derived from high sulphur coal and low rank coal is not very porous and is quite dense (*www.caer.uky.edu*). The published literature shows wide variation in physical properties of coal bottom ash. Table 1.1 shows the physical properties of coal bottom ash reported in the published literature.

Table 1.1 Physical properties of coal bottom ash

Physical properties	Yuksel & Genc (2007)	Kou and Poon (2009)	Bai et al. (2005)	Kim & Lee (2011)	Naik et al. (2007)	Ghafoori & Bucholc	Singh and Siddique (2014)
Specific gravity	1.39	2.19	1.5	1.87	2.09	2.47	1.39
Water absorption (%)	6.10	28.9	30.4	5.45	13.6	7.0	31.58
Fineness Modulus	-	1.83	-	2.36	-	2.8	1.37

1.2.2 Chemical Properties of Coal Bottom Ash

Coal ash produced on burning of lignite or sub bituminous coal contains high calcium oxide content. This type of coal ash has cementitious properties in addition to pozzolanic

properties. Anthracite or bituminous coals on burning result in low-calcium coal ash which has pozzolanic properties and very small fraction of calcium oxide (ASTM C 618-03). Coal bottom ash is mainly composed of silica, alumina and iron with small amounts of calcium, magnesium, sulphate etc. Its chemical composition is controlled by the source of the coal. The data reported in published literature shows variation in chemical composition of Coal bottom ash. Table-1.2 shows the chemical composition of coal bottom ash reported in published literature.

Table 1.2 Chemical composition of coal bottom ash

Chemical composition (%)	Yuksel & Genc (2007)	Bai et al. (2005)	Aramraks (2006)	Kasemchaisiri & Tangtermsirikul (2007)	Muhardi et al.	Gafoori & Bucholc (1996)	Singh and Siddique (2014)
SiO_2	57.90	54.8	46.20	38.64	42.7	41.70	56.44
Ai_2O_2	22.60	28.5	23.11	21.15	23.00	17.10	29.24
Fe_2O_3	6.50	8.49	8.62	11.96	17.00	6.63	8.44
CaO	2.00	4.2	12.12	13.80	9.80	22.50	0.75
MgO	3.20	0.35	2.90	2.75	1.54	4.91	0.40
Na_2O	0.086	0.08	0,55	0.90	0.29	1.38	0.09
K_2O	0.604	0.45	2.13	2.06	0.96	0.40	1.29
TiO_2	-	2.71	-	-	1.64	3.83 (P_2O_5, TiO_2, etc.)	3.36
P_2O_5	-	0.28	-	-	1.04		-
SO_3		-	0.42	0.61	1.22	0.42	0.24
LOI	2.40	2.46		7.24	-	1.13	0.89

1.2.3 Mineralogy Characteristics of Coal Bottom Ash

Results of X-ray diffraction (XRD) analysis of pure coal bottom ash carried out by Muhardi et al. (2010) show that mullite ($Al_6Si_2O_{13}$), silicon oxide (SiO_2) and silicon phosphate are the predominant crystalline form substances. They observed that silica (SiO_2) is present partly in the crystalline forms of quartz (SiO_2) and partly in combination with the alumina as mullite ($Al_6Si_2O_{13}$). The iron appears partly as the oxide magnetite ($Fe_3O_{4)}$ and hematite (Fe_2O_3). The composition of coal bottom ash depends on the composition of coal and furnace condition. Alumino silicates such as clays melt or

decompose to form glass or mullite ($Al_6Si_2O_{13}$). Carbonates including calcite ($CaCO_3$), dolomite [$CaMg(CO_3)_2$], ankerite [$CaMgxFe_{(1-x)}(CO_3)_2$] and siderite ($FeCO_3$) decompose, release CO_2 and form lime (CaO), calcium ferrite ($CaFe_2O_4$), hematite (Fe_2O_3), magnetite ($Fe_3O_{4)}$ and periclase (MgO). Sulphides such as pyrite (FeS_2) oxidize, loose SO_2 and form sulfates (SO_3). Iron oxides such as hematite (Fe_2O_3) and magnetite ($Fe_3O_{4)}$, chlorides volatilize as NaCl and KCl. Quartz (SiO_2) generally remains unaltered.

1.2.4 Pozzolanic Property of Coal Bottom Ash

The study carried out by Cheriaf et al. (1999) indicates that pozzolanic activity of coal bottom ash starts after 14 days. They observed that after 14 days, the coal bottom ash particles started reacting with calcium hydroxide and after 90 days of hydration, the consumption of calcium hydroxide was very significant. Fig 1.2 shows that the hydrate is covering the spherical particle and the particle is not yet disintegrated. They also noted that pozzolanic activity of coal bottom ash was considerable after 90 days of hydration. Results of their study show that coal bottom ash is a suitable material for use in concrete. The strength activity index of coal bottom ash with Ordinary Portland cement at 14, 28 and 90 days of hydration was 0.764, 0.88 and 0.97, respectively. The values of strength activity index higher than 0.75 at 28 days and 0.85 at 90 days, required by the European standard EN 450 prove pozzolanic activity of coal bottom ash.

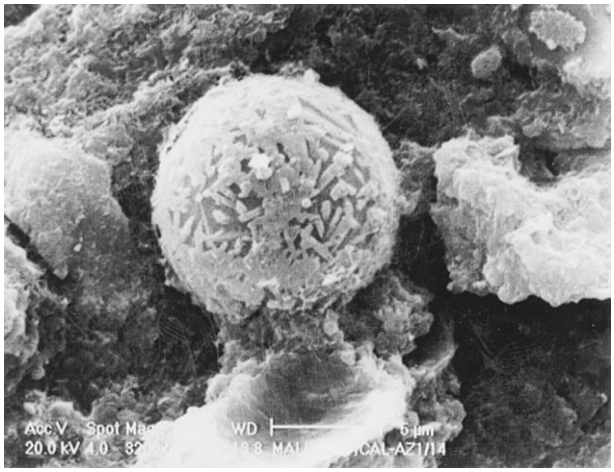

Fig. 1.2: Coal bottom ash particle starting to react with $Ca(OH)_2$ (Cheriaf et al. 1999)

1.2.5 Disposal of Coal Ash

Coal ash disposal site is shown in Fig. 1.3. Coal ash is sluiced in the form of slurry containing nearly 80% water to ash ponds near the power plants where it settles down, decantation takes place and dries. At some thermal power plants, fly ash is collected in dry

form and is supplied to various users. The remaining unused fly ash along with coal bottom ash is sluiced to ash ponds. Large stretches of land are used for disposal of coal ash. In Punjab (India), large stretches of prime agricultural land are in use for disposal of coal ash at six coal fired thermal power plants. Since the ash dykes can be raised up to a certain height, on filling the ash pond to its full capacity, new ash ponds are generally built on the additional land for the disposal of coal ash.

Fig. 1.3: Coal ash disposal site (www.thehindu.com/todays-paper/tp-national/tp-andhrapradesh/slurry-from-ntpc-ash-pond-affects-horticulture-crops/article483533.ece)

1.2.6 Environmental Impact of Coal Bottom Ash

The current method of disposal of coal bottom ash in ponds poses risk to human health and to the environment. The hazardous constituents in coal bottom ash migrate and can contaminate ground water or surface water, and hence affect living organisms. In addition, there is danger of ash dyke spills and filling the area surrounding to the ash pond with coal ash. In year 2008, ash dyke at Kingston plant, USA, failed and coal ash flooded 12 homes, spilled in to nearby Watts Bar Lake, and contaminated the Emory River. Nearly 5.4 million cubic yard of ash spilled which covered about 400 acres of adjacent land. Fig. 1.4 shows the site of ash dyke failure at Kingston plant (USA). The clean up operation cost was about $200 million. It took about 6 years to clean up the area from the ash slurry. This spill is termed as one of the worst environmental disasters in the history of the United States (www.sourcewatch.org). Ash dyke failures at NTPC's Simhadri plant in Vishakhapatnam (India) in 2010 and Rajiv Gandhi thermal power plant, Hissar, Haryana (India) in 2012 have also been reported. Ash dykes of Hindalco captive power plant breached in 2012 and

damaged crops at Hirakud,(India). Thousands of tons of coal ash flowed into the Satluj River due to a breach in the southern ash dyke of the Guru Gobind Singh Super Thermal Plant (GGSSTP), Ropar, Punjab (India) in 2002. Ash dykes at GGSSTP, Ropar had breached number of time. The people living in the nearby area are under constant threat of ash dyke breaches. Due to continuous seepage of water from ash ponds, land adjoining to pond site has converted into water logged land.

Fig. 1.4: Coal ash dyke spill at Kingston plant, USA
(http://www.sourcewatch.org/index.php/File:SPILL2.JPG)

The dunes made by dumping of coal ash are becoming environmental hazards to the surrounding communities. In view of environmental problems posed by dumping of coal ash, it is imperative to utilize coal ash and devise ways and means to cut down the growth of coal ash accumulation. The productive utilization of the coal ash is the only environment friendly solution to the problems associated with its disposal.

1.2.7 Uses of Coal Bottom Ash

Coal bottom ash can be beneficially utilized in a variety of manufacturing and construction applications. Fig.1.5 illustrates the common uses of bottom ash. At present in USA, coal bottom ash is predominantly being used for the following applications:-

- Road base and sub-base
- Structural fill
- Backfill
- Drainage media

- Aggregate for concrete, asphalt and masonry
- Abrasives/traction
- Manufactured soil products
- Snow and ice control

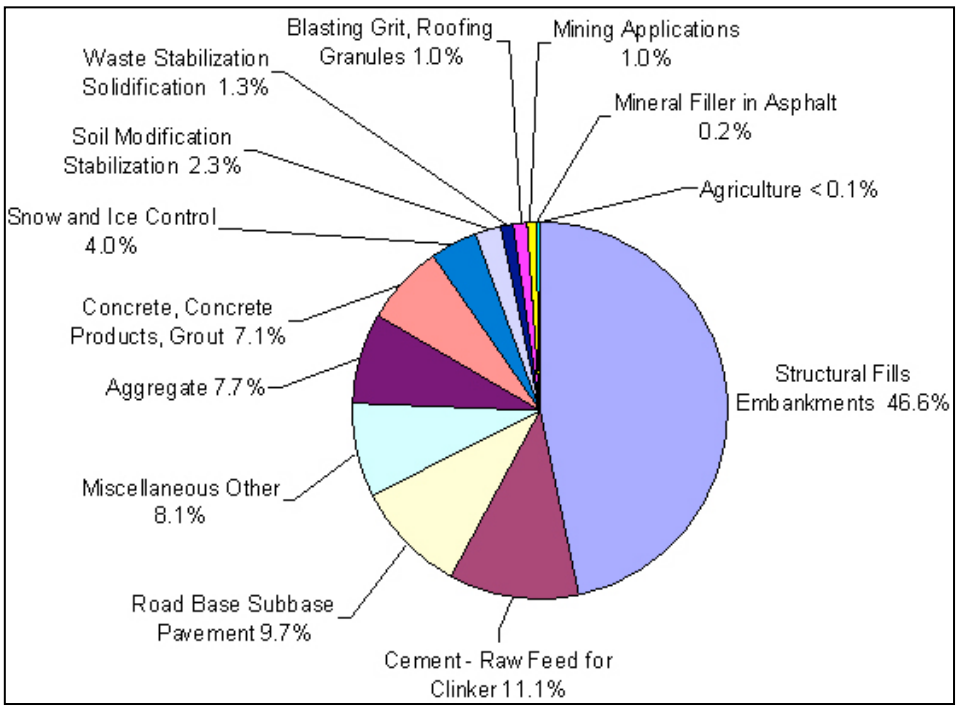

Fig. 1.5: Coal bottom ash applications as a percentage of totals reused (ACAA, 2006)

1.3 SIGNIFICANCE OF RESEARCH

Degradation of environment takes place mainly due to: i) accumulation of industrial waste products; ii) excessive extraction of the natural resources, which are depleting gradually. In the developing countries like India, large volumes of coal ash are getting accumulated near the coal fired power plant sites and are becoming environmental nuisance for the surrounding community.

There has been growing trend of utilization of the waste materials worldwide. Fly ash has been in use in manufacturing of cement and concrete since long. However, use of coal bottom ash as an admixture or fine aggregate in production of concrete is not common throughout the world. It is therefore required to examine the coal bottom ash for its possible uses in concrete. Efforts have been made in the developed countries like USA to find the gainful uses of high-calcium coal bottom ash. In a few research works high-calcium coal bottom ash has been targeted as fine aggregate in concrete. However, in

India, no significant effort has been made in this respect. The published literature is insufficient to bring coal bottom ash in practical use. As such, coal bottom ash is not used in any form. The use of coal bottom ash will serve two purposes, firstly the disposal of this waste material, secondly, use as construction material, and helping in preserving the natural resources. The utilization of an industrial by product has an important bearing on maintaining the ecological balance and economy of a country in general and construction industry in particular.

1.4 GAP IN THE RESEARCH AREA

Limited research work is published on use of low-calcium coal bottom ash as fine aggregate in concrete and that too is confined to strength properties of concrete only. Coal bottom ash produced in India has no cementitious property, contains low-calcium oxide content and has low specific gravity as compared to coal bottom ash studied abroad. Till date, Indian coal bottom ash has not been studied for its use as fine aggregate in concrete. The meticulous investigations of strength and durability properties of concrete containing low-calcium coal bottom ash as fine aggregate are required before it is widely accepted as raw construction material to be used in production of structural concrete. As no much work has been reported on strength and durability properties of concrete incorporating low-calcium coal bottom ash as fine aggregate, it was proposed through this research work to investigate the properties of concrete made with low-calcium coal bottom ash.

1.5 OBJECTIVES AND SCOPE OF RESEARCH WORK

The present research work has following main objectives:-

- Study the effect of coal bottom ash as partial or total replacement of natural river sand on the properties of fresh concrete.
- Study the effect of coal bottom ash as partial or total replacement of natural river sand on strength properties of hardened concrete.
- Study the effect of coal bottom ash as partial or total replacement of natural river sand on durability properties of hardened concrete.

The scope of the present research work includes the following:

- Characterization of material
- Design of conventional concrete mix
- Preparation of concrete mixtures with varying sand replacement levels

- Studying the properties of fresh control concrete as well as bottom ash concrete mixture
- Casting of specimens of control concrete as well as bottom ash concrete mixtures
- Testing for strength properties of hardened control concrete as well as bottom ash concrete mixtures
- Testing for durability properties of hardened control concrete as well as bottom ash concrete mixtures

To achieve the aim, following tests were performed in this research work:

(a) Characterization of Material

- Specific gravity test
- Sieve analysis
- Chemical analysis of coal bottom ash
- Water absorption measurement

(b) Cement Tests

- Setting time measurement
- Consistency measurement
- Compressive strength

(c) Concrete Tests

- Slump and compaction factor test
- Water loss through bleeding measurement
- Air content measurement
- Water loss through air drying measurement
- Unit weight measurement
- Compressive strength test
- Splitting tensile strength test
- Modulus of elasticity test
- Permeable pore space and water absorption test
- Drying shrinkage test
- Scanning Electron Microscopy (SEM)
- Energy Dispersive Spectroscopy (EDS) Analysis
- X-Ray diffraction(XRD) analysis
- Pulse velocity test
- Sorptivity test

- Rapid Chloride Penetration test
- Sulphate resistance test
- Acid resistance test
- Abrasion resistance test

1.6 METHODOLOGY

Research was conducted in two phases. In first phase, after characterization of material, two control concrete mixtures designated as Concrete 'A' and Concrete 'B' was designed. Properties of fresh concrete mixtures and strength properties of bottom ash concrete as well as control concrete were determined in the first phase. Durability properties of concrete containing coal bottom ash in partial or total replacement of river sand were examined in the second phase.

1.7 THESIS OVERVIEW

Chapter-1 Introduces the aim of the research, coal bottom ash production, physical and chemical properties of coal bottom ash, problems associated with its disposal, environmental concerns, utilization of coal bottom ash, objectives and scope of the research work.

Chapter -2 Presents detailed review of published literature on the effect of coal bottom ash as fine aggregate on strength and durability properties of concrete. Brief review of solid waste materials as supplementary cementitious materials and as aggregate replacement in concrete and mortars is also discussed in this chapter.

Chapter-3 This chapter describes the procedure of test methods applied in this research work for characterization of materials and laboratory test performed to evaluate the properties of concrete mixtures.

Chapter-4 This chapter presents the test results of characterization of materials, properties of fresh concrete, strength and durability properties of hardened concrete mixtures. Analysis of Scanning Electron Micrograph and phase identification done using X-Ray diffractogram are also presented in this chapter. The influence of coal bottom ash on properties of fresh concrete, strength and durability properties of hardened concrete mixtures incorporating coal bottom ash as partial or total replacement of river sands having varying fineness modulus is also discussed in this chapter.

Chapter-5 Gives the main conclusions of this research work.

CHAPTER-2
LITERATURE REVIEW

This chapter presents the brief review of published literature on use of waste materials either as cement supplementary material or as replacement of aggregate in concrete. Detailed review of literature on effect of coal bottom ash as fine aggregate replacement on properties concrete has been presented in this chapter.

2.1 WASTE MATERIALS

In developing countries like India, rapid industrialization has resulted in increase in the production of solid waste materials. Various industries generate numerous solid waste materials. Disposal of these solid waste materials is a major environmental issue. Disposal of solid waste materials should be managed in such a way that it should pose minimum environmental problems. The productive use of these solid waste materials is the best way to alleviate the problems associated with their disposal. The use of industrial by-products is an important factor in the economics of many industries. The solid waste materials can be put in numerous uses depending upon their physical and chemical properties. The construction industry has enormous potential for use of waste materials as construction material. Based upon their properties, these solid waste materials can either be used as supplementary cementitious materials or as replacement of aggregate in concrete or mortars. Governments should create economic incentives for managing the solid waste materials in a more environmentally beneficial manner (Regev et al., 2014).

In the published literature, solid waste materials such as fly ash (FA), rice husk ash (RHA), sewage sludge ash (SSA), baggase fly ash (Bag), municipal solid waste incineration (MSWI) fly ash, titanium fume (TF), silica fume (SF), glass residue and grounded granular blast furnace slag (GGBFS) has been targeted for their use as replacement of cement in manufacturing of concrete/mortars. Waste materials such as meat and bone meal (MBM) bottom ash, coal bottom ash, recycled aggregate, waste foundry sand, ceramic waste, plastic waste, marble dust, crusher stone dust and copper slag have been tried as replacement of aggregate in production of concrete. Use of demolition waste materials such as crushed bricks has also been reported in the published literature. The brief literature review of solid waste materials as supplementary cementitious material and as replacement of aggregate in concrete is given as under:

2.1.1 Waste Materials as Supplementary Cementitious Material

Roman were the first to use waste materials such as volcano ash as pozzolanic material in production of concrete for the construction of structures. The fist study on use of fly ash as pozzolanic ingredient was reported in 1937. The fly ash was brought in practical use as cement replacement in concrete in the construction of access roads and construction of RCC oil tank at Didcot Power Station, USA in 1981-82 (Dustan, 1983). However, In India, use of fly ash started in early 90's in manufacturing of cement. Metakaolin (MK), grounded granular blast furnace slag (GGBFS) and silica fume (SF) have also been used as the replacement of cement in mortar and concrete.

Mishra et al. (1994) studied the effect of blast furnace slag, fly ash and silica fume on permeability of concrete and concluded that on use of these waste materials in concrete, the chloride permeability decreased. Khan and Lynsdale (2002) produced high performance concrete using fly ash and silica fume as cement supplementary materials and observed that the incorporation of 8–12% SF as cement replacement yielded the optimum strength and permeability values. They reported that fly ash when used alone resulted in decrease in the compressive strength of concrete at all ages but when blended with 10% silica fume, resulted in increase in compressive strength of high performance concrete. Addition of more than 10% silica fume did not show any improvement in compressive strength.

Khan (2003) investigated the permeation-related properties of high performance concrete utilizing fly ash and micro-silica as cement replacing materials. The incorporation of 8–12% micro-silica as cement replacement yielded the optimum permeability, porosity, and sorptivity values. Khatib (2008) observed that up to 60% replacement of cement with fly ash in self compacting concrete (SCC) resulted in an increase in compressive strength whereas SCC with 80% fly ash showed less than 2% absorption value and two third reduction in shrinkage as compared to the reference concrete at 56 days of curing age. Gupta et al. (2006) concluded that the shrinkage strain of high strength concrete (HSC) increased with age. The shrinkage strain of concrete with replacement of cement by 10% of Fly ash and Silica fume, respectively, at various ages were more (6 to 10%) than the shrinkage strain of concrete without Fly ash and Silica fume.

Younsi et al. (2013) observed that hydration slowed down on inclusion of fly ash or blast furnace slag as replacement of ordinary Portland cement in concrete. Addition of fly ash or

blast furnace slag also resulted in lower portlandite content in concrete. Water cured concrete mixtures incorporating mineral additives displayed same or finer pore structure and lower resistance to accelerated carbonation than that of reference concrete.

Hemalatha et al. (2014a) proposed mix design for production of self compacting concrete incorporating fly and silica fume after giving due consideration to delayed gain in strength of SCC having fly ash and silica fume after 28 days of curing age. Hemalatha et al. (2014b) observed that due to presence of more fines in SCC smaller interfacial transitional zone exists in concrete at all curing ages. After 28 days of curing age, substantial change in micro and macro properties were observed in self compacting concrete made with fly ash and silica fume, whereas no significant change was observed in SCC having no fly ash and silica fume.

Khatib et al. (2014) observed that 10% replacement of cement with MK was the optimum which caused maximum increase in compressive strength of mortar. The replacement more than 20% did not result in any increase in compressive strength. The enhancement in compressive strength of mortar containing 20% MK can attain a value around 50% compared with control mortar (Khatib et al., 2012). Inclusion of GGBFS as replacement of cement in concrete reduces the compressive strength at early curing age. The decrease in compressive strength at early curing age can be compensated with the addition of 10% metakaolin (Khatib and Hibbert, 2005). The strength increases during the first 14 days of hydration on use of metakaolin in concrete. The increase in compressive strength of concrete may be attributed to the filling effect, pozzolanic reaction of MK, and acceleration of cement hydration (Wild et al., 1996).

Figueiredo et al. (2014) reported that concrete incorporating metakaolin as cement replacement demonstrated a very good potential in the protection against the action of chlorides. Paiva et al. (2012) studied the effect of metakaolin dispersion on fresh and hardened state properties of concrete. They observed that water demand increased on use of metakaolin as cement replacement in concrete, consequently increase in porosity of concrete. Due to pozzolanic activity of metakaolin, there was no negative effect of presence of agglomerate on compressive strength of concrete. However, on use of water reducing agents, the dispersion of metakaolin was more effective, the porosity decreased and compressive strength increased even up to 30% on replacement of cement with metakaolin.

Cwirzen (2008) produced ultra high strength (UHS) concrete using silica fume and observed that 28-day compressive strength of heat treated (90°C) and non heat treated (20°C) specimens varied between 170-202 MPa and 30-150 MPa, respectively. They reported that the shrinkage values were two times higher for the UHS mortars in comparison with the UHS concretes. No significant change in microstructure of heat treated and non heat treated specimens was observed. Scott and Singh (2011) reported similar results of ultra high performance silica fume concrete. Cwirzen and Penttala (2005) investigated the influence of the cement paste–aggregate interfacial transition zone (ITZ) on the frost durability of high-performance silica fume concrete (HPSFC). They observed that the addition of silica fume in moderate quantity densified the microstructure of interfacial transition zone (ITZ) and resulted in improved durability of concrete.

Esteves et al. (2010) studied the effect of fine aggregate on the rheology properties of high performance cement-silica systems. They concluded that fine aggregate particles in the size range of 75 and 1000 µm via surface area act as water fixation point and for particles of higher diameter, frictional force may be the governing factor for resistance to flow. Cachim et al. (2014) observed that because of increasing concerns related with environmental and sustainable issues, the utilization of waste materials is the need of the hour. They reported that the glass residue, metakaolin and diatomaceous earth can be used as a partial replacement of cement in concrete.

Cyr et al. (2006) observed that usage of 25% waste materials such as MSWI fly ash, SSA, Bag and TF as replacement of cement showed the strength activity index as 60, 90, 70 and 90%, respectively. Inclusion of 25 and 50% SSA as cement replacement in mortars resulted in the decrease in workability and increase in the setting times (Cyr et al., 2007). Behim et al. (2011) observed that strength activity depends on fineness of slag. At high fineness (4000 cm^2/g) and for all ages, mortars containing up to about 40% of slag showed strength equivalent to that of the reference mortar. For 50% of slag, the relative strength was more than 90%. Tripathy and Barai (2006) concluded that up to 40% replacement of cement with crusher stone dust, compressive strength of autoclave cured mortars was either equal or more than that of reference normal cured mortar.

2.1.2 Waste Materials as Aggregate

Siddique (2003a, b) studied the effect of fly ash as fine aggregate replacement in concrete and observed increase in compressive strength of concrete and decrease in abrasion

resistance of concrete with the increase in replacement level of sand with fly ash. Cyr et al. (2005) observed that MBM bottom ash can be used as replacement of sand in mortars. Compressive strength of mortar incorporating up to 17% MBM bottom ash as replacement of sand did not change. Cyr et al. (2006) observed that on use of rubber sand, the strain of concrete improved by 25% but there was a negative effect on compressive strength.

Cachim et al. (2014) reported that materials such as recycled aggregate from construction and demolition wastes, ceramic wastes, copper slag and plastic waste can be used as partial replacement of aggregate in production of concrete. Cachim (2009) observed that strength and stiffness properties of concrete made with crushed bricks as replacement of natural aggregate up to 15% was almost same as that of conventional concrete. For 30% of natural aggregate substitution, there was a reduction of concrete properties. Khatib (2005) studied the effect of recycled aggregate as fine aggregate on mechanical properties of concrete. He concluded that after 28 days of curing age, the rate of development of strength of concrete incorporating recycled aggregate was higher than that of control concrete. Evangelista and Brito (2007) observed that up to 30% use of fine recycled aggregate, there was no negative effect on mechanical properties of concrete.

Rao et al. (2007) reported that good quality concrete can be made with the use of recycled aggregate. Rakshvir and Barai (2006) observed that compressive strength of concrete incorporating recycled aggregate decreased up to 10% with the increase in recycled aggregate content. Water absorption of recycled aggregate was more than that of natural aggregate. Chakradhara Rao et al. (2011) studied the compressive strength, indirect tensile strength, modulus of elasticity, chloride penetration and water absorption of concrete incorporating recycled coarse aggregate. They observed that volume of voids and water absorption of recycled aggregate concrete was 2.61 and 1.82% higher than normal concrete. Concrete cured in air after 7 days wet curing showed better strength than concrete cured completely under water for 28 days.

Chakradhara Rao et al. (2011) observed that there was no influence on strength on incorporating of 25% recycled coarse aggregate. They found that for a given impact energy the reactions and strains of recycled aggregate concrete with 50 and 100% recycled coarse aggregate was significantly lower and higher, respectively, than those of normal concrete and recycled aggregate concrete with 25% recycled aggregate. Prince and Singh (2014 a, b) investigated the bond behaviour of recycled aggregate concrete and deformed steel bar

and observed that normalized bond strength of 8, 10 and 12 mm dia bars was higher for recycled aggregate concrete as compared to natural coarse aggregate concrete. The bond strength of concrete increased with increase in replacement level.

Khatib and Ellis (2001) studied the effect of foundry sand as fine aggregate on mechanical properties of concrete. They reported that compressive strength decreased and drying shrinkage increased on use of foundry sand as fine aggregate in concrete. Siddique et al. (2009) observed that there was a marginal increase in compressive strength, splitting tensile strength, modulus of elasticity and flexural strength on use of foundry sand as fine aggregate in concrete. The increase ranged between 4.2 and 9.8% in compressive strength; 3.6 and 9% in splitting tensile strength; 5.2 and 12% in modulus of elasticity; and 2.0 and 9.0% in flexural strength, when the sand replacement in concrete increased from 10 to 30%. Guney et al. (2010) reported decrease in compressive strength and splitting tensile strength of concrete with the increase in foundry sand content. Compressive strength of concrete mixture containing 10% foundry sand as fine aggregate was almost identical to that of normal concrete.

Menadi et al. (2009) observed that incorporation of 15% limestone dust as fine aggregate in concrete caused decrease in compressive strength; and increase in chloride ion penetration and gas permeability of concrete. However, they observed decrease in water permeability and negligible effect on capillary water absorption on use of 15% lime stone dust in concrete. Sahu et al. (2003) reported increase in compressive strength, splitting tensile strength and modulus of elasticity on incorporation of up to 40% stone dust as fine aggregate in concrete. Kosior-Kazberuk (2011) observed that compressive strength of concrete containing 25% SSA as fine aggregate was comparable to the reference concrete and water absorption characteristics was within acceptable range. Yuksel et al. (2006) observed that GGBFS/sand ratio is the governing factor for effect on strength and durability properties of concrete. Strength decreased while durability properties of concrete improved on incorporation of GGBFS.

2.1.3 Coal Bottom Ash as Fine Aggregate

Based on the research reports some waste materials such ash fly ash, silica fume, grounded blast furnace slag etc are in use in manufacturing of either cement or concrete. Concrete is the most widely used construction material. Cement, coarse aggregate and river sand are its

main constituent materials. Natural resources of river sand are getting depleted gradually. The scarcity of river sand has resulted in the increase in the cost of production of concrete. In Punjab, India, the construction industry is plagued due to scarcity and high cost of river sand. On the other hand, coal fired thermal power plants have been accumulating tremendous volumes of coal bottom ash for decades. Deposits of coal bottom ash are becoming environmental hazard for the surrounding community. Appreciating the environmental problems posed by coal bottom ash, many researchers have targeted coal bottom ash as fine aggregate in concrete in their studies. They have reported encouraging results on use of coal bottom ash either as partial or as total replacement of river sand in concrete.

Cheriaf et al. (1999) reported that at 28 and 90 days of hydration, strength activity index of coal bottom ash with Ordinary Portland cement was 0.88 and 0.97 respectively. These values are higher than 0.75 at 28 days and 0.85 at 90 days, required by the European standard EN 450. The higher values of strength activity index indicate the pozzolanic activity of coal bottom ash. They also reported that pozzolanic activity of coal bottom ash starts at 14 days and consumption of calcium hydroxide was significant after 90 days of hydration. According to European standard EN 450, coal bottom ash is a suitable material to be used in concrete.

Particles of coal bottom ash range from fine sand to fine gravel. Coal bottom ash appears similar to natural river sand. These properties of coal bottom ash attracted the researchers to investigate its use as fine aggregate in the production of concrete. Many researchers have investigated the properties of concrete containing coal bottom ash as a replacement of natural sand in the past. Based on their studies, effects of coal bottom ash on properties of concrete containing coal bottom ash as fine aggregate are discussed in next section.

2.2 PROPERTIES OF FRESH BOTTOM ASH CONCRETE

2.2.1 Workability

The requirement of water for desired workability of concrete mainly depends on the properties of fine aggregate used in concrete. Coal bottom ash particles are angular and rough textured. Pop corn type particles of coal bottom ash are porous. The angular particles of coal bottom ash have interlocking characteristics. Coal bottom ash contains higher proportions of particles finer than 75 μm as compared to the natural river sand. In comparison natural river sand particles are dense, smooth textured and regular shaped. The

river sand particles become smooth due to weathering action. On use of coal bottom ash as replacement of natural sand in concrete, the number of irregular shaped, rough textured and porous and finer than 75 μm particles increases. When coal bottom ash is used in concrete, interlocking characteristic of particles increases the inter particles friction. This increased inter particle friction hinders the flow characteristics of fresh concrete made with coal bottom ash. Secondly, the porous coal bottom ash particles absorb part of water added internally. As such quantity of water available for lubrication of particles gets reduced. Consequently, for the fixed water-cement ratio, the workability of bottom ash concrete reduces on use of coal bottom ash as sand replacement. The most of the published reports show that in comparison to conventional concrete, the requirement of water to achieve same slump increases on use of coal bottom ash as replacement of sand in concrete. However, there are few reports that show increase in slump or decrease of quantity of water for same slump on use of coal bottom ash in concrete. The following independent reports which shows decrease in workability of concrete on use of coal bottom ash as fine aggregate in concrete

Ghafoori and Bucholc (1997) investigated properties of fresh concrete mixtures incorporating high-calcium coal bottom ash (CBA) as natural sand replacement. In their study, the control concrete mixtures were designed to develop 28-day compressive strength of 21 (3000), 28 (4000), 34 (5000) and 41 MPa (6000 psi). They observed that in comparison to control concrete, for bottom ash concrete mixtures, the requirement of water increased to achieve same slump on incorporation of coal bottom ash as substitute of sand. Water absorption of coal bottom ash used in their study was 7.0%. For combined mixture (50% CBA + 50% sand) water requirement reduced significantly but still was higher than that of control concrete. It further improved on use of water reducing admixture but was still higher than that of control concrete mixture except in case of 41 MPa (6000 psi) mixture. In case of bottom ash concrete mixture which contains cement content of 474 kg/m^3, the requirement of water was 189.6 kg/m^3 against 194.3 kg/m^3 for control concrete on use of higher dosage of water reducing admixtures. They observed that for the same slump, the difference in requirement of water of bottom ash concrete mixtures and control concrete mixture narrows down with the increase in cement content.

Ghafoori and Bucholc (1996) investigated the impact of water reducing admixtures on properties of fresh concrete mixtures incorporating lignite based coal bottom ash as natural

sand replacement In their study, four control concrete mixtures with varying cement content of 297, 356, 424, and 474 kg/m^3 were designed to develop 28-day strength of 21 (3000), 28 (4000), 34 (5000) and 41 MPa (6000 psi). Water absorption of coal bottom ash used in their study was 7.0%. They observed that for fixed water cement ratio concrete containing coal bottom ash displayed far less workability than the control concrete. The bottom ash concrete mixtures were fairly stiff. They noted that for the same slump**,** bottom ash concrete required 269.6 kg/m^{3}of mixing water against 183.7 kg/m^3 for control concrete containing 297 kg/m^3 cement. However, on use of water reducing admixtures, the water requirement reduced but was still higher than control concrete. Bottom ash concrete mixtures yielded an average of 7% higher volume of mixture. With the use of water reducing admixtures, the increase in volume dropped to 4%. For bottom ash concrete mixtures, the gap in volume decreased with the increase in cement content. However, on use of high dosage of water reducing admixture, in comparison to control concrete, for bottom ash concrete mixtures, the requirement of water reduced to achieve same slump.

Aramraks (2006) examined the water requirement of concrete mixtures incorporating 50 and 100% coal bottom ash as replacement of sand. Lignite based coal bottom ash grains (passing through No. 4 sieve) were used as fine aggregate in concrete. Water absorption of coal bottom ash used in their study was 5.45%. He observed that the mixtures using coal bottom ash required approximately 25 to 50% more quantity of mixing water than normal concrete to obtain suitable workability. Aggarwal et al. (2007) investigated the workability of bottom ash concrete mixtures in terms of compaction factor, and observed that compaction factor values decreased with the increase in the replacement level of sand with coal bottom ash. The mix proportions of control concrete was 426.7 kg/m^3 cement, 532.7 kg/m^3 sand and 1225 kg/m^3 coarse aggregate. Water absorption of coal bottom ash was not studied by them. The compaction factor reduced almost linearly from 0.9 to 0.82 with the increase in replacement level of sand with coal bottom ash from 0 to 50%. Chun et al. (2004) also observed that workability of concrete incorporating pond ash decreased with increase in quantity of pond ash. Water absorption of pond ash used in their study was 5.45%. They also noted that the air content declined with increase in the pond ash content.

However, there are some contrary reports in the published literature which show increased workability on use of coal bottom ash as a sand replacement in concrete. The reports which show increase in slump of concrete on use of bottom ash are discussed below:-

Bai et al. (2005) observed that when natural sand was replaced with coal bottom ash, for fixed water-cement ratios of 0.45 and 0.55, the slump of bottom ash concrete mixtures containing 382 kg/m^3 cement content increased with increase in bottom ash content. For the controlled slump in the range of 0-10 mm and 30-60 mm, the requirement of free water decreased with increase in quantity of coal bottom ash as fine aggregate in concrete. Consequently, there was decrease in free w/c ratio due to the fact that the cement content was kept the same for all the mixtures. Water absorption of coal bottom ash used in their study was 30.4%. They considered that ball bearing effect of the spherical shape of coal bottom ash particles as compared to irregular natural sand particle resulted in increase in slump.

Yuksel and Genc (2007) studied the properties of concrete mixtures containing varying percentage from 10 to 50% of coal bottom ash as sand replacement, 35 kg/m^3 of fly ash, 350 kg/m^3 of cement and 167 litres of mixing water. The slump values of fresh bottom ash concrete increased up to 40% replacement level and thereafter decreased marginally. Water absorption of coal bottom ash used in their study was 6.10%. Slump of bottom ash concrete mixture containing 50% coal bottom ash as replacement of sand, was 50 mm as against 60 mm of control concrete. However, when coal bottom ash was used in combination (natural sand+ GBFS+BA), there was an improvement in the workability at all sand replacement levels as to control concrete.

Kou and Poon (2009) examined the effect of coal bottom ash as a sand replacement at levels of 0, 25, 50, 75 and 100% by mass at fixed water-cement ratio and fixed slump on workability of concrete. Water absorption of coal bottom ash used in their study was 28.9%. They used saturated surface dried coal bottom ash in all bottom ash concrete mixtures. They observed that the slump values increased with increase in quantity of coal bottom ash in the concrete. This was due to higher water absorption and lower water retention values of coal bottom ash than river sand. As such, coal bottom ash made more free water available to increase the fluidity of fresh concrete. Kim and Lee (2011) investigated the flow characteristics of fresh concrete incorporating coal bottom ash as the replacement of sand. Water absorption of coal bottom ash used in their study was 5.45%. They observed that flow characteristics of concrete reduced marginally on use of fine coal bottom ash as sand replacement. The reduction in slump flow values on use of fine coal bottom ash can be neglected.

2.2.2 Bleeding

The amount of bleeding water in concrete depends largely on the water cement ratio. The properties of cement and the physical properties of fine aggregate such as water absorption, particles finer than 150 μm, etc. have impact on the bleeding. The use of coal bottom ash as replacement of sand in concrete affects the bleeding property of fresh concrete to great extent. It is believed that on use of coal bottom ash as replacement of sand in concrete, its porous particles absorb part of water internally during the mixing process in addition to water absorbed in inter particle voids present in the concrete mixture. Moreover, coal bottom ash particles have a lesser water retention capacity as compared to the natural river sand. With the passage of time, coal bottom ash particles release the internally absorbed water to the concrete mixture. The water released by coal bottom ash particles results in higher loss of water through bleeding in bottom ash concrete as compared to that in natural sand concrete. The published research data indicates that water reducing chemical admixtures had a profound effect on the amount of bleeding exhibited by the bottom ash concrete.

Andrade et al. (2009) found that the presence of coal bottom ash as replacement of sand in concrete increased the amount of bleeding water, the bleeding time and the water release rate. Higher the quantity of coal bottom ash in the concrete the greater is the effect. The total amount of bleeding water for 25 and 50% coal bottom ash content concrete mixtures was very close to the control concrete. For concrete mixtures containing 75 and 100% coal bottom ash, amount of bleeding water was more than control concrete. This may be due to higher quantity of water added in bottom ash concrete mixtures as compared to control concrete. The amount of water added in bottom ash concrete mixtures containing 75 and 100% coal bottom ash was 373 kg/m^3 and 378 kg/m^3, respectively, against 219 kg/m^3 added in control concrete.

Ghafoori and Bucholc (1996) demonstrated that the bottom ash concrete mixtures displayed higher degree of bleeding than the control concrete. The quantity of water added in bottom ash concrete mixtures was much higher than added in control concrete. The quantity of water added in bottom ash concrete mixtures varied from 251.2 kg/m^3 to 269.6 kg/m^3 as compared to 182.7 kg/m^3 to 194.3 kg/m^3 added in control concrete. The bottom ash concrete mixtures displayed, about 84% higher total amount of bleeding water in low cement content mixtures. On use of low dosage of admixture, the amount of bleeding water

decreased by approximately 50% of those obtained for bottom ash concrete without admixtures. With the use of high dosage of admixtures, the amount of bleeding was significantly lower than that of equivalent control concrete.

Ghafoori and Bucholc (1997) observed that for concrete mixture containing 297 kg/m^3 cement, bleeding percentage increased from 2.2 to 4.0 and 2.79 on use of 100 and 50% coal bottom ash as replacement of sand in concrete, respectively. With increase in quantity of cement in concrete mixtures, the bleeding percentage in fully bottom ash concrete mixtures decreased from 4.0 to 0.84 as compared to from 2.2 to 0.08 decreases in control concrete. With the use of water reducing admixture, bleeding percentage of bottom ash mixtures was nearly identical to that of respective control concrete mixture (2.0 to 0.36%). This may be due to fact that water cement ratio of bottom ash mixtures with water reducing admixtures was lower than respective control concrete mixture.

2.2.3 Setting Times

The initial setting time of concrete is the moment at which the concrete shows certain level of stiffness. The research reports published reveal that the replacement of sand with coal bottom ash in concrete increases the setting times of concrete. It is believed that the increased demand of mixing water on use of coal bottom ash is the possible reason for increased setting times. Higher quantity of mixing water in the concrete mixtures lowers the pH value of the medium and increases the distance between cement hydration products. The above factors result in delay or decrease in hydration activities of the cement particles and thus increase in setting times of concrete incorporating coal bottom ash as replacement of sand. The water reducing admixtures has little effect on setting times of bottom ash concrete with low proportion of cement. For bottom ash concrete mixtures with higher proportions of cement, the setting times decrease with the increase in dosage of water reducing admixtures.

Ghafoori and Bucholc (1996) studied effect of water reducing admixtures on setting times of concrete incorporating high calcium coal bottom ash as replacement of sand and observed that the average initial and final setting times for bottom ash concretes were 6.3 and 9.5% higher than the control concrete, respectively. The setting times of bottom ash concrete mixtures were unchanged on use of water reducing admixtures in concrete mixtures with low proportion of cement. However, setting times of bottom ash concrete mixtures with high proportion of cement decreased slightly. For concrete mixtures having

cement content of 474 kg/m^3, the initial setting times decreased from 3.3 to 3.0 hr and 2.5 hr on use of 369.7 (12.5) and 769.3 mL (25 oz) of water reducing admixture per 45.3 kg (100 lb) of cement, respectively. The final setting times of bottom ash concrete mixture decreased from 4.4 to 4.0 hr and 3.7 hr on use of 369.7 (12.5) and 769.3 mL (25 oz) water reducing admixture per 45.3 kg (100 lb) of cement, respectively. Ghafoori and Bucholc (1997) observed that setting times of concrete mixtures with partial replacement of sand with coal bottom ash were identical to control concrete. On use water reducing admixtures, the initial and final setting times of concrete mixtures incorporating 50% coal bottom ash as replacement of sand dropped approximately by 9 and 13.5%, respectively.

Andrade et al. (2009) investigated the influence of coal bottom ash as replacement of sand in concrete on its setting times. They observed that initial setting times of bottom ash concrete mixtures were higher than control concrete. For bottom ash concrete mixtures in which quantities of coal bottom ash were corrected according to the moisture content, initial setting time increased with increase in coal bottom ash content. Up to 75% replacement of sand with coal bottom ash, initial setting time increased from 230 min to 350 min. The initial setting time of concrete mixture incorporating 100% coal bottom ash was 270 min. Final setting time of the bottom ash concrete increased with increase in quantity of coal bottom ash in concrete. For concrete mixtures in which quantities of coal bottom ash were not corrected according to moisture content, initial and final setting times of bottom ash concrete mixtures except mixture containing 25% coal bottom ash were lower than control concrete Initial and final setting times of bottom ash concrete mixtures containing 25% coal bottom ash were 240 min and 340 min as compared to 230 min and 330 min of control concrete, respectively.

Jaturpitakkul and Cheerarot (2003) studied the effect of coal bottom ash as cement replacement on properties of cement paste. They observed that initial and final setting times of cement paste delayed as the coal bottom ash replacement level increased. Initial and final setting times of cement paste containing 30% coal bottom ash were longer than control paste by 23 minutes and 30 minutes, respectively. Final setting time of coal bottom ash cement pastes was between 195 and 210 min. The reduction in tricalciumsilicate in the paste on replacement of cement with coal bottom ash resulted into longer setting times.

2.2.4 Plastic Shrinkage

The loss of water by evaporation from its surface of concrete causes plastic shrinkage. Greater the loss of water by evaporation greater is the plastic shrinkage. From the published literature, it can be concluded that coal bottom ash has significant affect on plastic shrinkage of concrete. The published literature show that bottom ash concrete exhibits greater dimensional stability as compared to the conventional concrete. It is believed that the porous particles of coal bottom ash act as water reservoir in the bottom ash concrete mixtures. With the passage of time, the water absorbed by the coal bottom ash particles is released to the concrete mixture. The released water helps in reducing the plastic shrinkage. Greater bleeding capacity and higher bleeding rate of the bottom ash concrete mixtures also helps in reducing plastic shrinkage.

Ghafoori and Bucholc (1996) observed that the bottom ash concrete mixtures displayed better dimensional stability than that of control concrete. Plastic shrinkage strain of bottom ash concrete was 0.309% as compared to 0.467% of control concrete. Bottom ash concrete mixtures displayed 35% less average shrinkage than control concrete mixture. Low dose (369.7 mL per 45.36 kg [12.5 oz per 100 lb] of cement) of water reducing admixture has insignificant affect on plastic shrinkage of bottom ash concrete and control concrete. On use of high dose (739.3 mL per 45.36 kg [25 oz per 100 lb] of cement) of water reducing admixture, the plastic shrinkage of bottom ash concrete mixtures increased but remained 13% less than that of control concrete mixture. Ghafoori and Bucholc (1997) observed that early plastic shrinkage of bottom ash concrete containing 50% coal bottom ash was approximately 20% lower than control concrete. Plastic shrinkage of this mixture increased on use of water reducing admixtures. It was approximately 50% higher than bottom ash concrete but was lower than control concrete.

Andrade et al. (2009) concluded that bottom ash concrete resulted in lesser total deformations. For bottom ash concrete mixtures in which quantity of coal bottom ash was corrected according to moisture content, the maximum deformation reduced from 0.031 mm/m to 0.009 mm/m on increase in coal bottom ash content in concrete. For concrete mixtures in which quantity of coal bottom ash was not corrected for moisture content, maximum deformations of bottom ash concrete mixtures except concrete mixture containing 25% coal bottom ash was between 0.065 mm/m and 0.088 mm/m as compared to 0.031 mm/m for control concrete.

2.3 PROPERTIES OF HARDENED COAL BOTTOM ASH CONCRETE

2.3.1 Density

The published research data shows appreciable decrease in unit weight of concrete on use of coal bottom ash as a replacement of natural sand in concrete. Compared to natural sand, unit weight of coal bottom ash is comparatively low and its structure is porous. The increased demand of mixing water on use of coal bottom ash in concrete results in increase in number and size of pores and thus result in porous structure of concrete. These factors contribute to lower unit density of bottom ash concrete. Higher is replacement of sand with coal bottom ash in concrete more is the decrease in its unit weight.

Andrade et al. (2007) observed that the use of coal bottom ash having specific gravity of 1.67 g/cm^3 and fineness modulus of 1.55 as replacement of natural sand in concrete resulted in the decrease in density of concrete by 25% from 2170 kg/m^3 to 1625 kg/m^3. Kim and Lee (2011) studied the effect of fine and coarse coal bottom ash on density of concrete. The mix proportions of concrete used in their investigations consisted 143 kg/m^3 of silica fume, 14 kg/m^3 of superplasticizer, 187 kg/m^3 of water and 607 kg/m^3 of cement in all the specimens with varying percentages of coal bottom ash as replacement of sand, coarse aggregate replacement and combined replacement of both sand and coarse aggregate. They observed that density of hardened concrete decreased linearly as the replacement ratio of fine and coarse bottom ash increased. The density of high strength concrete was less than 2000 kg/m^3 when both 100% fine coal bottom ash and 100% coarse coal bottom ash were used. The decrease in density was 109 kg/m^3 (4.6%) and 228 kg/m^3 (9.6%) when sand was replaced with fine bottom ash and coarse aggregate was replaced with coarse coal bottom ash, respectively.

Topcu and Bilir (2010) investigated the effect of coal bottom ash as a replacement of sand on 7 and 28-day density of mortar. The mix proportions of mortar consisted 500 kg/m^3 cement, 3 kg/m^3 high range water reducing admixtures and varying percentages of coal bottom ash of specific gravity 1.39 g/cm^3 as replacement of natural sand. They observed that the weight of specimens decreased with increase in coal bottom ash content. The unit weight at the age of 7 and 28 days ranged between 1.23 kg/dm^3 and 2.23 kg/dm^3; and 1.35 and 2.28 kg/dm^3, respectively.

Ghafoori and Bucholc (1996) observed that bottom ash concretes exhibited lower unit weight as compared to the control concrete. One-day unit weight of bottom ash concrete

was 2263.4 kg/m^3 (141.3 lb/ft^3) as compared to 2343.5 kg/m^3 (146.3 lb/ft^3) of control concrete. Unit weight of bottom ash concrete increased on use of water reducing admixtures. The unit weight increased by an average of 0.8% on use of low dosage of 369.7 mL per 45.36 kg (12.5 oz per 100 lb) of cement and an additional 0.25% when high admixture dosage of 739.3 mL per 45.36 kg (25 oz per 100 lb) of cement was applied. Arumugam et al. (2011) observed that the average density of bottom ash concrete decreased linearly with increase in quantity of pond ash in concrete. The decrease in density of bottom ash concrete was due to lower specific gravity.

2.3.2 Compressive Strength

The strength development of concrete is influenced by porosity of hydrated paste. Further porosity is controlled by water/cement ratio and the bond cracks present at the interface of aggregate and hydrated paste. The strength of individual constituent material of concrete also has influence on the strength of concrete. The published reports show that for the same workability, water cement ratio of concrete mixture increases on use of coal bottom ash as substitute of natural sand. The increased water cement ratio result in increase in volume of all pores: pores left by water, fissures formed by bleeding etc. and low density of bottom ash concrete mixture. Since bottom ash concrete has higher bleeding, there are more chances of more bleeding water getting trapped below the aggregates. This trapped water results in the formation of the more number of small pores close to the aggregate surfaces. These pores prevent the excellent bonding of cement paste with the aggregate. Therefore the transition zone between the aggregate and cement paste becomes weak and porous which ultimately results in reduction in strength of bottom ash concrete. The weak microstructure obtained with the use of coal bottom ash is responsible for the decrease in compressive strength.

Ghafoori and Bucholc (1996) studied the effect of high-calcium coal bottom ash on compressive strength of concrete and observed that compressive strength development pattern of bottom ash concrete was similar to that of control concrete. At early curing age, compressive strength of bottom ash concrete was lower than that of control concrete but at 180 days of curing age, it was almost comparable for all the concrete mixtures. At the age of 7 days, bottom ash concrete mixtures having cement content of 297 kg/m^3, 356 kg/m^3, 424 kg/m^3 and 474 kg/m^3 achieved 67, 81, 78 and 86% of the 28-day compressive strength, respectively. At an early curing age of 3 and 7 days, average compressive strengths of

bottom ash concrete were 30% and 25% lower than those of control concrete, respectively. This difference dropped to 17% and 7% at 28 and 180 days, respectively. Compressive strength of bottom ash concrete at all levels of cement content improved on the use of low dosage of admixture. Compressive strength of bottom ash concrete at the age of 28 days increased by nearly 20% than the concrete mixture produced without admixture and by 3.5% than that of control concrete. Compressive strength of combined mixture of 50% bottom ash and 50% natural sand surpassed those of control concrete mixture on use of high range water reducing admixture.

Ghafoori and Bucholc (1997) found that compressive strength of bottom ash concrete mixture containing 50% coal bottom ash as replacement of river sand was lower than that of control concrete. The average differences in compressive strength at the curing age of 3 and 7 days were 12% and 14.5%, respectively. With age, the difference in compressive strength of bottom ash concrete and that of control concrete decreased. Compressive strength of bottom ash concrete mixtures was lower by 10 and 1.5% at 28 and 180 days, respectively. On use of high range water reducing admixture, compressive strength of bottom ash concrete mixture containing 50% coal bottom ash as replacement of river sand, surpassed that of control concrete at all levels of age. At the age of 7, 28, 90 and 180 days, the compressive strength increased by 30, 24, 21.4 and 19%, respectively.

Andrade et al. (2007) observed that concrete mixtures made with coal bottom ash as equivalent volume replacement, correcting coal bottom ash quantities according to the moisture content showed very significant loss in compressive strength. However in case of concrete mixtures prepared with the addition of coal bottom ash as non equivalent volume replacement, without correcting coal bottom ash quantities according to the moisture content the compressive strength of bottom ash concrete was similar to that of control concrete.

Kou and Poon (2009) investigated the effect of coal bottom ash on the properties of concrete. Saturated surface dry sand and coal bottom ash were used in their study. They observed that at a fixed water-cement ratio, the compressive strength of bottom ash concrete mixtures decreased with the increase in the coal bottom ash content at all the ages. However, at fixed slump range, the compressive strength of bottom ash mixtures was higher than that of control concrete at all the ages. The improvement in compressive strength could be attributed to the decrease in free water-cement ratio. For a given slump,

the higher water absorption by coal bottom ash lead to reduction in demand of free water. Kim and Lee (2011) investigated the effect of fine coal bottom ash as a replacement of sand in concrete on compressive strength at 7 and 28 days. They observed that the compressive strength of bottom ash concrete mixtures was not strongly affected by the replacements of sand with fine coal bottom ash. The effect of coal bottom ash on compressive strength was lower due to higher cement paste in concrete.

Sani et al. (2010) found that at 3 days, the compressive strength of bottom ash concrete mixtures containing 20% and 30% washed coal bottom ash as replacement of sand was the highest as compared to compressive strength of other washed bottom ash concrete mixtures. Bottom ash concrete mixture containing 30% washed coal bottom ash as sand replacement recorded highest compressive strength at all the curing ages up to 60 days. They concluded that 30% replacement of sand with washed coal bottom ash in concrete is the optimum amount in order to get favourable strength, environment saving and a lowering cost.

Topcu and Bilir (2010) examined the effect coal bottom ash as fine aggregate replacement on the compressive strength of cement mortar at the age of 7 and 28 days. They observed that compressive strength of cement mortar decreased with the increase in coal bottom ash content and the decrease rate in 7-day compressive strength was similar to 28-day compressive strength. Compressive strength values of mortar incorporating coal bottom ash were lower than that of control mortar sample. Ghafoori and Cai (1998) investigated the effect of coal bottom ash on properties of roller compacted concrete. They observed that compressive strength development of bottom ash roller compacted concrete was similar to that of conventional concrete. At 7 days, bottom ash concrete mixtures achieved nearly 75% of the 28-day compressive strength. For bottom ash concrete mixtures containing 9, 12 and 15% cement, 90-day compressive strength exceeded 28-day compressive strength by an average of 19, 15 and 12%, respectively. At the end of 180 days of curing, the 28-day compressive strength was surpassed by 26%.

Yuksel and Genc (2007) investigated the possibilities of using coal bottom ash as fine aggregate in concrete. They found that 28-day compressive strength of bottom ash concrete mixtures decreased with increase in bottom ash content. Compressive strength of bottom ash concrete mixture containing 50% coal bottom ash as sand replacement was lower by 31.8% than that of control concrete. With 10% sand replacement with coal bottom ash, 90-

day compressive strength of concrete decreased by 6.9%. This shows that coal bottom ash retards the gain in compressive strength of bottom ash concrete mixtures. Aramraks (2006) demonstrated that the compressive strength of bottom ash concrete mixtures incorporating 50 and 100% coal bottom ash as sand replacement was approximately 20 to 40% lower than that of natural sand concrete mixtures.

Aggarwal et al. (2007) investigated the effect of coal bottom ash with varying levels from 20 to 50% as sand replacement on properties of concrete. They observed that compressive strength of bottom ash concrete mixtures was lower than that of control concrete mixture at all the ages. The difference in compressive strength of bottom ash concrete mixtures and control concrete mixture was less distinct after 28 days. Compressive strength of bottom ash concrete mixtures continued to increase with the age. At 90 days, bottom ash concrete mixture containing 30% and 40% coal bottom ash as sand replacement, achieved compressive strength equivalent to 108% and 105% of compressive strength of normal concrete at 28 days, respectively.

Bai et al. (2005) studied the effect of coal bottom ash as fine aggregate on compressive strength of concrete mixtures designed with fixed water-cement ratio and slump range. They observed that at fixed water-cement ratio, compressive strength decreased with the increase in bottom ash content in concrete mixture, while at fixed slump range of 30-60 mm, there was an improvement in compressive strength over that of control concrete at all the ages. For fixed slump range, the improvement in compressive strength could be attributed to reduction in water demand on use of coal bottom ash in concrete. Arumugam et al. (2011) observed that concrete mixtures incorporating 20% pond ash as sand replacement showed improvement in compressive strength over the control concrete at all the curing ages. However, compressive strength of concrete mixtures reduced with further addition of pond ash as sand replacement level from 20%.

Chun et al. (2004) noticed that the compressive strength of concrete differed by the content of pond ash collected from each disposal site. With increase in content of pond-ash, there was relatively greater increase in compressive strength, compared to normal concrete, and such trend might be a consequence of decreased water-cement ratio induced by the absorption of mixing water. Kurama and Kaya (2008) studied the effect of coal bottom ash as partial replacement of cement in concrete and observed that compressive strength increased with increase in quantity of coal bottom ash replacement up to 10%. At 56 days,

compressive strength of concrete mixture containing 10% coal bottom ash as cement replacement surpassed by 5% to the compressive strength of control concrete. The additions of coal bottom ash higher than 10% lead to decrease in compressive strength at lower age of 7 and 28 days. However, at 56 days, compressive strength of bottom ash concrete mixtures at replacement levels up to 15% was higher than that of control concrete mix. Compressive strength of bottom ash mixtures with 25% replacement level was marginally lower than that of control concrete. Yuksel and Bilir (2007) observed that compressive strength decreased slightly on incorporation of grounded blast furnace slag and bottom ash as fine aggregate in concrete.

2.3.3 Flexural Strength

Bottom ash concrete displays similar trend in development of flexural strength and compressive strength. The published research data shows that flexural strength of concrete decreased on substitution of sand with coal bottom ash at all the curing ages. The flexural strength of concrete mainly depends upon the quality of paste in concrete mixture. The paste in concrete becomes weak and porous on use of coal bottom ash. Volume of all pores in concrete increases and microstructure of concrete becomes porous on use of coal bottom ash. As such bottom ash concrete mixtures displays lower flexural Strength.

Ghafoori and Bucholc (1996) found that flexural strength of concrete mixtures incorporating high-calcium (CaO = 22.50%) coal bottom ash as sand replacement was lower than that of conventional concrete. On use of super plasticizer admixture, flexural strength of bottom ash concrete mixtures either equalled or slightly exceeded that of control concrete. The flexural strength improvement over the bottom ash concrete mixture without superplasticizer and containing cement content of 297, 356, 424 and 475 kg/m^3 was 29.76, 20.3, 11.4 and 7.5%, respectively. Flexural strength of bottom ash concrete decreased with increase in coal bottom ash content. However, with the addition of super plasticizer in concrete mixtures, flexural strength slightly improved at almost all the curing ages.

Yuksel and Genc (2007) demonstrated that flexural strength of bottom ash concrete was lower than that of control concrete. They observed that for 10% replacement of sand with coal bottom ash, the decrease in flexural strength was almost 10% of flexural strength of control concrete and with replacement higher than 10%, there was almost no change in tensile strength values of bottom ash concrete mixtures. Topcu and Bilir (2010) observed

that flexural strength of mortar mixtures incorporating coal bottom ash as replacement of sand was lower than that of control mortar mixture. They also observed that for bottom ash mortar mixtures, the decrease rate in 7-day flexural strength was similar to that of 28-day flexural strength. The flexural strength of bottom ash mortar mixtures was lower than that of control mortar mixture at all the curing periods. Ghafoori and Cai (1998) studied the effect of coal bottom ash on mechanical properties of roller compacted concrete. They investigated that flexural strength of bottom ash concrete increased with age and at the end of 90 days, it surpassed its 28-day flexural strength by about 17%. The ratios of flexural strength and compressive strength were fairly uniform with an average value of 1.55.

Kim and Lee (2011) demonstrated that the flexural strength of concrete decreased almost linearly as the replacement ratio of fine and coarse coal bottom ash was increased. The modulus of rupture decreased by 19.5 and 24.0% on 100% replacement of normal aggregates with fine and coarse coal bottom ash, respectively. Aggarwal et al. (2007) found that flexural strength of bottom ash concrete mixtures were lower than that of control concrete at all the ages. They observed that at 90 days, concrete mixtures containing 30 and 40% coal bottom ash, attained flexural strength in the range of 113-118% of 28-day flexural strength of concrete. Arumugam et al. (2011) observed that pond ash concrete showed similar behaviour in flexural strength to that of compressive strength. Concrete mixtures containing pond ash up to 20% as sand replacement showed improved flexural strength over the control concrete mixture at all the curing ages. With the increase in sand replacement level over 20%, the flexural strength reduced.

Kurama and Kaya (2008) observed that 28-day flexural strength of bottom ash concrete incorporating coal bottom ash as cement replacement was almost equal to that of control concrete specimen. At the curing age of 56 days, flexural strength of bottom ash concrete mixtures except concrete mixture containing 25% cement replacement exceeded that of control concrete sample. The reduction in flexural strength of concrete containing 25% coal bottom ash was due to low activity of bottom ash at the early curing ages.

2.3.4 Splitting Tensile Strength

The splitting tensile strength of bottom ash concrete progresses in the similar manner as that of normal concrete. Coal bottom ash has more influence on the development of splitting tensile strength than compressive strength of concrete. On use of coal bottom ash as sand replacement in concrete, splitting tensile strength decreases. One of the reasons for

reduction in splitting tensile strength is the increase in porosity and distribution of pores in bottom ash concrete. The use of chemical admixtures reduces the water requirement, improve the microstructure of bottom ash concrete, and hence result in improvement in the splitting tensile strength.

Yuksel and Genc (2007) observed that up to 10% sand replacement with coal bottom ash, there was no change in splitting tensile strength and thereafter, it decreased considerably with increase in coal bottom ash content. The maximum decrease in the splitting tensile strength was 58% for bottom ash concrete mixture containing 50% coal bottom ash as replacement of sand. The decrease in splitting tensile strength of bottom ash concrete mixtures was almost linear with increase in coal bottom ash content. Ghafoori and Bucholc (1997) in their investigation observed that splitting tensile strength of bottom ash concrete increased with the increase in curing age and in case of concrete mixture with 356 kg/m^3 of cement or higher, it exceeded the control concrete mixture at all the ages of curing. The bottom ash concrete mixture incorporating 50% coal bottom ash as sand replacement and containing 297 kg/m^3 cement displayed 5% lower splitting tensile strength but with the use of admixture it improved by 12% above control concrete mixture. Ghafoori and Bucholc (1996) investigated the effect of water reducing admixtures on splitting tensile strength of bottom ash concrete. They observed that on use of water reducing admixtures the splitting tensile strength of bottom ash concrete mixtures improved by 17% over that of bottom ash mixtures without water reducing admixtures.

Ghafoori and Cai (1998) demonstrated that the splitting tensile strength of bottom ash concrete mixtures decreased with increase in coal bottom ash content and correspondingly decrease in coarse aggregate. After 7 days of curing, bottom ash concrete mixtures containing 9 to 15% cement content and 50 to 60% coarse aggregate gained 65 to 76% of its 28-day splitting tensile strength. At the end of 90 and 180 days, splitting tensile strength of bottom ash concrete mixtures containing 15, 12 and 9% cement content surpassed its 28-day splitting tensile strength by 11, 20 and 18%; and 18, 32 and 36%, respectively. Ratios of splitting tensile strength to compressive strength at 28 and 180 days range from 0.101 to 0.153. Aggarwal et al. (2007) found that splitting tensile strength of bottom ash concrete mixtures were lower than that of control concrete mixture at all the ages. At 90 days of age, bottom ash concrete attains splitting tensile strength in the range of 121-126% of 28-day splitting tensile strength of normal concrete. Arumugam et al. (2011) observed

that splitting tensile strength of concrete containing 20% washed bottom ash as sand replacement was higher than that of control concrete. Splitting tensile strength of bottom ash concrete mixtures decreased with increase in sand replacement level from 20%.

2.3.5 Microstructure

Yuksel and Genc (2007) investigated that when natural sand was replaced with coal bottom ash in the concrete, the microstructure changed its network structure. Instead of irregular grains in case of natural river sand, the grains becomes circular and pores become smaller and more distributed on use of coal bottom ash. As the replacement of sand with coal bottom ash in concrete increased, the detachment of grains in the network structure increased. These discrete grains are the microstructure of bottom ash concrete.

2.3.6 Modulus of Elasticity

It is evident from the published literature that the use of coal bottom ash strongly affects the modulus of elasticity of concrete. The modulus of elasticity of bottom ash concrete mixtures decreases with increase in coal bottom ash content in concrete. Coal bottom ash particles are less stiff and dense than natural sand particles. The use of coal bottom ash in concrete results in weak and porous paste, which results in reduction of modulus of elasticity of concrete. The use of water reducing admixtures improves the modulus of elasticity of bottom ash concrete mixtures due to reduction in water cement ratio.

Ghafoori and Bucholc (1996) found that bottom ash concrete mixtures with all unit weights of cement displayed significant lower modulus of elasticity than that of control concrete. On use of low dose of water reducing admixtures, modulus of elasticity of bottom ash mixtures containing cement content of 297, 356, 424 and 475 kg/m^3 improved by 9.6, 6.3, 11.92, and 5.15%, respectively. Kim and Lee (2011) found that the modulus of elasticity decreased with the increase in replacement of fine and coarse coal bottom ash aggregates. The modulus of elasticity of bottom ash concrete containing 100% coal bottom ash as sand replacement decreased from 41.1 MPa to 34.9 MPa. The decrease in modulus of elasticity of bottom ash concrete was 15.1% of modulus of elasticity of control concrete. Modulus of elasticity of bottom ash concrete was 31.8 MPa i. e. 77.5% of modulus of elasticity of control concrete specimen, when 100% coarse coal bottom ash was used as coarse aggregate. Topcu and Bilir (2010) observed that Modulus of elasticity of bottom ash mortars decreased from 60 GPa to 17 GPa with the increase of coal bottom ash content from 0 to 60%. The porous structure obtained on use of coal bottom ash in concrete is

responsible for the decrease in modulus of elasticity. Andrade et al. (2009) demonstrated that the modulus of elasticity of concrete at 28 days of curing age, decreased from 25.8 GPa to 8.9 GPa when the replacement ratio of coal bottom ash increased to 100% and 300 kg/m^3 cement was used.

2.3.7 Drying Shrinkage

A limited literature has been published on drying shrinkage properties of bottom ash concrete. It is believed that the porous particle structure of coal bottom ash is beneficial for reducing the drying shrinkage of concrete. The porous particles of coal bottom ash acts as reservoirs. It is considered that the porous coal bottom ash particles slowly release the moisture during the drying phase of concrete and therefore result in reduced shrinkage.

Bai et al. (2005) observed that at fixed water-cement ratio of 0.45 and 0.55, drying shrinkage values of all bottom ash concrete were lower than that of control concrete, while at fixed workability, the drying shrinkage values were higher. At fixed water-cement ratio, the quantity of porous material in concrete increased with the increase of bottom ash content, which slowly released the water during drying of concrete and thus resulted in reduced drying shrinkage. At fixed slump range, with the increase in coal bottom ash content, they found that drying shrinkage increased contrary to the decrease in drying shrinkage on reduction of free water content.

Ghafoori and Cai (1998) in their study found that the one year drying shrinkage strain of bottom ash roller compacted concrete varied from 203×16^{-6} to 298×10^{-6} which is nearly half to that of vibratory placed conventional concrete mixtures. Similar to conventional concrete, drying shrinkage of bottom ash roller compacted concrete increased with time. Ghafoori and Bucholc (1996) observed that despite higher water-cement ratio, bottom ash concrete displayed lesser drying shrinkage in comparison to control concrete. Swelling properties of bottom ash concrete were 200% higher than the volume increase exhibited by the equivalent natural sand concrete. Water reducing admixtures had negligible effect on the swelling characteristics of the coal bottom ash.

Ghafoori and Bucholc (1997) observed that bottom ash concrete mixtures displayed better dimensional stability as compared to the conventional concrete. They believed that higher bleeding resulted in lower drying shrinkage strain value of bottom ash concrete. Drying shrinkage strain values of bottom ash concrete mixture containing 50% coal bottom ash

was lower that that of control concrete but higher than that of fully bottom ash concrete mixture. Kou and Poon (2009) demonstrated that at the fixed slump range, the drying shrinkage values of all the bottom ash concrete mixtures were lower than that of control concrete. This was due to the fact that with the increase in coal bottom ash content, the required free water content in bottom ash concrete mixtures decreased.

2.4 DURABILTY PROPERTIES OF BOTTOM ASH CONCRETE

2.4.1 Permeability

The permeability of concrete depends upon the size, distribution and continuity of pores present in cement paste and permeability of aggregates. The published research reports indicate that bottom ash concrete has higher permeability as compared to the natural sand concrete. Permeability of bottom ash concrete mixtures increases with increase in coal bottom ash content. The key aspects which affect permeability characteristics of bottom ash concrete mixtures are porous microstructure of coal bottom ash, increased demand of mixing water and higher loss of water through bleeding. The replacement of sand with coal bottom ash in concrete results in porous microstructure. The increased water demand and higher bleeding exhibited by bottom ash concrete mixtures results in increase in pores and their continuity. Concretes with lower water to binder ratio and longer curing age, exhibits marginally lower permeability.

Ghafoori and Bucholc (1996) found that as per AASHTO T-277 specifications, the chloride permeability of bottom ash concrete was higher than that of control concrete. The permeation of chloride ions into the bottom ash concrete mixtures decreased drastically on use of low dosage of superplasticizer. The bottom ash concrete mixtures without admixtures allowed on an average 120% greater current flow than that through control concrete and with the use of admixture it reduced to 61% above that of control concrete. The results of accelerated chloride permeability of their research show that bottom ash concrete is more permeable than that of control concrete at all levels of cement contents.

Aramraks (2006) found that chloride permeability of bottom ash concrete was better than normal concrete. Total charge passed through bottom ash concrete containing 100% coal bottom as the replacement of sand was 1975 coulombs as compared to 4178 coulombs passed through control concrete. The bottom ash concrete mixture containing 100% coarse grain (passing no.4 and retaining on no. 50 standard sieves) coal bottom ash as replacement

of fine aggregate and with 2% superplasticizer showed the lowest chloride permeability. Kou and Poon (2009) demonstrated that at fixed water-cement ratio, the resistance to chloride-ion penetration of the concrete mixtures decreased with increasing percentages of coal bottom ash as a replacement of river sand. The availability of more free water in bottom ash concrete mixtures than in control concrete leads to looser microstructure.

2.4.2 Freeze-Thaw Resistance

Limited research data published on freeze-thaw resistance of bottom ash concrete may not be sufficient to draw any conclusion. The published data indicates that bottom ash concrete exhibits resistance to freezing and thawing similar to that of the control concrete. The water reducing admixtures have insignificant effect on freezing and thawing resistance of bottom ash concrete.

Ghafoori and Cai (1998) observed that when bottom ash roller compacted concrete containing high-calcium (22.50%) coal bottom ash as fine aggregate subjected to an environment with repeated freezing and thawing cycles, it performed well. They reported that mass loss and durability factor of bottom ash roller compacted concrete mixtures after 300 rapid freezing and thawing cycles was 2.3 and 91.2%, respectively. Both cumulative mass loss and durability factor exhibited linear relationship with freezing and thawing cycles. With an increase in cement content from 9 to 12% and 15%, cumulative mass loss decreased by 57 and 67%, whereas durability factor increased by 21 and 20%, respectively. The cumulative mass loss decreased with increase in quantity of coarse aggregate in concrete mixture. Mass loss decreased by 38 and 25%, when coarse aggregate percentage in concrete mixture increased from 50 to 60% and 55 to 60%, respectively.

Ghafoori and Bucholc (1996) observed that bottom ash concrete mixtures incorporating high-calcium (22.50%) coal bottom ash displayed remarkable resistance to freezing and thawing cycles. The resistance displayed by bottom ash concrete mixtures was slightly higher than that of control concrete. The use of water reducing admixtures has negligible affect on freezing and thawing resistance of the bottom ash concrete. Chun et al. (2004) noticed that increased content of pond-ash leads a relatively lower freezing and thawing resistance than normal concrete, while the trend of lowering resistance was mainly due to a decrease in air content and an influence of absorption water. Yuksel and Bilir (2007) observed that resistance to freezing and thawing improved on use of blast furnace slag and bottom ash as fine aggregate in concrete.

2.4.3 Resistance to Sulfate Attack

Ghafoori and Cai (1998) studied the effect of high-calcium (22.50%) coal bottom ash as replacement of sand in roller compacted concrete on its long term durability. They concluded that roller compacted concrete containing dry coal bottom ash as fine aggregate can exhibit excellent resistance to external sulfate attacks. After 28 days of immersion in sodium sulfate solution, the bottom ash roller compacted concrete specimens showed a mean expansion value of 0.0017%. After 365 days of immersion in 5% sodium sulfate solution, roller compacted concrete containing coal bottom ash experience expansion strain ranging from 0.00203 to 0.0388%. No mass loss was detected during this period. Compressive strength of samples which were water cured for 180 days was identical to that of the equivalent samples cured in a 5% sodium sulfate solution for six month period. They also observed that the resistance to external sulfate attack improved with the increase in coarse aggregate content in bottom ash roller compacting concrete. After 365 days of immersion period, the expansion strains reduced by 18 and 13% when cement content in concrete increased from 9 to 12% and to 15%, respectively.

Ghafoori and Bucholc (1996) observed that bottom ash concrete and natural sand concrete showed identical resistance to external sulfate attack. They found that after 180 days of immersion in 5% sodium sulfate solution, bottom ash concrete containing 600 lb/yd^3 (356 kg/m^3) cement without admixture showed 0.035% expansion strain. However, bottom ash concrete containing 474 kg/m^3 cement displayed expansion almost similar to that of control concrete. Ghafoori and Bucholc (1997) observed that expansion strain of bottom ash concrete mixtures when subjected to external sulfate attack was slightly higher than that of control concrete mixture. Expansion strain of bottom ash and concrete containing 50% coal bottom ash as replacement of sand and low dosage of water reducing admixture reduced significantly but was still higher than that of control concrete. However, when cement content in concrete mixtures increased to 474 kg/m^3, expansion strain values of bottom ash mixtures were identical to that of control concrete. The improvement in quality of paste of the matrix may be the possible explanation to the increased resistance against external sulfate attack.

2.4.4 Abrasion Resistance

The abrasion resistance of concrete floors and paved surfaces is very important for their service life. Concrete pavement surfaces must be able to resist grinding from sand trapped beneath vehicle wheels. The key aspects which influence the abrasion resistance of

concrete are its compressive strength, aggregate properties and quality of surface finishes. The other factors which also affect the abrasion resistance of concrete are the hardness of the aggregate and quality of bond between aggregate and paste. Further, the bond between aggregate and paste is influenced by the shape, texture, grading and soundness of aggregate. Resistance to abrasion is also affected by the cement paste and fine aggregate of top mortar. The top mortar is highly susceptible to moisture content. Coal bottom ash particles are porous and less stiff as compared to dense and stiffer particles of natural sand. Thus the use of coal bottom ash as fine aggregate in concrete can affect the resistance to abrasion of concrete. Published research literature indicates that bottom ash concrete show lower resistance to abrasion. Due to porous microstructure of coal bottom ash, it is more venerable to moisture than river sand, as such its use as a replacement of sand in concrete results in reduction in abrasion resistance. However, the use of water reducing admixtures in bottom ash concrete improves its resistance to abrasion.

Ghafoori and Cai (1998) found that the depth of wear of bottom ash roller compacted concrete decreased with increase of cement content. Under air–dry conditions, the resistance to abrasion of roller compacted concrete containing high-calcium coal bottom ash was far superior to that under wet conditions. The depth of wear of bottom ash roller compacted concrete under wet conditions was 7.25 times that under dry conditions. This ratio dropped to 6.42 and 6.00 when cement content increased from 9 to 12% and 15%, respectively. This indicates that higher cement content produces stronger paste and smoother surface layer.

Ghafoori and Bucholc (1996) found that the bottom ash concrete containing high-calcium coal bottom ash displayed 40% lower abrasion resistance than that of control concrete. However, with the use of water reducing admixture, abrasion resistant bottom ash concrete mixtures was superior to that of control concrete. Ghafoori and Bucholc (1997) investigated the effect of high-calcium coal bottom ash on resistance to abrasion of concrete. They observed that bottom ash concrete containing 50% coal bottom ash displayed 13% higher resistance to abrasion as compared to control concrete. Bottom ash concrete mixtures incorporating 100% coal bottom ash as fine aggregate and containing 356 and 474 kg/m^3 cement content displayed 47.5 and 35.2%, respectively, higher average depth of wear than that of control concrete. Aramraks (2006) noticed that the weight loss of bottom ash concrete mixtures containing 100% fine and coarse coal bottom ash under

abrasion test were 3.29 and 3.34 times that of normal concrete. The bottom ash concrete mixture containing 50% coarse grain (passing no.4 and retaining on no. 50 standard sieves) coal bottom ash as replacement of sand and with the use of 2% super plasticizer was the most suitable concrete mixture regarding both abrasion resistance and compressive strength properties. Yuksel et al. (2007) observed that chemical and physical properties of blast furnace slag and bottom ash affects the durability properties of concrete. Resistance to abrasion increased on use of blast furnace slag and coal bottom ash as fine aggregate in concrete.

CHAPTER-3
EXPERIMENTAL PROGRAM

This chapter describes the test methods applied in this research work for characterization of materials used in manufacturing the concrete and evaluation of the effect of coal bottom ash as replacement of river sand on properties of concrete.

3.1 INTRODUCTION

Experimental program consisted laboratory tests on properties of constituent materials of concrete, casting, curing and testing of specimens to evaluate the effect of coal bottom ash as replacement of sand on properties of concrete. Experimental program is illustrated in Fig 3.1.

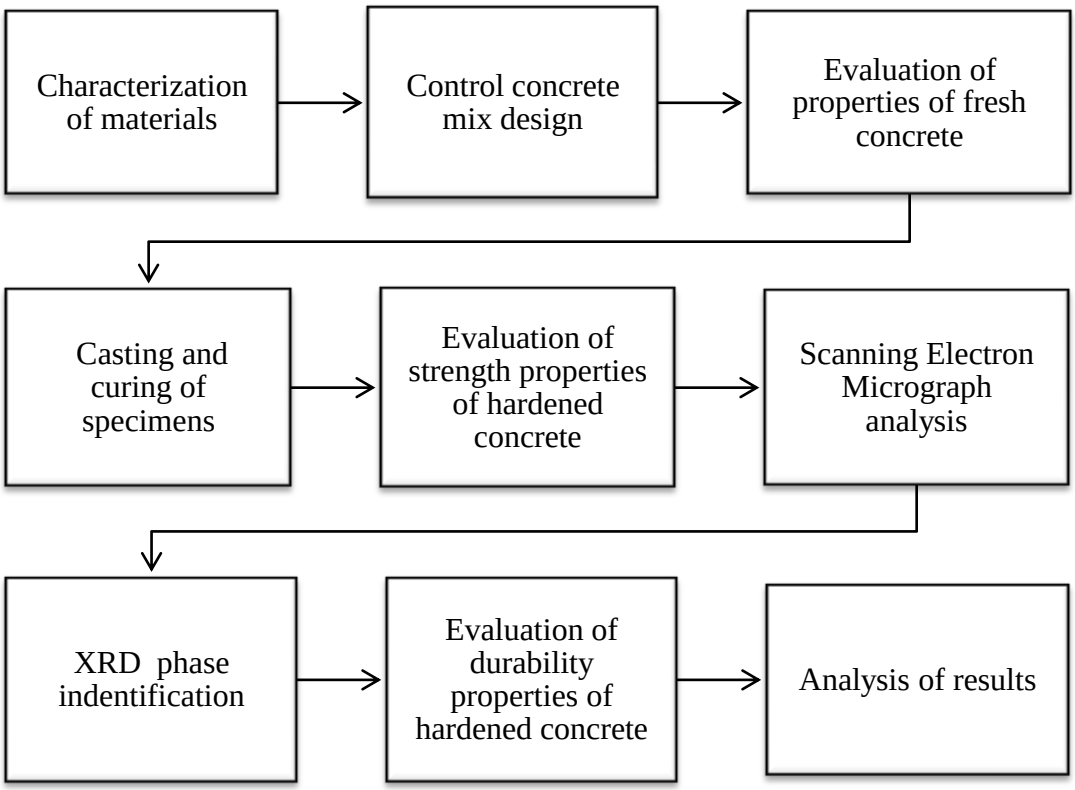

Fig. 3.1: Schematic diagram of experimental program

3.2 CHARACTERIZATION OF MATERIALS

3.2.1 Cement

Ordinary Portland cement grade 43 conforming to BIS: 8112-1989 was used in this study. Consistency, compressive strength and setting times of cement were determined as per BIS: 4031-1988.

a) Consistency

The standard consistency of a cement paste is defined as that consistency which will permit the Vicat plunger to penetrate to a point 5 to 7 mm from the bottom of the Vicat mould. Consistency of cement was determined as per procedure given in BIS: 4031 (Part-4) – 1988. Paste of 500 g cement was prepared and placed in Vicat mould. The top surface of mould was levelled and after that mould was shaken gently to expel the air. The mould along with non-porous plate was placed below the rod-bearing plunger of the Vicat apparatus. The plunger was lowered to touch the surface of paste and quickly released allowing to sink into the paste. Trial pastes with varying percentages of water were tested as described above until the amount of water necessary for making up the standard consistency was found.

b) *Setting times*

Setting times of cement was determined as per procedure given in BIS: 4031 (Part-5)-1988. Paste of neat cement was prepared by gauging the cement with 0.85 times the water required to give a paste of standard consistency. Vicat mould was filled with cement paste and top surface was levelled with the help of trowel. Vicat mould along with non-porous plate was placed below rod-bearing needle of Vicat apparatus. The needle was lowered to touch the surface of paste and then it was quickly released allowing to penetrate in to the paste. This process was repeated until the needle failed to pierce the block beyond 5.0 ± 0.5 mm measured from the bottom of the mould. The period elapsing between the time when water was added to the cement and the time at which the needle failed to pierce the test block to a point 5.0 ± 0.5 mm measured from the bottom of the mould was the initial setting time.

Then needle of the Vicat apparatus was replaced with the needle with an annular attachment. The cement was considered as finally set when, upon applying the needle gently to the surface of the paste, the needle makes an impression thereon, while the attachment fails to do so. The period elapsing between the time when water was added to the cement and the time at which the needle made an impression on the surface of test block while the attachment failed to do so was the final setting time.

c) Compressive strength

Cubes of size 69.5 mm x 69.5 mm x 69.5 mm were cast as per BIS: 4031 (Part-6)-1988 for testing for compressive strength of cement. Standard sand conforming to BIS: 650-1966

was used to make the cubes in 1:3 cement-sand mix ratios. The quantities of ingredients of cement sand mixer are given as below:

Cement = 200 g

Standard Sand = 600 g

Water = (P/4 +3.0) percent of combined mass of cement and sand,

Where,

P = the percentage of water required to produce a paste of standard consistency.

Cubes were compacted using a vibrating machine with frequency, 200 Hz, applied for two minutes. The cubes were de-moulded after 24 hr of adding water. After demoulding, the cubes were cured in a water bath at 27±1^{o}C. Compressive strength of cubes was determined at 3, 7, and 28 days of curing age. The cube specimens were loaded uniformly at 35 N/ mm^{2}/ min.

3.2.2 Fine Aggregate and Coal Bottom Ash

Two types of natural river sands from different sources in Punjab, India were used in this research work. Sand collected from Ghaghar River was conforming to zone III and Pathankot was conforming to zone II as per BIS 383-1960. Both sands and coal bottom ash were sieved through 4.75 mm sieve to remove the particles coarser than 4.75 mm before use in concrete. Particle size distribution, specific gravity and water absorption of river sand and coal bottom ash were determined as per procedure given in BIS: 2386 (Part I and II)-1963.

a) Particle size distribution

Samples of natural sand and coal bottom ash were oven dried at 100^{o}C for 24 ±1 hr and thereafter cooled down to room temperature. 500 g of each sample was mechanically sieved through set of sieves starting with 4.75 mm sieve at top, 2.36 mm, 1.18 mm, 600 µm, 300 µm, 150 µm, 90 µm and pan at bottom. The material retained on each sieve for each sample was recorded. Fineness modulus of samples was calculated by dividing the sum of cumulative percentage of mass retained on each sieve up to 150 µm sieve by 100.

b) Specific gravity and water absorption

Specific gravity of natural sand and coal bottom ash was determined using pycnometer as per procedure illustrated in BIS: 2386 Part III-1963. The 500 g of each sand and coal bottom ash was placed in tray and was covered with water. The entrapped air was removed by gentle agitation with a rod. The samples remained immersed in water for 24±1 hr.

Thereafter, water was drained from the samples by decantation through filter paper. After draining the water, the samples were allowed to dry at room temperature until no free surface moisture was seen. The saturated and surface dry samples of sand and coal bottom ash were weighed (weight A). The saturated and surface dry aggregate was placed in the pycnometer which was filled with water. Trapped air was released by rotating the pycnometer on its sides. The pycnometer was topped with water and weighed (weight B). The pycnometer was emptied and re-filled with water to the same level and then weighed (weight C). Sand and coal bottom ash samples obtained after empting the pycnometer were dried in oven at 110°C for 24±1 hr. Thereafter, the samples were cooled to room temperature and weighed (weight D). Specific gravity and water absorption were calculated as under:

$$\text{Specific gravity} = D/[A - (B - C)]$$

$$\text{Water absorption} = [100 \times (A - D)]/D$$

where

A = weight of saturated surface dry sample, g.

B = weight of pycnometer containing sample and filled with water, g.

C = weight of pycnometer filled with water, g.

D = weight of oven dried sample, g.

3.2.3 Coarse Aggregate

Crushed stone coarse aggregate was taken from quarry located near Pathankot, Punjab, India. Maximum size of coarse aggregate was 20 mm. Fineness modulus, specific gravity and water absorption of coarse aggregate were determined as per procedure laid in BIS: 2386 Part III- 1963. About 3.0 kg of coarse aggregate was submersed in water for 24 ±1 hr. Thereafter, the sample was allowed to dry at room temperature until no free surface moisture was seen. The saturated surface dry aggregate sample was weighed (weight A). Coarse aggregate was placed in basket filled with water and weighed (weight B). Coarse aggregate was removed from the basket and dried in oven at 110°C for 24±1 hr, and then weighed (weight C). Specific gravity and water absorption were calculated as follows

$$\text{Specific gravity} = C/(A - B)$$

$$\text{Water absorption} = [100 (A - C)]/ C$$

where

A = weight of saturated surface dry aggregate in air, g.

B = weight of saturated aggregate in water, g

C = weight of oven dry aggregate in air, g

3.3 MIX DESIGN

Two control concrete mixtures designated as Concrete 'A' and Concrete 'B' were designed as per guidelines given in BIS 10262-1982 to achieve 28-day compressive strength of 38.0 and 34.0 N/mm^2, respectively. Concrete 'A' was made with Ghaghar River sand conforming to grading Zone III of BIS: 383-1970 and having fineness modulus of 1.97. Concrete 'B' was made using Pathankot quarry sand conforming to grading Zone II of BIS: 383-1970 and having fineness modulus of 2.58.

Concrete A

28 day Compressive strength = 30 N/mm^2

Degree of quality control = Good

Maximum size of coarse aggregate = 20 mm

Degree of workability (Compaction Factor) = 0.9

Type of Exposure = Mild

Target 28 day compressive strength = 38.0 N/mm^2

Concrete B

28 day Compressive strength = 25 N/mm^2

Degree of quality control = Good

Maximum size of coarse aggregate = 20 mm

Degree of workability (Compaction Factor) = 0.9

Type of Exposure = Mild

Target 28 day compressive strength = 34.0 N/mm^2

Table 3.1 Mix proportions of control concrete mixtures

Mix	**Sand Conforms to grading Zone as per 383-1970**	**Water-cement ratio**	**Cement (kg/m^3)**	**Sand (kg/m^3)**	**Aggregate (kg/m^3)**	**Water (kg/m^3)**	**Superplasticizer (kg/m^3)**
Concrete A	III	0.45	479	479	1175	215.5	-
Concrete B	II	0.5	400	520	1200	200	2.0

3.4 CASTING AND CURING OF SPECIMENS

The ingredients of concrete were mixed in 0.06 m^3 capacity mixer. Weighed quantities of cement, sand and coal bottom ash were dry mixed until uniform colour was obtained without any cluster of cement, sand and coal bottom ash. Then weighed quantity of coarse aggregate was added and mixed in dry state until homogenous mixture was obtained. Measured quantity of water was added in two equal parts. Super plasticizer was mixed in second part of water added to the mixture and ingredients were mixed in the mixer. All the moulds were oiled before casting the specimens. Cube specimens of size 150 mm x 150 mm x 150 mm of each concrete mixture were cast to determine the compressive strength, splitting tensile strength, compressive strength after immersion in sulphate solution. Cylindrical specimens of size 150 mm x 300 mm were cast to measure the modulus of elasticity of concrete. Cylindrical specimens of size 100 mm x 200 mm were cast to determine the sorptivity, chloride ion penetration and water loss through air drying. Cube specimens of size 100 mm x 100 mm x 100 mm were cast to determine the resistance of concrete to external acid attack. Prism specimen of size 75 mm x 285 mm were cast to measure the length change when the specimens were exposed to air drying and immersed in sulphate solution. Concrete tile specimens of size 300 mm x 300 mm were cast to determine the resistance to abrasion. The specimens were de-moulded after 24 ±1 hr of adding water to concrete mixture. After demoulding the specimens were cured in water at room temperature. Figs. 3.2 show the casting of specimens.

Fig.3.2: Casting of concrete cubes for compressive strength

3.5 TEST PROCEDURE FOR EVALUATION OF PROPERTIES OF CONCRETE

3.5.1 Workability

Workability of concrete mixtures was measured by performing slump and compaction factor tests as per procedure given in Indian standard BIS: 1199-1959.

a) *Slump Test*

The mould was cleaned from inside and was filled in four layers with concrete. Each layer was compacted by twenty-five strokes of the rounded end of 16 mm diameter tamping rod. The strokes were distributed uniformly over the cross section of the mould. The excess mass of concrete was struck off with the help of trowel after tamping the top layer. The mould was removed from concrete immediately by raising it slowly and carefully in a vertical direction. As shown in Fig. 3.4, slump was measured immediately by determining the difference between the height of the mould and that of highest point of the specimen after subsidence of concrete.

Fig. 3.3: Experimental set up for measuring slump of fresh concrete

b) Compaction Factor Test

This test is more precise and sensitive than the slump test and is particularly useful for concrete mixtures of very low workability as are normally used when concrete is to be compacted by vibration; such concrete may consistently fail to slump. Sample of concrete was placed gently in the upper hopper. The hopper was filled with its brim and then the trap door was opened. When the concrete came to rest, cylinder was uncovered and the

trap door of the lower hopper was opened. The excess concrete remaining above the top level of cylinder was cut off by holding a trowel in each hand, with the plane of the blade horizontally and moving them, same time keeping them pressed on the top edge of cylinder. The weight of concrete in the cylinder was measured and was recorded as weight of partially compacted concrete. The cylinder was refilled in five layers and vibrated to obtain full compaction. The weight of concrete in the cylinder was then remeasured and was recorded as weight of fully compacted concrete. The compaction factor is the ratio of weight of partially compacted concrete and weight of fully compacted concrete.

3.5.2 Air Content

Air content of freshly mixed concrete was determined as per procedure specified in BIS: 1199–1959. Fig 3.6 shows the apparatus used to determine the air content in fresh concrete. Sample of fresh concrete was placed in the bowl in three layers. Each layer was fully vibrated. After cleaning the flange of bowl, the conical cover was clamped over it and water was added over the concrete with the help of tube until it rose to half way mark of stand pipe. Entrapped air above the concrete was removed by tilting the apparatus and tapping the conical cover lightly.

Fig 3.4: Experimental set up for measuring air content in fresh concrete

Water was filled up to zero mark. Then pressure (P) was applied to concrete by means of hand pump and water level was recorded ($h_{1)}$. Thereafter, applied pressure was released gradually and the bowl was tapped lightly for one min. The water level was again recorded (h_2).

Apparent air content (A1) $= h_1 – h_2$

The above process was repeated till the difference in two consecutive determination of apparent air content was within 0.2 percent. The air content of concrete was calculated as follows:

Air content $= A_1 – G$

where

G = aggregate correction factor, percentage by volume of concrete.

3.5.3 Bleeding

The quantity of mixing water that bleed from a sample of fresh concrete was measured as per procedure laid in ASTM C232–09. After mixing the ingredients of concrete, cylindrical container having internal diameter of 255±5 mm and inside height of 285 ±5 mm was filled in with freshly made concrete. The concrete in the container was vibrated after every layer. The top surface of the concrete was levelled with the help of trowel. Immediately after the trowelling the top surface of specimen, mass of concrete and container was recorded. Stop watch was set on and the container was covered to prevent the evaporation of the bleed water. The container was tilted by placing wedge under its one side and the accumulated water at the top surface of concrete was collected with the help of pipette at an interval of 10 min during first 40 min and at 30 min there after until cessation of bleeding as shown in Fig. 3.5. After the collection of bleed water, the container was brought to level position without jarring. Total volume and mass of bleeding water excluding the mass of solids was recorded. Percentage of accumulated bleeding water of net mixing water contained within the test specimen was calculated from following formula:-

C $= (w/W) \times S$

Bleeding (%) $= (D/C) \times 100$

where

C = mass of water in the test specimen, g.

W = total mass of the batch, kg.

w = net mixing water (total amount of water minus the water absorbed by the aggregate), kg.

S = mass of sample, g.

D = mass of bleeding water, g

Volume of bleeding water per unit area of surface was calculated as follows:-

$V = V_1 / A$

where

V_1 = total volume of bleeding water

A = area of exposed concrete, cm^2

Fig. 3.5: Experimental set up for collection of bleeding water from the surface of concrete

3.5.4 Water Loss through Air-Drying

Immediately after de-moulding the cylinders of size 100 mm x 200 mm, the weight of each specimen was recorded and specimens were kept in room for air drying in identical environment. The temperature and humidity in the room was controlled. The weight of each specimen was recorded at an interval of 24-±1 hr over a period of 28 days. The loss of weight of specimen represented the weight of water loss through air-drying during that period. Average weight loss of three specimens per concrete mixture was considered as the water loss through air drying of concrete mixture.

3.5.5 One-day Unit Weight

Weight of concrete cubes was recorded immediately after de-moulding. The average of weight of 15 no. concrete cubes divided by the volume of cube was termed as one-day unit weight of concrete specimen.

3.5.6 Permeable Pore Space and Water Absorption

Permeable pore space, water absorption, and dry density of concrete were determined as per ASTM C 642–97. Three specimens were tested for permeable pore space, water absorption, and dry density of the mix. After initial curing, the concrete specimens were oven dried at a temperature of 110^{o}C for a period of 24 hr. Thereafter, the specimen was cooled down to room temperature and weighed. The process was repeated until the difference in consecutive readings of weight of specimen taken at interval of 24 hr was less than 0.5 percent. Then the specimen was immersed in water for period of 24 hr. Weight of specimen was recorded. Specimen was again immersed in water until the difference in consecutive readings of weight of specimen taken at interval of 24 hr was less than 0.5 percent. Thereafter the specimen was placed in boiling water for 5 hr. The specimen was cooled down to room temperature and weighed. Weight of specimen in water was also recorded. Bulk dry density, water absorption and permeable pore space were calculated as follows:

Dry bulk density	$= [A/(C - D)] \times \rho$	$= g_1$
Apparent density	$= [A/(A - D)] \times \rho$	$= g_2$
Water absorption, (%)	$= [(B - A)/A] \times 100$	
Permeable pore space,(%)	$= (g_2 - g_1)/g_2 \times 100$	

where

A	=	mass of oven dried sample in air, g
B	=	mass of saturated surface dry sample in air, g
C	=	mass of saturated surface dry sample after boiling in air, g
D	=	mass of saturated sample in water, g
ρ	=	density of water = 1 g/cm^3

3.5.7 Sorptivity

Water Sorptivity of concrete specimens was measured as per procedure specified in ASTM C 1585–04. Three specimens per concrete mixture were tested for water sorptivity. This

test was performed to determine the susceptibility of an unsaturated concrete specimen to the penetration of water. Concrete specimens were oven dried at a temperature of 50 ± 2^{o}C for 3 days. After the 3 days, the specimen was placed in sealable container for 15 days. After 15 days, weight of specimen was recorded to nearest of 0.01 g and sides were sealed. Average diameter of specimen was also recorded and top surface was also sealed. Then the mass of sealed specimen was measured and recorded as initial mass. As shown in Fig.3.7, the specimens were placed in water and stop watch was started. The mass of specimen was recorded at interval 1 min, 5 min, 10 min, 20 min, 30 min, 1 hr, 2 hr, 3 hr, 4 hr, 5 hr, 6 hr, 1 day, 2 days, 3 days, 5 days, 6 days, 7 days, and 8 days.

Fig. 3.6: Experimental set up for measuring sorptivity of concrete

The absorption was calculated as follows:

$$I = m_t / [a/d]$$

where

I = the absorption

m_t = the average increase in specimen mass in g, at time t

a = the exposed area of the specimen, in mm^2

d = the density of the water in g/mm^3

3.5.8 Compressive Strength

Compressive strength of concrete specimens was measured as per BIS: 516-1959. Immediately after removing the cubes from the water at the specified curing age, surface water and grit was wiped off and the cube was placed in compression testing machine of 3000 KN capacity as shown in Fig 3.8. The cube was placed in machine in such a manner that load was applied to opposite sides of the cube as cast. The load was applied without shock and increased continuously at the rate of 4.5 kN/sec until the resistance of the cube to the increasing load breaks down and no greater load can be sustained. The maximum load applied to the cube was recorded.

Fig. 3.7: Compression testing machine (Capacity 3000 kN)

Three cubes were tested for each test. Compressive strength of specimen was calculated by dividing the maximum load applied during the test by the cross- sectional area of the cube. Average of three values was recorded as the compressive strength of the concrete mixture.

$$f_{ck} = P/A$$

where:

P = maximum load applied, kN

A = surface area of cube of size 150 mm x 150 mm x 150 mm

3.5.9 Splitting Tensile Strength

Splitting tensile strength of concrete specimens was determined as per procedure given in BIS: 5816-1999. In this study, cube specimens were used to determine the splitting tensile strength of concrete mixtures. As shown in Fig. 3.9, cube specimen was placed in Universal Testing Machine of 1000 kN capacity and load was applied without shock and increased continuously at a rate of 1.2 N/mm^2 to 2.4 N/mm^2 until the failure. The maximum load applied was recorded for each specimen. Average value of three specimens was considered as the splitting tensile strength of concrete mix. Splitting tensile strength was calculated as under:

$$f_{ct} = 0.5187 \times P / S^2$$

where

P = maximum load applied, kN

S = side of cube, mm

Fig. 3.8: Experimental set up for measuring Splitting tensile strength of concrete

3.5.10 Modulus of Elasticity

Modulus of elasticity of concrete specimens was determined as per procedure given in BIS: 516-1959. Immediately after removing the specimen from water, surface was wiped

with cloth and to record the stains, LVDT was fixed on the cylindrical specimen. Then specimen was placed in the testing machine as shown in Fig. 3.10. The cylinder specimens were loaded continuously at a rate of 14.0 N/mm^2/min until an average stress of (C+0.5) N/mm^2 was achieved, where C is one-third of the average compressive strength of cube. The load was maintained for one minute and was reduced gradually. The load was applied second time at the same rate until an average stress of (C+ 0.15) N/mm^2 was reached. The loading cycle was repeated until the difference in strain between two consecutive readings at (C+0.15) N/mm^2 does not exceeded 5 percent. The strains at the various loads in the last two cycles were plotted graphically against the stress. The straight line was drawn through the points and slope of straight line was determined. The average value of slope of straight lines of three specimens was recorded as modulus of elasticity of concrete.

Fig. 3.9: Experimental set up for measuring modulus of elasticity of concrete

3.5.11 Pulse Velocity

The test involves determination of pulse velocity through concrete as per procedure give in ASTM C 597-02. Battery operated Portable Ultrasonic Non-destructive Digital Indicating Tester was used to measure the pulse velocity through concrete. Pulses of longitudinal stress waves are generated by an electro acoustical transducer held in contact with one face

of concrete and are received by another transducer held in contact with other face of concrete specimen. The time (T) taken by pulse to pass through specimen of length (L) is known as transit time. The pulse velocity (V) is calculated by dividing the length of specimen (L) by transit time (T). Average value of three specimens was considered as the pulse velocity of concrete mix. The apparatus set for the test is shown in Fig 3.11 and values of pulse velocity for grading concrete as per BIS 13311-92 (Part-I) are given in Table 3.2.

Table 3.2 Concrete quality grading as per BIS 13311-92 (Part-I)

Pulse velocity (m/s)	**Concrete quality grading**
Above 4500	Excellent
3500 - 4500	Good
3000 - 3500	Medium
Less than 3000	Doubtful

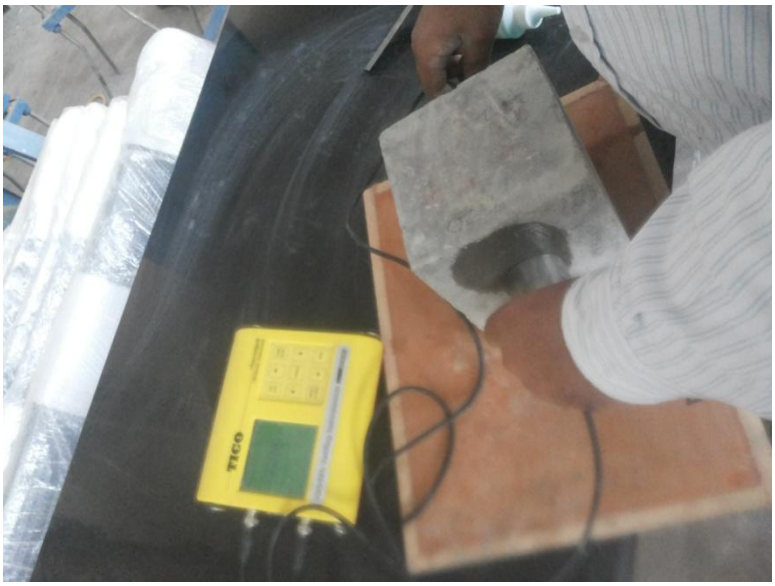

Fig. 3.10: Experimental set up for measuring pulse velocity through concrete

3.5.12 Drying Shrinkage

Loss of water from the hardened concrete causes drying shrinkage. Drying shrinkage of hardened concrete was measured as per ASTM C 157-03. Three specimens were used for this test. The length of prism was recorded as initial comparator reading after initial water curing period of 28 days and specimens were stored in the drying room. The comparator

readings were taken after period of air storage after curing of 4, 7, 14 and 28 days and after 8, 16, and 32 weeks as shown in Fig 3.12. The length change at any age after initial reading was calculated as follows

$$\Delta L_x = \frac{\text{CRD} - \text{Initial CRD}}{G} \times 100$$

where

ΔL_x = length change of specimen at any age, (%)

CRD = difference between the comparator reading of the specimen and reference bar at any age

G = the gauge length (250 mm)

Fig. 3.11: Experimental set up for measuring length change

3.5.13 Sulfate Resistance

Sulphate attack can take the form of expansion, loss in compressive strength and loss in mass of concrete. As such change in length, loss in compressive strength and loss in mass of concrete specimens after exposure to sulfate environment have been observed in the

study. The length change of concrete prism specimens immersed in sulphate solution was determined as per ASTM C 1012-10. Figs. 3.13 and 3.14 show the deterioration of specimens after 365 days of immersion in sulfate solution. After initial water curing period of 28 days, the length of prism specimens were recorded as initial reading and the specimens were immersed in 10% solution of magnesium sulphate. The comparator readings were taken after immersion in sulphate solution after curing of 1, 2, 3, 4, 8, 9,13 and 15 weeks and after 4, 6, 9 and 12 months. Three specimens were tested for each test. The length change at any age after initial reading was calculated as follows:

$$\Delta L_x = \frac{L_x - L_i}{L_g} \times 100$$

where

ΔL_x = length change of specimen at x age, (%)

L_x = the comparator reading of the specimen at x age

Li = the initial comparator reading of the specimen

L_g = the gauge length (250 mm)

Fig. 3.12: Control concrete specimens after 365 days period of immersion in 10% magnesium sulfate solution (Concrete 'A')

The compressive strength of cube specimens after immersion in 10% magnesium sulfate solution was measured at 28, 90, 180 and 365 days. The change in compressive strength of concrete specimens during immersion for each test period was calculated as per formula give below:

Change in compressive strength (%) = $[(S_2 - S_1)/S_1] \times 100$

where

S_1 = 28-day average compressive strength of concrete specimen

S_2 = Average compressive strength of concrete specimen after immersion in magnesium sulfate solution at the age of test.

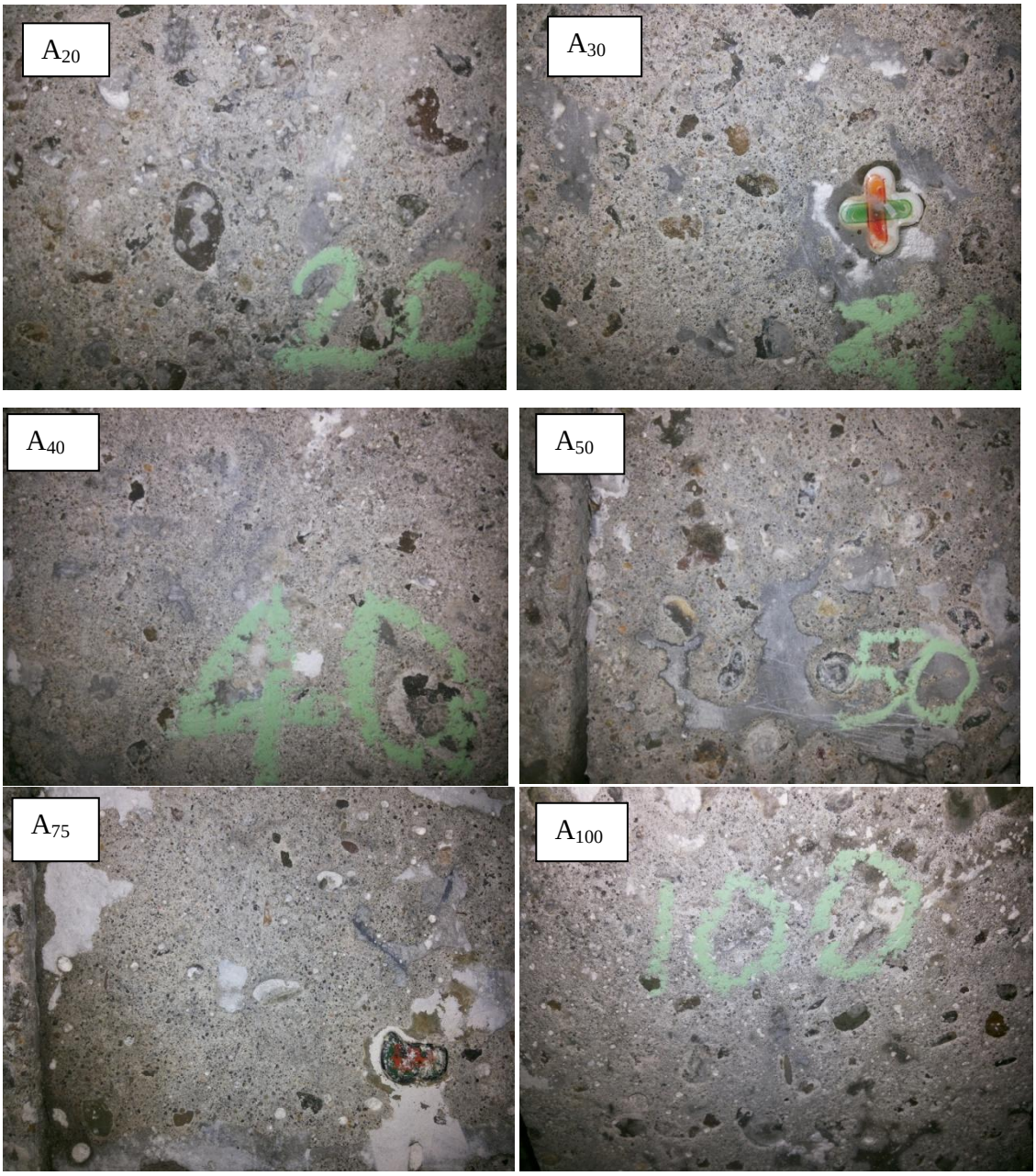

Fig. 3.13: Bottom ash concrete specimens after 365 days period of immersion in 10% magnesium sulfate solution (Concrete 'A')

3.5.14 Acid Resistance

Resistance of concrete specimens against external acid attack was evaluated as per ASTM C 267-01. The specimens were indentified using plastic numbers fixed with the help of adhesive. Each specimen of concrete was weighed on completion of initial water curing period of 28 days. Then the specimens were immersed in 3% sulphuric acid solution. During this test the changes in the following properties of specimens were determined after 7, 28, 56 and 84 days of immersion the specimens in 3% sulphuric acid solution. The Figs. 3.15 and 3.16 show the deterioration of specimens after 7 and 84 days of immersion in sulphuric acid solution respectively.

- Weight of specimen
- Appearance of specimen
- Compressive strength of specimen

The change in compressive strength of concrete specimens during immersion for each test period was calculated as per formula give below:-

$$\text{Change in compressive strength (\%)} = [(S_2 - S_1)/S_1] \times 100$$

where

S_1 = 28-day average compressive strength of concrete specimen

S_2 = Average compressive strength of concrete specimen after immersion in acid solution at the age of test.

Fig. 3.14: Deterioration of specimens after 7 days of immersion in 3% sulphuric acid solution (Concrete 'B')

The change in weight of concrete specimens during immersion for each test period was calculated as per formula give below:-

Weight change (%) = [(W – C)/C] x 100

where

C = Weight of specimen before immersion in acid solution

W = Weight of specimen after immersion in acid solution at the age of test.

Three specimens per mix were tested to study the effect of coal bottom ash on compressive strength and weight loss of concrete under external acid attack.

Fig. 3.15: Deterioration of specimens after 84 days of immersion in 3% sulphuric acid solution

3.5.15 Abrasion Resistance

Resistance to abrasion of concrete was measured as per procedure given in BIS: 1237-2012. The test specimens were oven dried at 110±5^{o}C for 24 hr and then weighed to the nearest 0.1 g. Thickness at four corners and at centre of dried specimens was measured. Fig. 3.17 shows the apparatus for measuring depth of wear of concrete specimens against abrasion. The Specimen was fixed in the holding device with surface to be ground facing the disc and was loaded at the centre with 300 N. Abrasive powder was spread evenly on the grinding disc during the test. Thickness and weight of specimens were measured after 1.5 min interval and specimen was turned about the vertical axis through an angle of 90^{o} in clockwise direction. At the end of test, thickness and weight of specimens were taken. The extent of wear was determined from the difference in thickness of specimen before and after the abrasion test.

These values were checked with the average loss in thickness from following formula:-

$$t = \frac{(W_1 - W_2)\, V_1}{W_1 \times A}$$

where

t	=	average loss in thickness in mm
W_1	=	initial mass of the specimen in g
W_2	=	final mass of the abraded specimen in g
V_1	=	initial volume of the specimen in mm^3
A	=	surface area of the specimen in mm^2

Fig. 3.16: Experimental set up for measuring abrasion resistance of concrete

Abrasion resistance of control as well as bottom ash concrete mixtures was measured at 28, 90, 180 and 365 days curing age. Average wear depth of three specimens were considered as wear depth of concrete mix.

3.5.16 Chloride Permeability

The rapid chloride penetration test was performed as per procedure given in ASTM C 1202-10. Total electrical charge in coulombs passed through 50 mm thick and 100 mm diameter size during 6 hr was measured in this test. A potential difference of 60 V DC was maintained across the ends of specimen. One end of the specimen was immersed in sodium chloride solution and the other end was immersed in sodium hydroxide solution. Average of total charge in coulombs passed through the three specimens was related to its resistant

to chloride ion penetration. The resistance to chloride ion penetration of concrete was rated as negligible, very low, low, medium and high as per Table 3.3. Prooveit data processor used in this study for measuring the chloride ion penetration is shown in Fig. 3.18. Fig 3.19 shows the display of charge passed through concrete during the test.

Fig. 3.17: Experimental set up for measuring chloride ion penetration

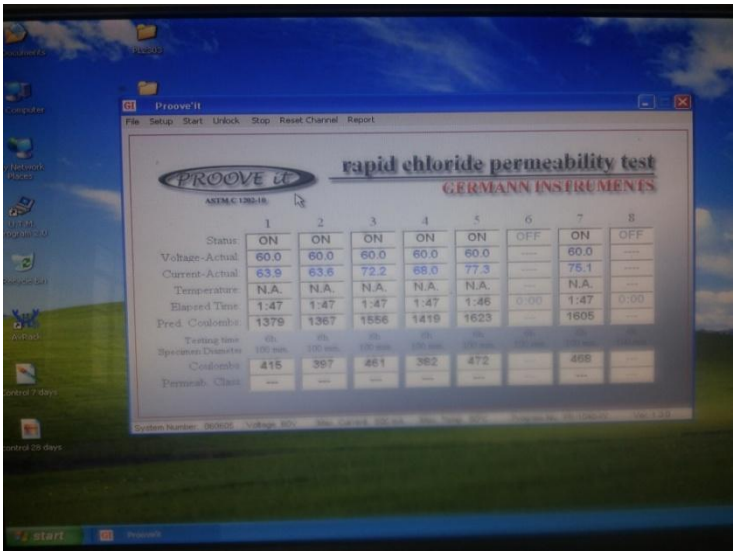

Fig. 3.18: Display of charge passed during the test

Table 3.3 Chloride ion penetration based on charge passed

Charge passed (coulombs)	Chloride ion penetration
>4000	High
2000 - 4000	Moderate
1000 - 2000	Low
100 - 1000	Very low
<100	Negligible

3.5.17 Scanning Electron Microscopy (SEM)

The microstructure of concrete consists of hydrated cement paste, aggregate and interfacial transitional zone. The scanning electron microscopy (SEM) plays a significant role in resolving the microstructure of concrete. Scanning electron microscopy provides both topographic and compositional analysis of materials. The application of scanning electron microscopy enhances the ability to characterize the concrete microstructure and helps in ascertaining the factors affecting the mechanical properties and durability of concrete. The concrete microstructure is integrated system consisting of CSH gel, calcium hydroxide, calcium sulfoaluminate hydrate (ettringite and monosulfate), coarse and fine aggregate and interfacial transition zone between aggregate and cement hydration products. Morphology structure of CSH varies from common fibrous type to irregular grains forming a reticular network. At the early age of cement hydration, prominent morphology structure of CSH is fibrous type but reticular network also occurs occasionally. Equant grain morphology of CSH appears as the hydration of cement proceeds. Another type of morphology of CSH has a dimpled appearance with either regular pores or closely packed equant grains. The calcium hydroxide appears in many shapes such as massive, platy crystals, large thin elongated crystals and blocky masses to finely disseminated crystals. Calcium sulfoaluminate hydrates have two morphologies that are ettringites and monosulfate. Ettringites appears as needle like crystals with no branching, whereas monosulfate appears as hexagonal platy crystals.

The fractured pieces of bottom ash concrete generated from compressive strength test were used for observing the scanning electron micrographs. In this study, fractured pieces of concrete were mounted on the SEM stub and images were obtained using secondary electron (SE) image mode. Scanning electron micrographs of concrete specimens were taken at the curing age of 28 and 90 days. The concrete specimens were coated with thin

layer of gold to make them electrically conductive before placing on the scanning electron microscopy (SEM) stem. The SEM images of concrete specimens were taken in the secondary electron (SE) mode. Secondary electrons are the low energy resulting from an inelastic collision of primary beam electron with an electron of a specimen atom. Secondary electron produced near the surface escape and result in image of surface topography. The experimental set up for scanning electron microscope is shown in Fig.3.20. Energy dispersive spectroscopy was used to perform the chemical analysis of concrete specimens.

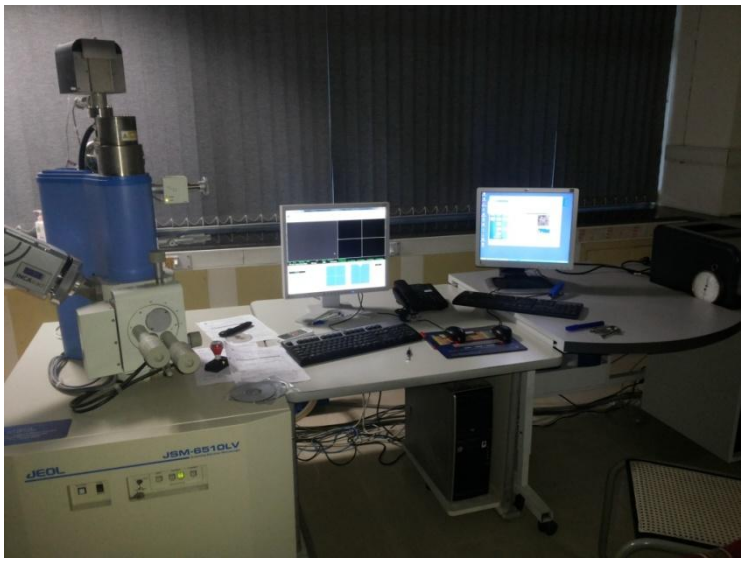

Fig. 3.19: Experimental set up for Scanning Electron Micrograph

3.5.18 X-Ray Diffraction (XRD) Analysis

XRD is a useful technique for identification of crystalline phases such as calcium hydroxide, ettringites, and calcium silicate hydrates etc. present in the concrete. The microstructure of the interfacial transitional zone of concrete differs from that of bulk cement paste. The amorphous phases of concrete result in weak peaks. In addition, the peaks of aggregate minerals interfere in XRD analysis of concrete. The weak diffraction peaks of poorly crystalline calcium silicate hydrate phase of concrete and interference of diffraction peaks of minerals present in aggregate make the identification of hydration phases present in concrete more complicated. The weak diffraction peaks of calcium silicate hydrate tend to be swamped by the diffraction peaks from calcium hydroxide. Every crystalline phase has its own diffraction image. The diffractogram is made up of succession of diffraction maximum points in which intensity of the diffracted radiation is plotted on ordinate and angle 2θ on abscissa. The X-ray diffraction technique was used for

identification of various phases present in the hardened bottom ash concrete as well as control concrete at the age of 28 and 90 days. The cement pastes were separated from the concrete samples and were sieved through 90 μm sieve. The XRD investigations were performed for diffraction angle 2θ ranged between 5° and 80° in steps of 2θ = 0.017°. The diffraction pattern, list of d-spacing and relative intensities of diffraction peaks was prepared. This data was compared with the standard peaks of compounds in the diffraction database released by International Centre for Diffraction Data (ICDD). Fig 3.21 shows the X-Ray diffraction (XRD) instrument.

Fig. 3.20: X-Ray diffraction (XRD) instrument

4.1 INTRODUCTION

This chapter presents the test results of characterization of materials and properties of fresh concrete, strength and durability properties of hardened concrete mixtures incorporating coal bottom ash as partial or total replacement of river. Micro-structural analysis of scanning electron micrographs and phase identification prepared using X-Ray diffractogram are discussed in this chapter. A comparative study of properties of fresh concretes, strength and durability properties of hardened concretes made with low-calcium coal bottom ash as partial replacement of sands having varying fineness modulus is also presented in this chapter.

4.2 CHARACTERIZATION OF MATERIALS

4.2.1 Cement

The test results of properties of cement are given in Table 4.1. The ordinary Portland cement used in this study fulfilled the requirements of BIS: 8112-1989.

Table 4.1 Chemical and Physical properties of cement.

Chemical composition			**Physical properties**		
Composition	**Test result**	**BIS value**	**Property**	**Test result**	**BIS value**
Lime saturation factor (lsf)	0.877	0.66< lsf<1.02	Fineness (m^2/kg)	278.6	> 225
Ratio of Alumina and Iron oxide	1.51	> 0.66	Initial setting time (min)	125	> 30
Loss on Ignition (%)	1.93	< 5.0	Final setting time (min)	175	< 600
Total sulphur content (SO_3) (%)	2.10	< 2.5	Compressive strength (N/mm^2)		
Magnesia (%)	0.97	< 6.0	3 days	32.0	> 23
Insoluble residue (%)	1.85	< 2.0	7 days	40.3	> 33
Alkalies (K_2O) (%)	0.4	< 0.6	28 days	51.5	> 43
Na_2O (%)	0.10		Consistency (%)	28	
Total chloride content (%)	0.020	< 0.05			

4.2.2 Coal Bottom Ash

Coal bottom ash was collected from Guru Hargobind Thermal Power Plant Bathinda, Punjab, India. The chemical composition and physical properties of coal bottom ash are presented in Tables 4.2 and 4.3 respectively. The chemical analysis of coal bottom ash was performed using energy dispersive spectrometer (EDS). Two samples from two different laboratories were got tested. The chemical analysis shows that coal bottom ash is mainly composed of silica, alumina and iron with small amounts of calcium, magnesium, sulfate etc. Total composition of silicon dioxide (SiO_2), aluminum oxide (Al_2O_3) and iron oxide (Fe_2O_3) present altogether in the coal bottom ash varied from 94.21% to 91.57% and as such coal bottom ash used in this study conformed to ASTM C 618-03 Class F ash. The loss of ignition of coal bottom ash was less than 1%. The specific gravity of coal bottom ash was measured by pycnometer method and was 1.39. X-Ray diffractogram and EDS spectra of coal bottom ash are shown in Figs. 4.1 and 4.2, respectively. The X-Ray diffractogram shows that quartz, tridymite, mullite, anorthite and hematite are the major phases present in coal bottom ash. As shown in Fig. 4.3, the particles of coal bottom ash are porous, angular and irregular in shape and have rough texture. Some spherical shaped and pop corn type particles are also present in coal bottom ash. Particle size distribution curve of coal bottom ash is presented in Fig.4.4. Coal bottom ash contains 17.3% particles finer than 90 µm as compared to 4.0% in Ghaghar sand and 3% in Pathankot quarry sand.

Table 4.2 Chemical composition of coal bottom ash

Compound	**Composition (%)**		
	Sample 1	**Sample 2**	**ASTM C 618-03 requirement (%)**
Silicon dioxide (SiO_2)	56.44	60.33	-
Aluminum oxide (Al_2O_3)	29.24	19.46	-
Iron oxide (Fe_2O_3)	8.44	11.78	-
SiO_2+ Al_2O_3+ Fe_2O_3	94.12	91.57	70 min
Potassium oxide (K_2O)	1.24	0.88	-
Calcium oxide (CaO)	0.75	0.62	-
Magnesium oxide (MgO)	0.40	0.26	5.0 max
Sulfur trioxide (SO_3)	0.24	0.24	5.0 max
Sodium oxide (Na_2O)	0.09	0.40	1.5 max
Loss on ignition (%)	0.89	1.0	6.0 max

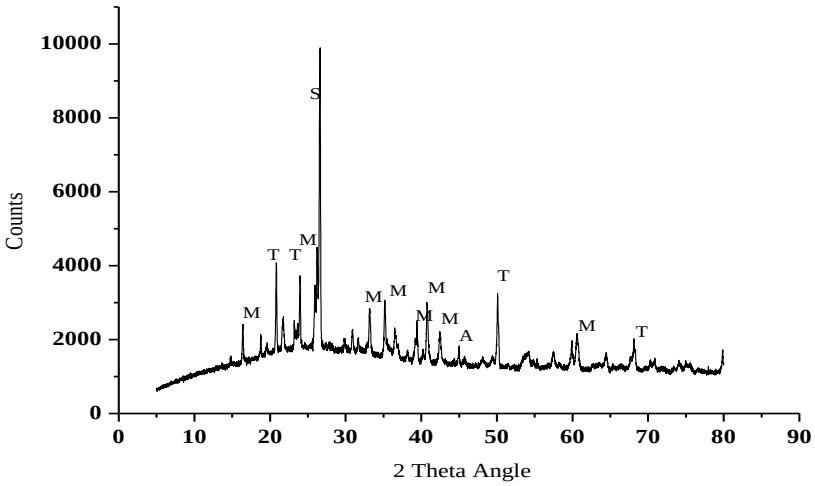

Fig. 4.1: X- Ray diffractogram of coal bottom ash (M = Mullite; T = Tridymite; S = α-SiO_2; A = Anorthite)

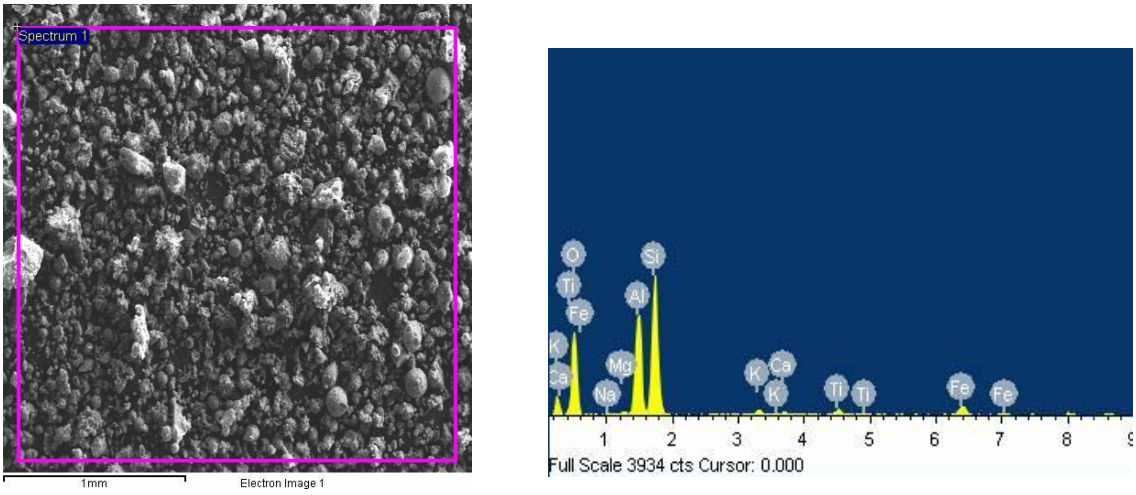

(a) (b)

Fig. 4.2: Scanning electron micrograph (SEM) and energy dispersive spectrometer (EDS) Spectra of coal bottom ash (a) SEM image (b) EDS Spectra

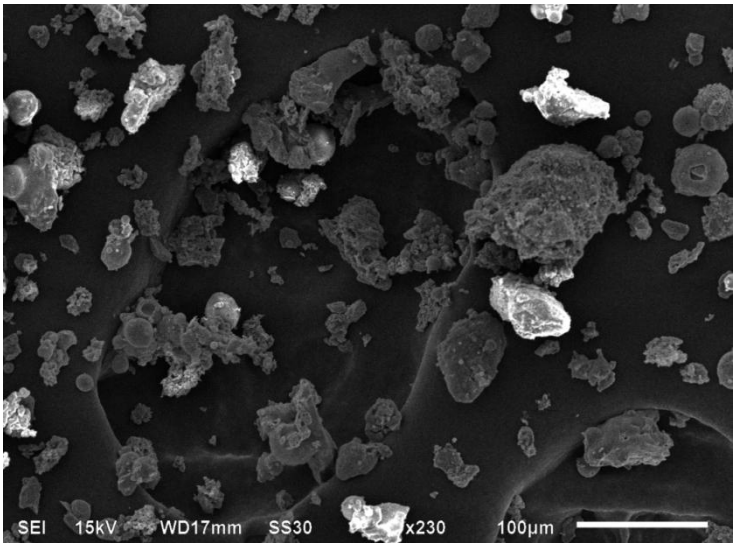

Fig. 4.3: Scanning electron micrograph of coal bottom ash

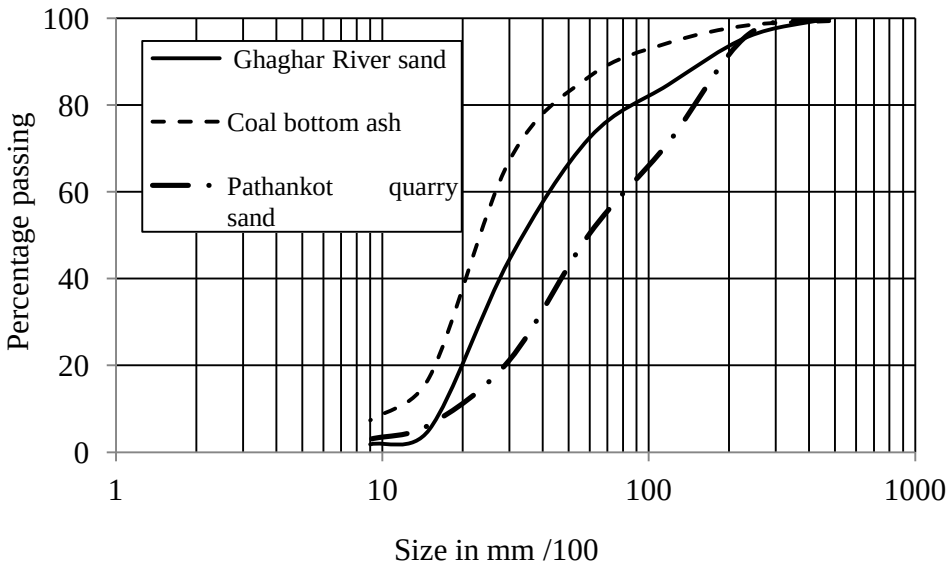

Fig. 4.4: Particle size distribution curve of coal bottom ash, Ghaghar sand and Pathankot quarry sand

4.2.3 River Sand and Coarse Aggregate

The physical properties of River sand and coarse aggregate are presented in Table 4.3. Scanning electron micrograph of Pathankot quarry sand and Ghaghar River sand are given in Figs. 4.5 and 4.6, respectively. Particle size distribution curves of both sands are shown in Fig.4.4

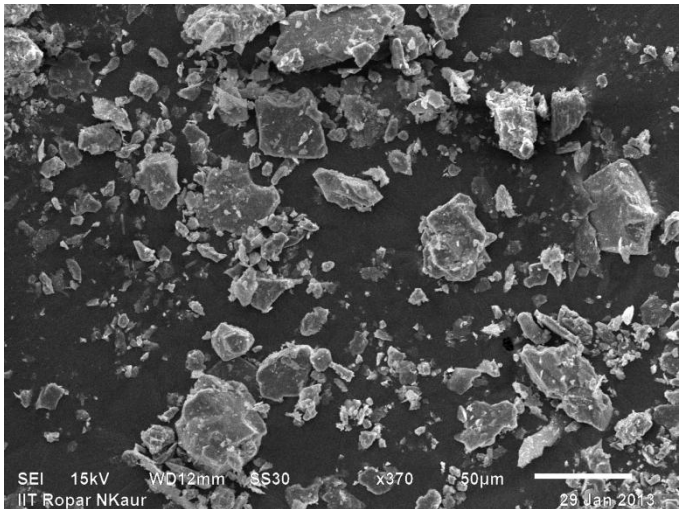

Fig. 4.5: Scanning electron micrograph of Pathankot quarry sand

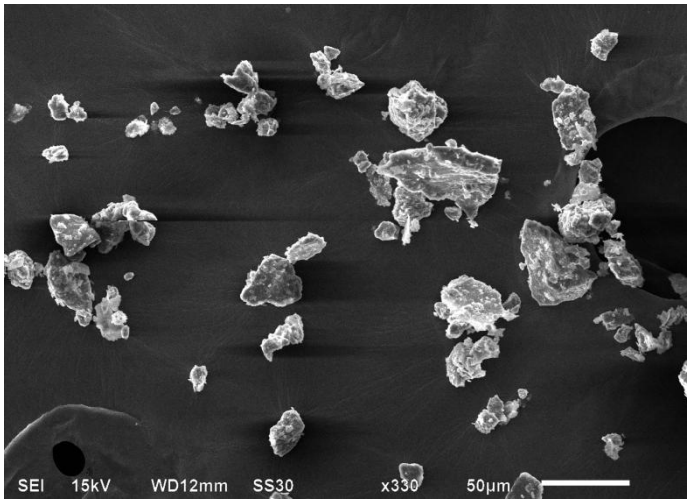

Fig. 4.6: Scanning electron micrograph of Ghaghar river sand

Table 4.3 Physical properties of sand, coal bottom ash and coarse aggregate

Property	**Ghaghar river sand**	**Pathankot quarry sand**	**Coal bottom ash**	**Coarse aggregate**
Specific gravity	2.60	2.59	1.39	2.68
Water absorption by mass (%)	2.46	2.06	31.58	0.38
Fineness modulus	1.97	2.76	1.37	6.28

Crushed stone aggregate was used in this study and was collected from Pathankot quarry. Specific gravity and water absorption of coarse aggregate were 2.68 and 0.38% respectively. The maximum size of coarse aggregate was 20 mm. The fineness modulus of coarse aggregate was 6.28.

4.3 PROPERTIES OF CONCRETE MADE WITH SAND HAVING FINENESS MODULUS OF 1.97 (*Concrete 'A'*)

4.3.1 Mix Proportions

The control concrete mixture was designed as per BIS: 10262-1982 to achieve strength of 38.0 N/mm^2 at 28 days curing age. The Ghaghar river sand used in control concrete was conforming to grading zone III specified in BIS: 383-1960. The designed concrete mix was designated as concrete 'A'. Both river sand and coal bottom ash were oven dried at 100^{o}C for 24 ±1 hr to remove moisture and then cooled downed to room temperature for another 24 ±1 hr before use in manufacturing of concrete mixtures. Coal bottom ash was collected in wet-state from thermal power plant and was oven dried to prevent outflow of water absorbed in it. Coal bottom ash has lesser water retention capacity. Moreover it is difficult to measure actual absorption of water by coal bottom ash during the mixing process. As such, no adjustment in unit water content to account for likely water absorption was made and a fixed quantity of water was added in all concrete mixtures. The river sand was replaced with coal bottom ash in concrete by mass at 20, 30, 40, 50, 75 and 100% levels. The detail of mix proportions of concrete 'A' are given in Table 4.4.

Table 4.4 Mix proportions of concrete (concrete 'A')

Mix	**Cement (kg/m^3)**	**w/c ratio**	**Sand (kg/m^3)**	**Sand replacement level (%)**	**Coal bottom ash (kg/m^3)**	**Coarse aggregate (kg/m^3)**	**Water (kg/m^3)**
Control concrete	479	0.45	479	0	0	1175	215.55
A_{20}	479	0.45	383.2	20	51.22	1175	215.55
A_{30}	479	0.45	334.6	30	76.82	1175	215.55
A_{40}	479	0.45	287.4	40	102.43	1175	215.55
A_{50}	479	0.45	239.5	50	128.04	1175	215.55
A_{75}	479	0.45	119.75	75	192.06	1175	215.55
A_{100}	479	0.45	0	100	256.08	1175	215.55

4.3.2 Properties of Fresh Concrete

4.3.2.1 Workability

Workability is that property of freshly mixed concrete, which determines the ease and homogeneity with which it can be mixed, placed, compacted, and finished. It is the amount of energy to overcome friction and cause full consolidation. Ease is related to rheology of fresh concrete, which includes performance parameters of stability, mobility and compactability. These parameters are predominantly dependent on consistency of the fresh concrete mixture. Thus, workability of fresh concrete is the complex system of two critical parameters, consistency and homogeneity. The usual measurement of consistency of concrete is slump. Homogeneity does not have standardized test method for its measurement. The workability of concrete mixtures was measured by performing slump test and compaction test.

Slump test

The test results are presented in Fig. 4.7. The test results show that at fixed water-cement ratio, slump values of bottom ash concrete mixtures decreased with the increase in coal bottom ash content in concrete mixture. Slump test results are in line with compaction factor test results. As shown in Table 4.3, the water absorption of coal bottom ash is higher than that of river sand. The porous and pop corn type particles of coal bottom ash absorbed more water rapidly during the mixing process than the solid particles of natural river sand. Thus the availability of free water for lubrication of particles reduced. The substitution of river sand with coal bottom ash also resulted in increase in specific surface area of fine aggregate in concrete. The rough texture and angular shape of coal bottom ash particles also played significant role in increasing the inter particle friction. All these factors contributed towards lowering the slump values. Therefore, it can be concluded that the decrease in workability of concrete on use of coal bottom ash is the result of increased specific surface area, increase in internal friction and rate of absorption of water internally by the dry and porous particles of coal bottom ash. The slump values decreased from 70 mm to 10 mm on incorporation of 100% coal bottom ash as substitute of sand in concrete. Ghafoori and Bucholc (1996, 1997), Aramraks (2006), Andrade et al. (2009) and Chun et al. (2008) also observed reduction in slump on use of coal bottom ash as substitute of sand in concrete. Kou and Poon (2009) observed that the slump values increased with increase in quantity of saturated surface dry coal bottom ash in the concrete mixtures. The water

absorption of coal bottom ash used in their study was 28.9%. However, Bai et al. (2005) reported increase in slump values on use of coal bottom ash in concrete at fixed water-cement ratio. Bai et al. (2005) believed that the ball bearing effect of spherical particles of coal bottom ash increased the slump of bottom ash concrete mixtures. Moreover, coal bottom ash used in their research work contained particles more than 40% finer than 150 µm and spherical in shape.

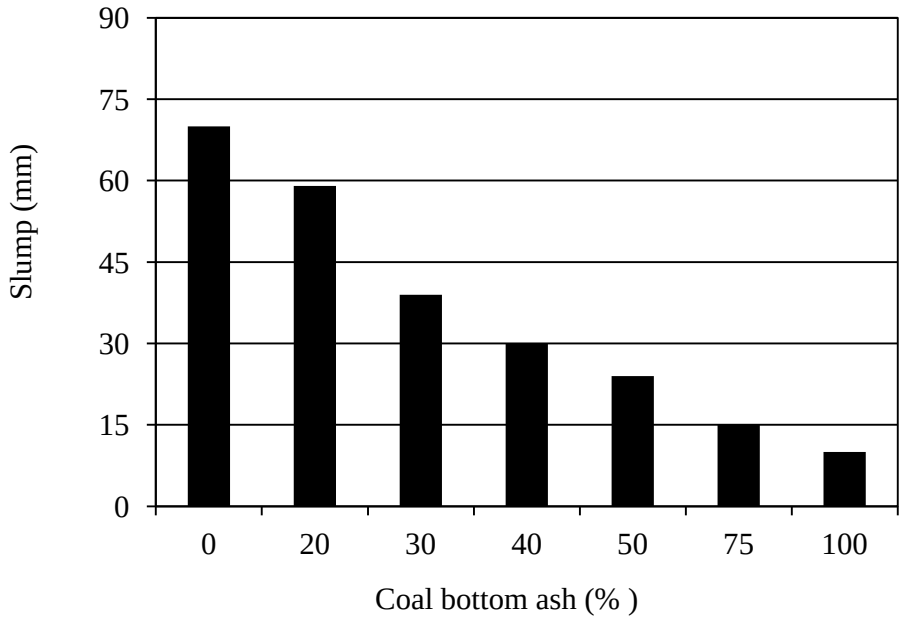

Fig. 4.7: Effect of coal bottom ash on slump values of concrete (Concrete 'A')

Whereas coal bottom ash used in the present study contains 17.2% particles finer than 150 µm and also the particles are angular shaped, rough textured and porous.

Compaction Factor

The compaction factor test results are presented in Fig. 4.8. The compaction factor values decreased almost linearly with the increase in coal bottom ash content in concrete. Higher value of coefficient of determination (R^2 = 0.9313) indicates good relevance between the curve and data points. The compaction factor decreased from 0.87 to 0.72 on incorporation of 100% coal bottom ash as fine aggregate in concrete. The compaction factor test results of bottom ash concrete mixtures confirm the slump test results. The results of present study are in good agreement with those reported by Aggarwal et al. (2009) for pond ash. They reported decrease in compaction factor from 0.90 to 0.82 on incorporation of 50% pond ash as fine aggregate in production of concrete.

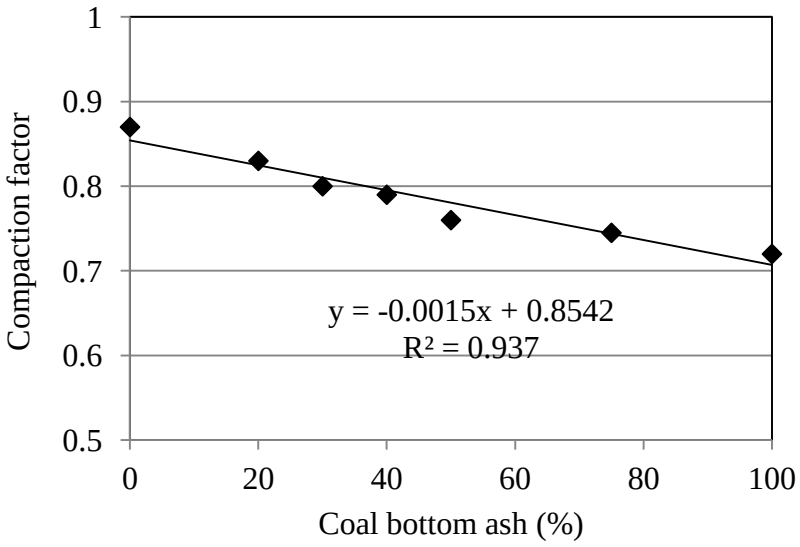

Fig. 4.8: Effect of coal bottom ash on compaction factor values of concrete (Concrete 'A')

4.3.2.2 Air Content

The air content test results are presented in Fig 4.9. The air content in bottom ash concrete mixtures varied between 2.45 and 3.55% as compared to 2.45% in control concrete.

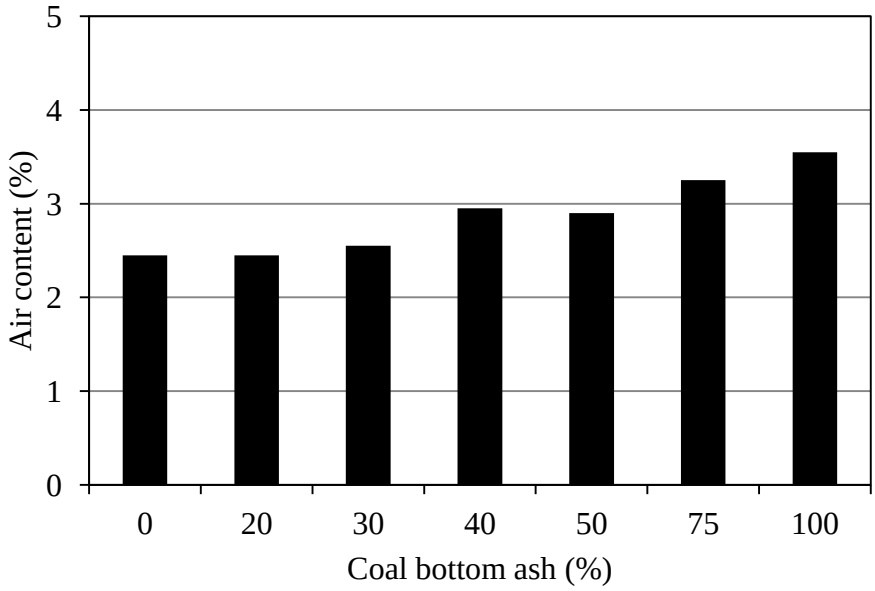

Fig. 4.9: Effect of coal bottom ash on entrapped air content in fresh concrete (Concrete 'A')

Bottom ash mixture containing 100% coal bottom ash as substitute of sand showed highest entrapped air content of 3.55%. The entrapped air content in bottom ash concrete mixtures containing up to 30% coal bottom ash as substitute of sand did not changed significantly.

More than 30% substitution of sand with coal bottom ash resulted in significant increase in entrapped air content in bottom ash concrete mixtures.

4.3.2.3 Bleeding

Immediately after leveling the newly placed concrete, the particles of aggregate and cement start settling to the bottom of the container. Due to the difference in weight of constituent materials of concrete, segregation starts taking place and the water rises to the surface of freshly placed concrete. The water accumulated at the top of the concrete surface is called bleeding. Bleeding results in the formation of porous, weak and non durable concrete layer at the top of placed concrete.

The test results of water loss through bleeding are presented in Fig. 4.10. The test results indicate that bleeding percentage decreased almost linearly with the increase in coal bottom ash content in concrete. The bleeding decreased from 3.14 to 1.66% on use of 100% coal bottom ash as substitute of sand in concrete. Total volume of bleeding water of concrete mixtures containing 20, 30, 40, 50, 75 and 100% coal bottom ash was 85, 87, 84, 57, 55 and 51 ml respectively as compared to 100 ml in control concrete. The volume of water collected per unit area of exposed surface of concrete decreased from 0.2017 g/cm^2 to 0.11 g/cm^2 on incorporation of 100% coal bottom ash as substitute of sand in concrete mixture. The low loss of water through bleeding of bottom ash concrete mixtures can be attributed to low free water-cement ratio. Less quantity of water was available in inter particle voids in the bottom ash concrete mixture because the dry and porous particles of coal bottom ash absorbed the part of water internally during the mixing process.

However, Andrade et al. (2009); and Ghafoori and Bucholc (1996, 1997) observed higher water loss through bleeding on incorporation of coal bottom ash in concrete. The amount of bleeding water in concrete depends largely on the water cement ratio. In the study carried out by Andrade et al. (2009); and Ghafoori and Bucholc (1996, 1997) the higher quantity of water was added in bottom ash concrete mixtures to achieve the desired slump which resulted in higher loss of water through bleeding. In the study carried out by Andrade et al. (2009), 378 kg/m^3 of water was added in bottom ash concrete mixture containing 100% coal bottom ash against 219 kg/m^3 of water added in control concrete mix. Whereas in the present study, a fixed water-cement ratio was maintained in bottom ash concrete mixtures as well as control concrete.

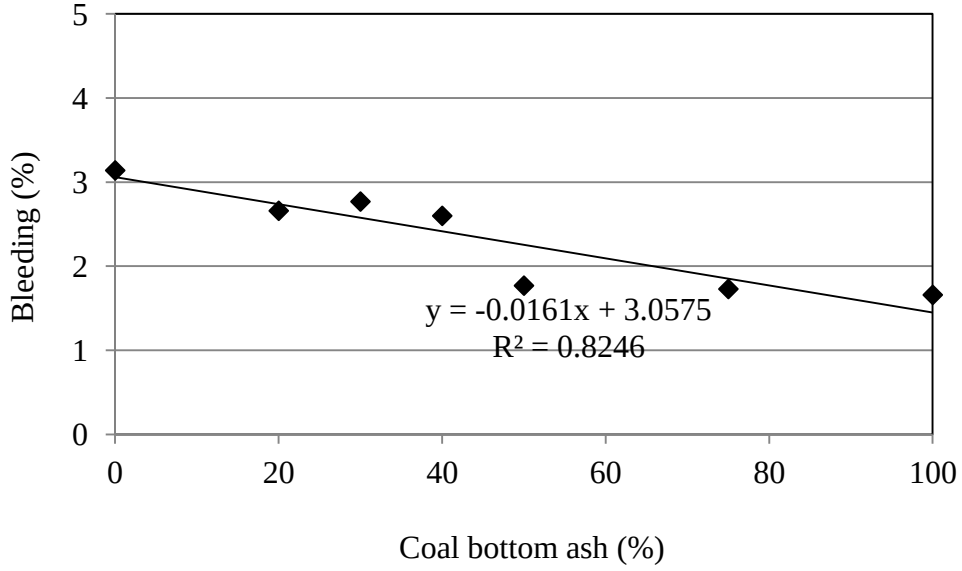

Fig. 4.10: Effect of coal bottom ash on loss of water through bleeding (Concrete 'A')

4.3.3 Strength Properties of Hardened Concrete

4.3.3.1 Unit Weight

As shown in Fig. 4.11, one-day unit density of concrete decreased almost linearly with the increase in coal bottom ash content in concrete. Higher value of coefficient of determination (R^2 = 0.9987) indicates good relevance between the curve and data points. The decrease in density of bottom ash concrete mixtures can be attributed to lower specific gravity and porous particles of coal bottom ash. On substitution of river sand with the coal bottom ash in concrete, heavy particles are replaced with the lighter particles. The increased voids in concrete on use of coal bottom ash as substitute of sand also resulted in lower density. One-day unit density of bottom ash concrete mixtures containing 50% and 100% coal bottom ash as substitute of sand decreased by 112 kg/m^3 (4.66%) and 214 kg/m^3 (9.8%), respectively. One-day unit density of concrete decreased from 2404 to 2189 kg/m^3, when 100% coal bottom ash was used as fine aggregate in concrete. The decrease in dry bulk density of bottom ash concrete mixtures was nearly equal to the difference in weight of sand and coal bottom ash used in manufacturing of concrete. The one-day unit densities of concrete mixtures measured by the average weight of cube by its standard volume indicate that each concrete mix yielded 2.36 to 2.98% less volume. However, the difference in standard volume and actual volume of concrete cube may also be the reason for the variation in density.

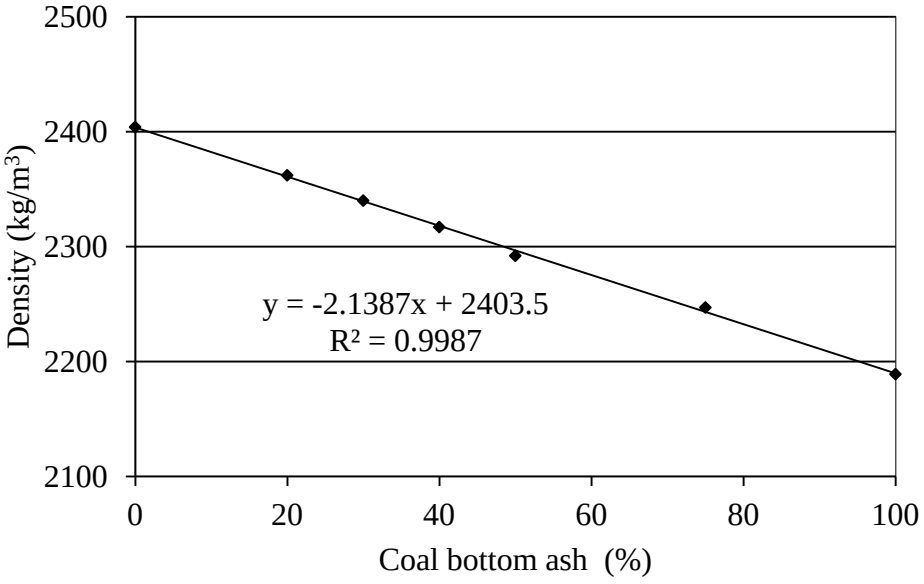

Fig. 4.11: Effect of coal bottom ash on one-day unit density of concrete (Concrete 'A')

The results of present study are in good agreement with the results reported by Ghafoori and Bucholc (1996, 1997), Andrade et al. (2007), and Kim and Lee (2011).

4.3.3.2 Water Loss from Air-Drying

The water loss from air-drying of bottom ash concrete and control concrete samples after demoulding is illustrated in Fig. 4.12. The water loss from air-drying increased with the increase in coal bottom ash content up to 40% in concrete. This might be due to higher permeable pore space and better connectivity of pores in bottom ash concrete mixtures. For bottom ash concrete mixture containing 50% coal bottom ash as sand replacement , the water loss from air-drying was lower than that for 40% substitution and was higher than that of the control concrete sample. For bottom ash concrete mixture containing 75% coal bottom ash and 25% river sand, the water loss from air-drying was lower than that of the control concrete mixture. After 28 days of air-drying, water loss of bottom ash concrete mixtures containing 20, 30, 40, 50, 75 and 100% coal bottom ash as fine aggregate was 58, 61, 65, 58, 48.5 and 50.5 gram, respectively, as compared to 53.5 gram water loss of control concrete. As the water cement ratio was kept identical in all concrete mixtures, the quantity of water present in inter particle voids reduced due to absorption of part of water internally by the dry and porous particles of coal bottom ash. This may be the reason for the lesser loss of water by the bottom ash concrete mixtures containing 75 and 100% coal bottom ash.

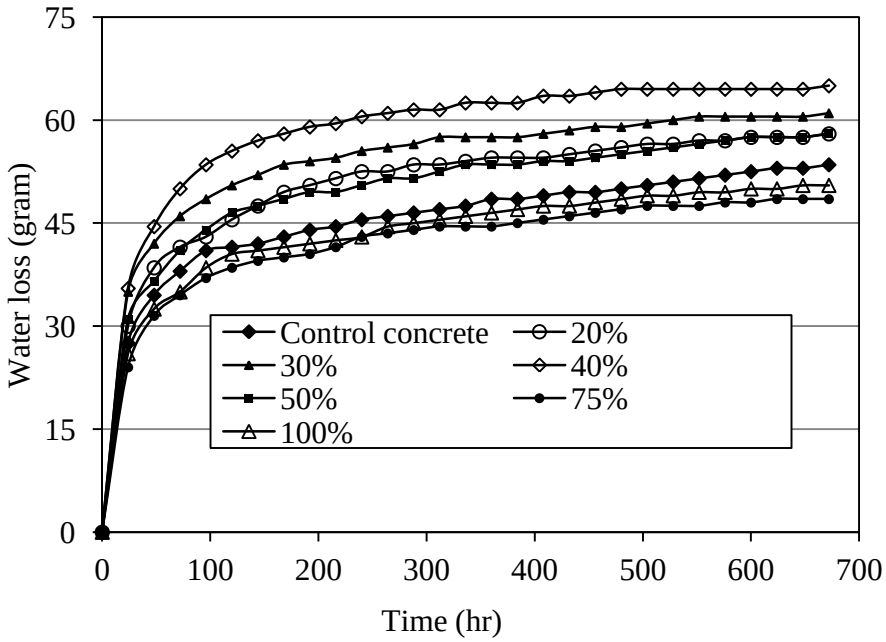

Fig. 4.12: Effect of bottom ash on water loss on air-drying of concrete (Concrete 'A')

4.3.3.3 Permeable Pore Space and Water Absorption

The results of permeable pore space and water absorption are illustrated in Table 4.5. At 28 days of curing age, permeable pore space in concrete and water absorption of concrete increased with increase in coal bottom ash content in concrete with the exception of bottom ash concrete mixture containing 40% coal bottom ash in which permeable pore space and water absorption was less than that of control concrete. At 90 days of curing age, permeable pore space and water absorption of bottom ash concrete mixtures were comparable to that of control concrete. At 28 days of curing age, on incorporation of 75 and 100% coal bottom ash as replacement of sand in concrete, permeable pore space in concrete increased from 10.82 to 11.65% and to 11.99%, respectively. Water absorption of bottom ash concrete mixtures containing 50, 75 and 100% coal bottom ash was 4.86, 5.25 and 5.56%, respectively, as compared to 4.68% of control concrete. The results proved the correlation between the permeable pore space and water absorption. At curing age of 28 days, the connectivity between the capillaries in the paste improved on incorporation of coal bottom ash in concrete. The permeable pore space and water absorption of bottom ash concrete mixtures reduced with progress of curing age. The permeable pore space in concrete mixture containing 100% coal bottom ash as fine aggregate reduced from 11.99% at 28 days to 9.46% at 365 days of curing age. The water absorption of concrete mixture

containing 100% coal bottom ash as fine aggregate reduced from 5.56% at 28 days to 3.85% at 365 days of curing age. The reduction in permeable pore space in bottom ash concrete mixtures with the progress of curing age is significant. The pozzolanic activity of the coal bottom ash is believed to be responsible for the reduction of permeable pore space in bottom ash concrete mixtures.

Table 4.5 Permeable pore space (void) and water absorption of concrete (Concrete 'A')

Mix	**Permeable pore space (%) at curing age (days)**				**Water absorption (%) at curing age (days)**			
	28	**90**	**180**	**365**	**28**	**90**	**180**	**365**
Control concrete (A_0)	10.82	10.46	10.00	9.29	4.68	4.55	4.22	3.97
A_{20}	10.92	10.65	10.22	9.04	4.74	4.67	4.42	3.79
A_{30}	10.86	10.20	10.00	9.88	4.67	4.37	4.34	4.19
A_{40}	10.46	10.49	10.07	10.21	4.53	4.64	4.39	4.38
A_{50}	10.96	10.43	9.88	9.48	4.86	4.38	4.34	3.97
A_{75}	11.65	9.44	9.41	9.24	5.25	4.23	4.19	3.89
A_{100}	11.99	10.54	9.98	9.46	5.56	4.54	4.46	3.85

4.3.3.4 Compressive Strength

The compressive strength test results presented in Figs. 4.13 and 4.14 show that the strength development pattern of bottom ash concrete at all the levels of sand replacement with coal bottom ash is similar to that of control concrete. It is evident from the test results that with increasing curing age, the improvement in compressive strength of bottom ash concrete mixtures is continuous and significant. At 7 days of curing age, concrete mixtures containing 20, 30, 40, 50, 75 and 100% coal bottom ash as fine aggregate gained 78.10, 72.46, 73.12, 69.45, 65.41 and 68.95% of their 28-day compressive strength, respectively, as compared to 74.4% of 28-day compressive strength gained by control concrete. The bottom ash mixtures A_{20}, A_{30}, A_{40}, A_{50}, A_{75} and A_{100} achieved 100, 94.58, 97.22 91.0, 86.28 and 84.84% compressive strength of control concrete, respectively. However, with the increase in curing period, there was a significant increase in compressive strength of bottom ash concrete mixtures as compared to that of control concrete mixture. At 28 days of curing period, although compressive strength of bottom ash concrete mixtures was slightly lower than that of control concrete but the gain over

their 7-day compressive strength was significant. At 28 days, compressive strength of bottom ash concrete mixtures containing 50 and 100% coal bottom ash in concrete decreased from 38.21 N/mm^2 to 37.25 N/mm^2 and to 34.98 N/mm^2, respectively. Bottom ash concrete mixtures containing 20, 30, 40, 50, 75 and 100% coal bottom ash gained 20.05, 38.01, 36.76, 44.27, 52.87 and 44.97% over their 7 day compressive strength, respectively, as compared to 34.40% gained by the control concrete mixture. After 90 days of curing age, compressive strength of above bottom ash concrete mixtures A_{20}, A_{30}, A_{40}, A_{50}, A_{75} and A_{100} exceeded by 17.86, 21.64, 14.79, 17.18, 11.84 and 19.10% of their 28-day compressive strength, respectively, as compared to an improvement of 6.83% over 28-day compressive strength by the control concrete. The bottom ash concrete mixtures A_{20}, A_{30}, A_{40}, A_{50}, A_{75} and A_{100} achieved 105.27, 112.29, 106.30, 106.93, 102.67, and 102.06% of 90-day compressive strength of control concrete, respectively. At 90 days of curing period, energy dispersive spectrometry (EDS) analysis of concrete mixtures containing 0, 30, 50, 75 and 100% coal bottom ash show Ca/Si ratio as 2.42, 2.39, 2.44, 2.27 and 2.14, respectively. Low Ca/Si ratio (2.14) CSH gel was formed in the bottom ash concrete mixture incorporating 100% coal bottom ash as replacement of river sand. Low calcium-silicate ratio (Ca/Si) CSH gel phase in bottom ash concrete mixtures demonstrates higher reactivity and thus achieving higher strength as compared to control concrete mixture. As seen in Figs. 5.49 to 5.50, at 90 days of curing period, the CSH gel is more evenly spread over the entire image than that at the earlier age. At 90 days of curing period, the finely spread of CSH gel and the formation of extra CSH gel due to consumption of portlandite by pozzolanic action of coal bottom ash resulted in higher compressive strength. At 180 days of curing period, compressive strength of bottom ash concrete mixtures containing 20, 30, 40, 50, 75 and 100% coal bottom ash was 100.13, 102.24, 107.16, 102.84, 104.52, and 99.25% of the compressive strength of control concrete, respectively. It is apparent from the test results of the present study that the difference in compressive strength of all concrete mixtures was insignificant at 180 days of curing period. At 365 days of curing period, all bottom ash concrete mixtures except concrete mixture containing 75% coal bottom ash as fine aggregate displayed compressive strength almost comparable to that of control concrete. Concrete mixture containing 75% coal bottom ash achieved 5.57% higher compressive strength than that of control concrete. The test results of this study are in good agreement with those reported in previous studies (Kim and Lee, 2011; Chun et al., 2008). At early age of 7 days, the compressive strength of bottom ash concrete mixtures was lower than control concrete mixture. At 28 days of curing age, compressive strength of

bottom ash mixtures was almost comparable to control concrete mixture except bottom ash concrete mixture containing 100% coal bottom ash which showed 8.5% lower compressive strength. Between curing age of 28 and 90 days, bottom ash concrete mixtures gained more compressive strength than gained by control concrete mixture. At early curing age of 7 days, the factors responsible for lower compressive strength of bottom ash concrete mixtures can be summarized as: 1) the replacement of the stronger material with the weaker material; 2) absence of pozzolanic activity by the coal bottom ash; 3) the increased porosity of concrete.

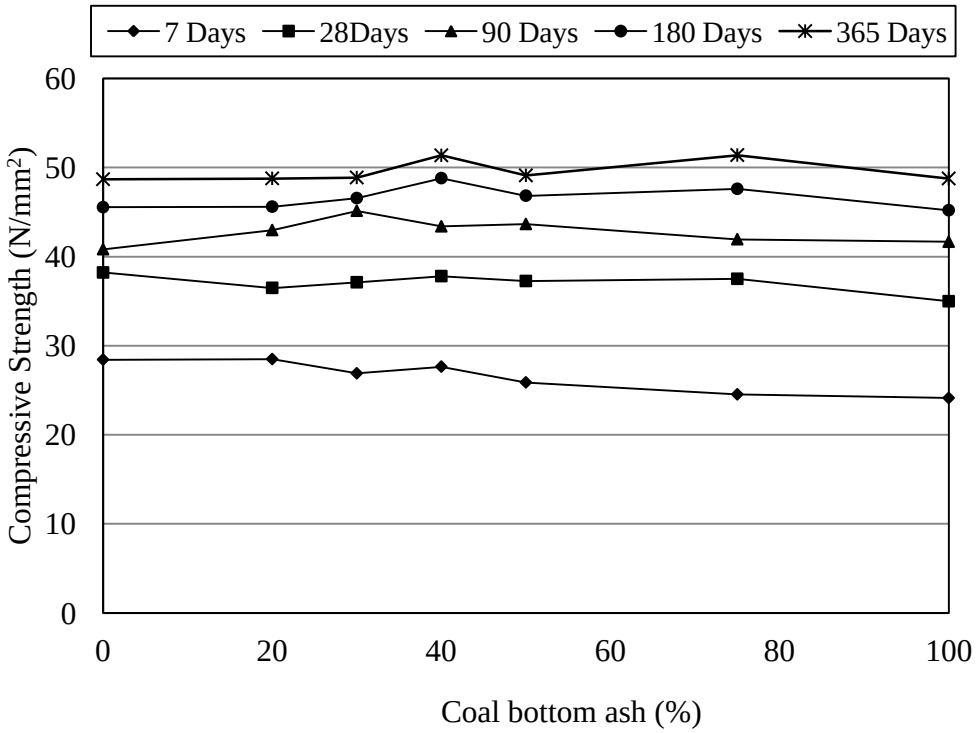

Fig. 4.13: Compressive strength of concrete versus coal bottom ash content (Concrete 'A')

The decrease in the free water-cement ratio of the bottom ash concrete mixtures due to absorption of part of water by the porous particles of the coal bottom ash internally during the mixing process also contributed to some extent in negating the effect of the factors responsible for lower compressive strength. In other words at early curing age, the compressive strength of bottom ash concrete mixtures improved to some extent due to the reduced free water-cement ratio but the net effect of all the factors mentioned above was reduction in compressive strength on use of coal bottom ash as fine aggregate. The previous studies showed that pozzolanic activity of coal bottom ash is slow till 14 days of curing age and after this period, the coal bottom ash particles start reacting with calcium hydroxide and forming CSH gel and needles (Cheriaf et al., 1999).

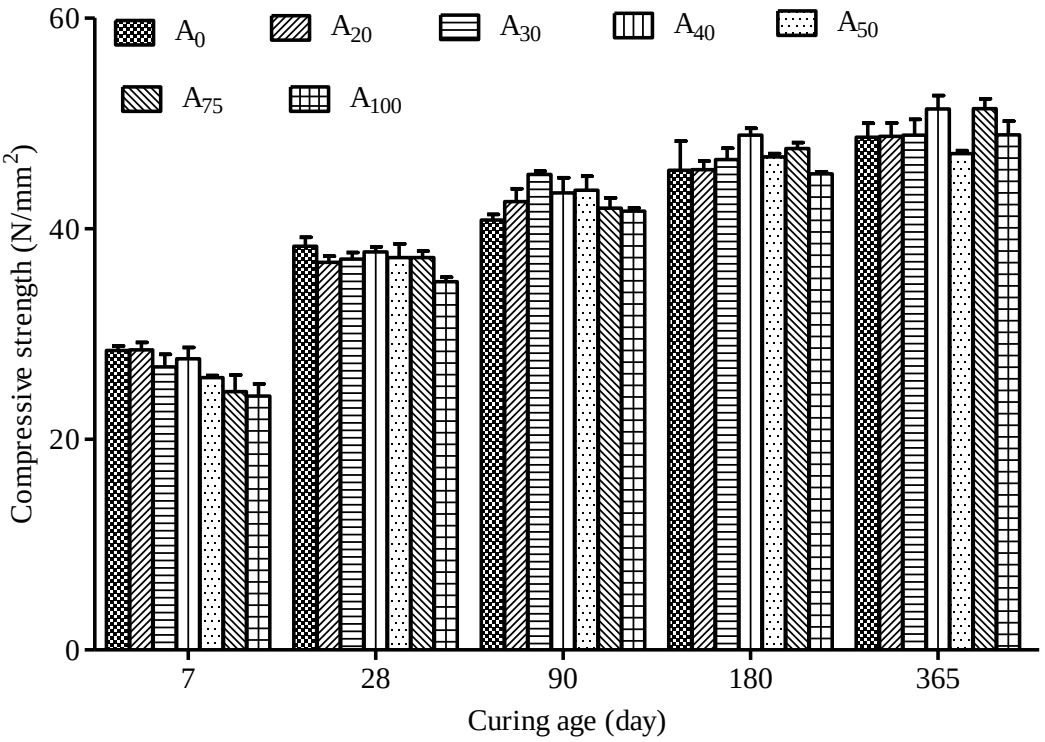

Fig. 4.14: Effect of coal bottom ash on compressive strength of concrete (Concrete 'A')

With the increasing age, reactive silica in the coal bottom ash reacts with alkali calcium hydroxide produced by hydration of cement and forms calcium silicate and aluminate hydrates. The formation of stable calcium silicate and aluminate hydrates by chemical reactions between cement paste constituents and aggregates result in filling the voids in the interfacial transition zone and in improving its compressive strength. At 28 days of curing age, the increased pozzolanic activity of the coal bottom ash negated the effect of factors responsible for reduction in strength and played its role in improving the compressive strength. As such, the decrease in compressive strength of bottom ash concrete mixtures was not significant except bottom ash mixture containing 100% coal bottom ash. After 28 days of curing age, pozzolanic effect of coal bottom ash overcame all the negative effects and enhanced the strength properties of bottom ash concrete mixtures.

Statistical significance of effect of coal bottom ash on compressive strength of bottom ash concrete was confirmed at 7 days. The empirical equation to determine the relationship between compressive strength, the curing age and coal bottom ash content in concrete was established from the test results. The empirical equation developed for compressive strength of bottom ash concrete mixtures containing 20 to 100% coal bottom ash as sand replacement is given as under:

$f_t = C \ln(t) + D$

$C = 3.6405\ a^{0.1265}$ $D = 20.22\ e^{-0.005a}$ $R^2 = 0.9769$

Higher value of determination coefficient (R^2) indicates good relationship between the data and regression curve. Similar empirical equations derived by M. a. a. Abd elaty (2014) for normal cement concrete are given as under:

For normal concrete (28-da compressive strength = 36.8 MPa and w/c = 0.4)

$f_t = 5.9036\ln(t) + 16.225$ $R^2 = 0.9894$

where,

f_t = Compressive strength of concrete in N/mm^2 at age (t)

t = Curing age in days

a = Coal bottom ash content in percentage (%)

4.3.3.5 Splitting Tensile Strength

The splitting tensile strength results of bottom ash concrete mixtures are shown in Figs. 4.15 and 4.16. The test results indicate that inclusion of coal bottom ash as fine aggregate in concrete improved the splitting tensile strength of concrete at all the curing ages. Coal bottom ash as fine aggregate in concrete affected the splitting tensile strength and compressive strength differently. The splitting tensile strength of concrete is more dependent on the quality of the paste than compressive strength. The properties of fine aggregate affect quality of paste and interfacial transition zone in the concrete, which affect the ratio of tensile strength and compressive strength. The pozzolanic properties of coal bottom ash improves the quality of the paste thereby result in increase in splitting strength of concrete (Ghafoori and Bucholc, 1997). At the early age, the presence of pores in the paste of bottom ash concrete might have helped in blocking the propagation of cracks and increasing the splitting tensile strength. The splitting tensile strength results of this investigation are in good agreement with those reported by Ghafoori and Bucholc (1996, 1997); and Chun et al. (2008). At curing age of 7 days, bottom ash concrete mixtures containing 20, 30, 40, 50, 75 and 100% of coal bottom ash as fine aggregate achieved 80.97, 77.6, 75.06, 77, 75.26 and 78.29% of their 28-day splitting tensile strength, respectively, in comparison to 78.4% of 28-day splitting tensile strength gained by control concrete. At curing age of 28 days, the splitting tensile strength of bottom ash concrete mixtures incorporating 100, 75 and 50% coal bottom ash as fine aggregate was 4.04, 8.99 and 11%, respectively, higher than that of the control concrete. The improvement in splitting tensile strength of bottom ash concrete mixtures containing 100, 75 and 50% coal

bottom ash as fine aggregate over control concrete at 180 days of curing age was 7.14, 6.55 and 5.95%, respectively. The incorporation of coal bottom ash in concrete shows significant increase in splitting tensile strength. At 90 days of curing age, the splitting tensile strength of all bottom ash concrete mixtures as well as the control concrete mixture was nearly 7.56% of their compressive strength. The splitting tensile strength and compressive strength ratios (%) shown in Table 4.6 are in good agreement with the data published in previous studies (Prince and Walter, 1951). For moderate strength conventional concrete, the splitting tensile strength-compressive strength ratio (%) is approximately 8 to 9. For higher strength conventional concrete, tensile strength is approximately 7% of compressive strength.

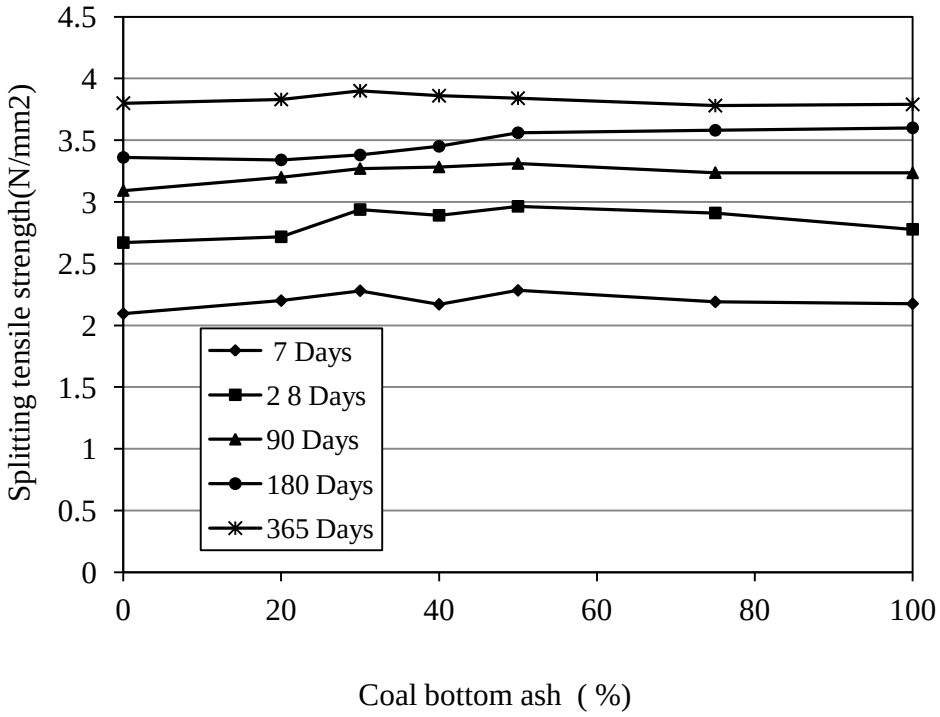

Fig. 4.15: Splitting tensile strength of concrete versus coal bottom ash content (Concrete 'A')

The properties of coarse and fine aggregate, curing age, water-cement ratio and air entrained affect the relationship between splitting tensile strength and compressive strength. In case of conventional concrete, the splitting tensile strength-compressive strength ratio decreases with the increase in curing age and decrease in water-cement ratio. The test results of present study revealed that ratio increased with the increase in bottom ash content in concrete. At 7 days of curing age, the ratio increased from 7.37 to 9.02 on 100% replacement of river sand with coal bottom ash in concrete. The splitting tensile

strength and compressive strength ratios (%) of bottom ash concrete decreased with the increase in curing age.

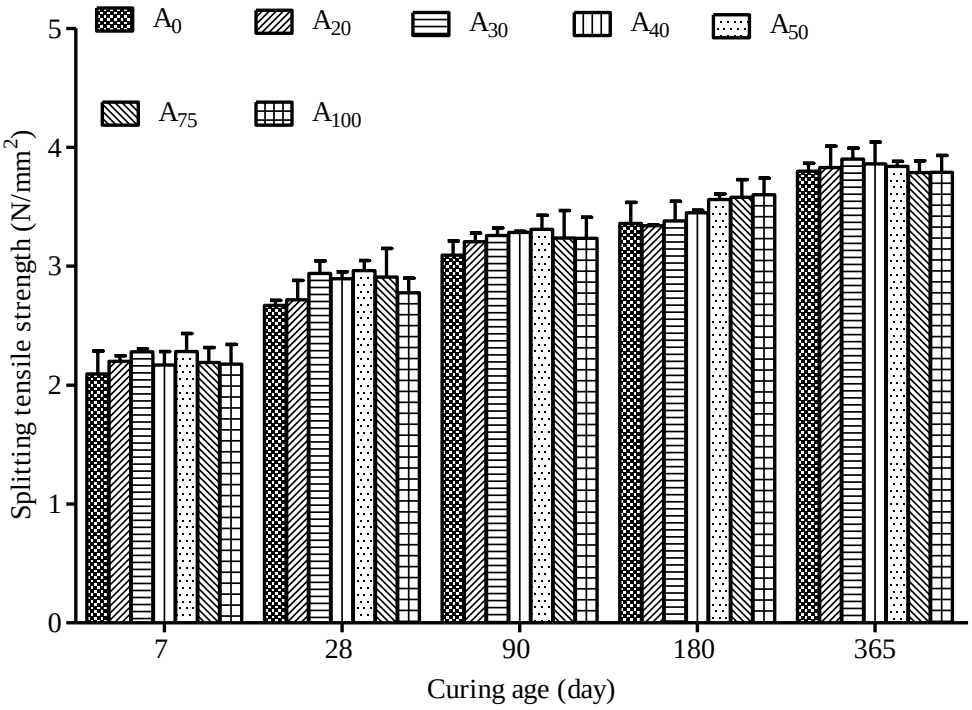

Fig. 4.16: Effect of coal bottom ash on splitting tensile strength of concrete (Concrete 'A')

Table 4.6 Splitting tensile and compressive strength ratios of bottom ash concrete mixtures and control concrete (Concrete 'A')

Mix	**Splitting tensile/Compressive strength ratio (%) at curing age (days)**				
	7	**28**	**90**	**180**	**365**
Control concrete (A_0)	7.37	6.99	7.57	7.38	7.65
A_{20}	7.72	7.45	7.45	7.32	7.85
A_{30}	8.48	7.92	7.25	7.26	7.98
A_{40}	7.85	7.65	7.57	7.07	7.52
A_{50}	8.82	7.96	7.59	7.60	7.82
A_{75}	8.93	7.76	7.72	7.52	7.36
A_{100}	9.02	7.94	7.77	7.96	7.86

At the curing age of 7, 28, 90, 180 and 365 days, the average values of ratios (%) of bottom ash concrete were 8.47, 7.78, 7.56, 7.45 and 7.73, respectively. The results show that similar to conventional concrete, the compressive strength and splitting tensile strength of concrete containing coal bottom ash as partial or total replacement of river sand

increased with the progress of curing age, but compressive strength improved at a faster rate than the splitting tensile strength.

4.3.3.6 Modulus of Elasticity

The test results are presented in Figs. 4.17 and 4.18. The modulus of elasticity of concrete deceased approximately linearly with the increase in coal bottom ash content in concrete. At all the curing ages, bottom ash concrete mixtures displayed lower modulus of elasticity than control concrete. At 28 days of curing age, bottom ash concrete mixtures containing 50 and 100% coal bottom ash achieved 88.62 and 79.30% of modulus of elasticity of control concrete, respectively. At 28 days of curing age, the modulus of elasticity of control concrete and bottom ash concrete mixtures containing 50 and 100% coal bottom ash as fine aggregate was 29.18 GPa, 25.93 GPa and 23.14 GPa, respectively. With age, modulus of elasticity of bottom ash concrete mixtures increased but remained lower than that of the control concrete mixture. At 180 days of curing age, bottom ash concrete mixtures containing 50 and 100% coal bottom ash as fine aggregate gained 92.5 and 84.21% of modulus of elasticity of control concrete, respectively. At 365 days of curing age, modulus of elasticity of bottom ash concrete mixtures containing 20, 30, 40, 50, 75, and 100% coal bottom ash as fine aggregate increased over their 28 day modulus of elasticity by 11.10, 10.36, 12.30, 13.68, 13.69 and 18.89%, respectively as compared to 9.49% increase in modulus elasticity of control concrete. The values of modulus of elasticity obtained in this study falls within the typical range of 20 GPa to 32 GPa for M 30 grade concrete given in BS 8110: (Part 2)-1985. As per expression $E = 1.7\rho^2 f^{0.33}$ for density between 14.00 kN/m^3 and 23.20 kN/m^3, modulus of elasticity of concrete containing 100% coal bottom ash and having dry bulk density of 21.01 kN/m^3 and compressive strength of 34.98 N/mm^2 works out as 24.22 GPa. Also as per ACI building code 318-99, modulus of elasticity works out as 22.04 GPa. For M 30 grade concrete having density of 21.01 kN/m^3, modulus of elasticity as per BS: 8110: (Part 2)-1985 and ACI building code 318-99 works out as 23.03 GPa and 20.41 GPa, respectively. The modulus of elasticity of bottom ash concrete mixture containing 100% coal bottom ash as fine aggregate is more than that worked out from the expressions given in BS: 8110: (Part 2)-1985 and ACI building code 318-99. Hence, as far as strength properties and modulus of elasticity are concerned, the concrete produced using coal bottom ash is suitable for structural purposes. The modulus of elasticity of bottom ash concrete decreased with the decrease in its unit density. The test results of modulus of elasticity of bottom ash concrete

of the present research work are in good agreement with those of semi light weight concrete and the results reported in previous studies on use of coal bottom ash as fine aggregate in concrete (Kim and Lee, 2011; Ghafoori and Bucholc, 1996).

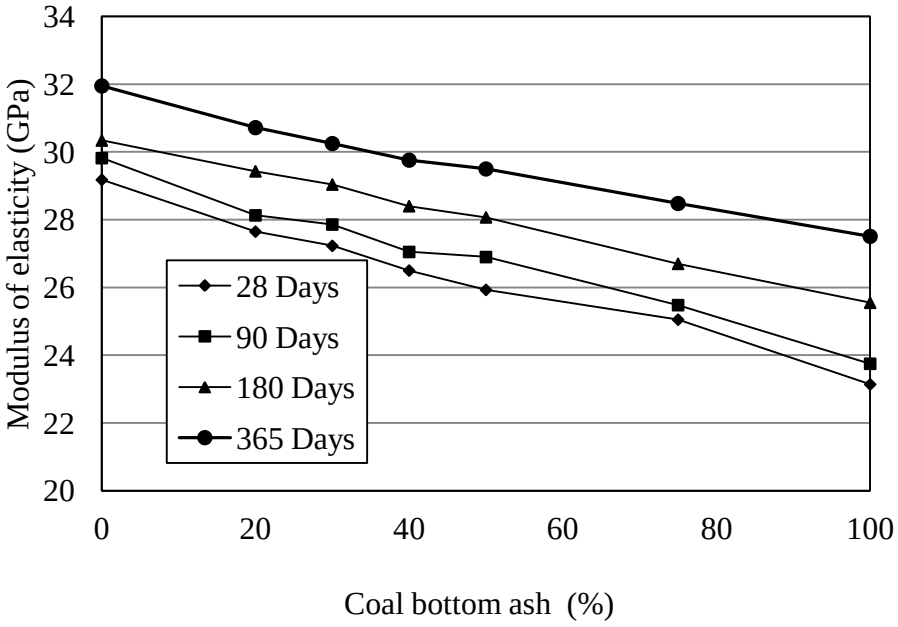

Fig. 4.17: Modulus of elasticity of concrete versus coal bottom ash content (Concrete 'A')

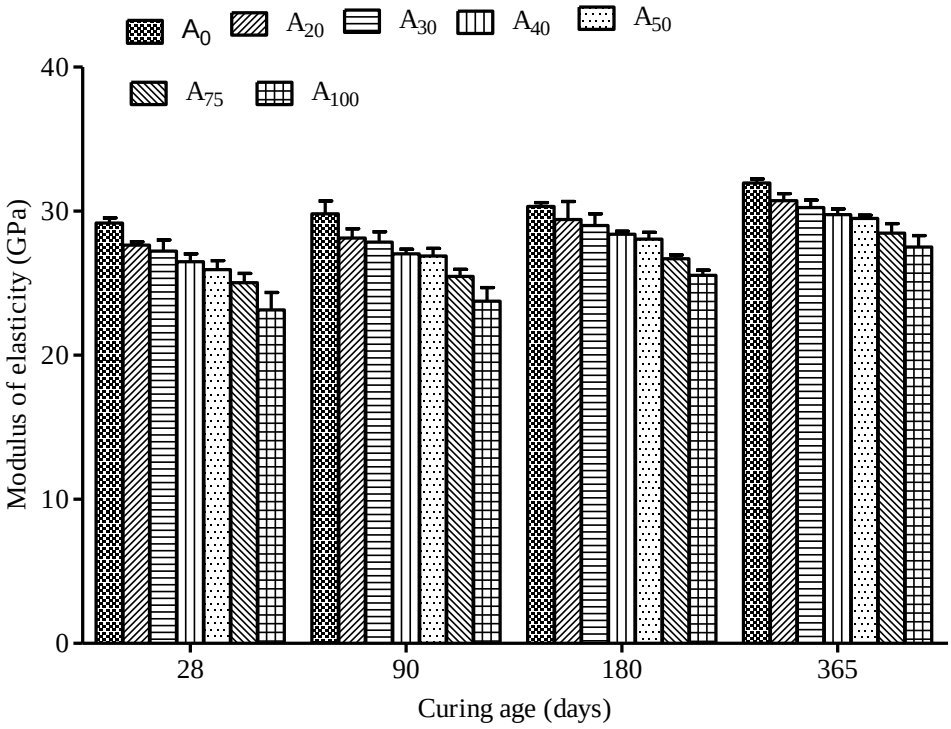

Fig. 4.18: Effect of coal bottom ash on modulus of elasticity of concrete (Concrete 'A')

Compared to control concrete, for the same compressive strength, the bottom ash concrete displayed lower the modulus of elasticity. At 90 days of curing age, the compressive strength and modulus of elasticity of concrete mixtures containing 100% coal bottom ash as fine aggregate were 42.95 N/mm^2 and 23.75 GPa, respectively, as compared to 40.82 N/mm^2 and 29.82 GPa of control concrete. Moduli of elasticity of bottom ash concrete mixtures as well as control concrete are given in Table 4.7.

Table 4.7 Modulus of elasticity of bottom ash concrete mixtures and control concrete (Concrete 'A')

Mix	**Modulus of elasticity (GPa) at curing age (days)**			
	28	**90**	**180**	**365**
Control concrete	29.18	29.82	30.34	31.95
A_{20}	27.65	28.13	29.43	30.72
A_{30}	27.23	27.86	29.04	30.25
A_{40}	26.5	27.05	28.40	29.76
A_{50}	25.95	26.91	28.07	29.50
A_{75}	25.05	25.48	26.71	28.48
A_{100}	23.14	23.75	25.55	27.51

4.3.3.7 Pulse Velocity

The pulse velocity test results are illustrated in Table 4.8 and Fig. 4.19. At 28 days of curing period, the pulse velocity values through bottom ash concrete mixtures were almost comparable to that through the control concrete mixture. The pulse velocity values through bottom ash concrete mixtures A_{75} and A_{100} was 0.6 and 1.27%, respectively, lower than that through the control concrete. The pulse velocity values decreased from 4393 to 4337 m/s on incorporation of 100% coal bottom ash as replacement of river sand in concrete. The decrease in pulse velocity values on use of coal bottom ash as replacement of river sand in concrete was not substantial. These results are in line with compressive strength results at 28 days of curing period. However, Topcu and Billir (2007) observed that on incorporation of coal bottom ash as replacement of fine aggregate in mortar, the pulse velocity decreased linearly. Comparing pulse velocity values obtained in this study with those given in BIS: 13311-92 and reproduced in Table 3.2, the quality of concrete made with coal bottom ash can be graded as good. It is evident from Fig. 4.20 that the pulse velocity through concrete increased with increase in curing period. The pulse velocity

values increased at a faster rate up to 180 day of curing period. Although, after 180 days of curing period, the pulse velocity value through concrete mixtures continued to increase but at a slower pace.

Table 4.8 Pulse velocity through concrete specimens (Concrete 'A')

Mix	Pulse velocity (m/s) at curing age (days)			
	28	90	180	365
Control concrete	4393	4587	4708	4768
A_{20}	4400	4565	4690	4747
A_{30}	4383	4555	4677	4750
A_{40}	4380	4580	4703	4733
A_{50}	4390	4545	4663	4723
A_{75}	4367	4500	4627	4735
A_{100}	4337	4480	4617	4713

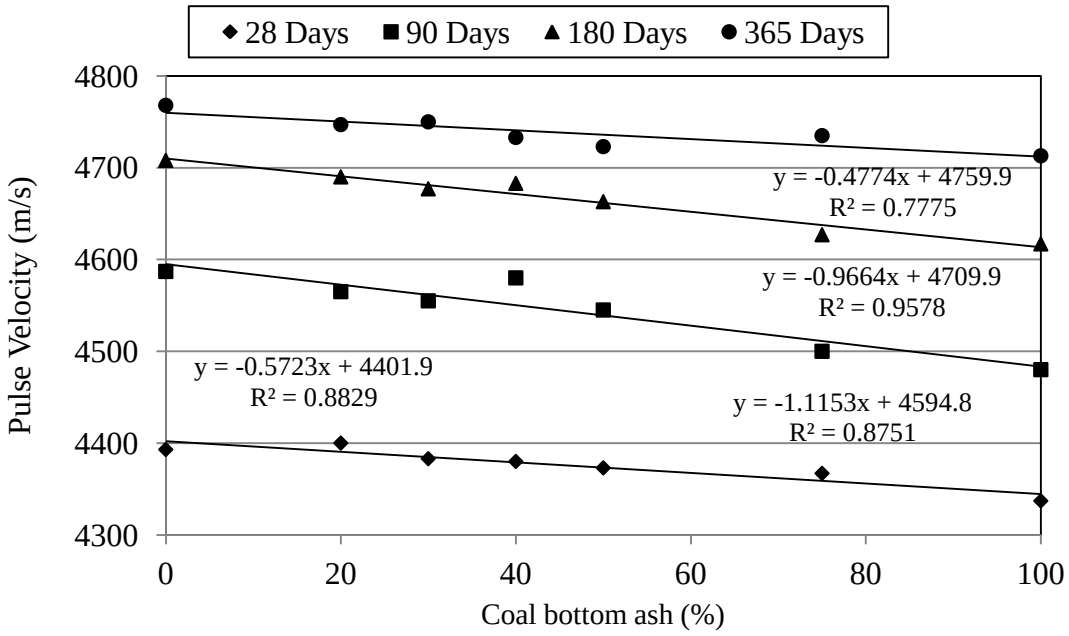

Fig. 4.19: Effect of coal bottom ash on pulse velocity through concrete (Concrete 'A')

At 365 days of curing period, pulse velocity values through bottom ash concrete mixtures were also comparable to that through the control concrete mixture. The difference in pulse velocity values through bottom ash concrete mixtures and the control concrete mixture was less than 1.15%. Higher values of pulse velocities obtained in this study indicate the quality of bottom ash concrete mixtures in terms of density, homogeneity and uniformity

was good. The increase in pulse velocity values indicates that there is the increase in the gel/space ratio due to continued hydration process with age.

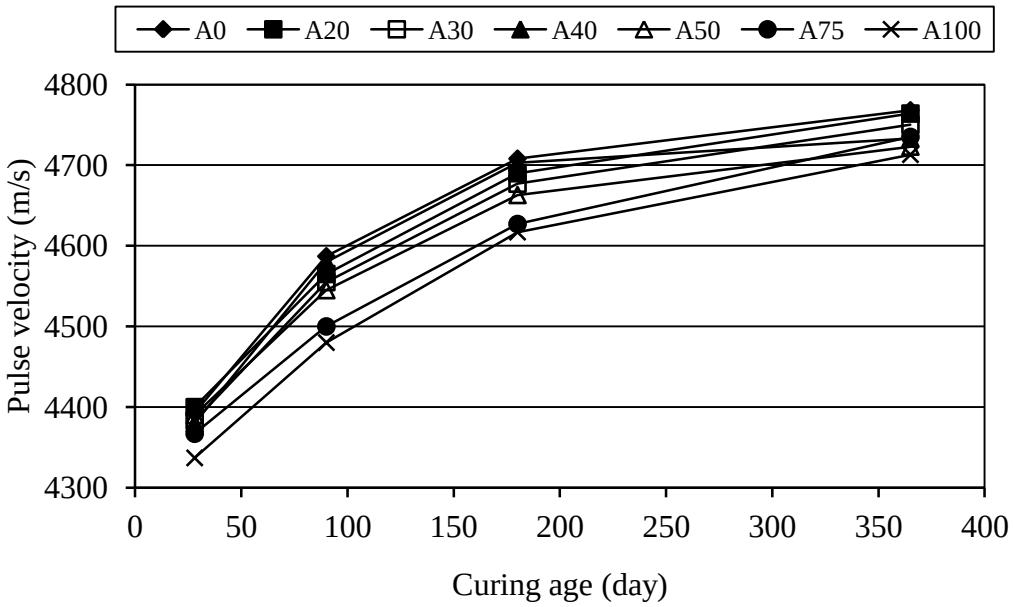

Fig. 4.20: Variation of pulse velocity with age (Concrete 'A')

This phenomenon was also confirmed by the permeable pore space test results shown in Table 4.5. Significant decrease in permeable pore space in bottom ash concrete mixtures resulted in higher values of pulse velocities. With increasing age, all the concrete mixtures achieved an almost equal increase in pulse velocity values. At 365 days of curing period, the pulse velocity values through bottom ash concrete mixtures A_{30} (30% CBA), A_{50} (50% CBA), A_{75} (75% CBA) and A_{100} (100% CBA) increased by 8.37, 7.59, 8.43 and 8.67%, respectively, over pulse velocity values at 28 days of curing age as compared to 8.54% that increased through control concrete.

4.3.4 Durability Properties of Concrete

4.3.4.1 Sorptivity

From Fig. 4.21, it can be seen that the sorptivity of concrete mixtures incorporating coal bottom ash as replacement of river sand increased with the increase in coal bottom ash content. These results are in line with water absorption results. For bottom ash concrete mixtures, initial rate of absorption of water increased with increase in replacement level of river sand with coal bottom ash. However, for all the bottom ash concrete mixtures as well as control concrete, the secondary rate of absorption of water was identical. The initial rate

of absorption of water increased from 12 x 10^{-4} to 19 x 10^{-4} mm/√s on 100% replacement of river sand with coal bottom ash in concrete. This means that bottom ash concrete mixtures took lesser time for rise of water by capillary action and thus bottom ash concrete mixtures were more porous than control concrete. At early curing period of 28 days, both permeable pore space test results and scanning electron micrographs also confirmed more voids in bottom ash concrete mixtures as compared to voids in control concrete. The absorption of more water at a faster rate by the porous particles of coal bottom ash and the rise of more water through higher number of capillary voids may be the possible explanation for higher initial water sorptivity of bottom ash concrete mixtures. Initial rate of absorption of water of bottom ash mixtures A_{20}, A_{30}, A_{40}, A_{50}, A_{75} and A_{100} was 12 x 10^{-4} mm/√s, 13 x 10^{-4} mm/√s, 14 x 10^{-4} mm/√s, 15 x 10^{-4} mm/√s, 16 x 10^{-4} mm/√s and 19 x 10^{-4} mm/√s, respectively, as compared to 13 x 10^{-4} mm/√s of control concrete. Secondary sorptivity of water was 2 x 10^{-4} mm/√s for all the bottom ash concrete mixtures and control concrete. Sorptivity of water of bottom ash concrete mixtures A_{20}, A_{30}, A_{40}, A_{50}, A_{75} and A_{100} was 6.03, 12.20, 12.93, 14.63, 27.64 and 38.75%, respectively, higher than that of control concrete. As shown in Fig. 4.22, total water sorptivity increased almost linearly with the increase in replacement level of river sand with coal bottom ash. Higher value of coefficient of determination (R^2 = 0.985) indicates good relevance between the curve and data points.

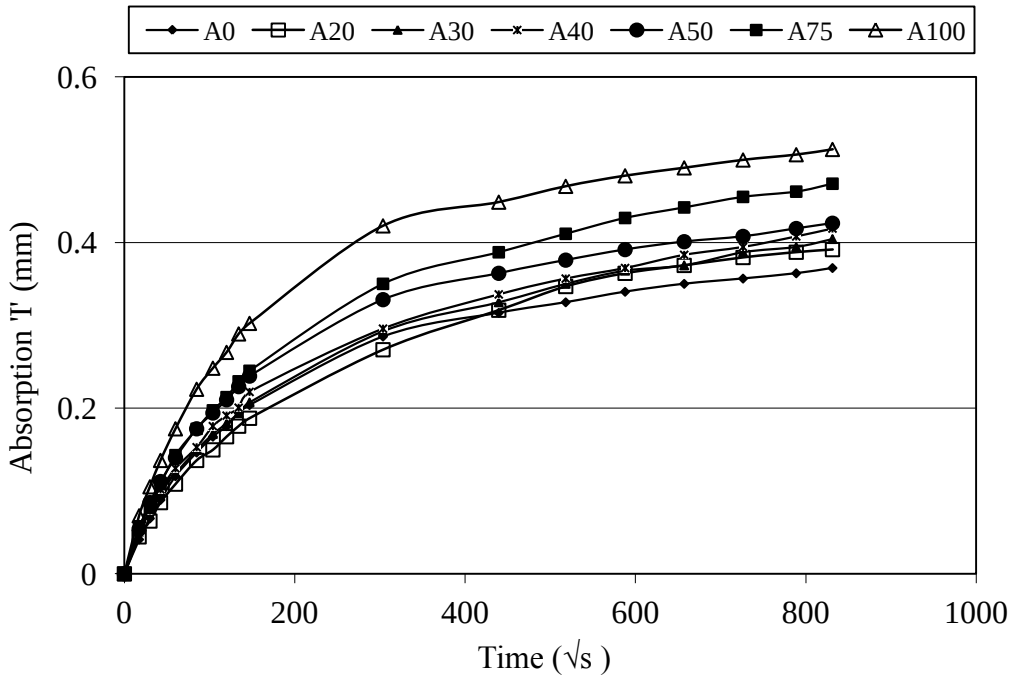

Fig. 4.21: Effect of coal bottom ash on water sorptivity of concrete (Concrete 'A')

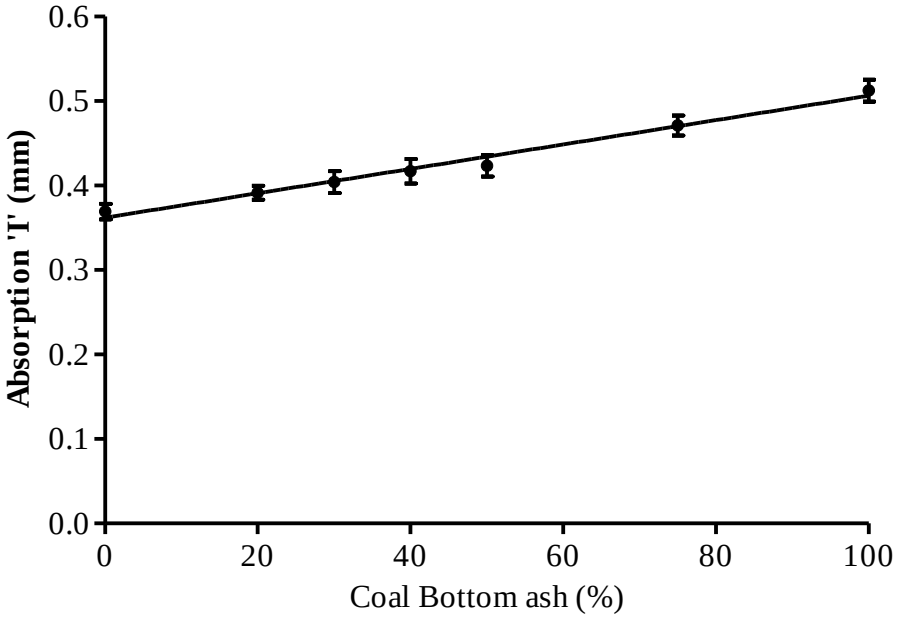

Fig. 4.22: Sorptivity versus coal bottom ash content in concrete (Concrete 'A')

4.3.4.2 Chloride Permeability

Resistance to chloride ion penetration depends largely on the volume and size of interconnected capillary voids present in the concrete and micro cracks present in the paste and at the aggregate - paste interface. Rapid chloride penetration test results of concrete mixtures are presented in Fig. 4.23 and Table 4.9. Total charge in coulombs (C) passed over a period of 6 hrs duration through concrete was measured at 28, 90, 180 and 365 days of curing age. As per ASTM C 1202-10, the chloride permeability of all bottom ash concrete mixtures $A_{20,}$ $A_{30,}$ $A_{40,}$ $A_{50,}$ A_{75} and A_{100} as well as control concrete (A_0) at 28 days of curing age was moderate. Total charge passed through bottom ash concrete mixtures $A_{20,}$ $A_{30,}$ $A_{40,}$ $A_{50,}$ A_{75} and A_{100} was 2624 , 2513, 2594, 2402, 2651 and 2623 coulombs, respectively, as compared to 2891 coulombs passed through the control concrete. The resistance of concrete to chloride ion penetration increased with age. At 90 days of curing age, total charge passed through bottom ash concrete mixtures except A_{40} and A_{50} was lower than that passed through the control concrete. After 90 days of curing age, resistance to chloride ion penetration of bottom ash concrete mixtures increased with increase in coal bottom ash content in concrete. From the results, it is evident that pozzolanic activity of coal bottom ash contributed significantly in improving the resistance to chloride ion penetration of bottom ash concrete mixtures. At 180 and 365 days of curing age, total charge passed through all bottom ash concrete mixtures was significantly lower

than that passed through the control concrete mixture. At 365 days of curing age, cumulative charge passed through bottom ash concrete mixtures A_{20}, A_{30}, A_{40}, A_{50}, A_{75} and A_{100} was 1064, 1037, 953, 790, 785 and 605 coulombs, respectively, as compared to 1326 coulombs passed through the control concrete.

Table 4.9 Charge passed through concrete specimens. (Concrete 'A')

Mix	**Charge(coulomb) passed at curing age (days)**			
	28	**90**	**180**	**365**
Control concrete (A_0)	2891	2248	1517	1326
A_{20}	2624	2115	1264	1277
A_{30}	2513	2013	1104	1037
A_{40}	2594	2254	1144	953
A_{50}	2402	2287	927	790
A_{75}	2651	1675	713	785
A_{100}	2623	1603	544	605

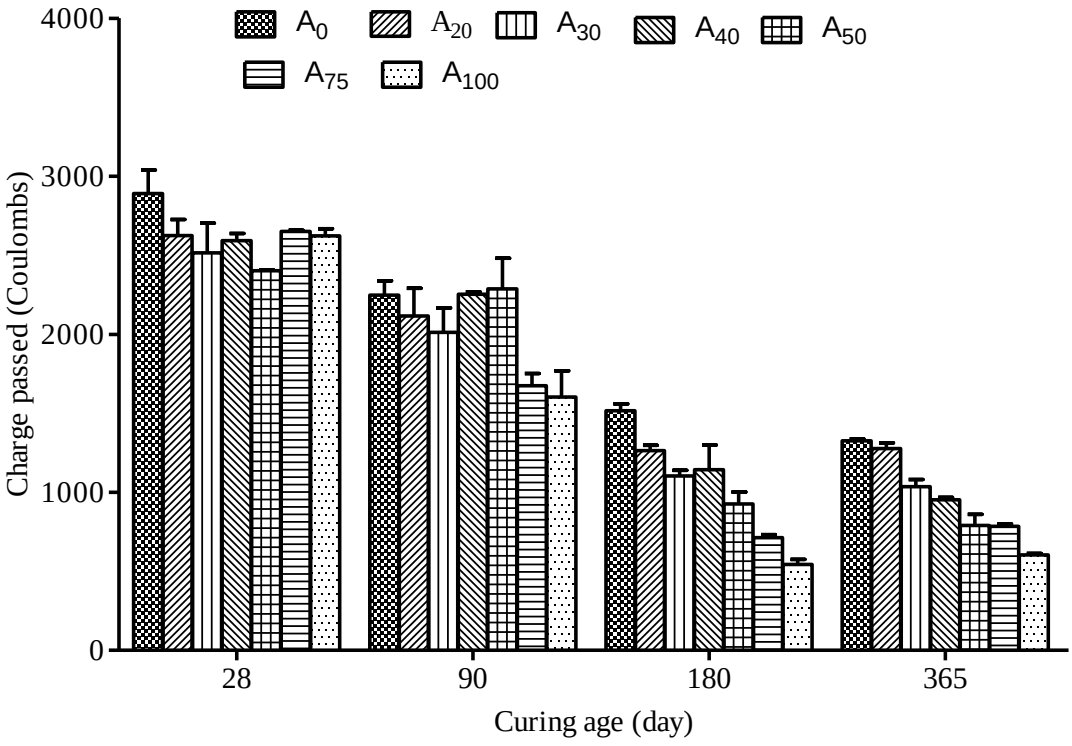

Fig. 4.23: Effect of coal bottom ash on chloride ion penetration in concrete (Concrete 'A')

Permeable pore space in bottom ash concrete mixtures $A_{50,}$ A_{75} and A_{100} was 9.48, 9.24 and 9.46%, respectively, against 9.26% in control concrete. The voids in bottom ash concrete mixtures also include voids in coal bottom ash particles. As such, actual voids in paste of bottom ash concrete mixtures may probably be less than that measured as per ASTM C 642-97.The reduction in alkalinity of pore solution of bottom ash concrete mixtures may be another possible explanation for lower charge passed through them at early 28 days of curing age. After 90 days of curing age, compressive strength results of bottom ash concrete mixtures also support the phenomenon of increased resistance to chloride ion penetration on use of coal bottom ash in concrete. Aramraks (2006) also observed that at 56 days of curing age, cumulative charge passed through bottom ash concrete mixtures was lower than that passed through the control concrete. Kou and Poon (2009) also observed that resistance to chloride ion penetration increased on use of bottom ash in concrete as fine aggregate.

4.3.4.3 Drying Shrinkage

Hardened concrete in unsaturated air experiences drying shrinkage. It is the movement of water, which causes expansion, or shrinkage of hardened concrete. Fig. 4.24 presents the drying shrinkage behaviour of bottom ash concrete mixtures and control concrete. Shrinkage strains decreased with the increase in coal bottom ash content in concrete. At 90 days of drying period, the shrinkage strains of bottom ash concrete mixtures $A_{20,}$ $A_{30,}$ $A_{40,}$ $A_{50,}$ A_{75} and A_{100} were 520 x 10^{-6}, 413.33 x 10^{-6}, 406.67 x $10^{-}6$, 366.67 x 10^{-6}, 320 x 10^{-6} and 300 x 10^{-6}, respectively. However, during the same period, shrinkage strain of control concrete was 493.33 x 10^{-6}. At 180 days of drying period, bottom ash concrete mixtures $A_{30,}$ $A_{40,}$ $A_{50,}$ A_{75} and A_{100} experienced 14.10, 10.25, 21.79, 34.62, and 37.17%, respectively, less shrinkage strain as compared to control concrete. However, the bottom ash concrete mixture A_{20} containing 20% coal bottom ash as fine aggregate experienced 6.40% higher drying shrinkage strain than the control concrete. The shrinkage strain values of bottom ash concrete specimens except A_{20} specimen were lower than that of control concrete during the entire drying period of the test. The reduced shrinkage strain exhibited by bottom ash concrete mixtures was probably due to lower free water-cement ratio. The porous particles of dry coal bottom ash absorbed part of water internally during the mixing process. Coal bottom ash has lesser water retention capacity. It is also believed that, the porous coal bottom ash particles released the water during drying of specimens.

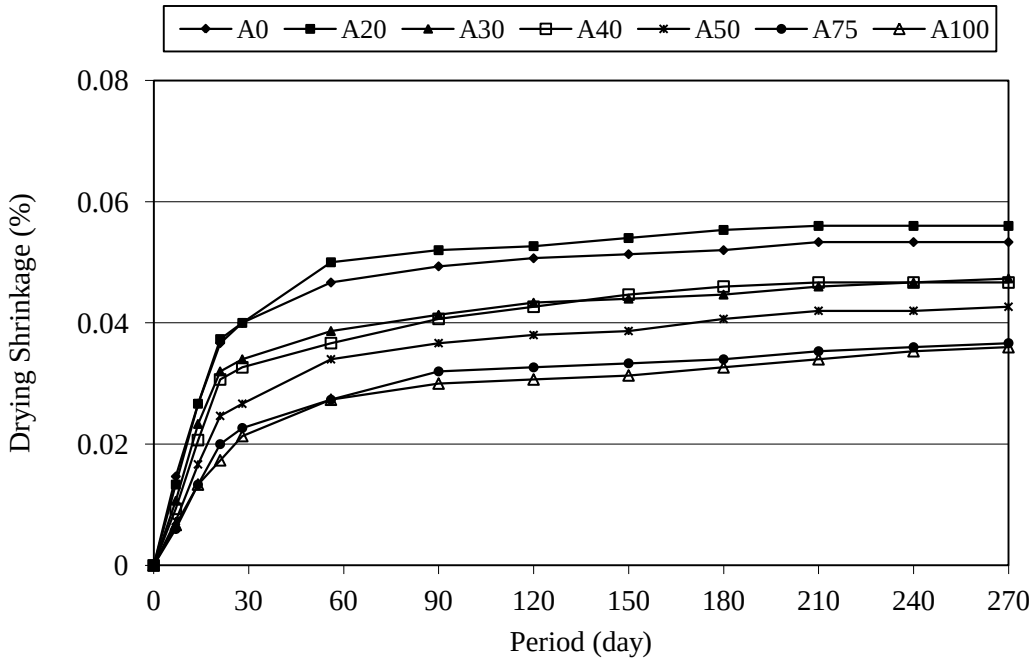

Fig. 4.24: Effect of coal bottom ash on drying shrinkage of concrete (Concrete 'A')

This resulted in lesser shrinkage strains on drying of bottom ash concrete mixtures. The drying shrinkage results of the present study compare well with study of Bai et al. (2005) and Ghafoori and Bucholc (1996, 1997). They have also observed that concrete containing coal bottom ash exhibited greater dimensional stability as compared to conventional concrete. Ghafoori and Cai (1998) has also observed lower shrinkage strains of roller compacted concrete made with coal bottom ash.

4.3.4.4 Sulphate Resistance

Permeability of concrete plays an important role in protecting it against external sulphate attack. Sulphate attack can take the form of expansion, loss in compressive strength and loss in mass of concrete. The sulphate related expansion of concrete is associated with the formation of etteringites and gypsum. Since magnesium sulphate attack is more severe on concrete, the concrete specimens were immersed in a 10% solution of magnesium sulphate. The test results of change in length of prism specimens due to external sulphate attack at various immersion ages are presented in Fig. 4.25. The expansion of bottom ash concrete specimens increased with progress of immersion age in a similar pattern as that of the control concrete specimen. At 28 days of immersion period, the expansion values of bottom ash concrete mixtures $A_{20,}$ $A_{30,}$ $A_{40,}$ $A_{50,}$ A_{75} and A_{100} were 53.33 x 10^{-6}, 60 x 10^{-6}, 66.67 x10^{-6}, 60 x10^{-6}, 53.33 x10^{-6}, and 53.33 x10^{-6}, respectively, as compared to 50 x10^{-6} of control concrete. At 150 days of immersion period, the expansion strains of bottom

ash concrete mixtures $A_{20,}$ $A_{30,}$ $A_{40,}$ $A_{50,}$ A_{75} and A_{100} was 5.56, 16.67, 27.78, 33.33, 33.33, and 38.89%, respectively, higher than that of control concrete. At 180 days of immersion period, the expansion strains of bottom ash concrete specimens increased by 175, 166.67, 160, 200, 237.52 and 250%, respectively, over the expansion strains at 28 days of immersion period as compared to 180% increase of 28-day expansion strain of control concrete. After 210 days of immersion in sulphate solution, the total expansion of bottom ash concrete mixtures incorporating 30, 50, 75 and 100% coal bottom ash was 180 x 10^{-6}, 193.33 x 10^{-6}, 200 x 10^{-6} and 200 x 10^{-6}, respectively, as compared to 160 x 10^{-6} that of control concrete. At the end of test i.e. 365 days, total expansion of bottom ash concrete mixtures $A_{20,}$ $A_{30,}$ $A_{40,}$ $A_{50,}$ A_{75} and A_{100} was 350 x 10^{-6}, 373.3 x 10^{-6}, 380 x 10^{-6}, 373.33 x 10^{-6}, 406.67 x $10^{-6}$and 436.67 x 10^{-6}, respectively, as compared to 333.33 x 10^{-6} of control concrete. Total expansion of bottom ash concrete mixture containing 100% coal bottom ash concrete was 31% more than that in control concrete. The results obtained in the present study are comparable with those reported by Ghafoori and Bucholc (1996, 1997); and Ghafoori and Cai (1998).

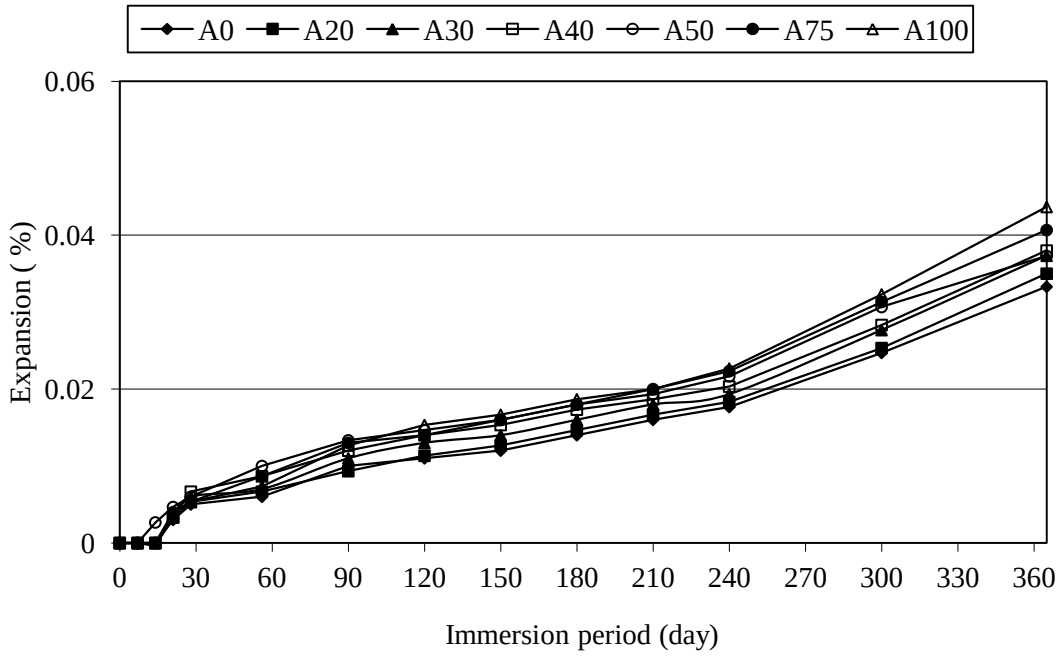

Fig. 4.25: Effect of coal bottom ash on expansion of concrete due to external attack of sulphate (Concrete 'A')

Mass Loss

Up to 240 days of immersion period, no cracks and spalling were observed in bottom ash concrete as well as control concrete specimens. After 365 days of immersion in 10%

magnesium sulphate solution, mass loss in bottom ash concrete specimens $A_{20,}$ $A_{30,}$ $A_{40,}$ $A_{50,}$ A_{75} and A_{100} was 0.56, 0.57, 0.66, 0.68, 0.51 and 0.24%, respectively, as compared to 0.72% in control concrete.

Change in Compressive Strength

Test results of compressive strength after immersion in 10% magnesium sulphate solution are presented in Fig. 4.26. The test results show that no reduction in compressive strength took place after immersion in 10% magnesium sulphate solution, rather it continued to increase during the test period. The increase in compressive strength of concrete mixtures after immersion in magnesium sulphate solution over their 28-day compressive strength is illustrated in Fig. 4.27. After 28 days of immersion period, percentage increase in compressive strength of bottom ash concrete mixtures was lower than that of control concrete. However, after 90 days of immersion period, increase in compressive strength of bottom ash concrete mixtures A_{40}, A_{75} and A_{100} was higher than that of control concrete. After 180 days of immersion period, the increase in 28-day compressive strength of bottom ash concrete mixtures $A_{20,}$ $A_{30,}$ $A_{40,}$ $A_{50,}$ A_{75} and A_{100} was 25.36, 27.11, 29.92, 32.97, 30.48 and 30.65%, respectively, as compared to 26.75% increase in 28 day compressive strength of control concrete. After 365 days of immersion period, compressive strength of bottom ash concrete mixtures $A_{20,}$ $A_{30,}$ $A_{40,}$ $A_{50,}$ A_{75} and A_{100} was 45.02, 46.27, 42.84, 42.48, 43.89 and 40.09 N/mm^2, respectively, as compared to 47.73 N/mm^2 of control concrete. This indicates that the cement continued to hydrate in magnesium sulphate solution over the test period.

The increase in strength of concrete may be attributed to continuous hydration and the filling of pores with compounds formed by the reaction of sulphate. The reason for insignificant mass loss and no reduction in compressive strength and continued expansions may be the formation ettringites within the confined voids. The continued hydration of concrete specimens and formation of ettringites interrupted the continuity of pores, which resulted in further reduction in its permeability. The reduced continuity of voids prevented the penetration of sulphate ions into the concrete. Low permeability of bottom ash concrete specimens may also be the reason for the better performance against sulphate attack.

Irassar et al. (1996) reported that the compressive strength of concrete containing 40% fly ash as cement replacement increased by 86% and 144% over their 28-day compressive strength after 1 year and 5 year immersion period respectively. Brown (1981) reported that the compressive strength of mortars increased initially after the immersion in a sulphate solution. After certain expansion strains, the compressive strength started decreasing. The beginning of loss of compressive strength of mortars corresponds to 0.1% expansion (Ouyang et al., 1988; Ouyang, 1989). In the present study, even after 365 days of immersion period, the expansion strains of all bottom ash concrete mixtures remained well below than 0.1%.

Table 4.10 Compressive strength of concrete after 28 days of water curing (Concrete 'A')

Mix	A_0	A_{20}	A_{30}	A_{40}	A_{50}	A_{75}	A_{100}
28-day compressive strength (N/mm^2) - Water cured	38.21	36.48	37.11	37.80	37.25	37.5	34.98

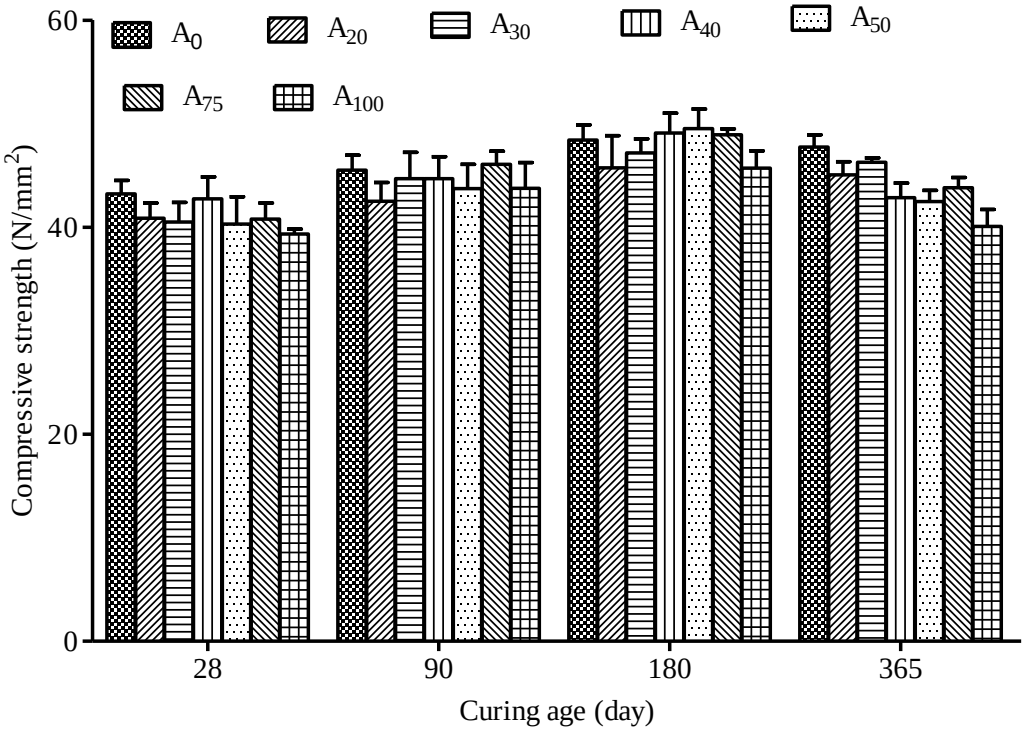

Fig. 4.26: Compressive strength of concrete after immersion in sulphate solution (Concrete 'A')

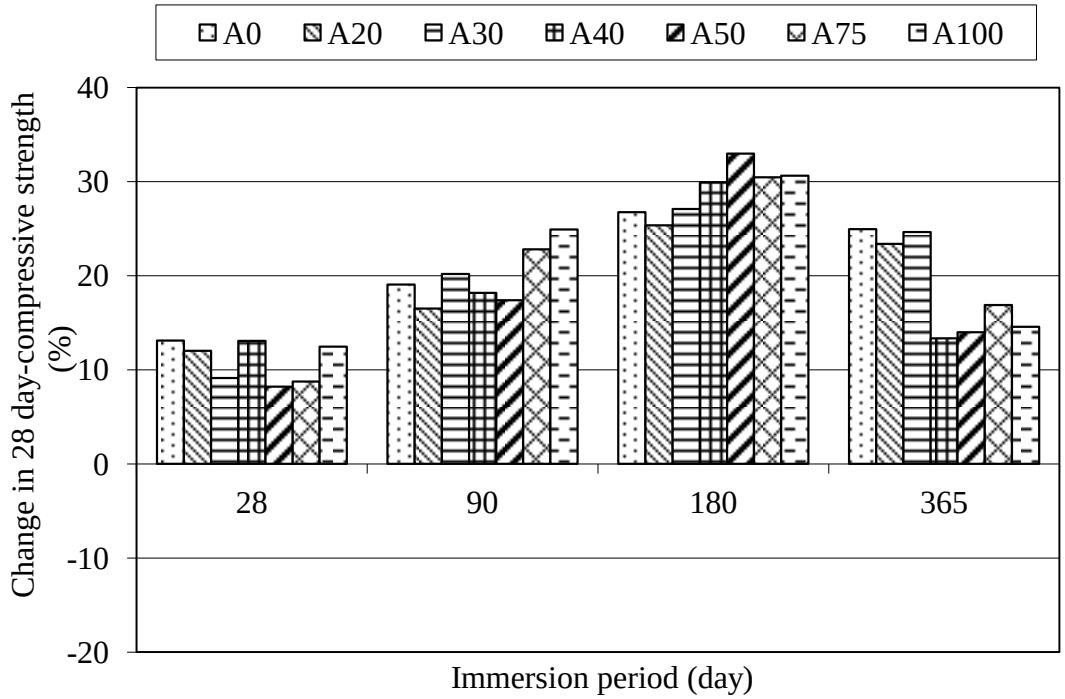

Fig. 4.27: Change in 28-day compressive strength after immersion in sulphate solution (Concrete 'A')

Microstructure

Scanning electron micrographs (SEM) of concrete mixtures after 180 days of immersion in 10% magnesium sulphate solution are shown in Figs. 4.28 to 4.30. In this study, fractured pieces of concrete were mounted on the SEM stub and images were obtained using secondary electron (SE) image mode. The concrete specimens were coated with thin layer of gold to make them electrically conductive before placing on the scanning electron microscopy (SEM) stem. It is apparent from the SEM images that sulphate ion diffusion did not take place even to a depth near to the surface. No signs of gypsum and monosulfate morphologies, which can indicate the attack by sulphate, were observed in either of the concrete mixtures. At higher resolution, very small ettringite needles in few voids were observed in the concrete mixtures. All the SEM images show dense and evenly spread calcium silicate hydrate gel. Energy dispersive spectroscopy (EDS) analysis results are presented in Table 4.12. The small fraction of sulphur content in the concrete mixtures observed in EDS analysis might have been due to sulphur trioxide present in cement or coal bottom ash.

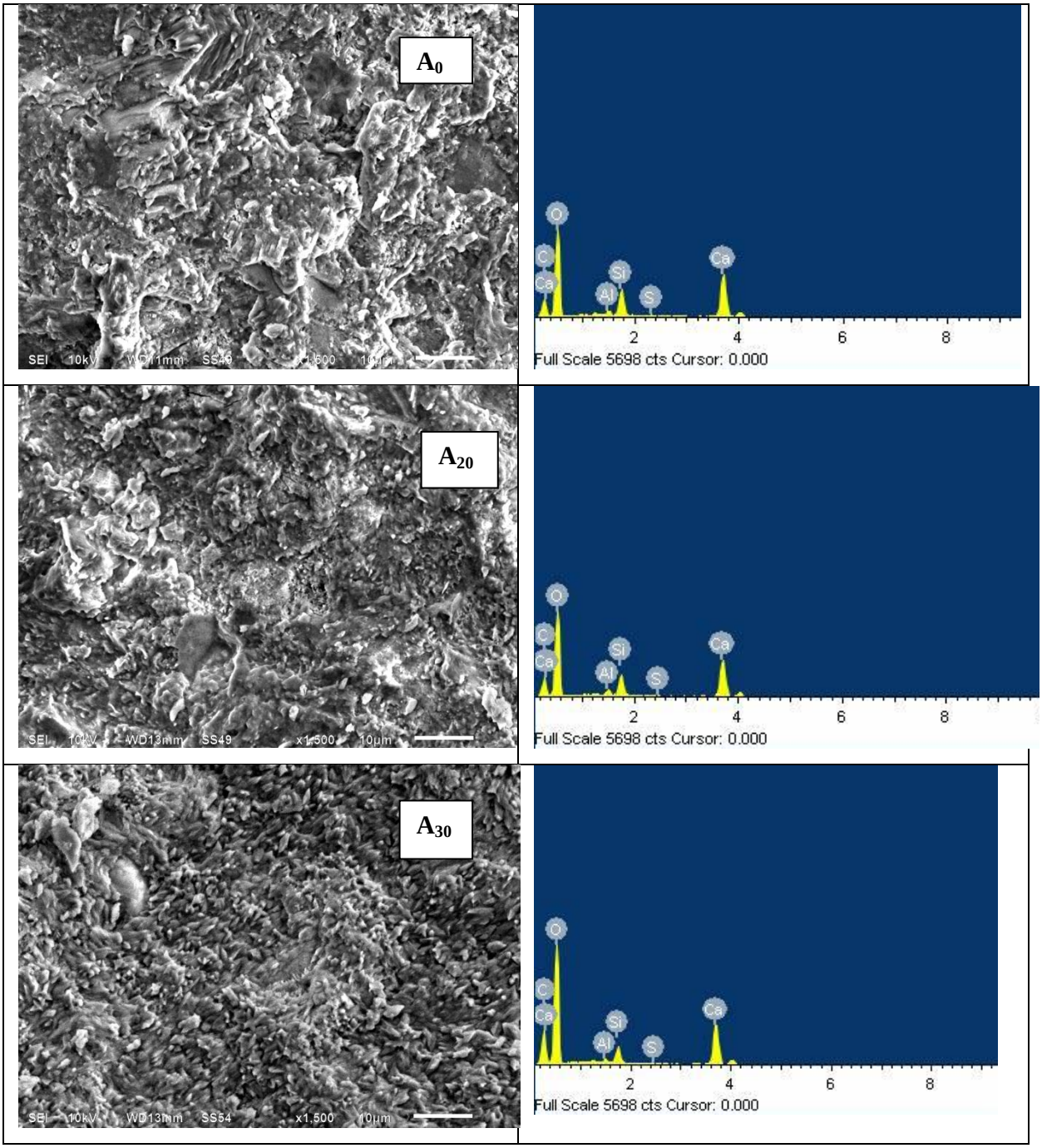

Fig. 4.28: Scanning electron micrograph and EDS spectrum of bottom ash concrete (A_{20} and A_{30}) and control concrete after 180 days of immersion period in magnesium sulfate solution

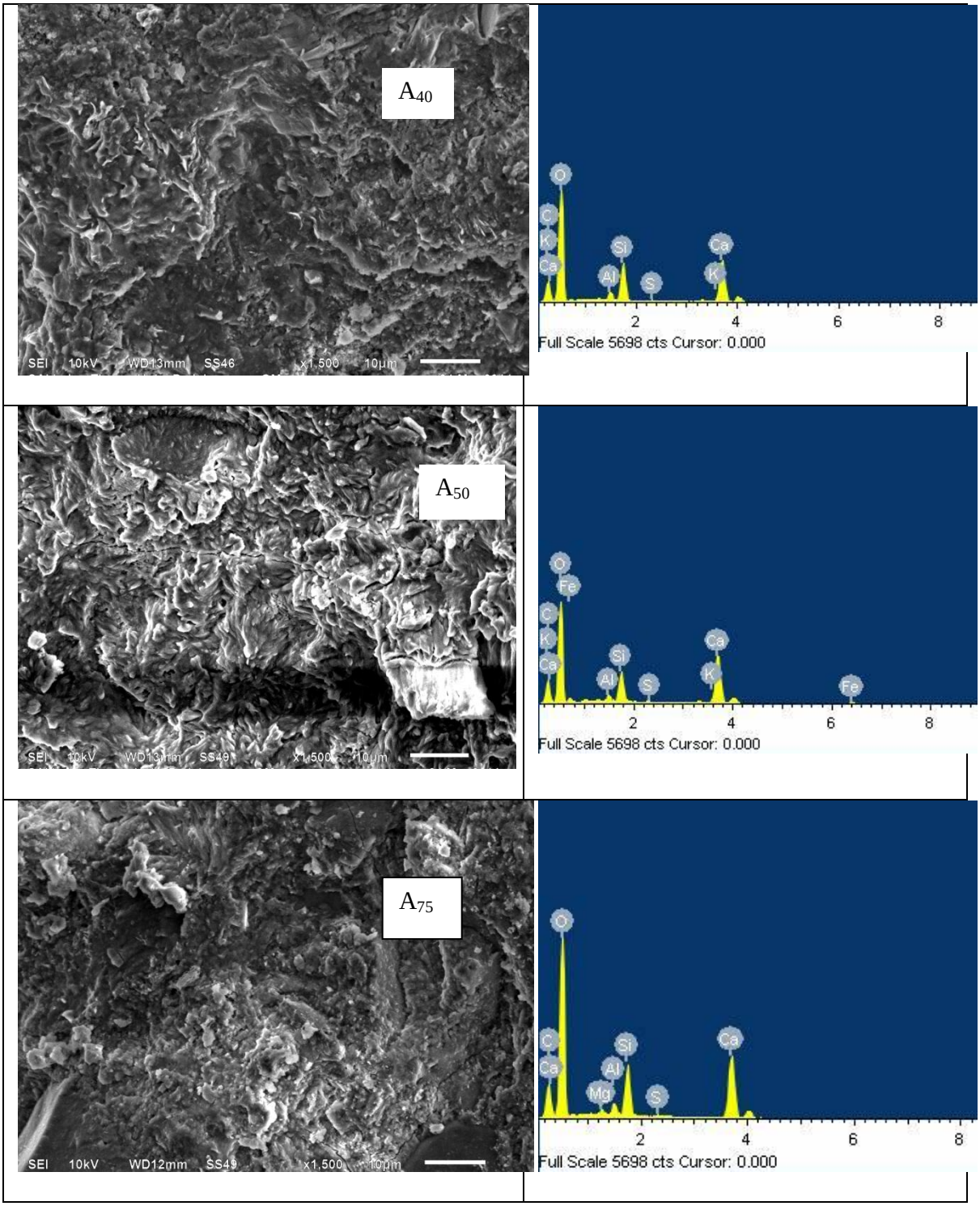

Fig. 4.29: Scanning electron micrograph and EDS spectrum of bottom ash concrete ($A_{40,}$ $A_{50,}$ A_{75}) after 180 days of immersion period in magnesium sulfate solution

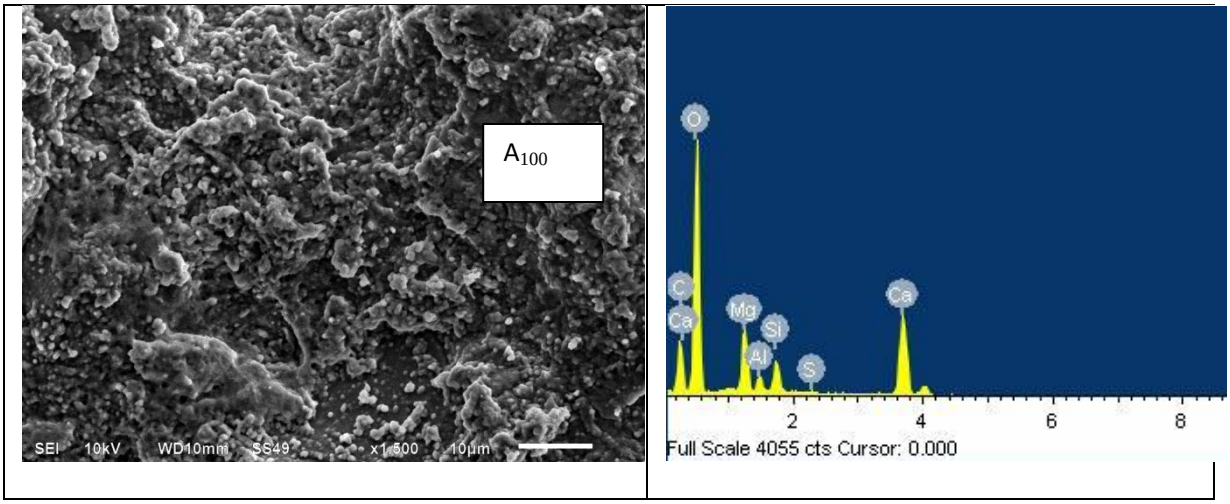

Fig. 4.30: Scanning electron micrograph and EDS spectrum of bottom ash concrete (A_{100}) after 180 days of immersion period in magnesium sulfate solution

Table 4.11 Chemical composition of concrete after immersion in 10% magnesium sulfate solution for 180 days (Concrete 'A')

Element	**Weight (%) in concrete mixtures**						
	A_0	**A_{20}**	**A_{30}**	**A_{40}**	**A_{50}**	**A_{75}**	**A_{100}**
Ca	12.16	11.08	9.06	15.63	16.84	9.88	8.06
Si	4.85	4.08	2.23	8.67	6.60	4.97	2.06
Al	0.77	0.92	0.42	1.87	1.25	1.11	0.9
K	-	-	-	0.52	0.48	-	-
Mg	-	-	-	-	-	0.42	4.92
C	19.23	20.16	22.29	15.04	15.61	19.72	20.22
O	62.71	63.69	65.97	58.14	57.66	63.70	63.69
S	0.28	0.07	0.03	0.13	0.15	0.21	0.15
Fe	-		-	-	1.42	-	-

XRD Phase Identification

X-Ray spectrums of concrete mixtures after 180 days of immersion period in 10% magnesium sulphate solution are shown in Figs. 4.31 to 4.33. The cement pastes were separated from the concrete samples and were sieved through 90 µm sieve. The XRD investigations were performed for diffraction angle 2θ ranged between 5° and 80° in steps

of 2θ = 0.017°. The diffraction pattern, list of d-spacing and relative intensities of diffraction peaks was prepared. This data was compared with the standard peaks of compounds in the diffraction database released by International Centre for Diffraction Data (ICDD). Peaks of gypsum and calcium sulfoaluminate hydrates were not observed in the XRD spectrums of either of concrete mixtures. The XRD and SEM analysis indicate the bottom ash concrete specimens were not damaged by the external attack of sulphate. The increase in compressive strength of bottom ash concrete also supports that sulphate ions could not penetrate and deteriorate the concrete specimens up to the age of the test. After 180 days of immersion period in a 10% solution of magnesium sulphate, no change in phase composition of concrete was observed in XRD spectrums. Analysis of XRD spectrums indicates that the absolute intensity of portlandite peaks of bottom ash concrete mixtures except A_{20} mixture was lower than that in control concrete. The total intensity of portlandite (d = 4.90°A and 2.62°A) in bottom ash mixtures A_{20}, A_{30}, A_{40}, A_{50}, A_{75}, and A_{100} was 2073, 1715, 1523, 1610, 1488 and 1715 counts, respectively, as compared to 1901 counts in control concrete. Assuming total intensity of a phase is connected with the amount of that phase present in the concrete mixture, the lower intensities of portlandite indicate that the influence of coal bottom ash is significant in case of portlandite phase.

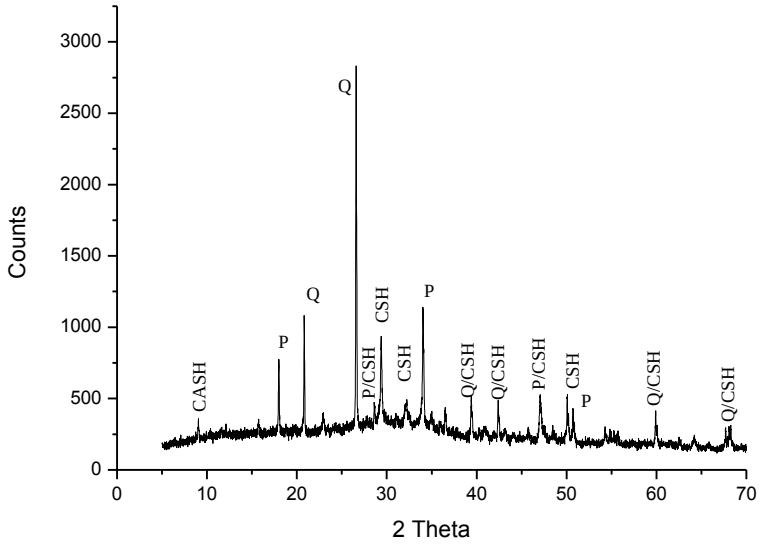

Fig. 4.31: XRD spectrum of control concrete (Concrete A) after 180 days of immersion period in magnesium sulfate solution (CASH = Calcium alumino silicate hydrate; CSH = Calcium silicate hydrate; P = Portlandite; Q = Quartz)

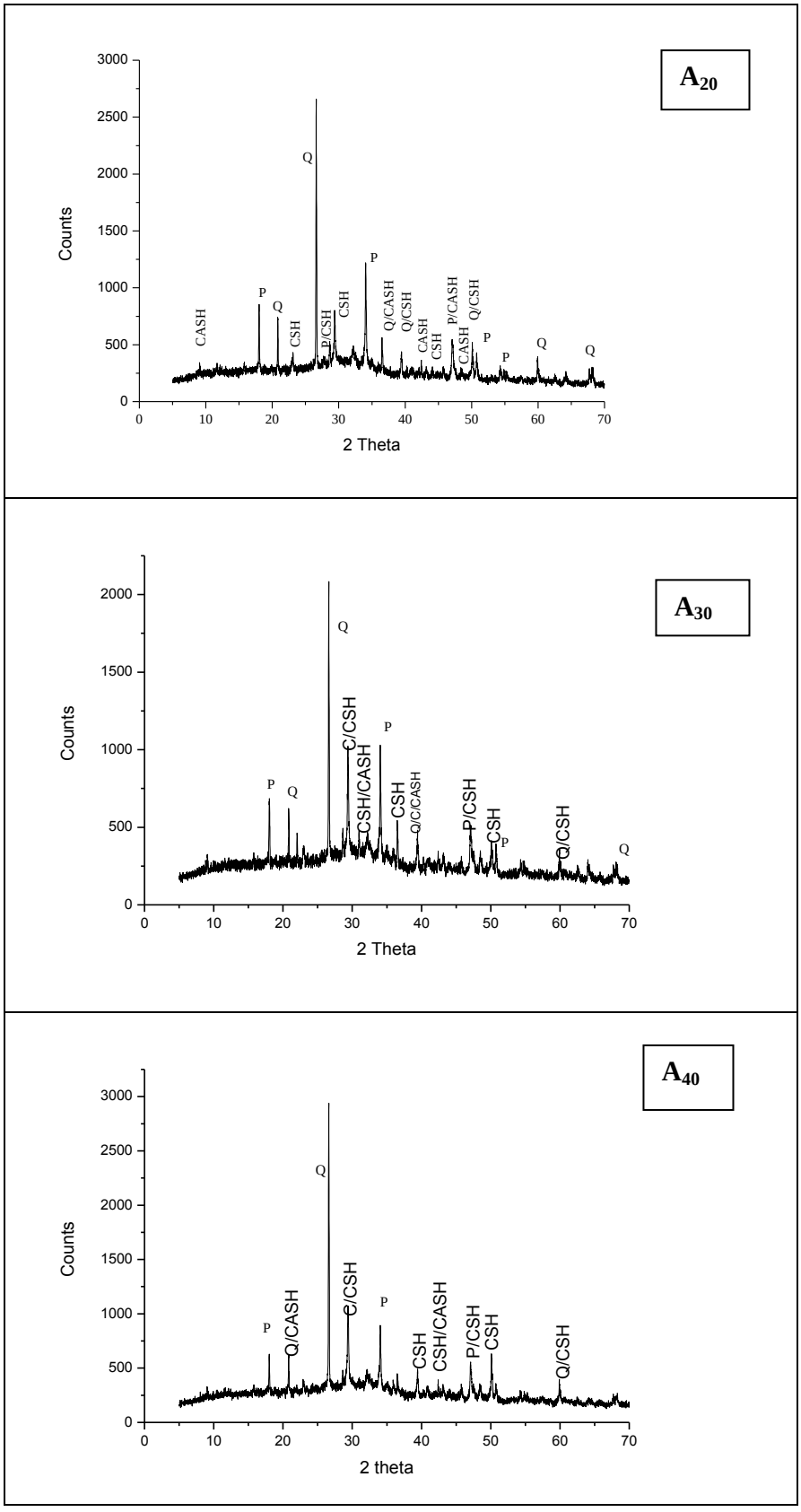

Fig. 4.32: XRD spectrum of bottom ash concrete (A_{20}, A_{30}, and A_{30}) after 180 days of immersion period in magnesium sulfate solution (CASH = Calcium alumino silicate hydrate; CSH = Calcium silicate hydrate; P = Portlandite; Q = Quartz)

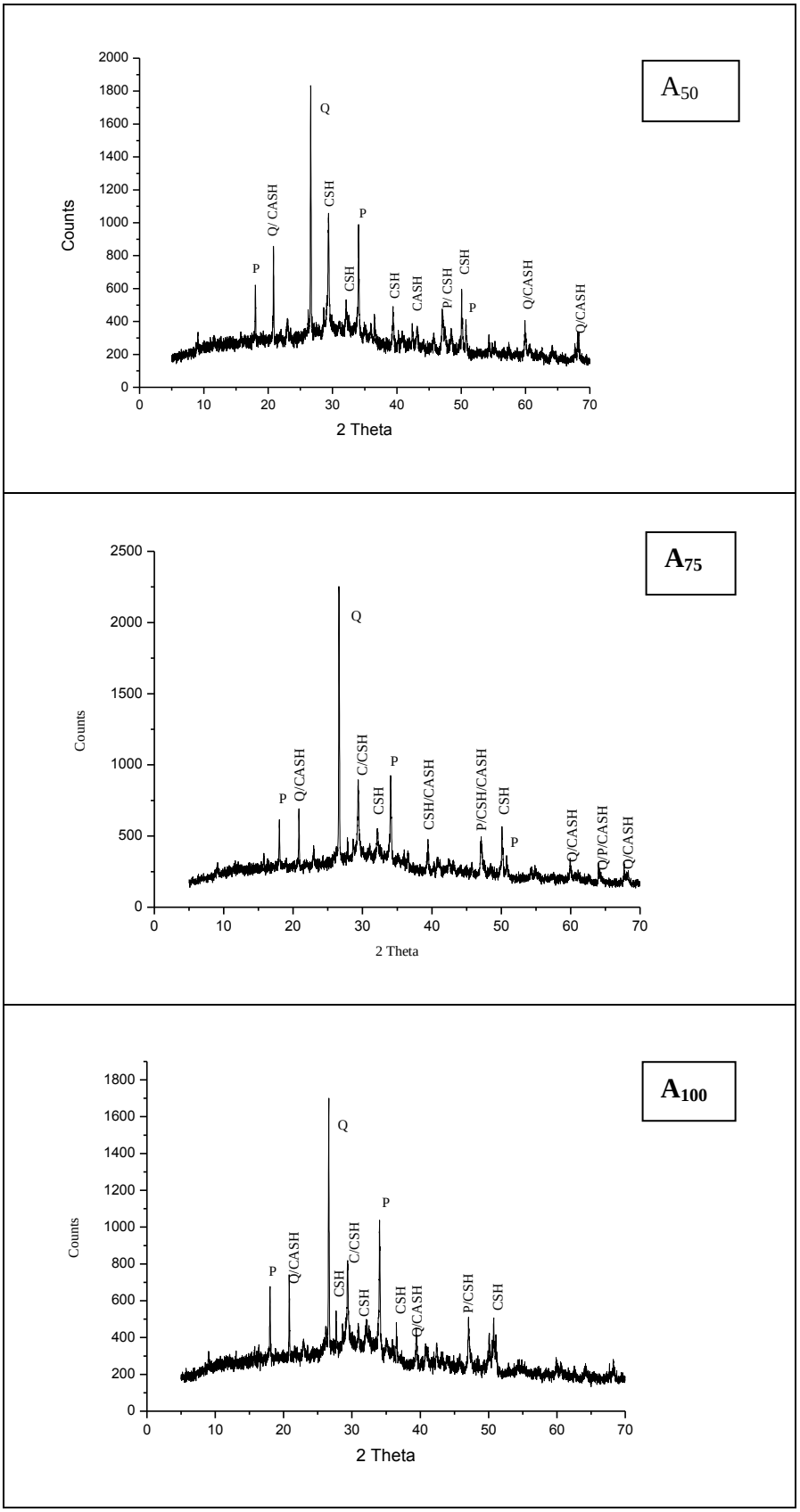

Fig. 4.33: XRD spectrum of bottom ash concrete (A_{50}, A_{75} and A_{100}) after 180 days of immersion period in magnesium sulfate solution (CASH = Calcium alumino silicate hydrate; CSH = Calcium silicate hydrate; P = Portlandite; Q = Quartz)

4.3.4.5 Acid Resistance

Concrete being alkaline in nature is susceptible to attack by sulfuric acid formed from either bacterium processes in sewage system or sulfur dioxide present in the atmosphere in the industrial areas. The sulfuric acid formed in the sewer pipes by bacterium causes corrosion of concrete sewer lines. The anaerobic and aerobic environments are required to produce sulfuric acid in sewer pipes. *Desulfovibrio,* an anaerobic bacterium utilizes sulphates in sewer as an oxygen source and reduce the sulfate compounds to sulfide. The sulfide reacts with dissolved hydrogen to form hydrogen sulfide. Hydrogen sulfide gas rises to the top of the sewer pipe and reacts with oxygen and forms sulfate. *Thiobacilli* bacterium combines the hydrogen with sulfate through oxidation and forms sulfuric acid. Sulfuric acid so formed attack the paste and produces gypsum, which is soluble in water. Sulfuric acid reacts with calcium hydroxide and produces calcium sulfate ($CaSO_4$). The reaction of sulfuric acid with calcium silicate hydrate also results in forming of silicate oxide in aqueous state. Weight loss and compressive strength of the test specimens versus immersion time in sulphuric acid solutions are shown in Figs. 4.34 and 4.35, respectively. Compressive strength and Loss of weight are an average of three specimens of the same mix. The data for the individual specimens varied less than 5 percent of the average values.

Mass Loss

Fig.4.34 shows the percentage loss of weight of concrete specimens after immersion in 3% sulphuric acid solution. Bottom ash concrete specimens performed slightly better than the control concrete, when immersed in 3% sulphuric acid solution. After 28 days of immersion period, the weight loss of bottom ash concrete mixtures $A_{20,}$ $A_{30,}$ $A_{40,}$ $A_{50,}$ A_{75} and A_{100} was 9.53, 10.05, 8.97, 8.94, 8.75, and 7.89%, respectively, as compared to 10.87% weight loss of the control concrete. Percentage loss of weight of bottom ash concrete specimens decreased with increase in coal bottom ash content in concrete. At 56 days of immersion period, weight loss of bottom ash concrete mixtures $A_{20,}$ $A_{30,}$ $A_{40,}$ $A_{50,}$ A_{75} and A_{100} increased to 11.84, 11.23, 10.8, 11.38, 10.75, and 10.2%, respectively. However, weight loss of control concrete during the same period was 11.98%. At 84 days of immersion period, percentage weight loss decreased from 13.01 to 11.65% on incorporation of 100% coal bottom ash as fine aggregate in concrete. The lower percentage weight loss of bottom ash concrete mixtures can be attributed to lower permeability of bottom ash concrete mixtures as compared to that of control concrete.

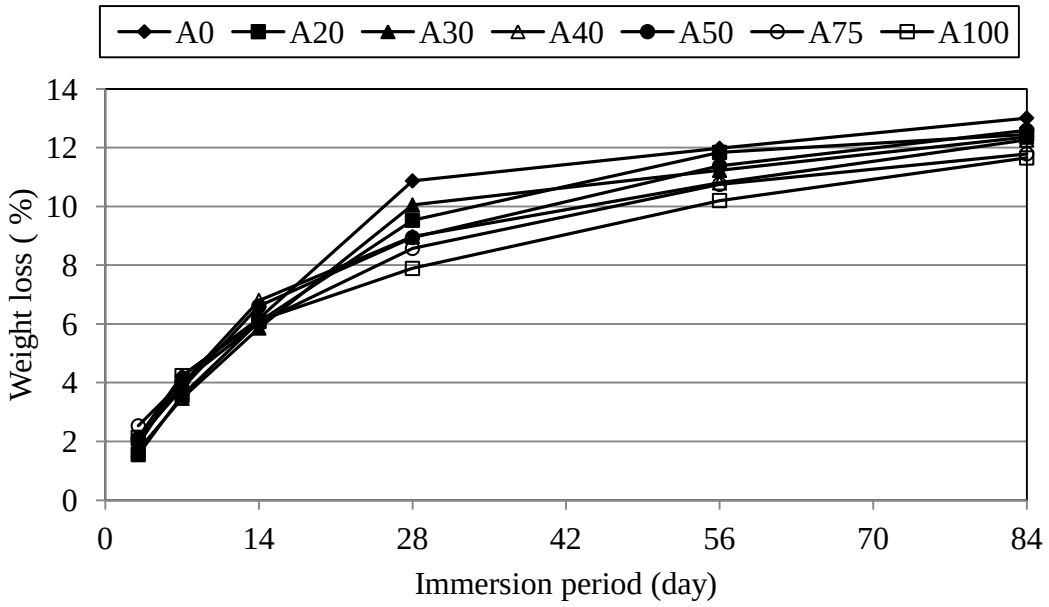

Fig. 4.34: Effect of coal bottom ash on resistance of concrete to external attack of acid -weight loss (Concrete 'A')

Reduction in 28- day Compressive Strength

Fig.4.35 shows the compressive strength of concrete specimens after immersion in 3% sulphuric acid solution. After 7 days of immersion in sulphuric acid solution, compressive strength of bottom ash concrete mixtures $A_{20,}$ $A_{30,}$ $A_{40,}$ $A_{50,}$ A_{75} and A_{100} decreased by 26.26, 25.95, 19.84, 20.94, 28.00 and 25.82%, respectively, as compared to 25.94% decrease in compressive strength of control concrete. 28-day compressive strength of control concrete and bottom ash concrete mixture incorporating 100% coal bottom ash decreased from 38.21 to 28.3 N/mm^2 and from 34.98 to 25.95 N/mm^2, respectively, after 7 days of immersion period. After 28 days of immersion period, 28-day compressive strength of all specimens decreased drastically. The loss in 28-day compressive strength of control concrete, $A_{20,}$ $A_{30,}$ $A_{40,}$ $A_{50,}$ A_{75} and A_{100} was 49.23, 48.76, 50.00, 49.10, 40.32, 35.52 and 37.11%, respectively. After 84 days of immersion period, loss in 28 day compressive strength of the above mixes increased to 65.72, 65.84, 58.37, 59.66, 58.77, 59.63 and 56.40%, respectively. The percentage loss of 28-day compressive strength decreased with increase in coal bottom ash content in concrete. Weakening of concrete matrix, loss of cement paste and reduction in size of specimens due to sulphuric acid attack resulted into reduction in 28-day compressive strength of concrete. It is believed that lower permeability and pozzolanic activity of bottom ash concrete mixtures contributed to resistance to external sulphuric acid attack.

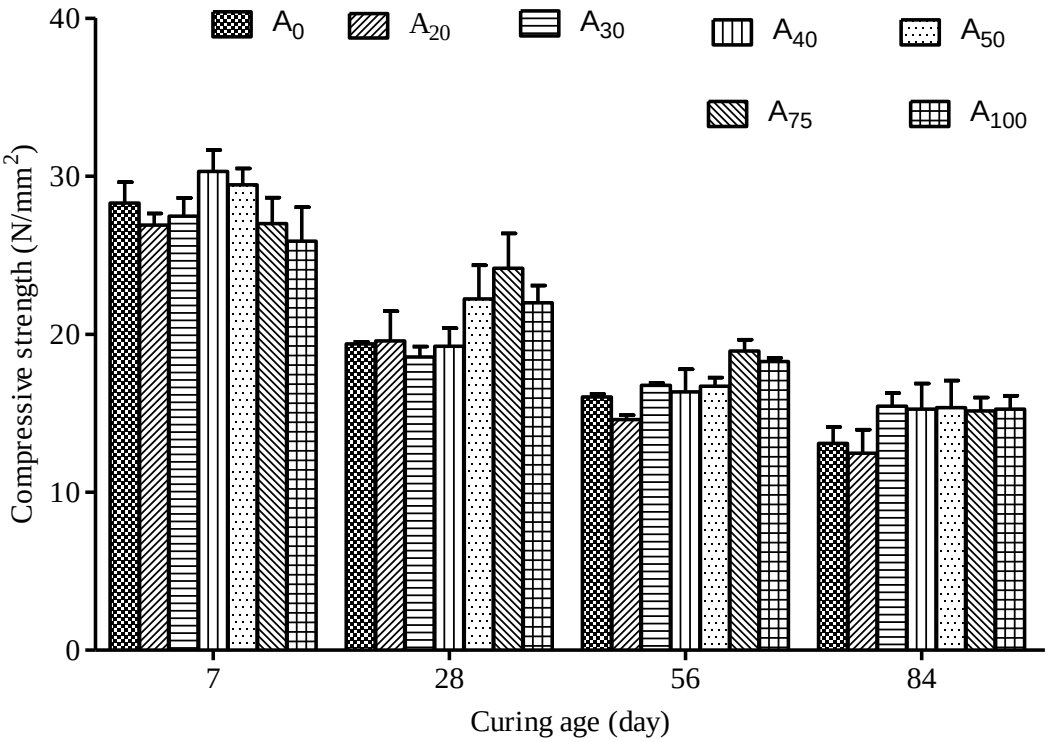

Fig. 4.35: Effect of coal bottom ash on resistance of concrete to external attack of acid - loss of compressive strength (Concrete 'A')

4.3.4.6 Abrasion Resistance

The test results of wear depth of bottom ash concrete and control concrete are shown in Figs 4.36 to 4.39. The test results show that average depth of wear increased with the increase in abrasion time. It can be seen from the test results that average depth of wear of control concrete mixture as well as bottom ash concrete mixtures decreased with increase in curing period. This indicates improvement in resistance to abrasion of all concrete mixtures with age. The continued hydration and densification of the concrete matrix with increasing age may be the possible explanation for decrease in average depth of wear of concrete. However, at all curing periods, average depth of wear of bottom ash concrete mixtures increased with the increase in substitute rate of river sand with coal bottom ash. Fig. 4.37 shows variation in the average depth of wear with coal bottom ash content in concrete. At 28 days of curing period, average depth of wear of bottom ash concrete mixtures A_{20} (20% CBA), A_{30} (30% CBA), A_{40} (40% CBA), A_{50} (50% CBA), A_{75} (75% CBA) and A_{100} (100% CBA) for 15 min of wear time was 10.03, 20.00, 23.68, 27.52, 31.20 and 47.62%, respectively, higher than that of control concrete. However, average depth of wear after 7.5 min of wear time of bottom ash concrete mixture A_{100} was 0.78 mm

against 2 mm specified in BIS: 1237-1980 for heavy duty tiles. At 90 days of curing period, the average depth of wear for bottom ash concrete mixtures A_{20}, A_{30}, A_{40}, A_{50}, A_{75}, and A_{100} for 15 min of wear time was 0.802, 0.849, 0.856, 0.897, 0.956 and 1.013 mm, respectively, as compared to 0.7695 mm of control concrete. At 180 days of curing age, average depth of wear of bottom ash concrete mixtures A_{20}, A_{30}, A_{40}, A_{50}, A_{75}, and A_{100} reduced to 0.6213, 0.6514, 0.7289, 0.7873, 8657 and 0.9165 mm, respectively, whereas for control concrete, it reduced to 0.5519 mm. At 180 days of curing period, average depth of wear of bottom ash concrete mixtures $A_{20,}$ A_{30}, A_{40}, A_{50}, A_{75}, and A_{100} reduced by 24.96, 31.98, 26.15, 22.63, 17.32 and 19.45%, respectively, over average depth of wear at 28 days of curing period as compared to a reduction of 30.84% in average wear depth for control concrete. At 365 days of curing period, bottom ash concrete mixtures $A_{20,}$ A_{30}, A_{40}, A_{50}, A_{75}, and A_{100} were 4.10, 11.54, 14.75, 20.96, 28.65, and 33.08%, respectively, worse at resisting abrasion than control concrete. The compressive strength of concrete strongly influenced the average depth of wear. The test results showed that compressive strength has good relation with the abrasion resistance of bottom ash concrete specimens. Fig.4.40 shows that the average depth of wear increased almost linearly with increase in coal bottom ash content. Siddique (2013) also reported that there was decrease in abrasion resistance of self compacting concrete (SCC) mixtures with increase in bottom ash content in concrete. Further, the abrasion resistance of self compacting concrete (SCC) mixtures increased with the increase in age for all mixtures.

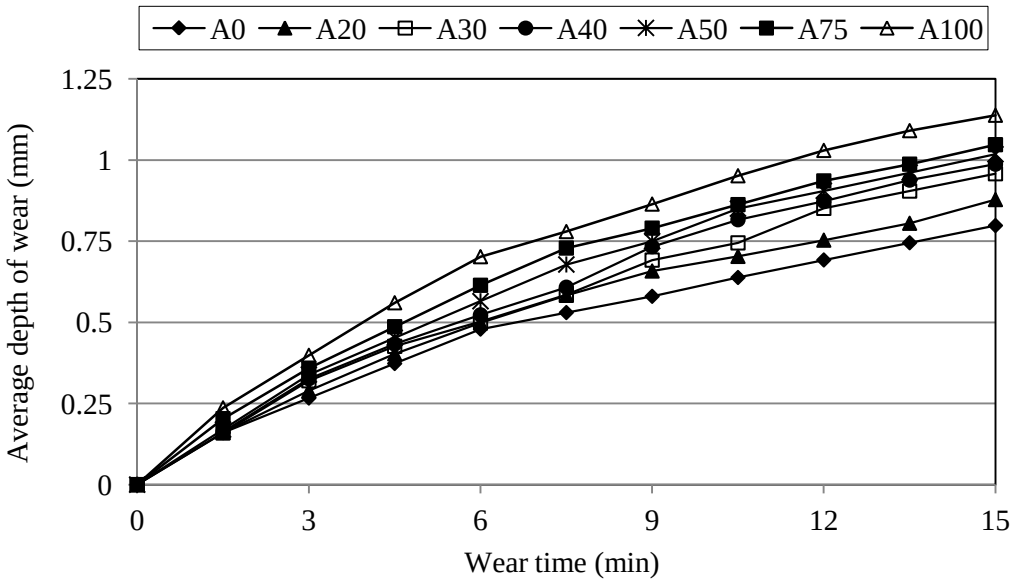

Fig. 4.36: Variation in depth of wear with coal bottom ash content in concrete at 28 days of curing age (Concrete 'A')

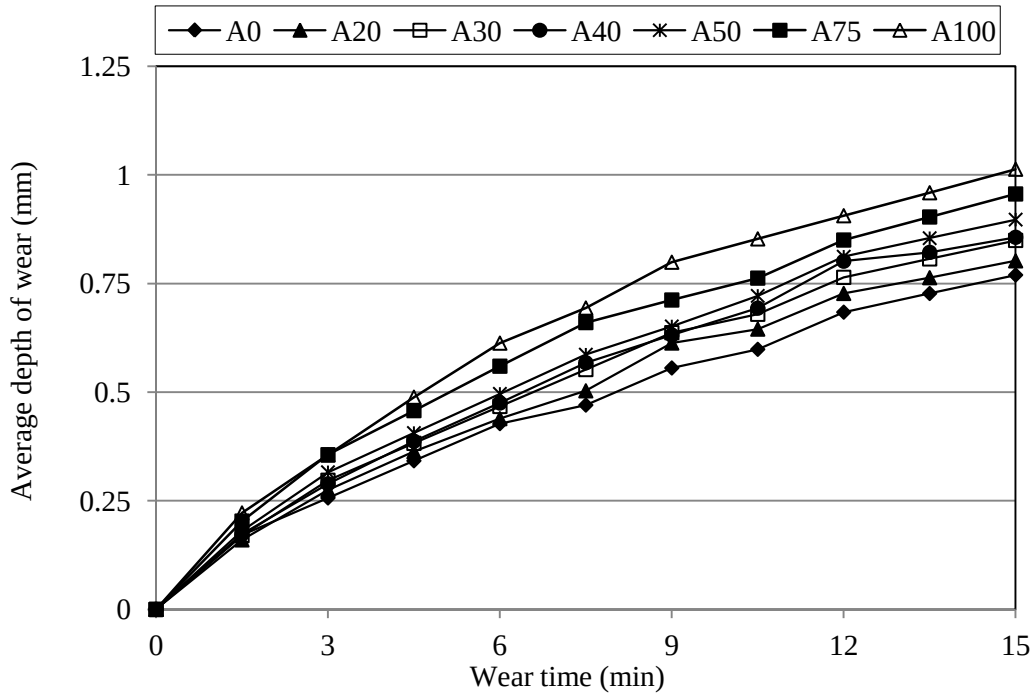

Fig.4.37: Variation in depth of wear with coal bottom ash content in concrete at 90 days of curing age (Concrete 'A')

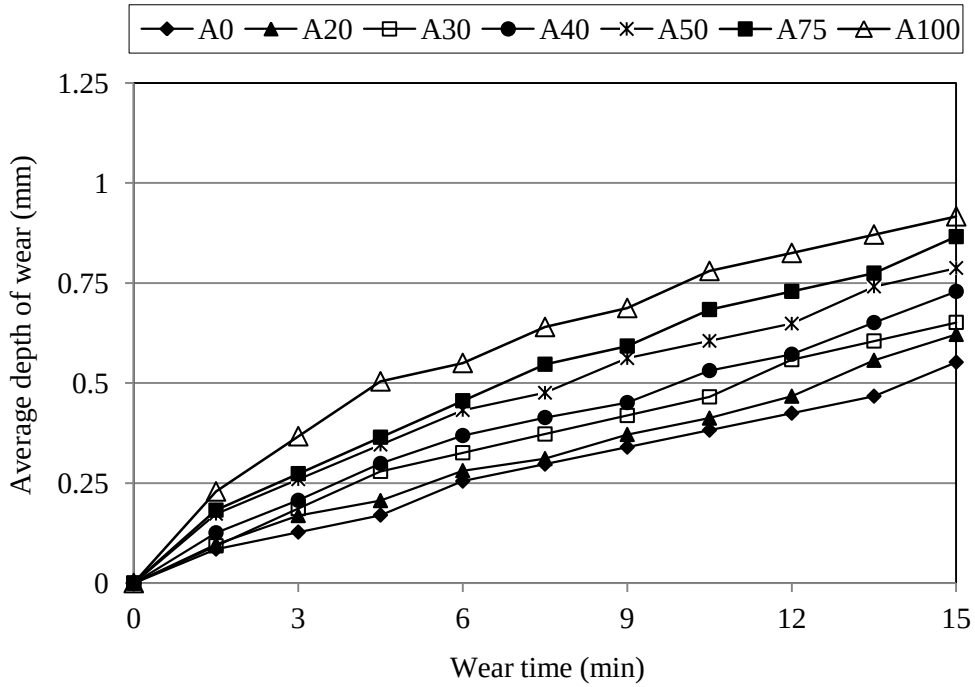

Fig. 4.38: Variation in depth of wear with coal bottom ash content in concrete at 180 days of curing age (Concrete 'A')

As seen in Fig. 4.63, average depth of wear decreased almost linearly with the increase in compressive strength of concrete.

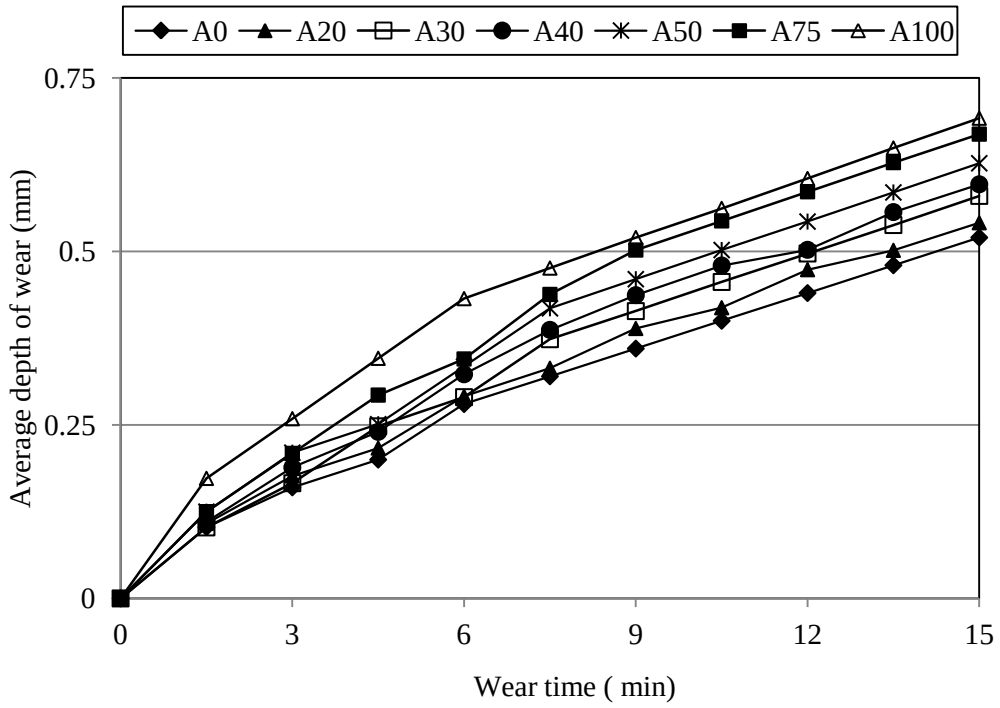

Fig. 4.39: Variation in depth of wear with coal bottom ash content in concrete at 365 days of curing age (Concrete 'A')

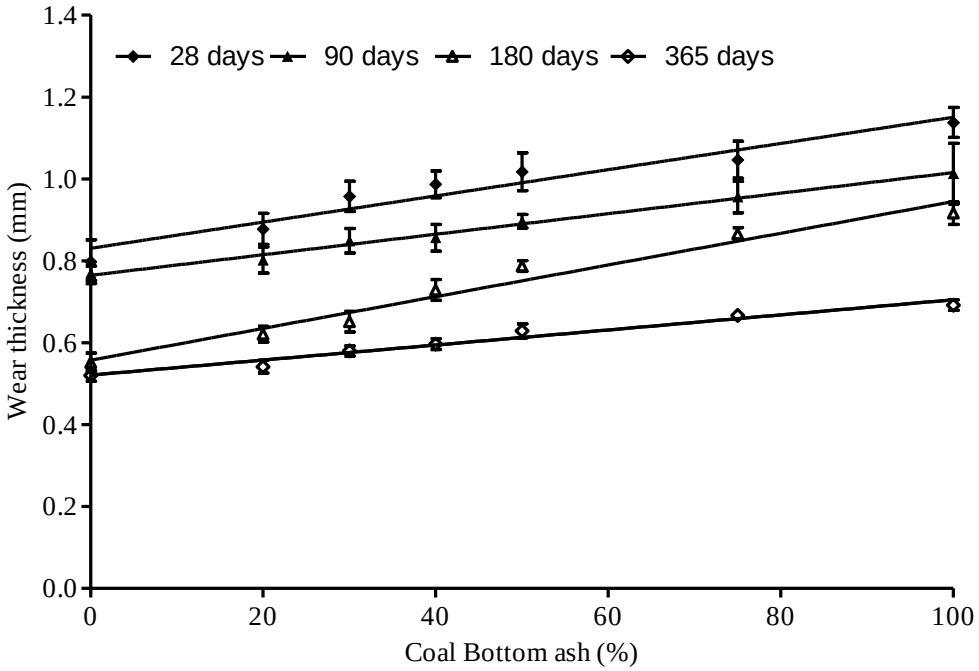

Fig. 4.40: Variation in abrasion resistance of concrete with coal bottom ash content (Concrete 'A')

4.3.5 Micro-Structural Properties of Concrete

The mechanical properties of concrete depend on its intrinsic microstructure. The concrete microstructure features are mainly affected by the hydration period, water cement ratio, addition of mineral admixtures and type of cement used in the production of concrete. The microstructure of concrete consists of hydrated cement paste, aggregate and interfacial transitional zone. The scanning electron microscopy (SEM) plays a significant role in resolving the microstructure of concrete. Scanning electron microscopy provides both topographic and compositional analysis of materials. In this study, fractured pieces of concrete generated from the compressive strength tests were mounted on the SEM stub and images were obtained using secondary electron (SE) image mode.

SEM images of control concrete and bottom ash concrete mixtures are shown in Figs. 4.41 to 4.50. Fig.4.41 shows dense, compact and continuous CSH gel, ettringite needles and large crystals of portlandite deposits in the cement paste of control concrete. In case of bottom ash concrete mixture containing 30% of coal bottom ash as shown in Fig. 4.43, the CSH gel structure is dense, compact and consists of crumpled sheets. The CSH gel is evenly spread over the entire image. At higher resolution, early products of C_3S hydration consisting of small foils and flakes were also observed. When the sand replacement level was increased from 50 to 100%, compact CSH structure of equant grains of a size less than 1.0 μm was observed in bottom ash concrete samples but the CSH gel structure was slightly less monolithic than that of control concrete. The comparatively small sized pores and portlandite crystals were observed in bottom ash concrete mixtures. The development of ettringite in the form of needles in the voids was also observed in bottom ash concrete as well as control concrete mixtures. In case of bottom ash concrete containing higher volumes of coal bottom ash, tiny air voids formed by the air released during absorption of water internally by the particles of coal bottom ash were also seen in the SEM images. As shown in Fig.4.47 at 100% sand replacement level, the number and size of voids comparatively increased. The slight decrease in compressive strength of bottom ash concrete at 28 days of curing age can be attributed to the variation in the microstructure of bottom ash concrete samples from that of control concrete due to slow pozzolanic activity of coal bottom ash. Figs 4.41 to 4.47 also show the morphology and energy dispersive spectroscopy spectrum of calcium hydroxide, calcium silicate hydrate, calcium alumino silicate hydrate, ettringite, calcium (alumino-ferrite) silicate hydrate, calcium aluminates and calcium silicate.

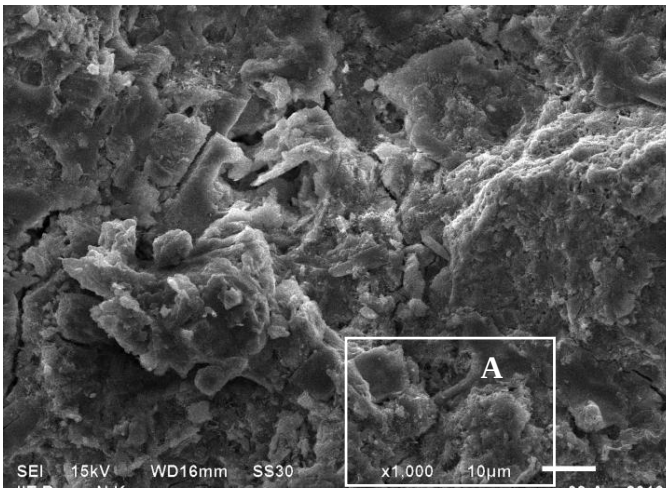

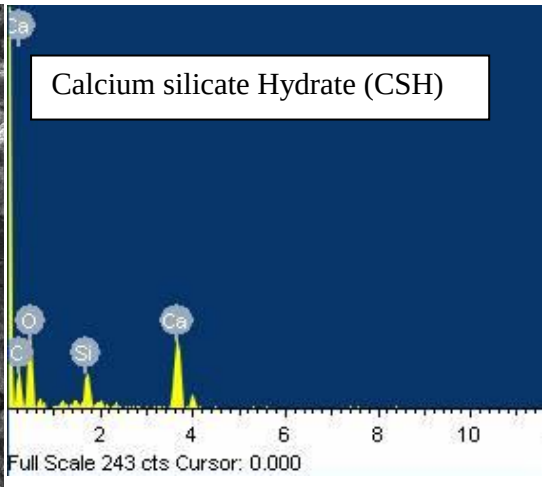

x 1000

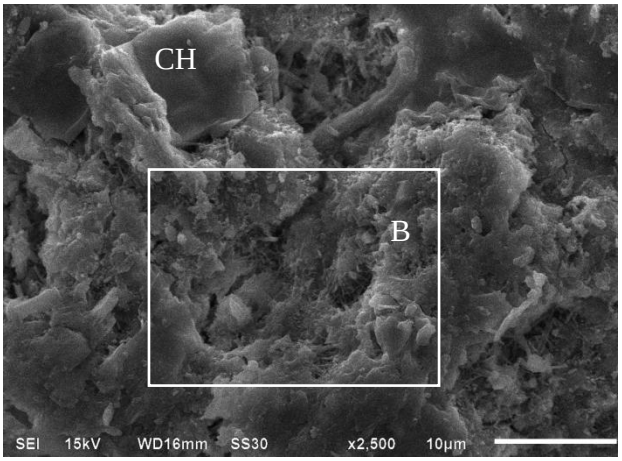

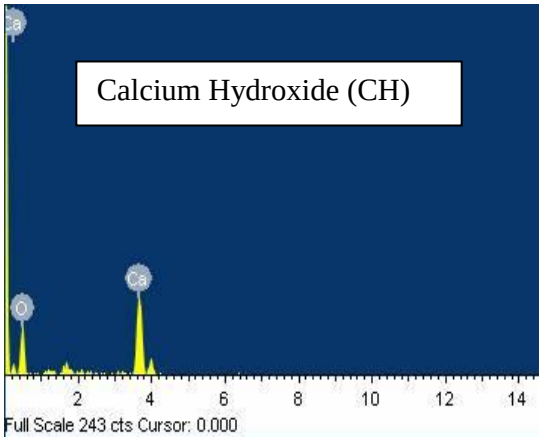

(A) x 2500

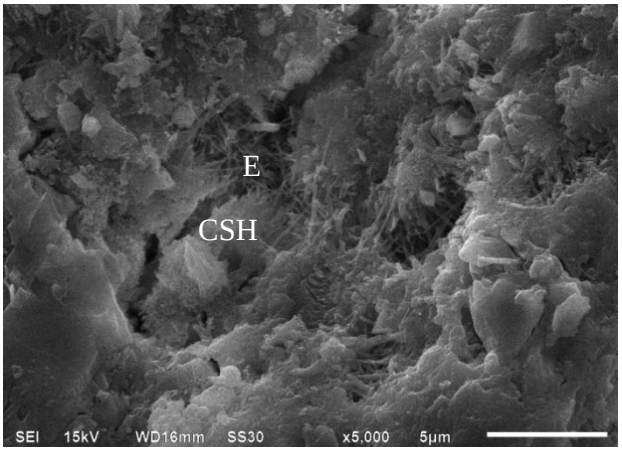

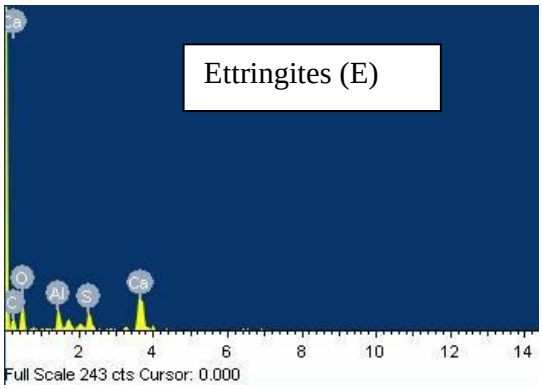

(B) x 5000

Fig. 4.41: Scanning electron micrograph and EDS spectrum of control concrete at 28 days of curing age (Concrete ‘A’)

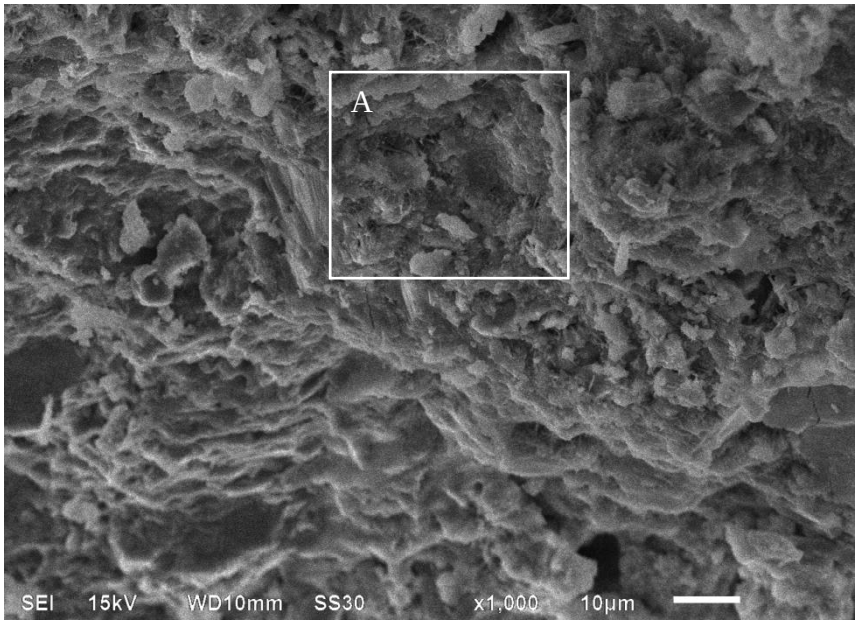

x 1000

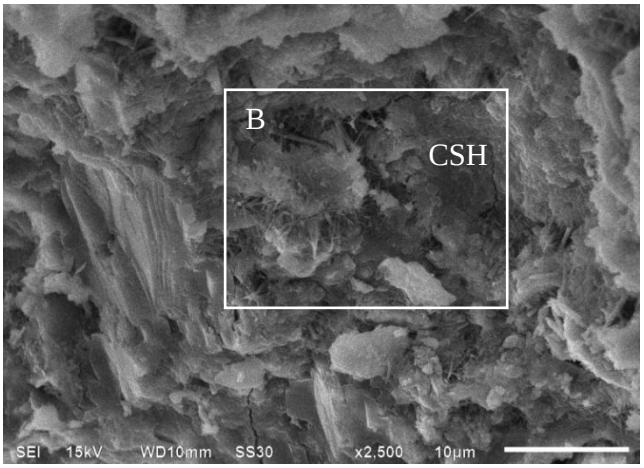

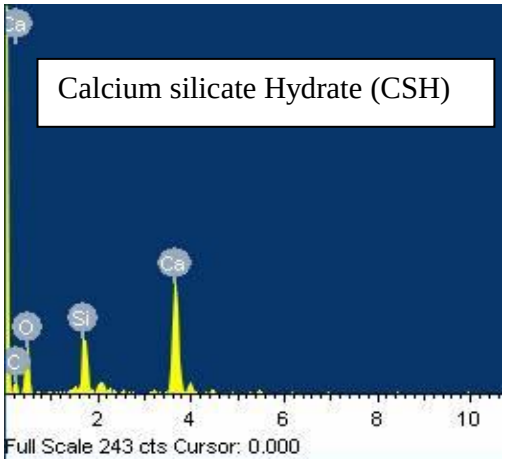

(A) x 2500

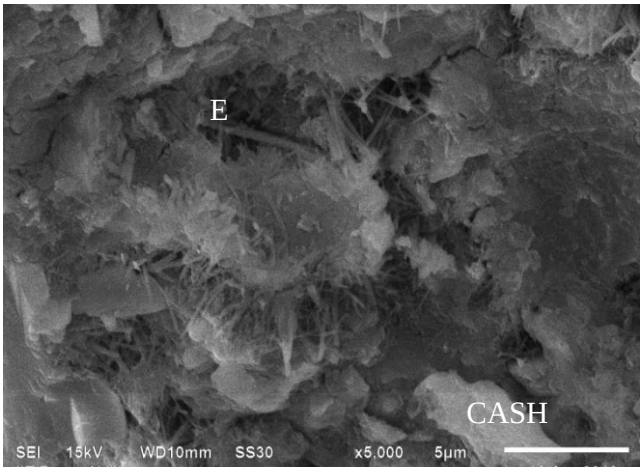

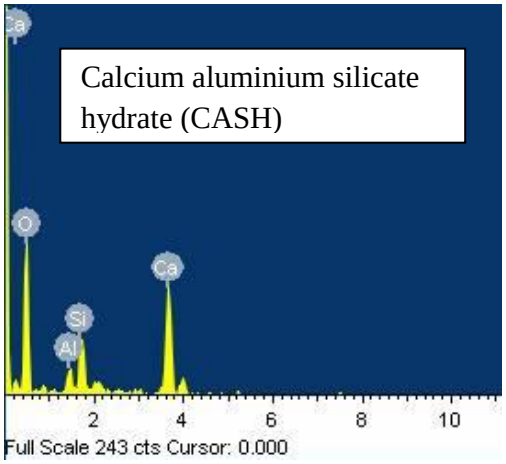

(B) x 5000

Fig. 4.42: Scanning electron micrograph and EDS spectrum of bottom ash concrete (A_{20}) at 28 days of curing age

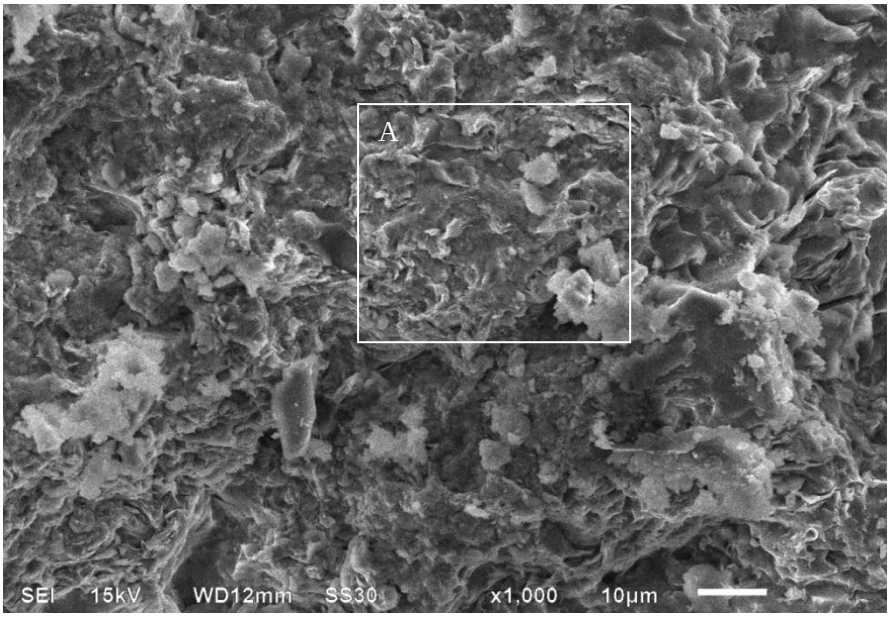

x 1000

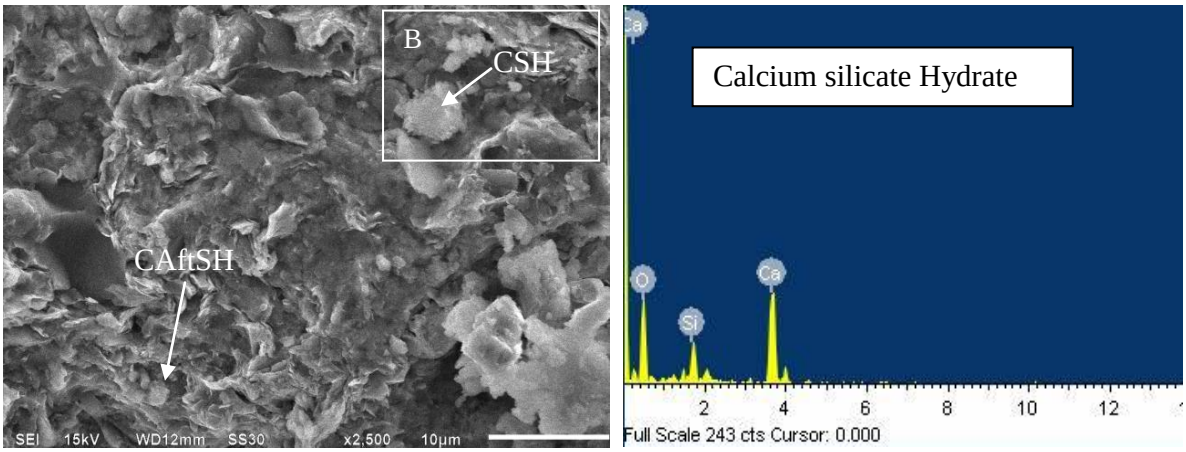

(A) x 2500

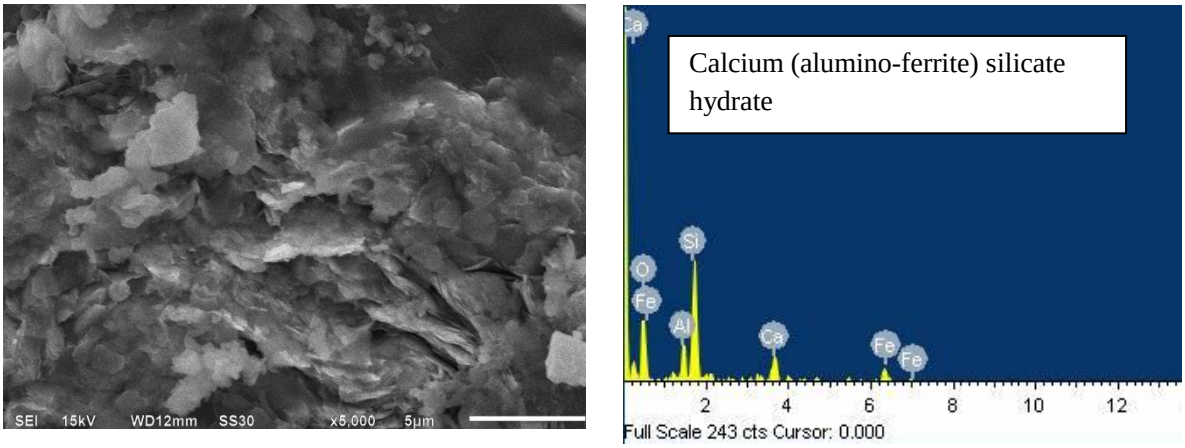

(B) x 5000

Fig. 4.43: Scanning electron micrograph and EDS spectrum of bottom ash concrete (A_{30}) at 28 days of curing age

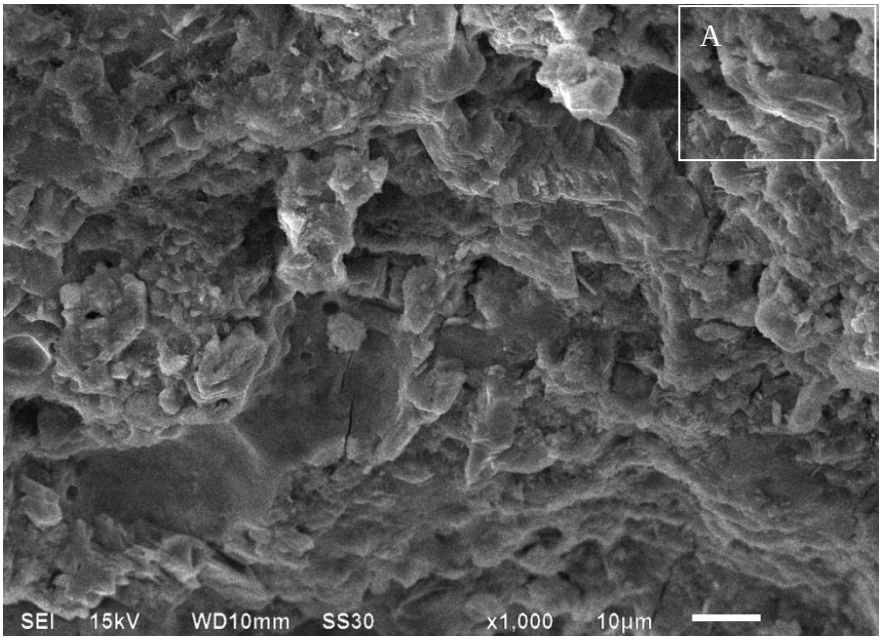

x 1000

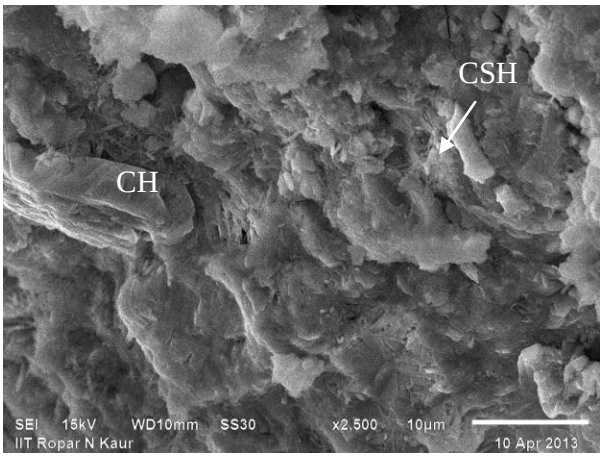

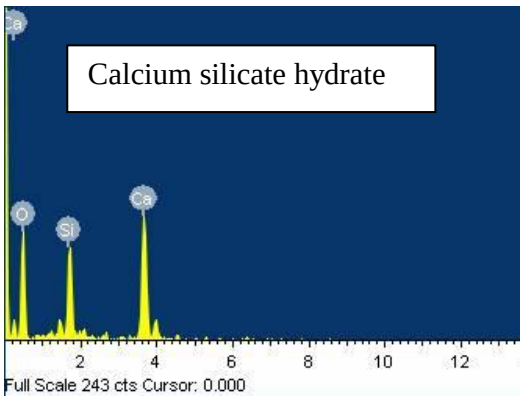

(A) x 2500

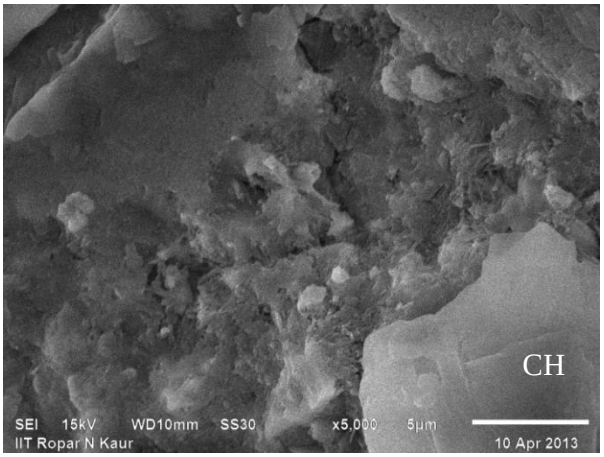

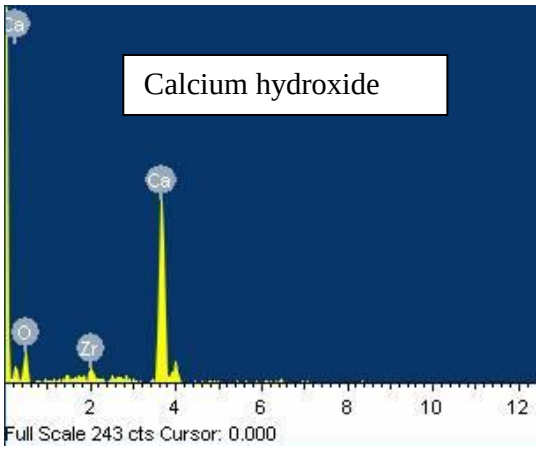

x 5000

Fig. 4.44: Scanning electron micrograph and EDS spectrum of bottom ash concrete (A_{40}) at 28 days of curing age

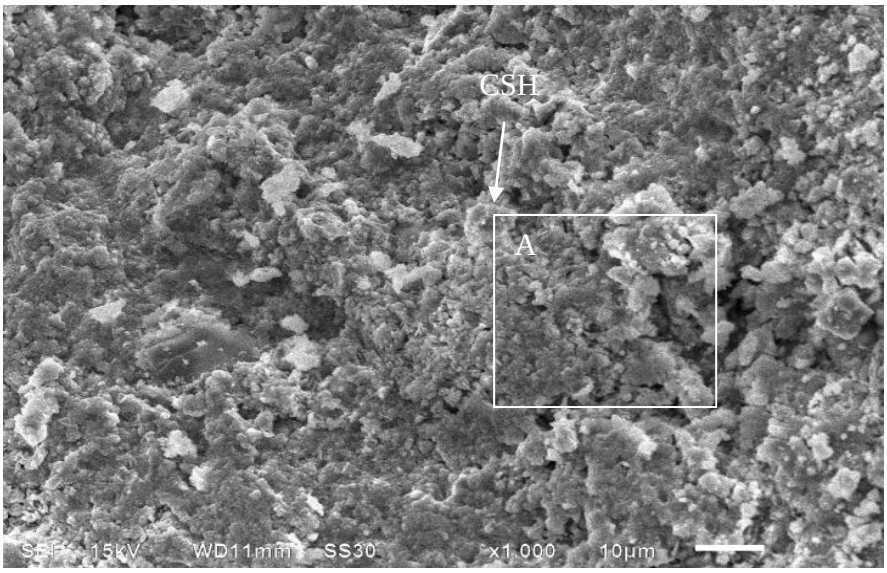

x 1000

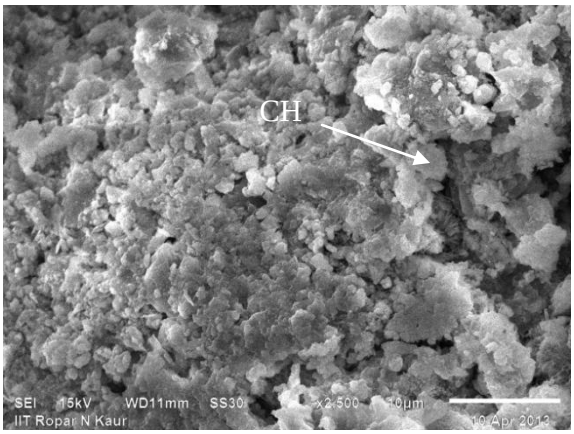

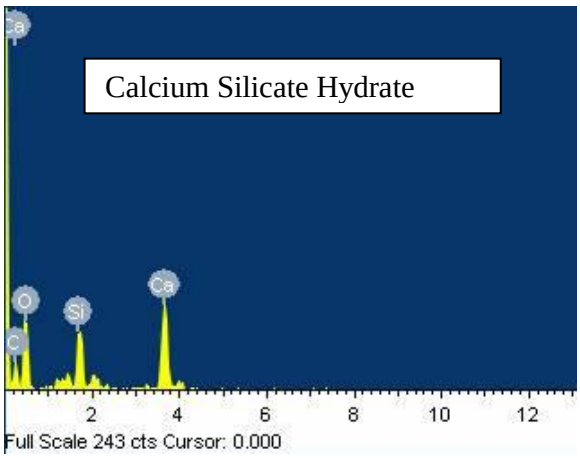

(A) x 2500

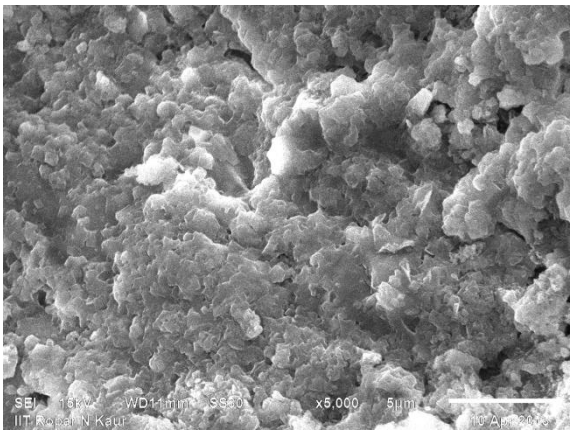

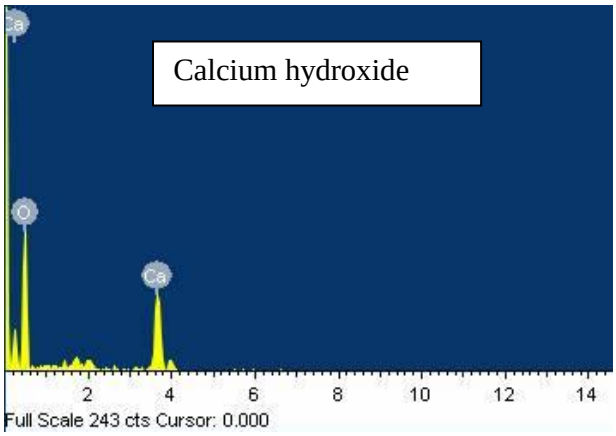

x 5000

Fig. 4.45: Scanning electron micrograph and EDS Spectrum of bottom ash concrete (A_{50}) at 28 days of curing age

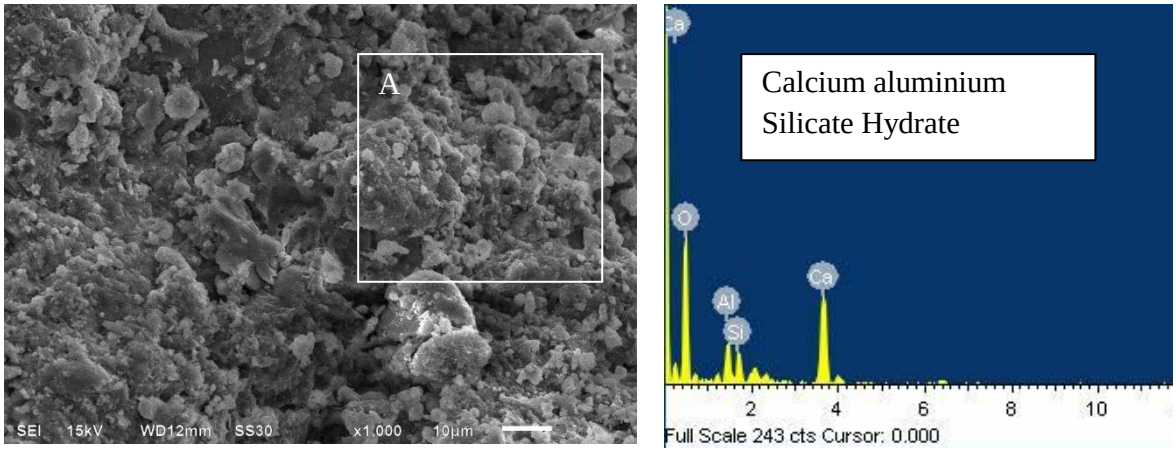

x 1000

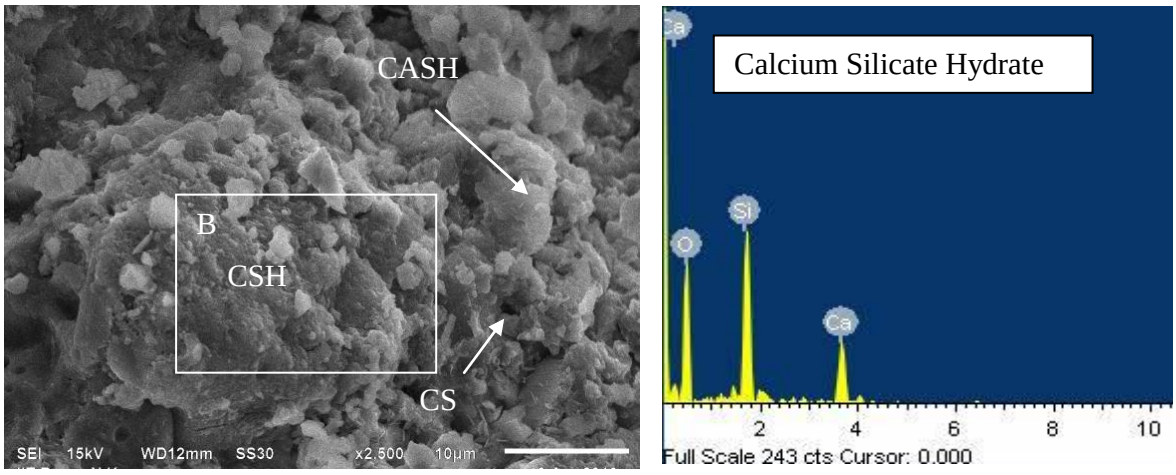

(A) x 2500

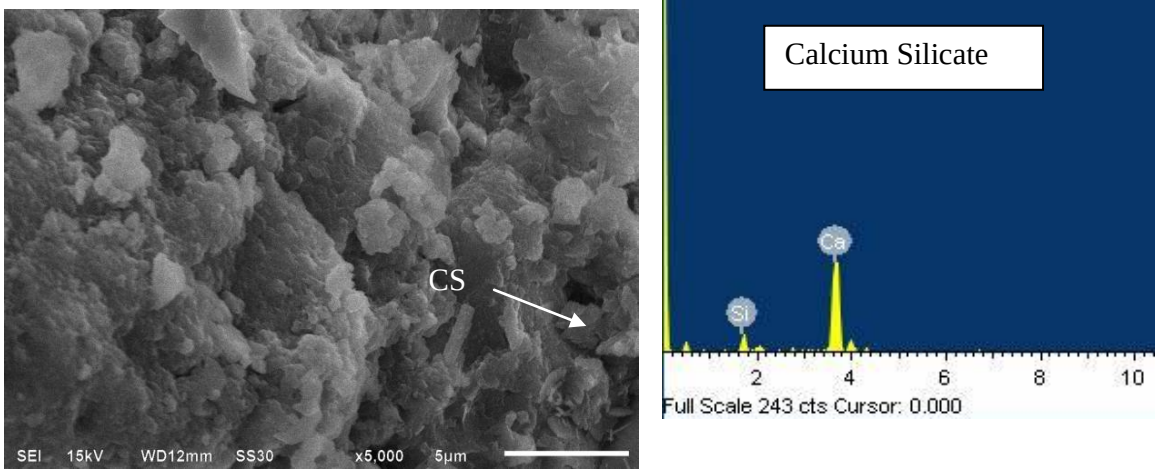

(B) x 5000

Fig. 4.46: Scanning electron micrograph and EDS Spectrum of bottom ash concrete (A_{75}) at 28 days of curing age

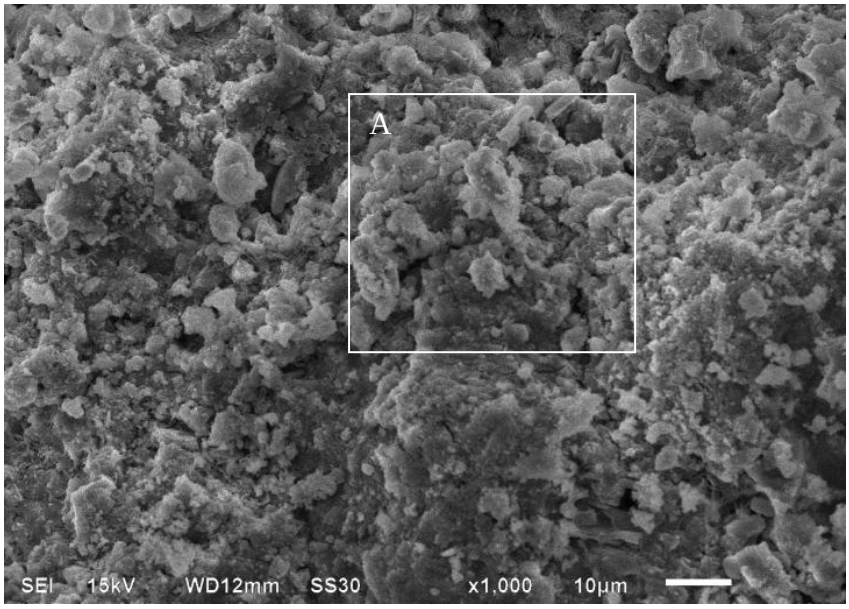

x 1000

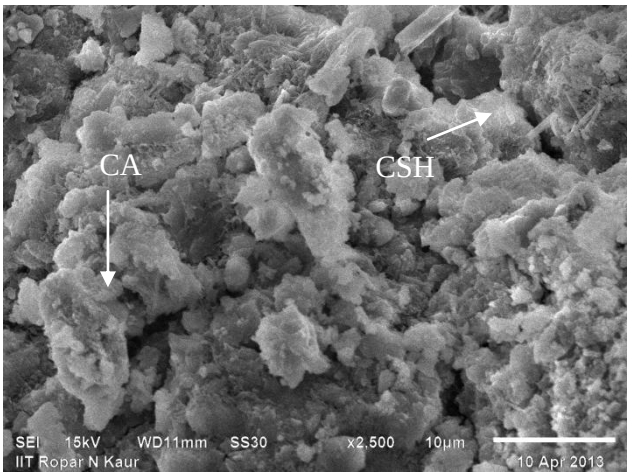

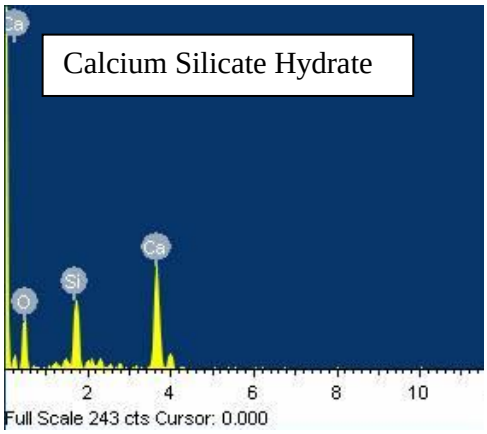

(A) x 2500

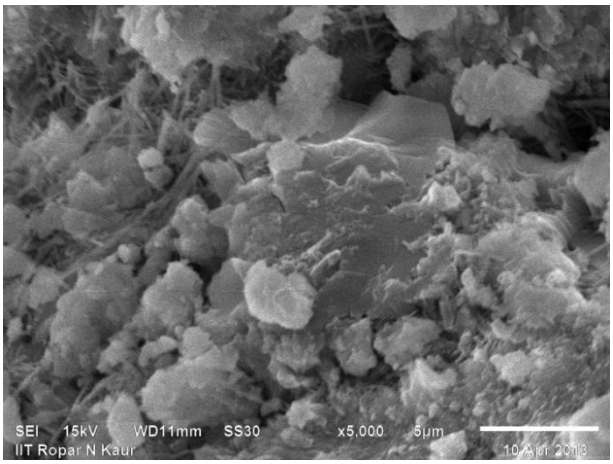

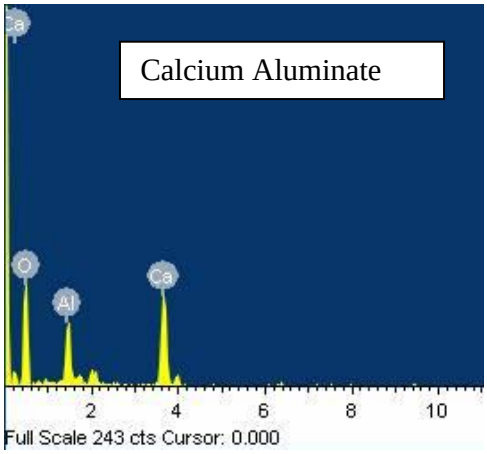

x 5000

Fig. 4.47: Scanning electron micrograph and EDS spectrum of bottom ash concrete (A_{100}) at 28 days of curing age

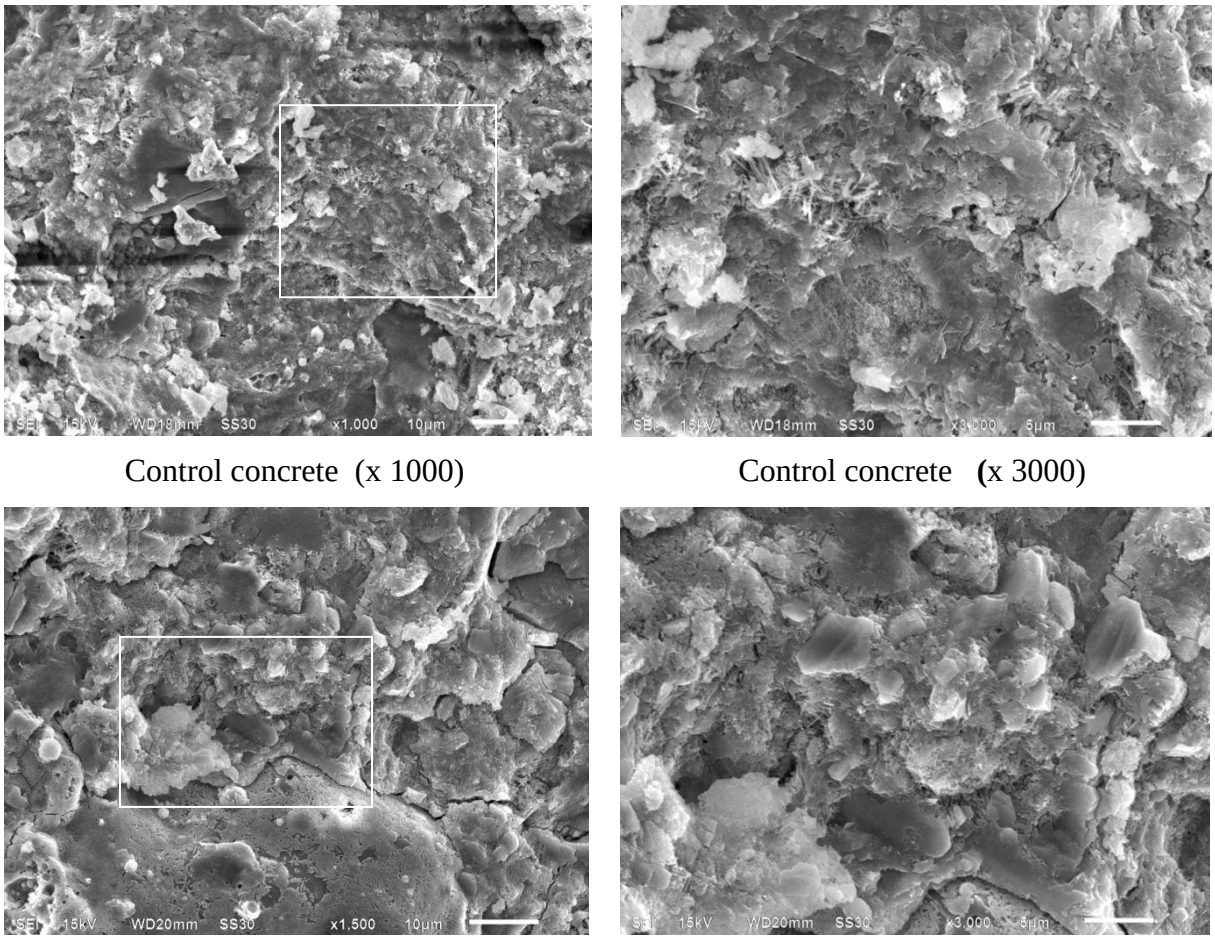

Control concrete (x 1000) Control concrete (x 3000)

A_{20} (x 1500) A_{20} (x 3000)

Fig. 4.48: Scanning electron micrograph of control concrete (Concrete 'A') and bottom ash concrete A_{20} at 90 days of curing age

Fig. 4.50 for bottom ash concrete mixture containing 100% coal bottom ash as fine aggregate shows more finely spread and compact CSH gel and fewer voids as compared to seen in Fig. 4.47. It is evident from SEM micrographs of bottom ash concrete mixture containing 50% coal bottom ash as fine aggregate shown in Figs 4.45 and 4.49 that voids reduced considerably with age. Improvement in CSH gel spread with age in control concrete and bottom ash concrete mixture containing 30% coal bottom ash was also visible from comparison of SEM micrographs shown in Figs. 4.41, 4.43, 4.48 and 4.49. At 90 days of curing age, CSH gel was more finely spread in bottom ash concrete mixtures as compared to that at 28 days of curing age. Pozzolanic action of coal bottom ash resulted in formation of extra CSH gel in bottom ash concrete mixtures after 28 days of curing period.

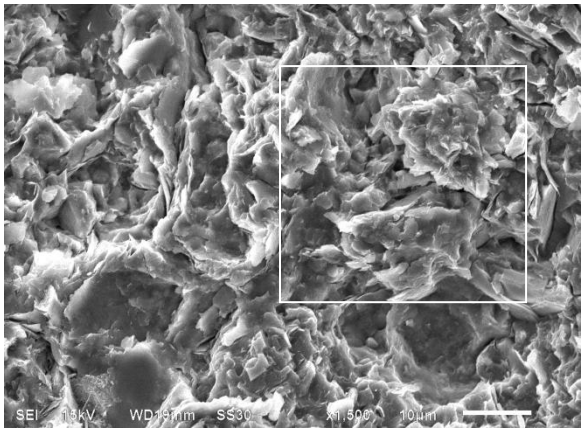

A_{30} (x 1500)

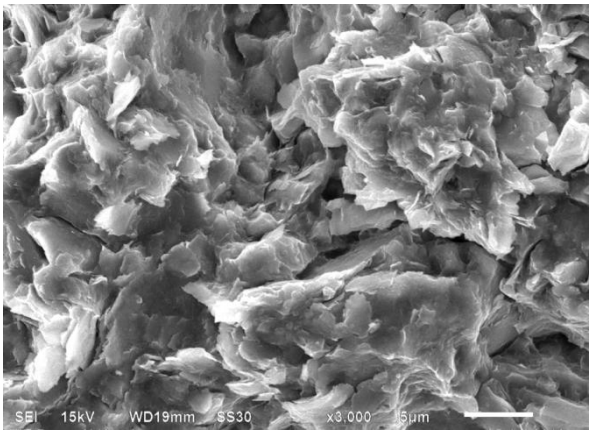

A_{30} (x 3000)

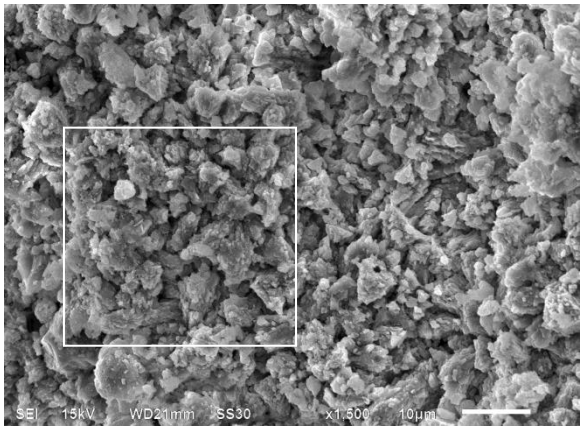

A_{40} (x 1500)

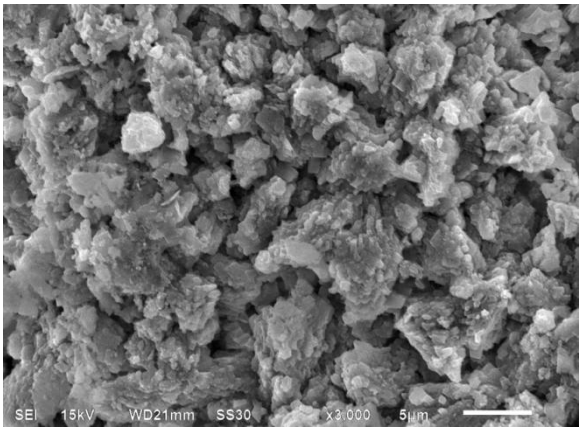

A_{40} (x 3000)

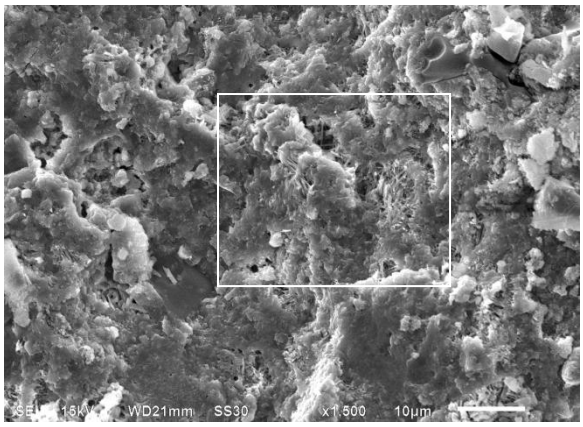

A_{50} (x 1500)

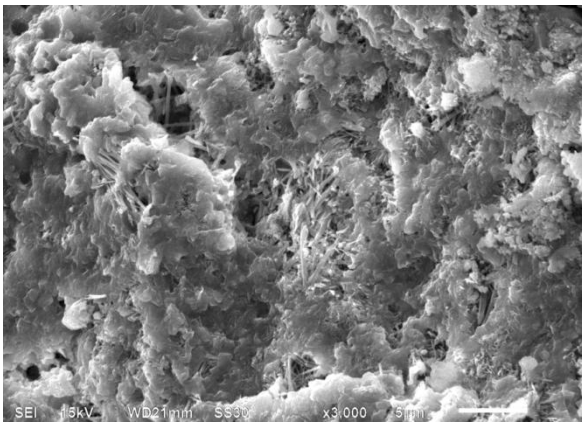

A_{50} (x 3000)

Fig. 4.49: Scanning electron micrograph of bottom ash concrete (A_{30}, A_{40} and A_{50}) at 90 days of curing age

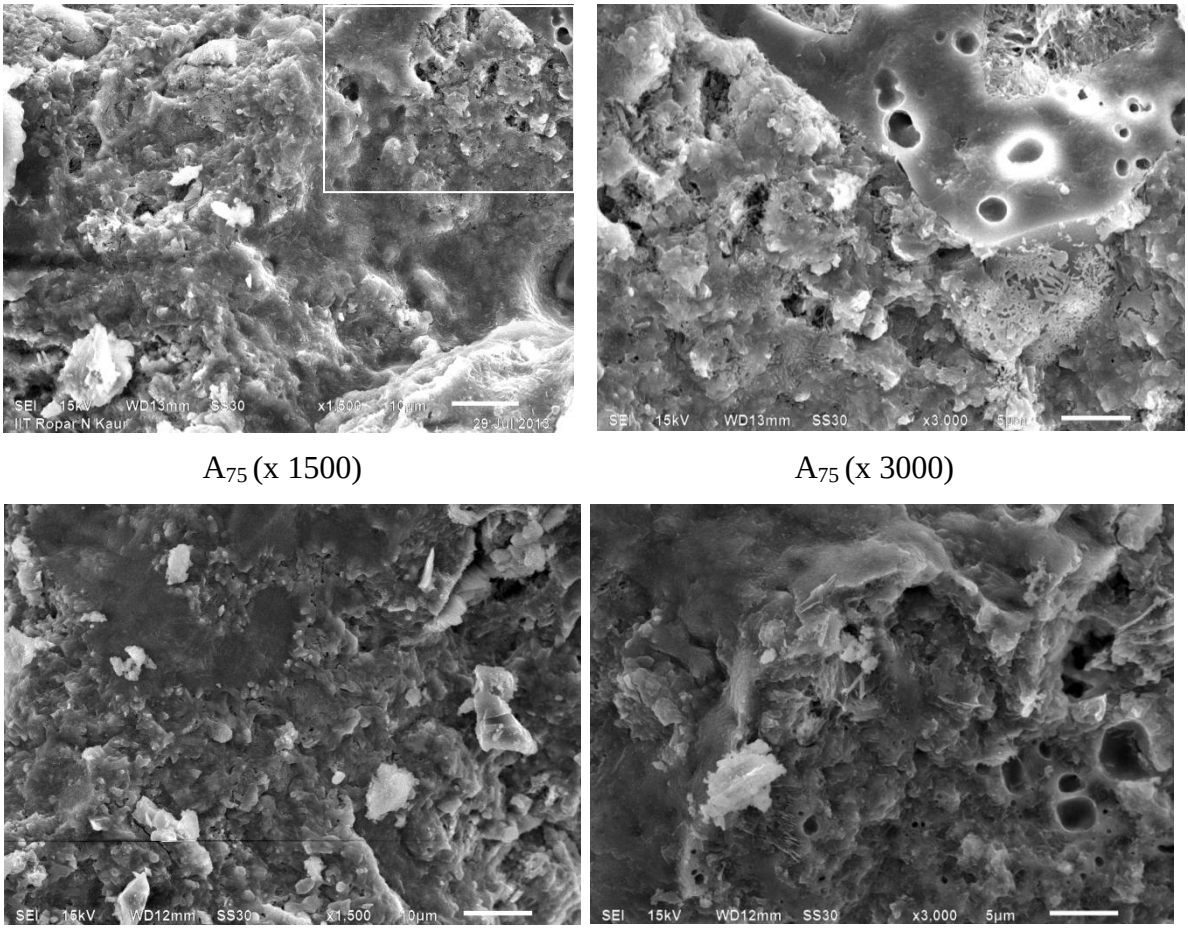

A_{75} (x 1500) A_{75} (x 3000)

A_{100} (x 1500) A_{100} (x 3000)

Fig. 4.50: Scanning electron micrograph of bottom ash concrete (A_{75} and A_{100}) at 90 days of curing age

4.3.6 XRD Phase Analysis

The microstructure of the interfacial transitional zone of concrete differs from that of bulk cement paste. The weak diffraction peaks of poorly crystalline calcium silicate hydrate phase of concrete and interference of diffraction peaks of minerals present in aggregate make the identification of hydration phases present in concrete more complicated. The weak diffraction peaks of calcium silicate hydrate tend to be swamped by the diffraction peaks from portlandite. The X-ray diffraction technique was used for identification of various phases present in the hardened bottom ash concrete as well as control concrete at the age of 28 and 90 days. The cement pastes were separated from the concrete samples and were sieved through 90 µm sieve. The XRD investigations were performed for diffraction angle 2θ ranged between 5° and 80° in steps of 2θ = 0.017°. XRD diffractograms of powder cement paste of control concrete and bottom ash concrete containing 20, 30, 40, 50, 75 and 100% coal bottom ash are presented in Figs. 4.51 to 4.56.

The XRD diffractograms show the presence of hydrated phases such as calcium hydroxide, quartz, ettringite, calcium silicate hydrate, calcium alumino silicate hydrate and calcium silicate in the concrete. The weak diffraction peaks of ettringite were also observed in all the concrete samples. It was also observed that the diffraction peaks of alite, belite and CSH overlapped each other and diffraction peak of silicon oxide present in the aggregate interfered with the peaks of hydration phases of concrete. The diffraction peak intensity of phase calcium silicate (d spacing = 3.02 °A) was more predominant in control concrete as compared to that in bottom ash concrete samples. The total intensity of ettringite was not changed with the addition of coal bottom ash in concrete. In this study total intensity of portlandite was assessed during the XRD analysis. While analyzing the XRD spectrums of concrete mixtures, it was assumed that total intensity of a phase is connected with the amount of that phase present in the concrete mixture. Total intensity of calcium hydroxide in concrete at 28 and 90 days of curing age are given in table 4.12. At 28 days of curing age, the evaluation of XRD spectrums intensities revealed that the total intensity of portlandite (d = 4.90 °A, 2.62 °A and 1.92 °A) in bottom ash concrete mixtures with the exception of concrete mixture A_{75} was higher than that in control concrete. The total intensity of portlandite (d = 4.90 °A, 2.62 °A and 1.92 °A) in concrete mixtures $A_{20,}$ $A_{30,}$ $A_{40,}$ A_{50} and A_{100} was 1.28, 11.79, 9.05, 13.75 and 6.85%, respectively, higher than that in control concrete. At 90 days of curing age, the total intensity of portlandite (d = 4.90 °A, 2.62 °A and 1.92 °A) in all bottom ash concrete mixtures $A_{20,}$ $A_{30,}$ $A_{40,}$ A_{50} and A_{75} was 8.54, 11.58, 16.73, 18.22 and 6.76%, respectively, lower than that in control concrete. Total intensity of portlandite in bottom ash concrete mixture A_{100} was 2.18% higher than that in control concrete. The relative evaluation of peak intensity revealed that the influence of coal bottom ash is significant in case of portlandite phase. At 28 days of curing age, total intensity of portlandite increased on incorporation of coal bottom ash in concrete. However, at 90 days, total intensity of portlandite decreased on use of coal bottom ash as fine aggregate in concrete. After 90 days of curing age, it is evident that the reduction in portlandite in bottom ash concrete mixtures was due to pozzolanic activity of coal bottom ash.

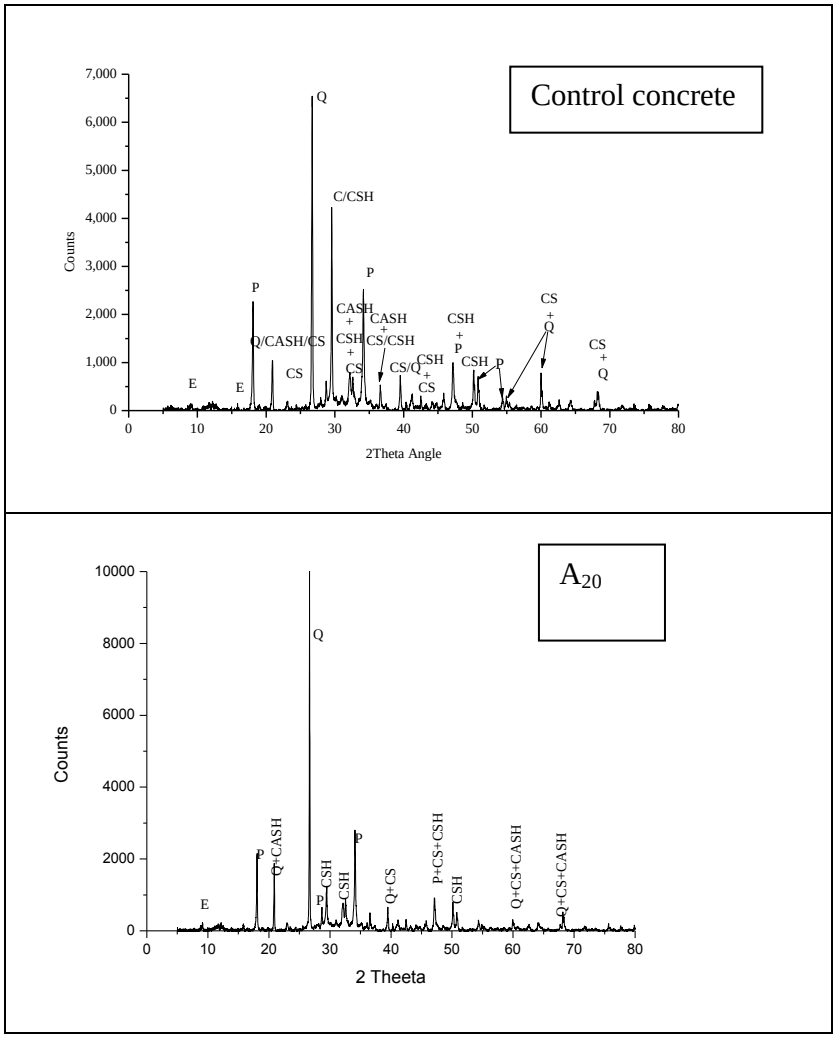

Fig. 4.51: XRD spectrum of control concrete (concrete Á') and bottom ash concrete (A_{20}) at 28 days of curing age (CASH = Calcium alumino silicate hydrate; CS = Calcium silicate; CSH = Calcium silicate hydrate; E = Ettringite; P = Portlandite; Q = Quartz)

Table 4.12 Intensity of calcium hydroxide peaks (Concrete 'A')

Mix	Total Intensity of Portlandite at d spacing (Counts)							
	28 days				90 days			
	4.90°A	2.62°A	1.92°A	Total	4.90°A	2.62°A	1.92°A	Total
Control concrete	2270	2523	1000	5793	611	818	316	1745
A_{20}	2151	2803	913	5867	597	712	287	1596
A_{30}	2913	2645	918	6476	642	641	260	1543
A_{40}	2539	2833	945	6317	519	628	306	1453
A_{50}	2809	2688	975	6472	527	606	294	1427
A_{75}	2402	2311	814	5527	728	673	226	1627
A_{100}	2689	2678	823	6190	845	604	334	1783

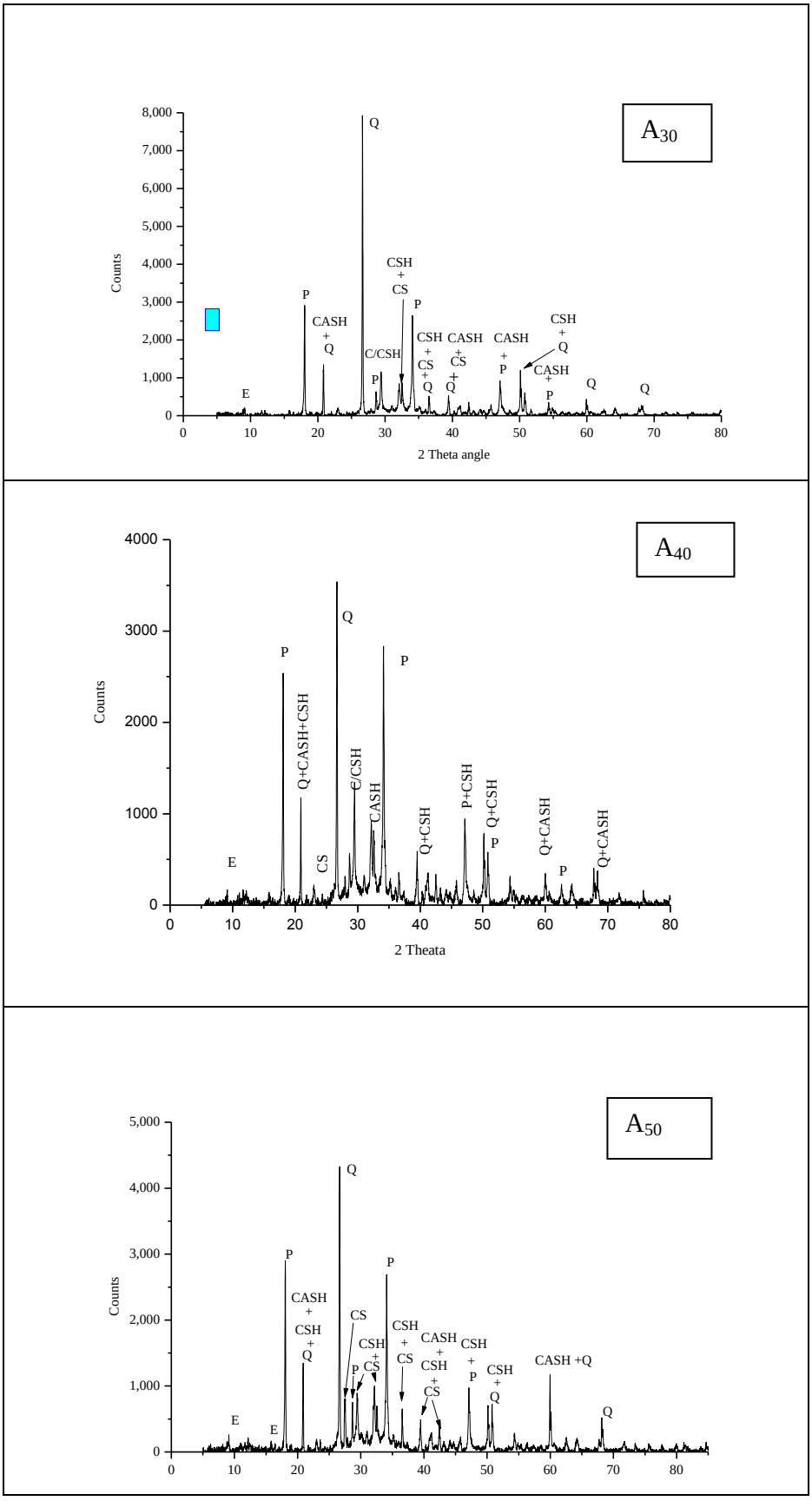

Fig. 4.52: XRD spectrum of bottom ash concrete (A_{30}, A_{40}, and A_{50}) at 28 days of curing age (CASH = Calcium alumino silicate hydrate; CS = Calcium silicate; CSH = Calcium silicate hydrate; E = Ettringite; P = Portlandite; Q = Quartz)

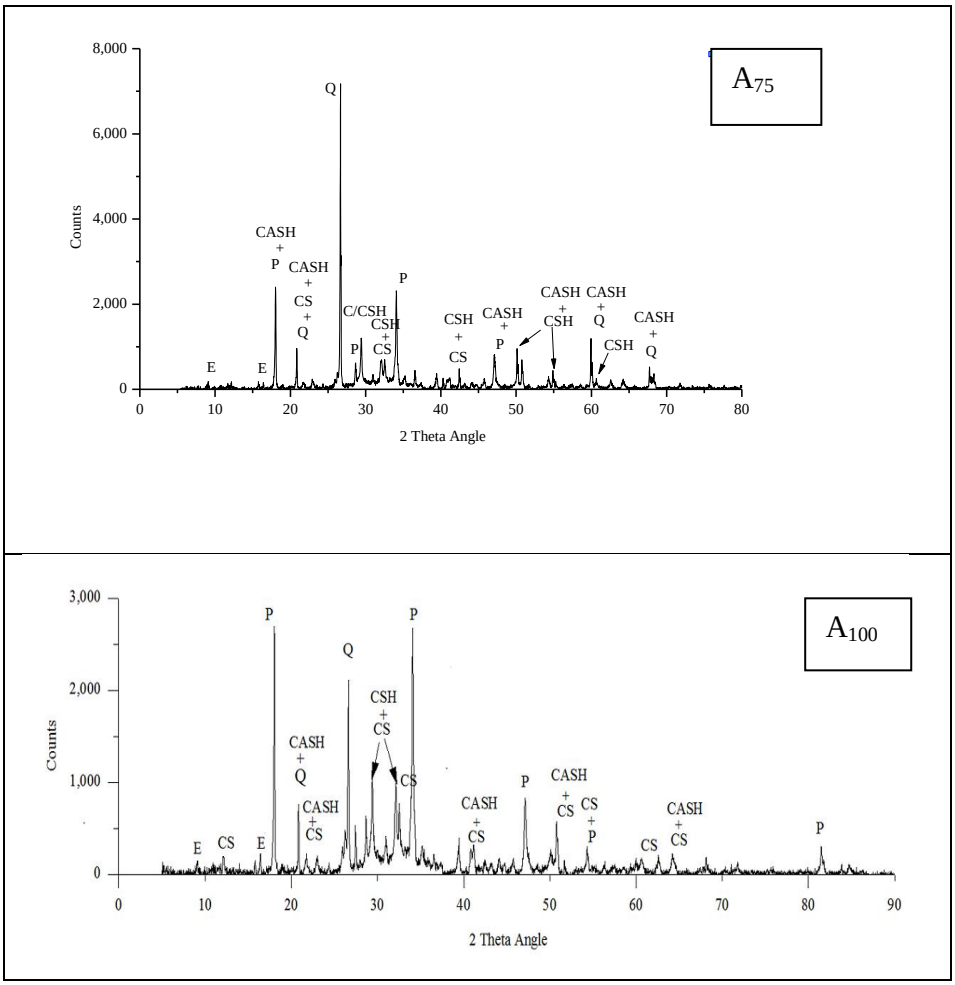

Fig. 4.53: XRD spectrum of bottom ash concrete (A_{75} and A_{100}) at 28 days of curing age (CASH = Calcium alumino silicate hydrate; CS = Calcium silicate; CSH = Calcium silicate hydrate; E = Ettringite; P = Portlandite; Q = Quartz)

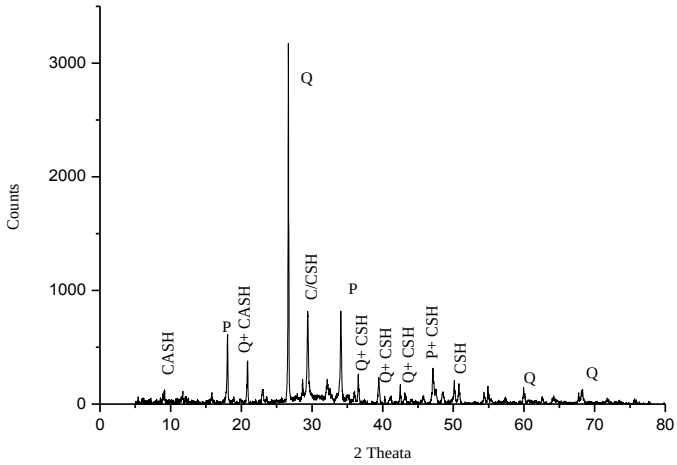

Fig. 4.54: XRD spectrum of control concrete (concrete 'A') at 90 days of curing age (CASH = Calcium alumino silicate hydrate; CS = Calcium silicate; CSH = Calcium silicate hydrate; E = Ettringite; P = Portlandite; Q = Quartz)

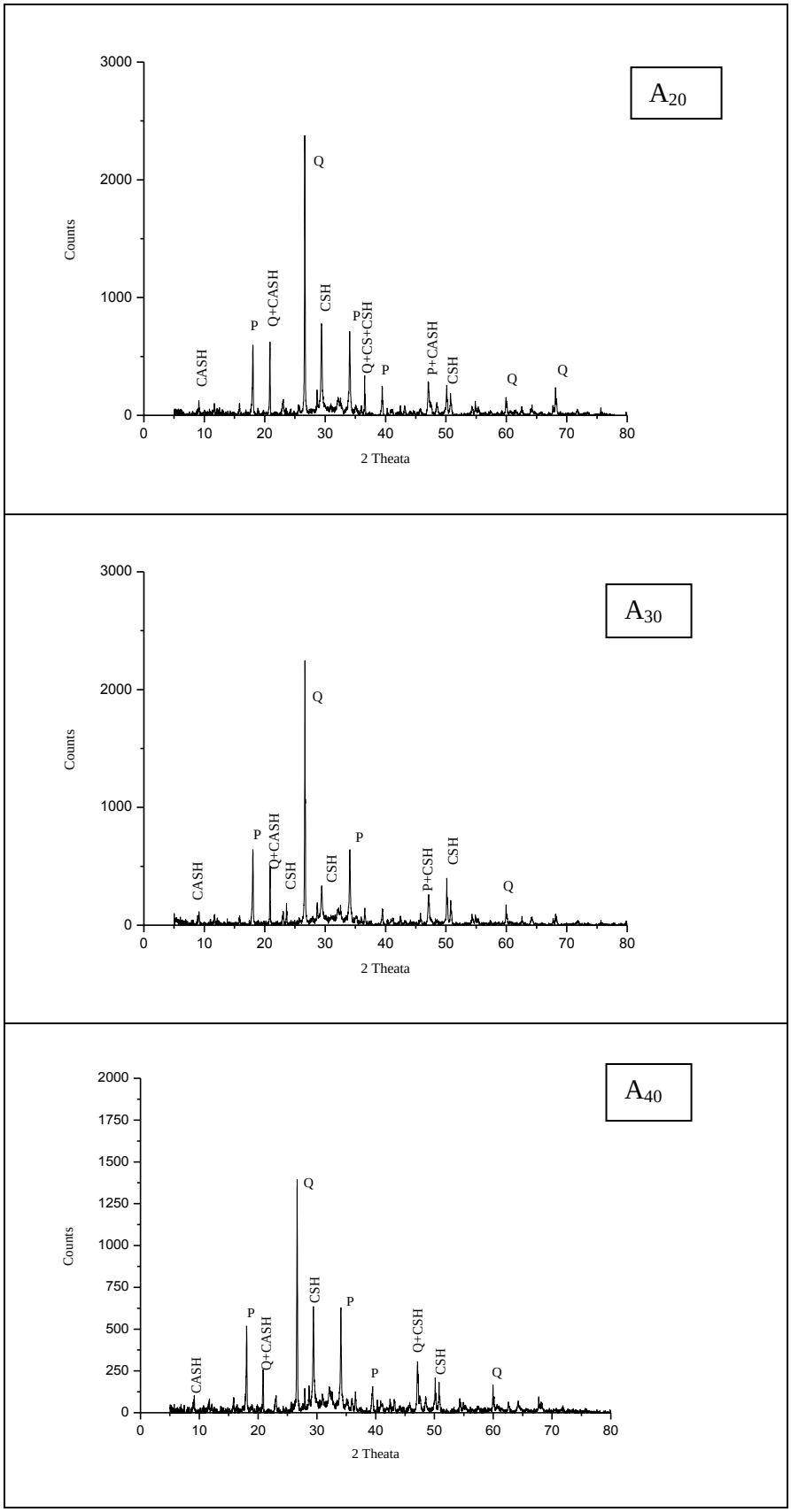

Fig. 4.55: XRD spectrum of bottom ash concrete ($A_{20,}$ $A_{30,}$ and A_{40}) at 90 days of curing age (CASH = Calcium alumino silicate hydrate; CS = Calcium silicate; CSH = Calcium silicate hydrate; E = Ettringite; P = Portlandite; Q = Quartz)

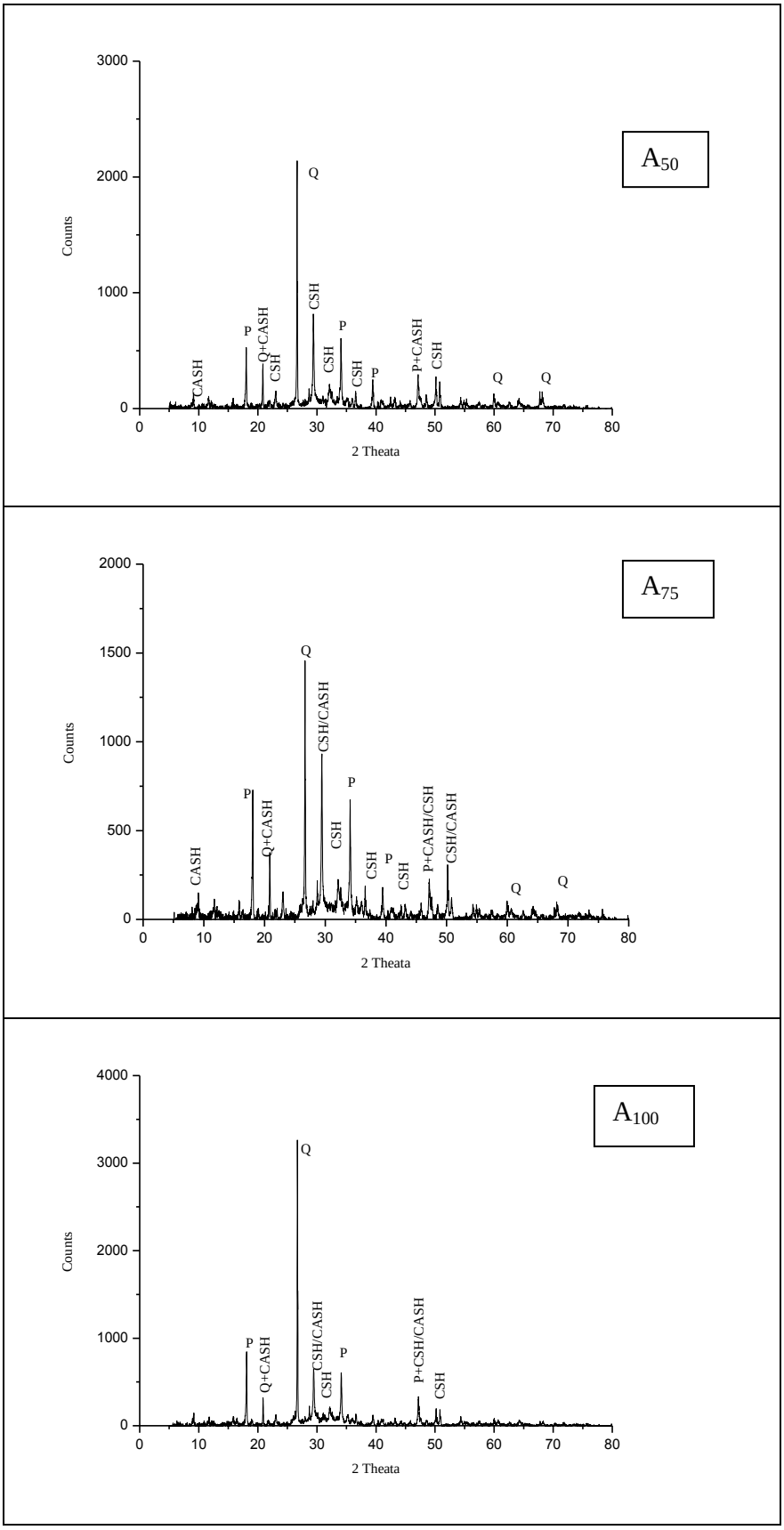

Fig. 4.56: XRD spectrum of bottom ash concrete ($A_{50,}$ A_{75}, and A_{100}) at 90 days of curing age (CASH = Calcium alumino silicate hydrate; CS = Calcium silicate; CSH = Calcium silicate hydrate; E = Ettringite; P = Portlandite; Q = Quartz)

4.3.7 Statistical Analysis of Results

4.3.7.1 Relationship between Compressive Strength and Splitting Tensile Strength

Fig. 4.57 demonstrates the relation between splitting tensile strength and compressive strength of bottom ash concrete containing 20 to 100% coal bottom ash as replacement of sand. The equation showing the relationships between compressive strength and splitting tensile strength together with the coefficients of determination R^2 derived from the test results of the present study is given below.

$$f_t = 0.1433 (f_{cu})^{0.834} \qquad R^2 = 0.9583$$

where

f_t = Splitting tensile strength of concrete in N/mm^2,

f_{cu} = Compressive strength of cube specimen of concrete in N/mm^2

The higher value of coefficient of determination R^2 indicates the good relation between regression curve and data points.

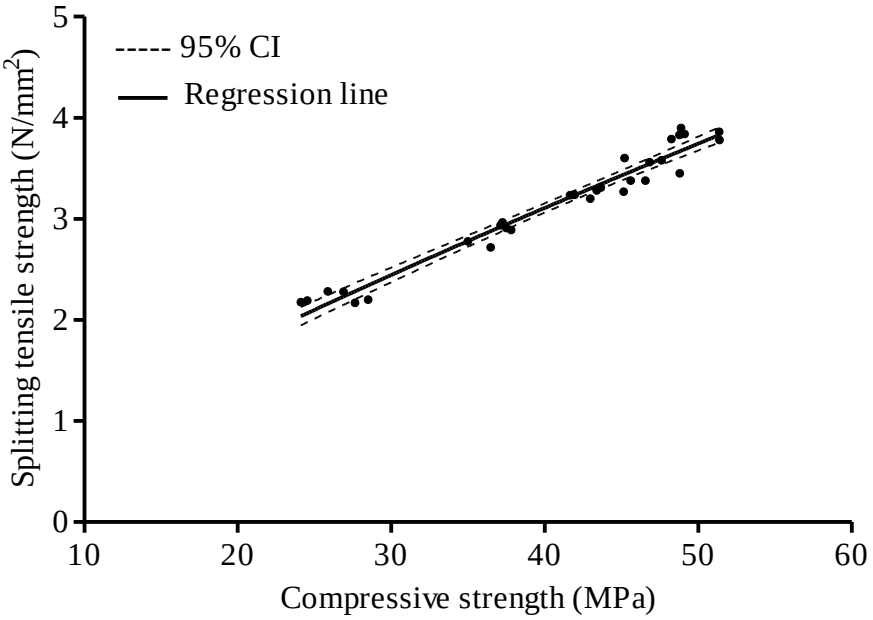

Fig. 4.57: Relation between compressive strength and splitting tensile strength of concrete (Concrete 'A')

The relationship is very close to relationship $f_t = 0.3(f_{cyl})^{2/3}$ where $f_{cyl} = 0.8f_{cu}$, recommended by CEB-FIP model code for concrete structures (1990). Comparison between relation given in CEB-FIP and derived from present study is given in Table 4.13.

Table 4.13 Comparison of relation given in CEB-FIP and derived from present study (Concrete 'A')

Cube Compressive strength (N/mm^2)	**Splitting tensile strength (N/mm^2) as per**		**Actual splitting tensile strength (N/mm^2)**
	$f_t = 0.3(f_{cyl})^{2/3}$	**$f_t = 0.1433\ (f_{cu})^{0.834}$**	
25.87	2.26	2.16	2.283
28.49	2.41	2.34	2.2
36.82	2.86	2.90	2.94
42.95	3.17	3.30	3.24
45.20	3.28	3.44	3.58
49.88	3.50	3.74	3.45

4.3.7.2 *Relationship between Compressive Strength, Dry Bulk Density and Modulus of Elasticity*

Fig. 4.58 shows the relationship obtained from the present study between compressive strength, dry bulk density and modulus of elasticity of concrete incorporating coal bottom ash as fine aggregate. The equation showing the relationships between compressive strength, dry bulk density and modulus of elasticity together with the coefficients of determination R^2 derived is given below. The empirical parameters of the equation obtained from the present study are almost similar to that given in BS 8110: (Part-2):1985. Higher value of coefficient of determination indicates good relevance between the data points and regression curve. Dry bulk density of bottom ash concrete mixtures varied between 2286 kg/m^3 and 2095 kg/m^3.

$E = 1.4425\ \rho^2\ \sigma^{0.33} + 2.832$ $\quad R^2 = 0.8422$ (Author)

$E = 1.7\ \rho^2\ \sigma^{0.33}$ BS: 8110: (Part 2):1985

where,

f = Cube compressive strength of concrete in N/mm^2

E = Modulus of elasticity of concrete in GPa

ρ = Dry bulk density of concrete in kg/m^3

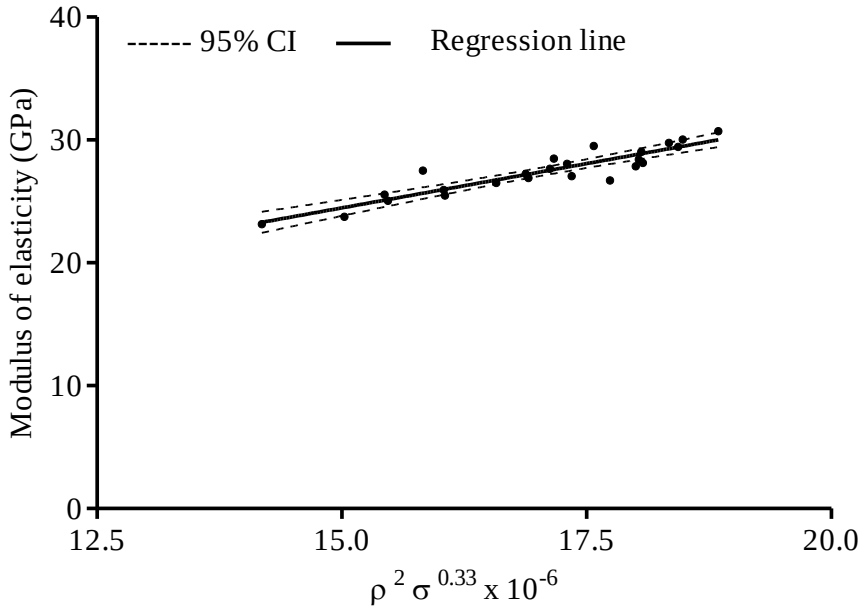

Fig. 4.58: Relationship between compressive strength, dry bulk density and modulus of elasticity of concrete (Concrete 'A')

4.3.7.3 Relationship between Chloride Permeability and Compressive Strength

Fig. 4.59 shows the relationship between cumulative charge passed and compressive strength of bottom ash concrete mixtures. Both chloride ion penetration and compressive strength of concrete are related to its pore structure. The equation showing the relationships between compressive strength (σ) and the cumulative charge passed (Q), together with the coefficient of determination (R^2) derived is given below.

$$\sigma = -0.005803Q + 53.627 \qquad R^2 = 0.7665$$

where

σ = Compressive strength of concrete in N/mm^2

Q = Total charge passed through specimen in coulombs

The value of coefficient of determination R^2 indicates the good relation between regression curve and data points.

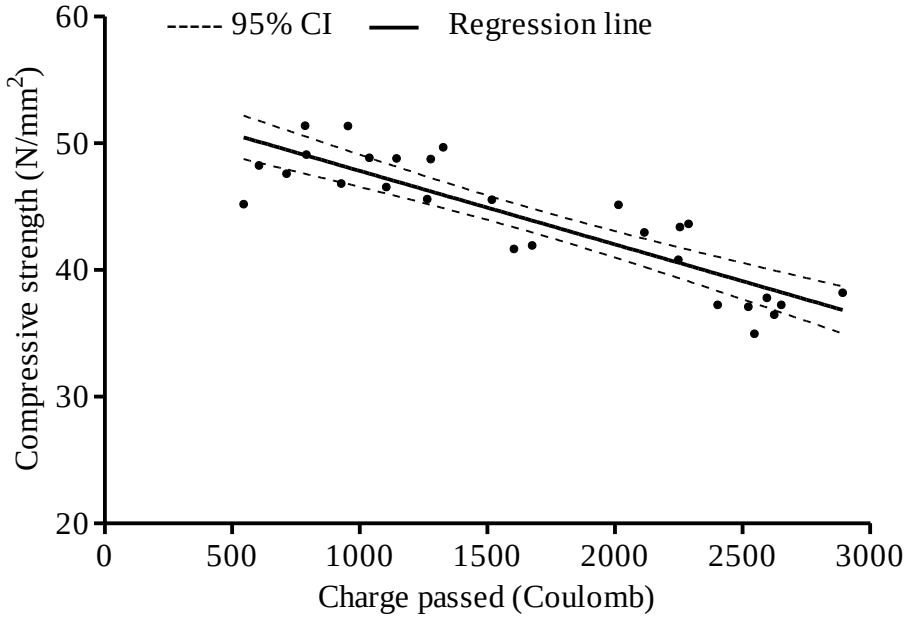

Fig. 4.59: Relation between chloride permeability and compressive strength of concrete (Concrete 'A')

4.3.7.4 Relationship between Chloride Permeability and Pulse Velocity

Fig. 4.60 shows the relationship obtained from the present study between ultrasonic pulse velocity and chloride permeability of bottom ash concrete.

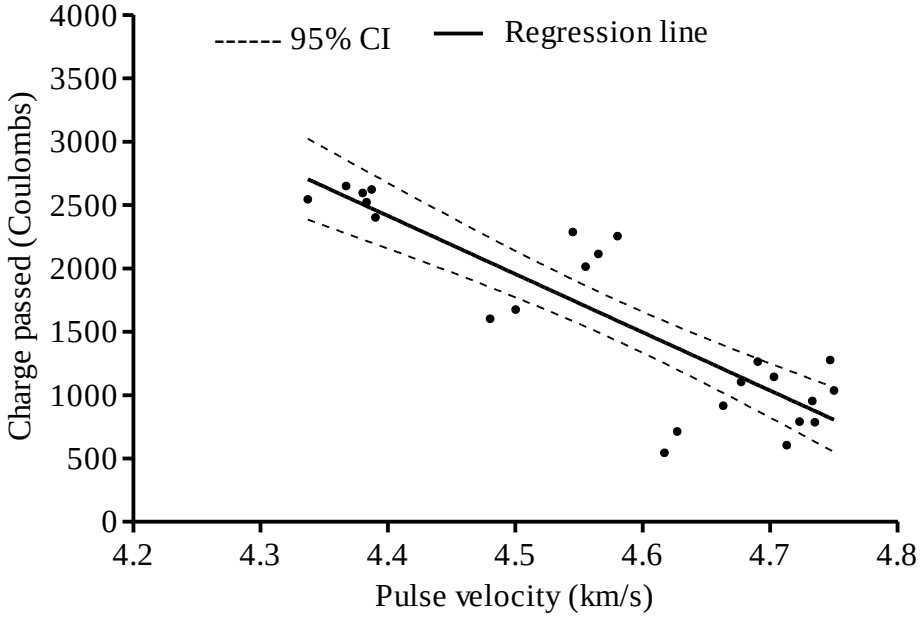

Fig. 4.60: Relation between pulse velocity and chloride permeability of bottom ash concrete (Concrete 'A')

The equation showing the relationships between chloride permeability and the pulse velocity of longitudinal waves (V), together with the coefficients of determination (R^2) derived is given below.

Q = -4596.8V + 22640 $R^2 = 0.7572$

Where

Q = Total charge passed through concrete in Coulomb

V = Pulse velocity through concrete specimen in km/s

4.3.7.5 Relation between Percentage Loss in Weight and Reduction in 28-day Compressive Strength

The relationship between reduction in 28-day compressive strength of bottom ash concrete specimens and their weight loss after immersion in 3% sulphuric acid solutions is shown in Fig. 4.61. The higher value of coefficient of determination (R^2) indicates the good relevance between the data points and the regression curve. The loss in compressive strength increased approximately linearly with the increase in mass loss of concrete specimens. The equation of relationship between mass loss and compressive strength loss of concrete due to external sulphuric acid attack is given as under

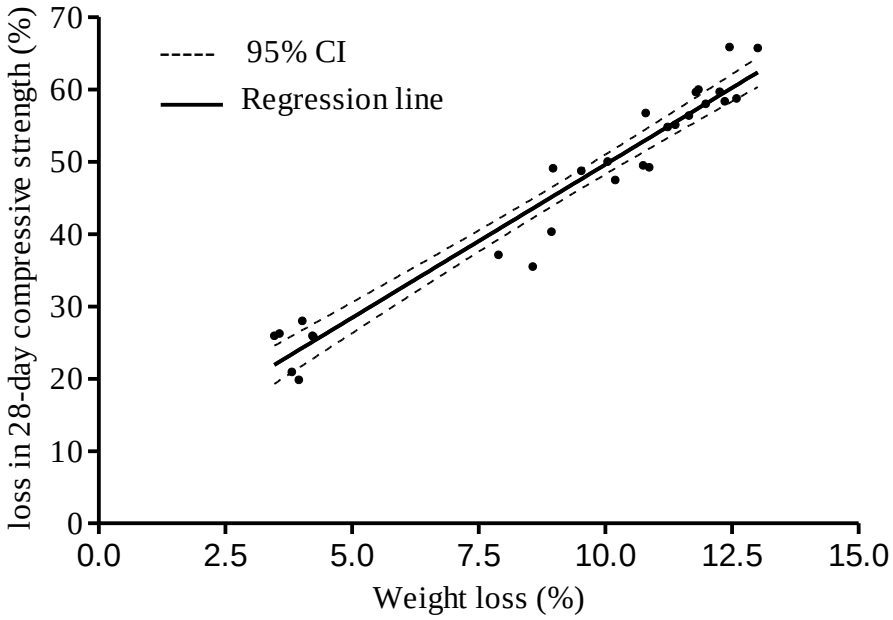

Fig. 4.61: Relation between loss in 28-day compressive strength and weight loss after immersion in 3% sulphuric acid solution (Concrete 'A')

$\Delta\sigma = 4.238\Delta m + 7.219$ $R^2 = 0.9476$ (Author)

Hewayde et al. (2007) reported similar relationship between mass loss of concrete specimens and loss in their compressive strength.

$\Delta\sigma$ = $2.3352\Delta m + 7.2081$ R^2 = 0.92 (Hewayde et al., 2007)

where

$\Delta\sigma$ = percentage loss in 28-day compressive strength of concrete

Δm = percentage loss in mass of concrete specimen

The linear regression line obtained in the present study suggests that percentage loss in 28-day compressive strength of bottom ash concrete mixtures is approximately 4.24 times the percentage loss in their mass.

4.3.7.6 Relationship between Compressive Strength and Pulse Velocity

Fig. 4.62 shows the relationship between ultrasonic pulse velocity and compressive strength of concrete obtained from the present study. The equation showing the relationships between compressive strength (σ) and the ultrasonic pulse velocity of longitudinal waves (V), together with the coefficients of determination R^2 derived is given below. The empirical parameters of the equation obtained from the present study are almost similar to that reported by Turgut (2004) and Nash't et al. (2005). However, the coefficient of determination, (R^2) is higher than that reported by them. Higher value of coefficient of determination indicates good relevance between the data points and regression curve.

σ = $1.13 \exp(0.7993V)$ $R^2 = 0.9493$ (Author)

σ = $1.146 \exp(0.77V)$ $R^2 = 0.80$ (Turgut, 2004)

σ = $1.19 \exp(0.715V)$ $R^2 = 0.59$ (Nash't et al., 2005)

where

σ = Compressive strength cube specimen of concrete in N/mm^2

V = Pulse velocity through concrete specimen in km/s

Verification of Proposed Relationship between Compressive Strength and Pulse Velocity

To verify the above relationship between compressive strength and pulse velocity, 10 cube specimens of concrete incorporating different proportions of coal bottom ash as substitute of river sand were cast. The specimens were tested at the curing age of 365 days for compressive strength and pulse velocity. The actual and predicted compressive strength

values are given in Table 4.14. All the predicted compressive strength values are within +7.23% and –8.92% variations from the actual compressive strength of concrete specimens. This verifies the proposed relationship for estimation of compressive strength from measured pulse velocity through concrete.

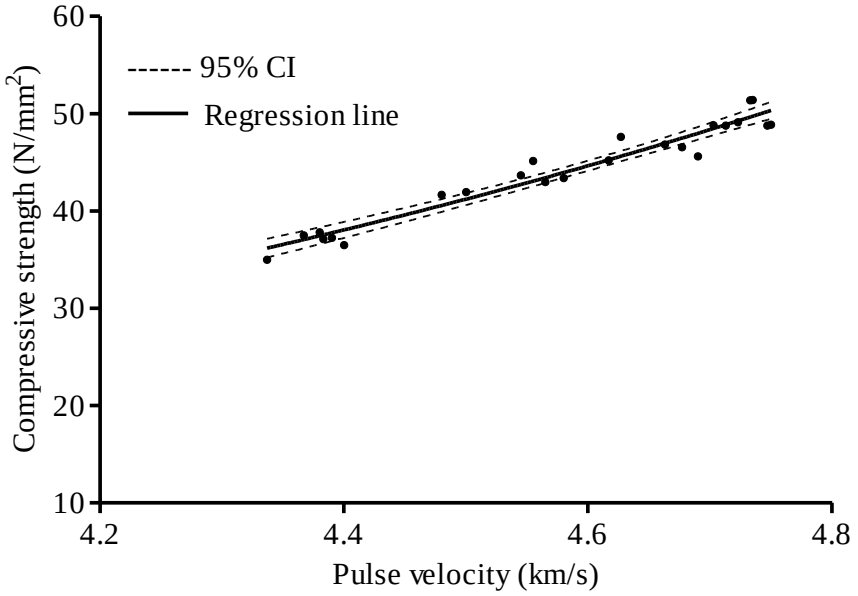

Fig. 4.62: Relationship between compressive strength and pulse velocity (Concrete 'A')

Table 4.14 Verification of relationship between pulse velocity and compressive strength (Concrete 'A')

Sample	**Pulse velocity (m/s)**	**Predicted compressive strength (N/mm^2)**	**Actual Compressive strength (N/mm^2)**	**Variation (%)**
1	4640	46.10	44.58	+3.41
2	4750	50.35	50.13	+0.44
3	4440	39.30	40.36	-2.7
4	4670	47.23	44.05	+7.22
5	4550	42.91	44.62	-3.99
6	4820	53.24	54.38	-2.09
7	4600	44.66	45.93	-2.77
8	4670	47.23	51.86	-8.92
9	4720	49.15	49.11	+0.10
10	4850	54.53	56.22	-3.00

4.3.7.7 Relationship between Compressive Strength and Abrasion Resistance

Fig. 4.63 shows the relationship between compressive strength and average depth of wear of concrete obtained from the present study. The equation showing the relationships between compressive strength (σ) and the average depth of wear (d) against abrasion of concrete, together with the coefficient of determination (R^2) derived is given below. The empirical parameters of the equation obtained from the present study are almost similar to that reported by Naik et al. (1995) for high strength concrete made with C type fly ash as replacement of cement. Higher value of coefficient of determination indicates good relevance between the data points and regression curve. Siddique (2013) observed that the abrasion resistance of self compacting concrete mixes is related with its compressive strength and increases with increase in compressive strength. Siddique (2010) observed that depth of wear of fly ash concrete against abrasion has very good correlation with compressive strength.

$d = -0.02859\sigma + 2.08$ $R^2 = 0.7279$ for 15 min of abrasion (Author)

$d = -0.03951\sigma + 4.0444$ $R^2 = 0.6724$ for 60 min of abrasion (Naik et al,1995)

$d = -1.5992Ln(x) + 7.7283$ $R^2 = 0.9044$ for 60 min of abrasion (Siddique, 2010)

where

d = Average depth of wear of concrete in mm

σ = Compressive strength of concrete in N/mm^2

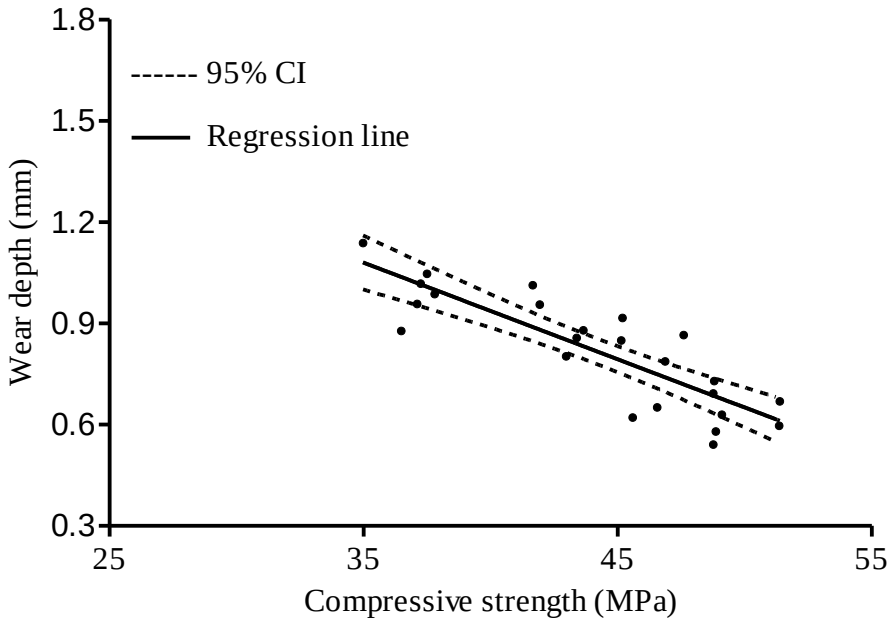

Fig. 4.63: Relationship between compressive strength and average depth of wear of concrete (Concrete 'A')

4.4 PROPERTIES OF CONCRETE MADE WITH SAND HAVING FINENESS MODULUS OF 2.58 (*Concrete* 'B')

4.4.1 Mix Proportions

The river sand collected from Pathankot quarry was conforming to grading zone II specified in BIS: 383-1960 and was used in manufacturing of control concrete. The fineness modulus of this sand was 2.58. The control concrete mixture was designed as per BIS: 10262-1982 to achieve 28 day compressive strength of 34.0 N/mm^2 and was designated as concrete 'B'. A fixed water-cement ratio of 0.5 was adopted in all the concrete mixtures. Superplasticizer at the rate of 0.5% by weight of cement was used in all the concrete mixtures. The river sand was replaced with coal bottom ash in concrete mixtures by mass at levels of 20, 30, 40, 50, 75 and 100%. The river sand as well as coal bottom ash was oven dried at 100^{o}C for 24 ±1 hr to remove moisture and then cooled downed to room temperature for another 24 ±1 hr before use in manufacturing of concrete mixtures. The detail of mix proportions of Concrete 'B' are given in Table 4.15.

Table 4.15 Mix proportions of Concrete 'B'

Mix	Cement (kg/m^3)	w/c	Sand (kg/m^3)	Sand replacement level (%)	Coal bottom ash (kg/m^3)	Coarse aggregate (kg/m^3)	Water (kg/m^3)	Super-plasticizer (kg/m^3)
Control concrete(B_0)	400	0.5	520	0	0	1200	200	2.0
B_{20}	400	0.5	416	20	55.82	1200	200	2.0
B_{30}	400	0.5	364	30	83.72	1200	200	2.0
B_{40}	400	0.5	312	40	111.63	1200	200	2.0
B_{50}	400	0.5	260	50	139.54	1200	200	2.0
B_{75}	400	0.5	130	75	209.30	1200	200	2.0
B_{100}	400	0.5	0	100	279.07	1200	200	2.0

4.4.2 Properties of Fresh Concrete

4.4.2.1 Workability

The workability of fresh concrete mixtures was measured by performing slump test and compaction test and the effect of coal bottom ash as replacement of sand on slump and compaction factor of concrete was observed.

Slump Test

The slump test results of control concrete as well as bottom ash concrete mixtures are illustrated in Fig. 4.64. For fixed water-cement ratio, the slump values decreased on incorporation of coal bottom ash as replacement of sand in concrete. Up to 30% replacement of sand with coal bottom ash in concrete, the slump values were not affected significantly. On 40 and 50% replacement of sand with coal bottom ash in concrete, there was significant decrease in slump values. The slump values decreased drastically on incorporation of 75 and 100% coal bottom ash in concrete. The slump values of bottom ash concrete mixtures $B_{20,}$ $B_{30,}$ $B_{40,}$ B_{50}, B_{75}, and B_{100} were 115, 105, 77, 65, 36, and 15 mm, respectively, as compared to 125 mm of control concrete.

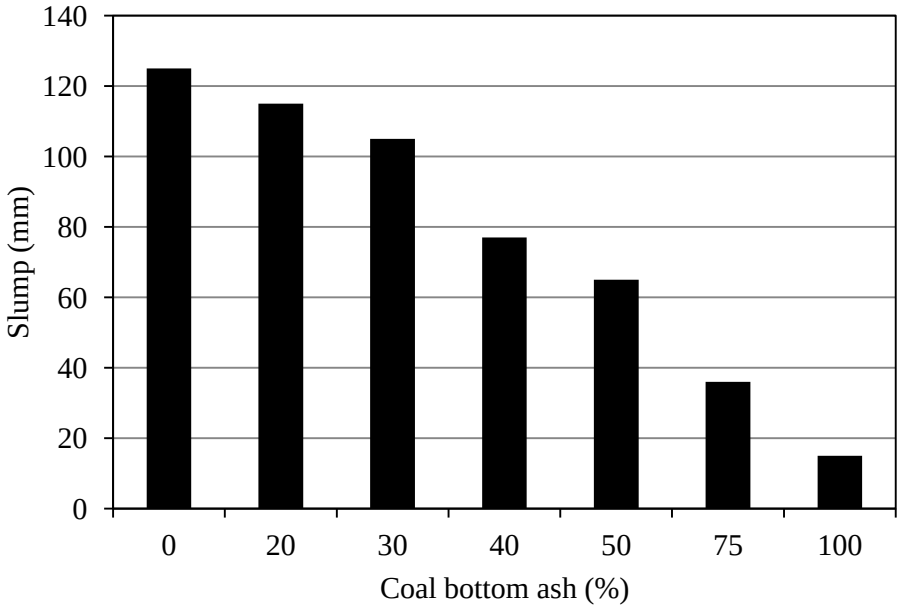

Fig. 4.64: Effect of coal bottom ash on slump values of concrete (Concrete 'B')

The results of the present study which demonstrate decrease in workability of concrete on incorporation of coal bottom ash as fine aggregate in concrete are in good agreement with the previous studies (Ghafoori and Bucholc, 1996, 1997; Kim and Lee, 2011). However, in some published research works (Kou and Poon, 2009; Bai et al., 2005) an increase in slump values of concrete on incorporation of coal bottom ash as fine aggregate is also reported. In research work of Kou and Poon, (2009), the use of saturated surface dry coal bottom ash in production of concrete resulted increase in workability of bottom ash concrete mixtures. Bai et al. (2005) believed that the ball bearing effect of spherical particles of coal bottom ash increased the slump of bottom ash concrete mixtures. Coal bottom ash used in their research work has spherical particles as compared to the angular

shaped, rough textured and porous particles of coal bottom ash used in the present study. The angular shaped, rough textured and dry particles of coal bottom ash used in the present study increased the internal friction between the particles and resulted in low the slump values. For the desired workability of concrete, the water demand is influenced by the properties of fines used in the concrete mixture. As shown in Table 4.3, water absorption of coal bottom ash is more than that of sand. The dry and porous particles of coal bottom ash absorbed more water internally during the mixing process of bottom ash concrete mixtures which resulted in decrease in quantity of free water for lubrication of particles. More the replacement of sand with coal bottom ash in concrete mixture, greater was the effect.

Compaction Factor

The compaction factor test results are presented in Fig. 4.65. Similar to slump values the compaction factor values were not affected significantly up to 30% replacement of river sand with coal bottom ash in concrete.

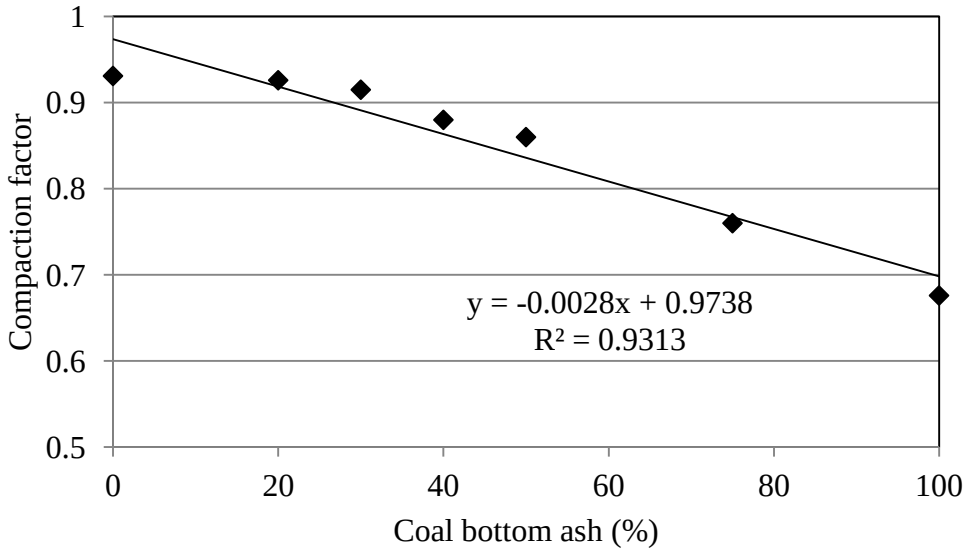

Fig. 4.65: Effect of coal bottom ash on compaction factor values of concrete (Concrete 'B')

However, higher than 30% replacement of sand with coal bottom ash in concrete resulted in significant reduction in compaction factor values of fresh concrete mixtures. Compaction factor values deceased drastically on incorporation of 75% and 100% coal bottom ash as fine aggregate in concrete. The compaction factor values decreased almost linearly with the increase in coal bottom ash content in concrete. The compaction factor

decreased from 0.931 to 0.676 on incorporation of 100% coal bottom ash as fine aggregate in concrete. Compaction factor test results are in line with slump test results. Higher value of coefficient of determination (R^2 = 0.9313) indicates good relevance between the curve and data points.

4.4.2.2 Air Content

The air content test results are presented in Fig. 4.66 The air content in bottom ash concrete mixtures varied between 1.40 and 3.05% as compared to 1.45% in control concrete.

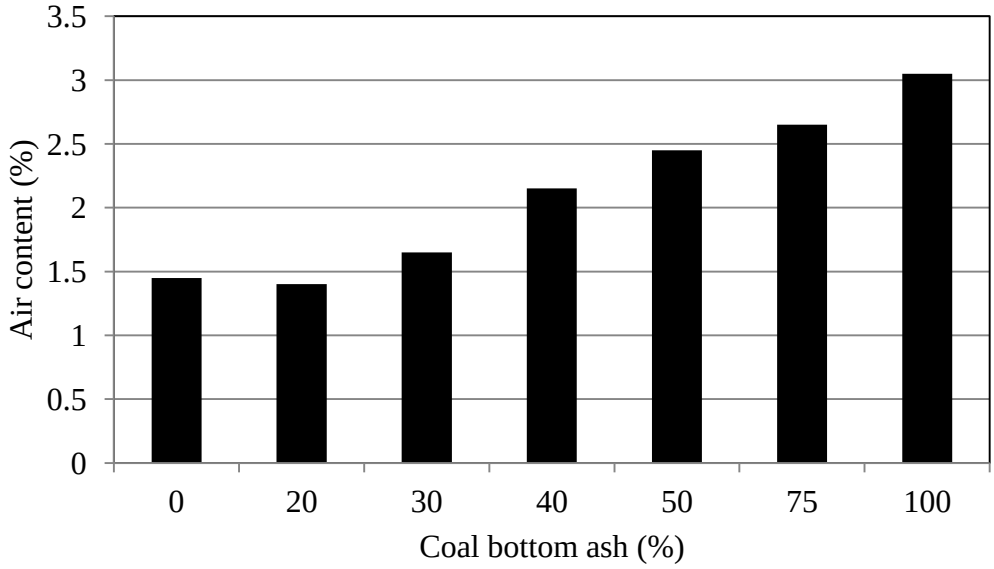

Fig. 4.66: Effect of coal bottom ash on entrapped air content in concrete (Concrete 'B')

Bottom ash concrete containing 100% coal bottom ash as replacement of sand showed highest entrapped air content of 3.05%. The entrapped air content in bottom ash concrete mixtures containing up to 30% coal bottom ash as replacement of sand did not changed significantly. Above 30% replacement of sand with coal bottom ash resulted in significant increase in entrapped air content in bottom ash concrete mixtures. Almost similar trend of air content in bottom ash concrete mixtures of concrete 'A' was observed.

4.4.2.3 Bleeding

The test results of water loss through bleeding are presented in Fig 4.67. The test results indicate that bleeding percentage decreased almost linearly with the increase in coal bottom ash content in concrete. The bleeding percentage decreased from 8.45 to 1.68% on use of 100% coal bottom ash as fine aggregate in concrete. Total volume of bleeding water of concrete mixtures containing 20, 30, 40, 50, 75 and 100% coal bottom ash was 180, 150,

130, 121, 100 and 51 ml, respectively, as compared to 252 ml in control concrete. The volume of bleeding water per unit area of exposed surface after leveling the top surface of freshly placed concrete decreased from 0.5134 to 0.1039 g/cm^2 on incorporation of 100% coal bottom ash as fine aggregate in concrete. The decreased bleeding percentage can be attributed to less quantity of water available in inter particle voids in the bottom ash concrete mixture because the dry and porous particles of coal bottom ash absorbed internally part of water added during the mixing process. However, Andrade et al. (2009) and Ghafoori and Bucholc (1996, 1997) observed higher water loss through bleeding on incorporation of coal bottom ash in concrete. The amount of bleeding water in concrete depends largely on the water-cement ratio. In study carried out by Andrade et al. (2009) and Ghafoori and Bucholc, (1996, 1997), the higher quantity of water was added in bottom ash concrete mixtures to achieve the desired slump which resulted in higher loss of water through bleeding.

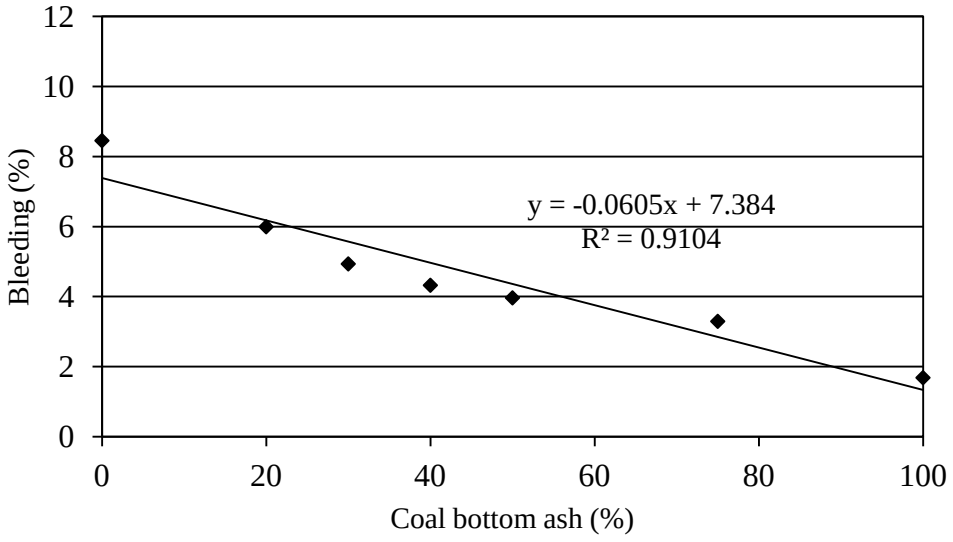

Fig. 4.67: Effect of coal bottom ash on loss of water through bleeding (Concrete 'B')

Andrade et al. (2009) in his research work, used 378 kg/m^3 of water in bottom ash concrete mixture containing 100% coal bottom ash against 219 kg/m^3 used in control concrete. Whereas in the present study, a fixed water-cement ratio was maintained in bottom ash concrete mixtures as well as control concrete mixture. The absorption of part of water by the dry and porous particles of coal bottom during the mixing process resulted in low free water-cement ratio in bottom ash concrete than in control concrete. Lower free water-cement ratio in bottom ash concrete mixtures resulted in lesser loss of water through

bleeding. Loss of water through bleeding was more in bottom ash concrete mixtures of concrete 'B' as compared to that in bottom ash concrete mixtures of concrete 'A'. Higher bleeding in bottom ash concrete mixtures of concrete 'B' than that in bottom ash concrete mixtures of concrete 'A' may be attributed to addition of higher amount of water and use of Na-based SNF superplasticizer (sodium sulfonate naphthalene formaldehyde). Na-based SNF superplasticizers increase the bleeding (Ramachandran, 1995).

4.4.3 Strength Properties of Hardened Concrete

4.4.3.1 Unit Weight

One-day unit density results of bottom ash concrete mixtures as well as control concrete are presented in Fig.4.68. One-day unit density of bottom ash concrete decreased linearly with the increase in levels of replacement of sand with coal bottom ash in concrete.

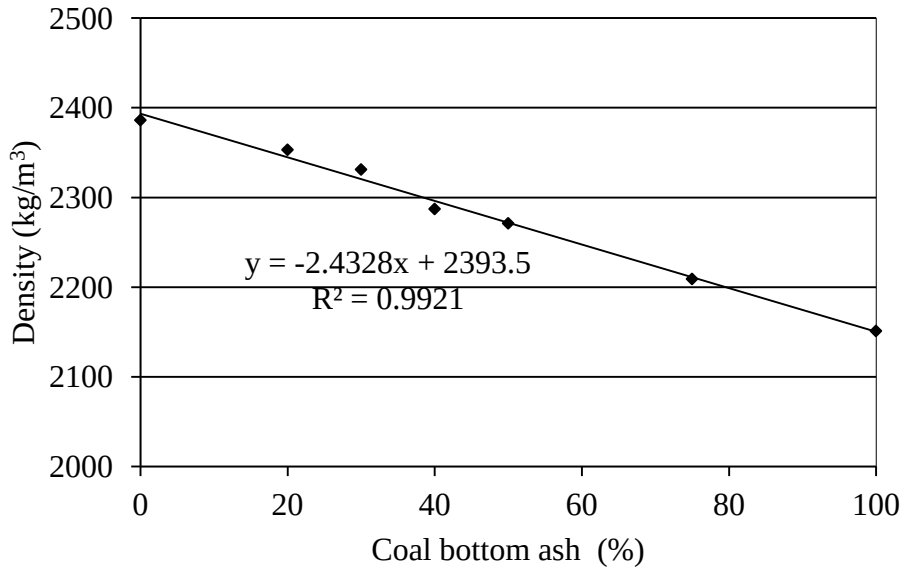

Fig. 4.68: Effect of coal bottom ash on density of concrete (Concrete 'B')

Higher value of coefficient of determination (R^2 = 0.99) indicates good relevance between the curve and data points. At 20, 30, 40, 50, 75 and 100% sand replacement levels, one-day unit density of concrete decreased by 33, 55, 99, 115, 177 and 235 kg/m^3, respectively. When 100 % coal bottom ash was used as fine aggregate, one-day unit density of concrete decreased from 2396 to 2161 kg/m^3. Andrade et al. (2007); Ghafoori and Bucholc (1996, 1997); and Kim and Lee (2011) have also reported decrease in unit density of concrete on use of coal bottom ash as fine aggregate. Topcu and Bilir (2010) have observed similar

trend of decrease in unit weight of mortars on use of coal bottom ash as fine aggregate. The low specific gravity and porous particles of coal bottom ash are responsible for the lower unit density of bottom ash concrete mixtures. On use of coal bottom ash in the concrete mixture, replacement of heavier material (sand) with lighter material (coal bottom ash) resulted in decrease in unit density of bottom ash concrete mixtures. The decrease in one-day unit density was equivalents to the difference in weight of river sand and coal bottom ash in concrete.

4.4.3.2 Water Loss from Air-Drying

Test results of water loss through air-drying of bottom ash concrete mixtures and control concrete are illustrated in Figs. 4.69 and 4.70.

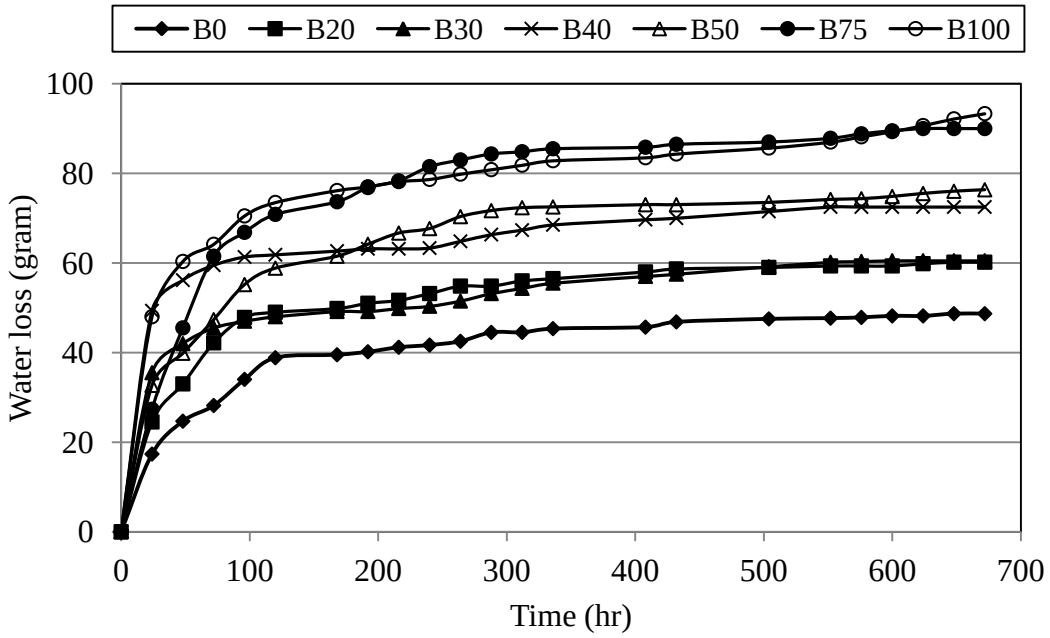

Fig. 4.69: Effect of coal bottom ash on loss of weight of concrete through air-drying (Concrete 'B')

The water loss from air-drying of bottom ash concrete mixtures after demoulding increased with the increase in coal bottom ash content in concrete. After 28 days of air-drying, water loss of bottom ash concrete mixtures containing 20, 30, 40, 50, 75 and 100% coal bottom ash as fine aggregate was 60.17, 60.5, 72.5, 76.33, 90 and 93.33 gram respectively as compared to 48.67 gram water loss of control concrete. Higher permeability and better connectivity of voids in coal bottom ash concrete mixtures at early age may the possible explanation for higher loss of water through air-drying.

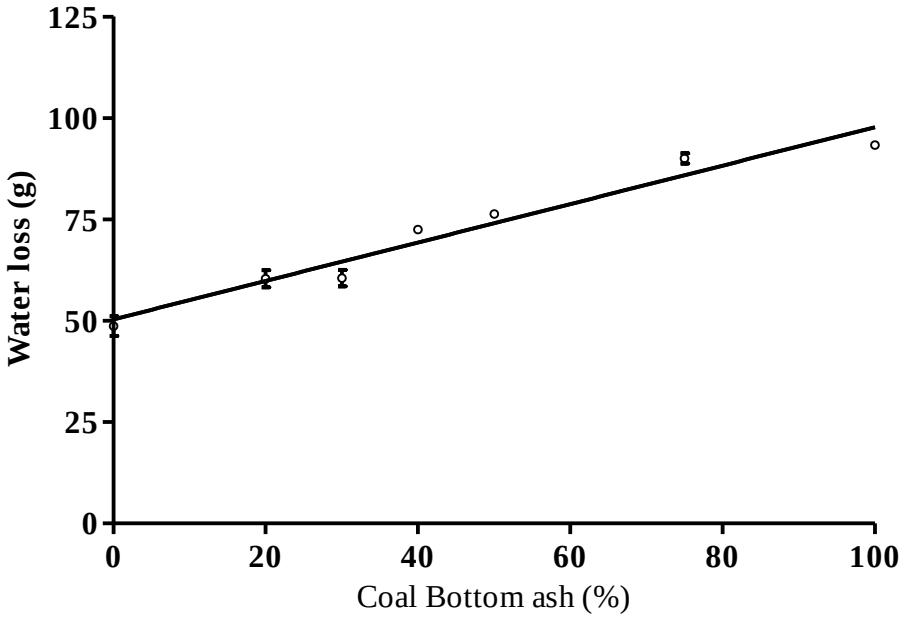

Fig. 4.70: Loss of water through air-drying versus coal bottom ash in concrete (Concrete 'B')

4.4.3.3 Permeable Pore Space and Water Absorption

Permeable pore space and water absorption of concrete specimens were determined as per the procedure given in ASTM C 642-97. The results of permeable pore space and water absorption are illustrated in Table 4.16. At 28 days of curing age, permeable pore space in concrete and water absorption of concrete increased with increase in coal bottom ash content in concrete with the exception of bottom ash concrete mixture containing 20% coal bottom ash in which permeable pore space and water absorption was less than control concrete. At 28 days of curing age, permeable pore space in concrete increased from 10.39 to 11.86% and to 11.58% on incorporation of 75 and 100% coal bottom ash in concrete, respectively. Water absorption of bottom ash concrete mixtures containing 50, 75 and 100% coal bottom ash was 4.56, 5.26 and 5.04%, respectively, as compared to 4.22% of control concrete. With the addition of coal bottom ash in concrete, at early curing age, the connectivity between the capillaries in the paste improved. The permeable pore space and water absorption of bottom ash concrete mixtures reduced with progress of curing age. The permeable pore space in bottom ash concrete mixture containing 100% coal bottom ash as fine aggregate reduced from 11.58% at 28 days to 9.73% at 365 days of curing age. The water absorption of bottom ash concrete mixture containing 100% coal bottom ash as fine aggregate reduced from 5.04% at 28 days to 4.45% at 365 days of curing age.

Table 4.16 Permeable pore space (void) and water absorption of concrete (Concrete 'B')

Mix	Permeable pore space (%) at curing age (days)				Water absorption (%) at curing age (days)			
	28	**90**	**180**	**365**	**28**	**90**	**180**	**365**
Control concrete(B_0)	10.39	9.76	9.23	8.85	4.22	4.13	3.64	3.60
B_{20}	10.26	9.61	8.59	8.25	4.25	3.57	3.33	3.28
B_{30}	11.02	10.03	9.21	8.89	4.37	4.0	3.93	3.77
B_{40}	10.78	10.28	10.09	9.99	4.8	4.46	4.14	4.02
B_{50}	11.14	10.68	10.01	9.82	4.56	4.64	4.30	4.14
B_{75}	11.86	10.56	9.64	9.27	5.26	4.60	4.05	4.17
B_{100}	11.58	10.48	10.04	9.73	5.04	4.45	4.43	4.45

The reduction in permeable pore space in bottom ash concrete mixtures with the progress of curing age is significant. The pozzolanic activity of the coal bottom ash is believed to be responsible for the reduction of permeable pore space in bottom ash concrete mixtures.

4.4.3.4 Compressive Strength

Compressive strength test results are illustrated in Figs.4.71 and 4.72. At early curing age of 7 days, bottom ash concrete mixtures B_{20}, B_{30}, B_{40}, B_{50}, B_{75} and B_{100} achieved 86.97, 85.06, 87.82, 82.5, 76.04 and 66.86%, respectively, of the compressive strength of the control concrete specimen. At 28 days of curing age, the above bottom ash concrete mixtures achieved 94.45, 95.12, 92.27, 86.96, 80.7 and 79%, respectively, of the compressive strength of the control concrete mixture. At early curing age, lower free water-cement ratio might have contributed in minimizing the negative effect of coal bottom ash on compressive strength of concrete. In addition other factors such as replacement of stronger material with weak material, the slow hydration due to addition of coal bottom ash in concrete may also be the possible explanation for lower compressive strength of bottom ash concrete mixtures. After 90 days of curing age, the compressive strength of bottom ash concrete mixtures B_{20}, B_{30}, B_{40}, B_{50}, B_{75} and B_{100} was 2.86, 2.79, 6.12, 8.20, 11.58 and 15.22%, respectively, lower than that of the control concrete. At 180 days of curing age, these margins dropped to 1.23, 3.47, 4.35, 0.86, 2.0 and 5.84%, respectively. From the above data, it is clear that with the progress of curing age, the gain in compressive strength of bottom ash concrete is consistent and significant. After 28 days

of curing age, bottom ash concrete mixtures achieved compressive strength at a faster rate than the control concrete. Up to 90 days of curing age, the compressive strength of bottom ash concrete mixtures remained lower than that of control concrete mixture. At 180 days of curing age, compressive strength of bottom ash concrete mixtures was comparable to that of control concrete. At 180 days of curing age, compressive strength of bottom ash concrete mixtures $B_{20,}$ B_{30}, B_{40}, B_{50}, B_{75} and B_{100} was 45.0, 44.0, 43.58, 45.2, 44.6 and 42.9 N/mm^2, respectively, which is comparable to 45.6 N/mm^2 of control concrete.

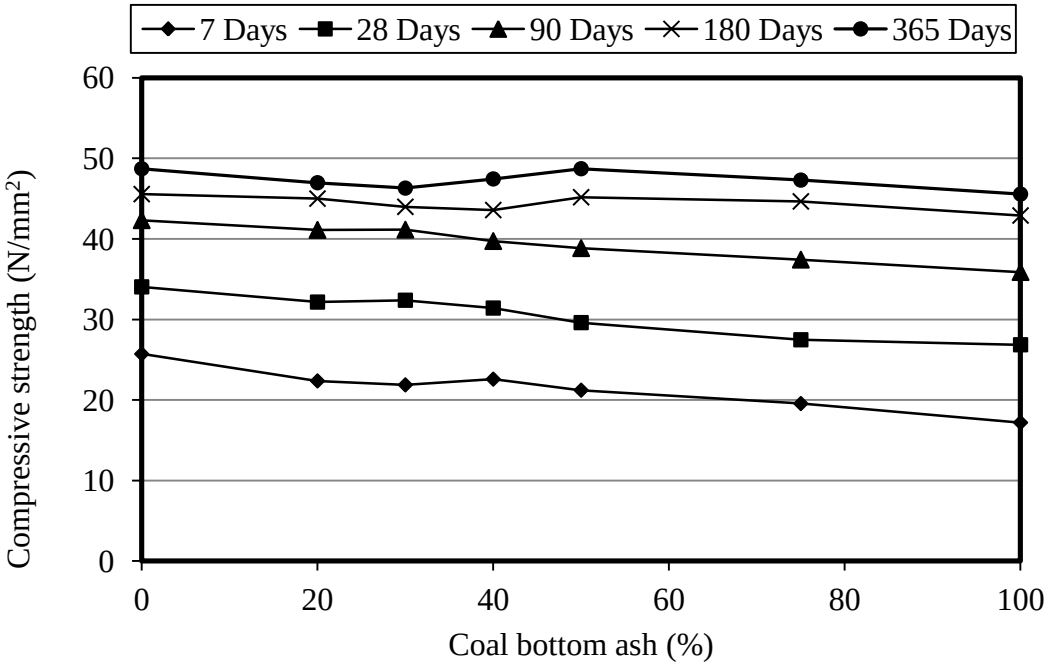

Fig. 4.71: Compressive strength of concrete versus coal bottom ash content (Concrete 'B')

At 365 days of curing age, bottom ash concrete mixtures B_{20}, B_{30}, B_{40}, B_{50}, B_{75} and B_{100} gained 146.10, 142.99, 151.03, 164.56, 172.19 and 169.68%, respectively, of their 28-day compressive strength as compared to 143.1% gained by control concrete. This may be attributed to the delayed hydration and pozzolanic activity of coal bottom ash after 28 days of curing age. At 180 and 365 days of curing period, bottom ash concrete containing 50% coal bottom ash achieved optimum compressive strength which may be due to combined effect of optimum packing of particles and pozzolanic action of coal bottom ash. The start of pozzolanic activity of coal bottom ash is evident from the scanning electron micrographs shown in Figs 4.100 and 4.101. The results of the present work are comparable to that reported by Ghafoori and Bucholc (1996, 1997) wherein they have observed that 28-day compressive strength of bottom ash concrete was lower by 17% than

the 28-day compressive strength of control concrete and this margin dropped to 7% at 180 days of curing age. Kim and Lee (2011) also observed that the compressive strength was not strongly affected on incorporation of coal bottom ash as fine aggregate in concrete.

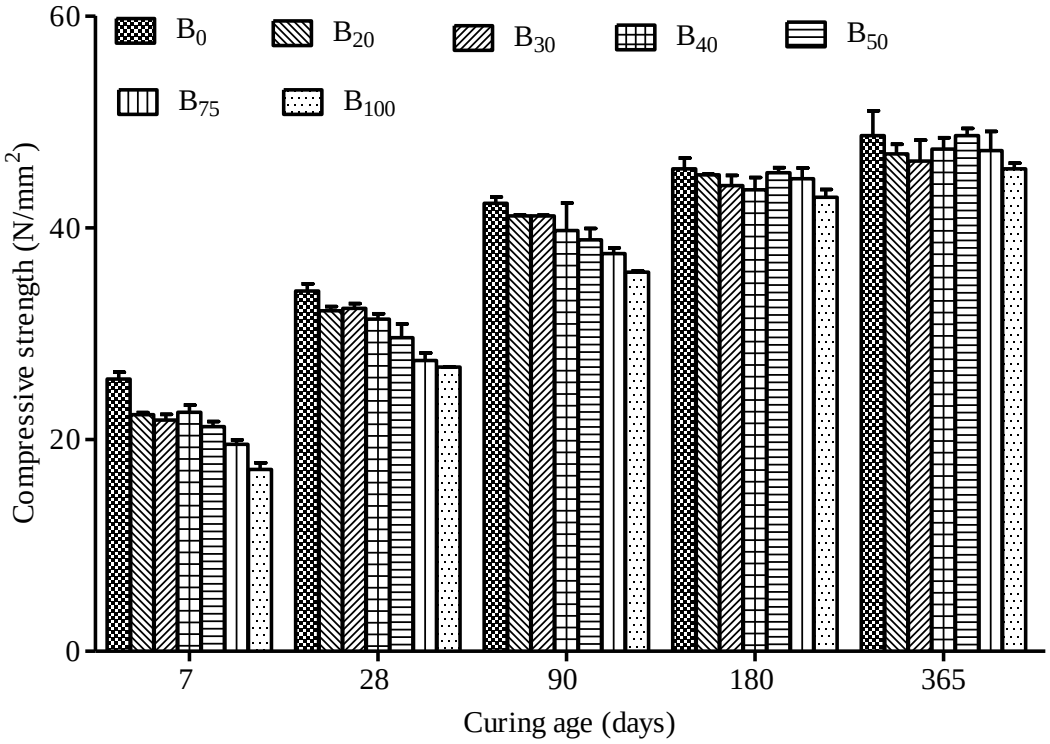

Fig. 4.72 Effect of coal bottom ash on compressive strength of concrete (Concrete 'B')

Statistical significance of effect of coal bottom ash on compressive strength of bottom ash concrete was confirmed at 7 days and 28 days. The empirical equation to determine the relationship between compressive strength, the curing age and coal bottom ash content in concrete was established from the test results. The empirical equation developed for compressive strength of bottom ash concrete mixtures containing 20 to 100% coal bottom ash as sand replacement is given as under:

$$f_t = C \ln(t) + D$$

$$C = 4.4077\, a^{0.1155}; \quad D = 18.288\, e^{-0.019a} \qquad R^2 = 0.9845$$

Higher value of determination coefficient (R^2) indicates good relationship between the data and regression curve. Similar empirical equations derived by M. a. a. Abd elaty (2014) for normal cement concrete are given as under:

For normal concrete (28-day compressive strength = 32 MPa and w/c = 0.6)

f_t = 6.2791ln(t) + 9.2031 R^2 = 0.9907

where,

f_t = Compressive strength of concrete in N/mm^2 at age (t)

t = Curing age in days

a = Coal bottom ash content in percentage (%)

4.4.3.5 Splitting Tensile Strength

The splitting tensile strength results of concrete mixtures are presented in Figs. 4.73 and 4.74. The results of the present study are comparable with those reported in previous studies (Ghafoori and Bucholc, 1996, 1997; Chun et al., 2008). At 7 days of curing age, bottom ash concrete mixtures B_{20}, B_{30}, B_{40}, B_{50}, B_{75} and B_{100} achieved 71.02, 70.03, 70.23, 68.23, 70.8 and 72.50%, respectively, of their 28-day splitting tensile strength as compared to 69.70% achieved by control concrete. At 28 days of curing age, the splitting tensile strength of bottom ash concrete mixtures B_{20}, B_{30}, B_{40}, B_{50}, B_{75} and B_{100} was 4.05, 2.41, 2.02 6.93, 12.38 and 15.73%, respectively, lower than that of the control concrete. With the progress of age, the splitting tensile strength of bottom ash concrete mixtures improved at a faster rate than that of control concrete. At 90 days of curing age, the splitting tensile strength of bottom ash concrete mixtures B_{20} and B_{30} was 3.83 and 2.85%, respectively, higher than that of control concrete. However, splitting tensile strength of bottom ash concrete mixtures B_{50}, B_{75}, and B_{100} was 1.79, 4.43 and 6.42%, respectively, lower than that of control concrete. At 180 days of curing age, bottom ash concrete mixtures B_{20}, B_{30} and B_{50} displayed 3.94, 2.42 and 0.91%, respectively, higher splitting tensile strength than the control concrete. Splitting tensile strength of bottom ash concrete mixtures B_{40}, B_{75} and B_{100} remained 0.9, 4.55 and 2.12%, respectively, lower than that of control concrete.At 365 days of curing age, bottom ash concrete mixtures B_{20}, B_{30}, B_{40}, B_{50}, B_{75} and B_{100} gained 159.90, 156.42, 153.02, 173.64, 165.78 and 170.52%, respectively, of their 28-day splitting tensile strength as compared to 160.05% gained by the control concrete. At 28 and 90 days of curing ages, the ratio of splitting tensile strength and compressive strength of bottom ash concrete increased from 0.0754 to 0.0806 and from 0.0715 to 0.0789, respectively, on incorporation of 100% coal bottom ash as fine aggregate. This suggests

that the incorporation of coal bottom ash had more effect on tensile strength than the compressive strength.

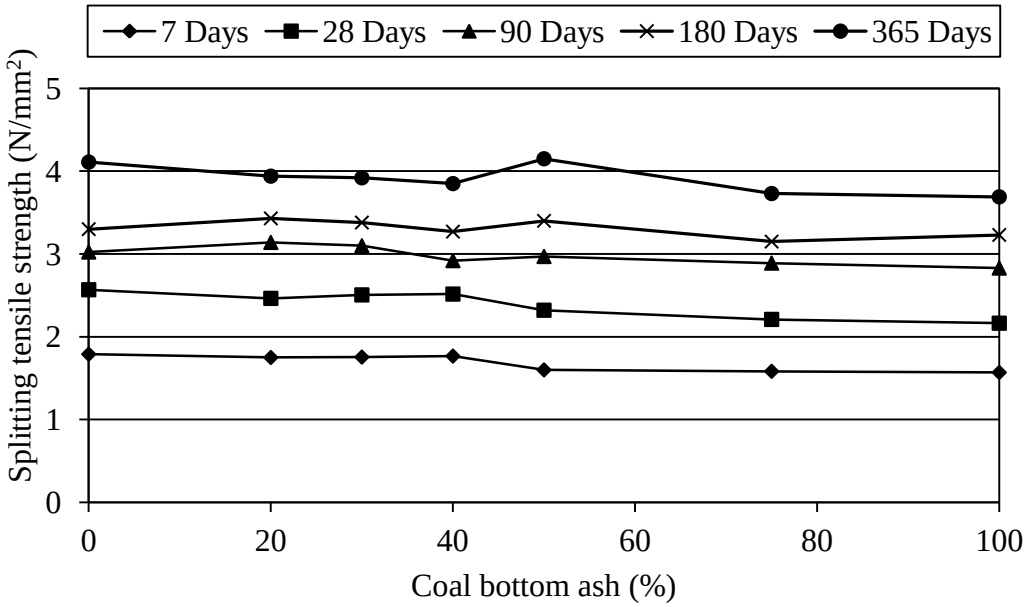

Fig. 4.73: Splitting tensile strength of concrete versus coal bottom ash content (Concrete 'B')

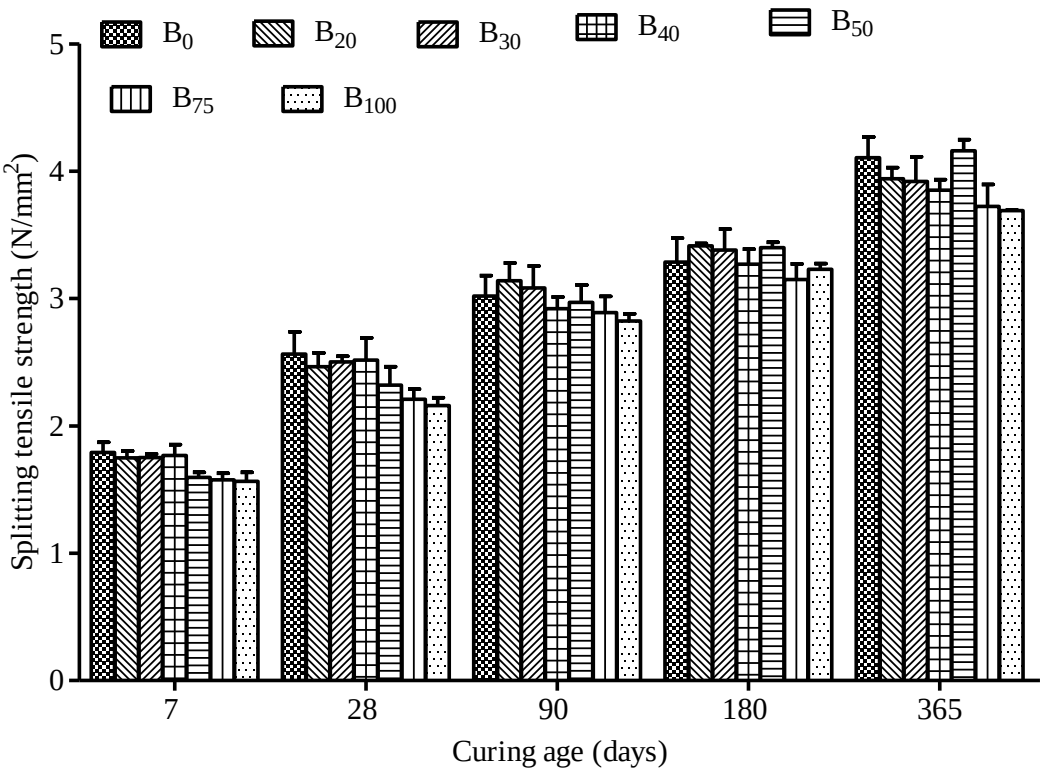

Fig. 4.74: Effect of coal bottom ash on splitting tensile strength of concrete (Concrete 'B')

Since the splitting tensile strength is more dependent on quality of paste than the compressive strength, the pozzolanic activity of coal bottom ash might have contributed more to splitting tensile strength than to compressive strength. The splitting tensile strength and compressive strength ratios shown in Table 4.17 are in good agreement with the data published in previous studies (Prince and Walter, 1951).

Table 4.17 Splitting tensile and compressive strength ratios of bottom ash concrete and control concrete (Concrete 'B')

Mix	**Splitting tensile / Compressive strength ratio (%) at curing age (days)**				
	7	**28**	**90**	**180**	**365**
Control concrete (B_0)	6.96	7.6	7.2	7.2	8.44
B_{20}	7.83	7.7	8.1	7.6	8.39
B_{30}	8.05	7.7	7.8	7.7	8.47
B_{40}	7.83	8.0	7.2	7.5	8.12
B_{50}	7.54	7.5	7.0	7.6	8.52
B_{75}	7.79	7.8	7.7	7.1	7.89
B_{100}	9.13	8.1	7.89	7.5	8.10

At 7 days of curing age, the splitting tensile strength and compressive strength ratio (%) increased from 6.96 to 9.13 on 100% replacement of river sand with coal bottom ash in concrete. The splitting tensile strength and compressive strength ratios (%) of bottom ash concrete mixtures decreased with the increase in curing age. At the curing age of 7, 28, 90, 180 and 365 days, the average values of splitting tensile strength and compressive strength ratios (%) of bottom ash concrete mixtures were 8.03, 7.8, 7.58, 7.50 and 8.25 respectively. The results show that similar to conventional concrete, the compressive strength and splitting tensile strength of concrete containing coal bottom ash as partial or total replacement of river sand increased with the progress of curing age, but compressive strength improved at a faster rate than the splitting tensile strength.

4.4.3.6 Modulus of Elasticity

Comprehensive study of elastic behaviour of a new concrete incorporating coal bottom ash as fine aggregate is must before its adoption as an engineering material. The deformation and deflection of structural member can only be calculated if the stress-strain relationship

of new concrete is known. Modulus of elasticity of new concrete incorporating coal bottom ash was determined at the curing age of 28, 90 180 and 365 days. The results of modulus of elasticity of coal bottom ash concrete and that of control concrete are presented in Figs. 4.75 and 4.76; and Table 4.18. The modulus of elasticity of bottom ash concrete mixtures up to 50% replacement level is comparable to that of control concrete at all the curing ages. However, on 100% replacement of river sand with coal bottom ash, at 28 days of curing age, modulus of elasticity decreased from 25.39 GPa to 21.32 GPa. At 28 days of curing age, concrete mixture incorporating 75% and 100% coal bottom ash achieved 92% and 83.97%, respectively, of modulus of elasticity of control concrete. With the progress of age, modulus of elasticity of bottom ash improved in a similar manner as in the case of control concrete. At 180 days of curing age, bottom ash concrete mixture incorporating 100% coal bottom ash gained 9.9% above its 28-day modulus of elasticity as compared to 6.42% gained by control concrete. Kim and Lee (2011) also observed the similar results in their study when 100% coal bottom ash was used as fine aggregate in concrete. The lower value of modulus of elasticity of concrete incorporating 100% coal bottom ash as compared to that of control concrete has also been reported by Ghafoori and Bucholc (1996, 1997).

Table 4.18 Modulus of elasticity of bottom ash concrete mixtures and control concrete (Concrete 'B').

Mix	**Modulus of elasticity at curing age (days)**			
	28	**90**	**180**	**365**
Control concrete (B_0)	25.39	26.46	27.02	28.84
B_{20}	25.38	26.06	26.42	28.51
B_{30}	24.95	26.14	27.06	28.32
B_{40}	25.97	26.65	27.18	28.4
B_{50}	25.04	26.01	26.42	27.53
B_{75}	23.36	24.73	25.79	26.81
B_{100}	21.32	22.4	23.43	25.38

The values of modulus of elasticity of coal bottom ash concrete observed in this research work are in good agreement with the values given for normal weight concrete BS: 8110; Part 2: 1980 and expression given in ACI Building Code 318-89.

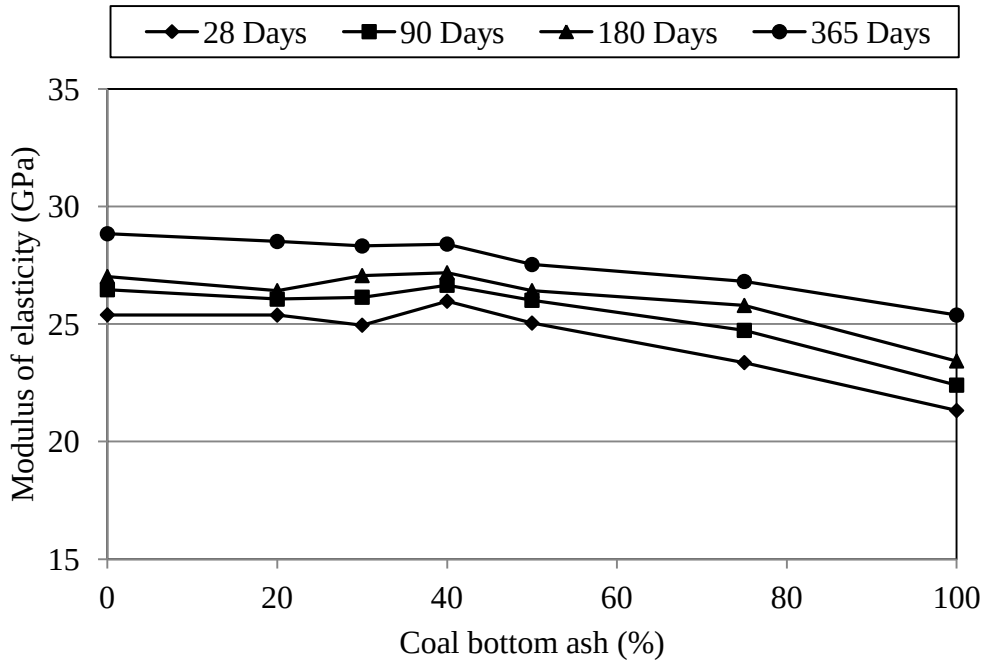

Fig. 4.75: Modulus of elasticity of concrete versus coal bottom ash content (Concrete 'B')

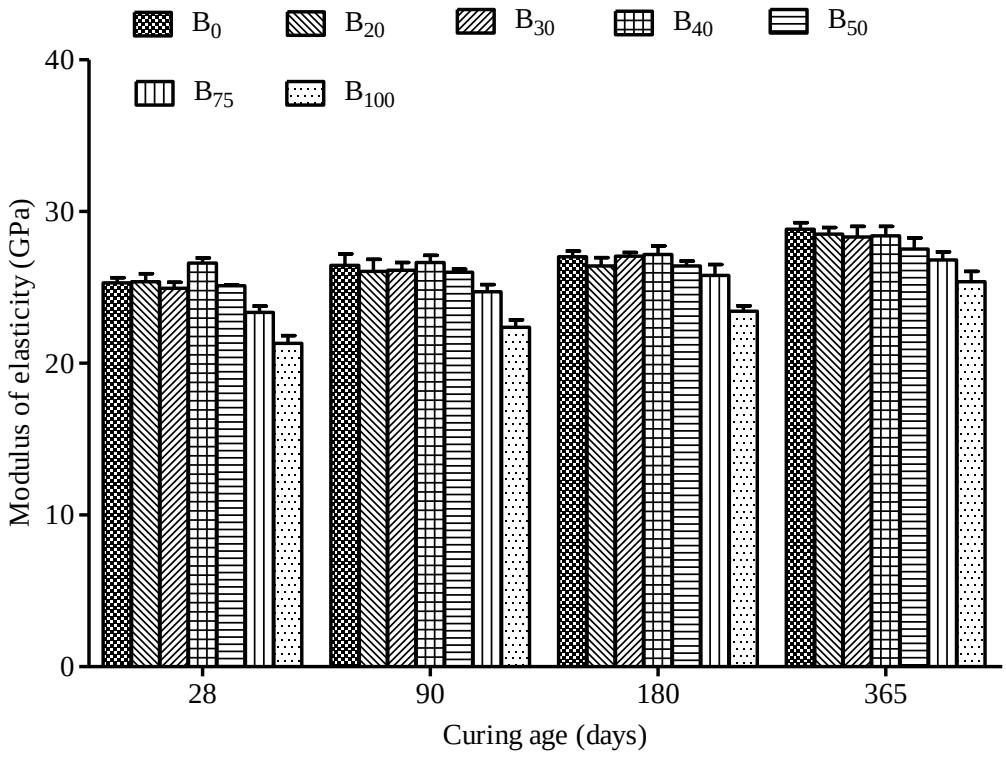

Fig. 4.76: Effect of coal bottom ash on modulus of elasticity of concrete (Concrete 'B')

4.4.3.7 Pulse Velocity

The values of pulse velocities obtained in this study are presented in Fig. 4.77 and Table 4.19. At 28 days of curing age, pulse velocity decreased from 4380 to 4130 m/s on incorporation of 100% coal bottom ash as fine aggregate in concrete. As shown in Fig. 4.77, the pulse velocity through concrete decreased almost linearly with increase in coal bottom ash content in concrete at all the curing ages. The results indicate that the pulse velocity through concrete increased with the progress of age in a similar form as the compressive strength increased. In the study (Topcu and Billir 2010) similar effect of coal bottom ash on pulse velocity through mortars is reported. At 28 days of curing age, the pulse velocity through bottom ash concrete mixtures B_{30}, B_{50}, B_{75} and B_{100} was 3.2, 2.28, 5.02 and 5.71%, respectively, lower than that through the control concrete. From the pulse velocities obtained at 28 days of curing age, the quality of concrete made with coal bottom ash as partial or total replacement of sand can be graded good as per BIS: 13311-92. It is apparent from Fig 4.78 that the pulse velocity through concrete increased with age. The rate of increase in pulse velocities was faster up to 180 days of curing age. After 180 days of curing age, the pulse velocities through concrete mixtures continued to increase but at a slower pace. At 365 days of curing age, pulse velocities through above bottom ash concrete mixtures were 1.67, 2.36, 6.07 and 5.86%, respectively, lower than that through control concrete. Higher values of pulse velocities obtained in this study indicate that the quality of bottom ash concrete mixtures in terms of density, homogeneity and uniformity was good.

Table 4.19 Pulse velocity through concrete specimens (Concrete 'B')

Mix	**Pulse velocity (m/s) at curing age (days)**			
	28	**90**	**180**	**365**
Control concrete (B_0)	4380	4505	4650	4780
B_{20}	4250	4430	4623	4650
B_{30}	4240	4440	4630	4700
B_{40}	4300	4410	4577	4630
B_{50}	4280	4350	4480	4667
B_{75}	4160	4360	4407	4490
B_{100}	4130	4310	4447	4500

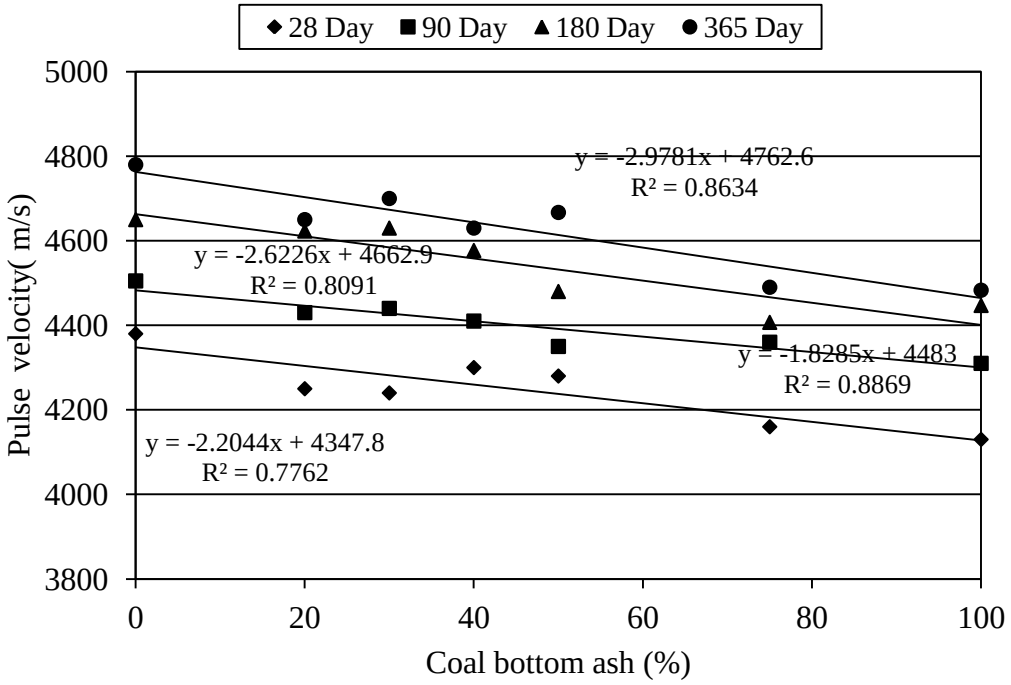

Fig. 4.77: Effect of coal bottom ash on pulse velocity through concrete (Concrete 'B')

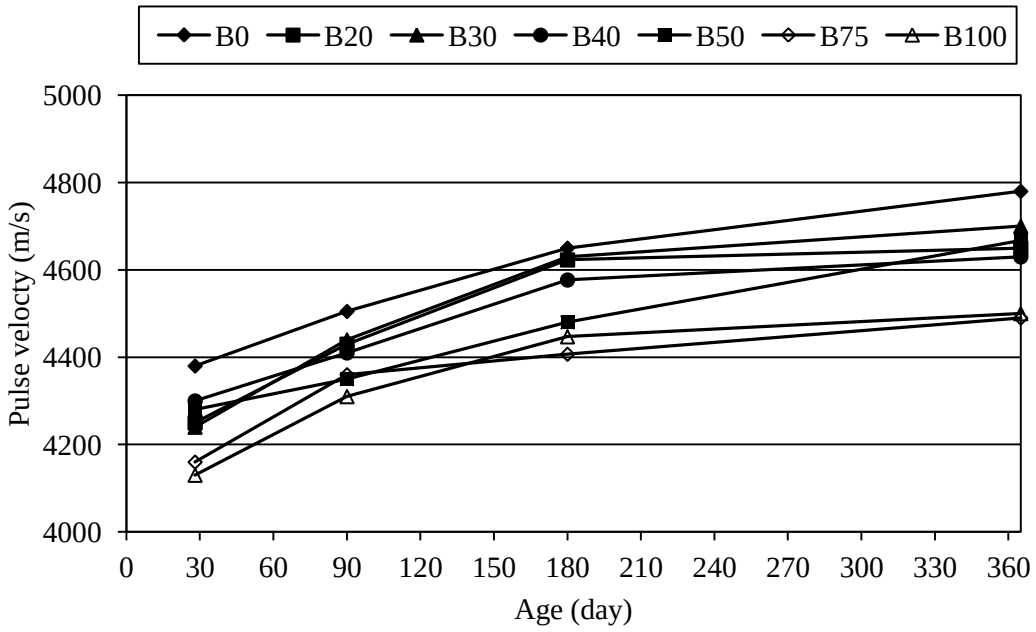

Fig. 4.78: Variation of pulse velocity with curing age (Concrete 'B')

The increased pulse velocity values indicate the increase in the gel/space ratio due to continued hydration process with age. At 365 days of curing period, the pulse velocity through bottom ash concrete mixtures B_{30}, B_{50}, B_{75} and B_{100} increased by 10.85, 9.04,

7.93 and 8.96%, respectively, over that at 28 days of curing age as compared to 9.13% increased through control concrete.

4.4.4 Durability Properties of Concrete

4.4.4.1 Sorptivity

Sorptivity test results are presented in Fig. 4.79. The variation of sorptivity of water with respect to coal bottom ash content in concrete is shown in Fig. 4.80. The water sorptivity of concrete mixtures incorporating coal bottom ash as substitute of river sand increased with the increase in coal bottom ash content in concrete. These results are in line with water absorption results. For bottom ash concrete mixtures, initial rate of absorption of water increased with increase in replacement level of river sand. Initial rate of absorption of water of bottom ash concrete mixtures B_{20}, B_{30}, B_{40}, B_{50}, B_{75} and B_{100} was 6 x 10^{-4} mm/√s, 7 x 10^{-4} mm/√s, 8 x 10^{-4} mm/√s, 7 x 10^{-4} mm/√s, 7 x 10^{-4} mm/√s and 9 x 10^{-4} mm/√s, respectively, as compared to 6 x 10^{-4} mm/√s of control concrete. However, for all the bottom ash concrete mixtures as well as control concrete mixture, the secondary rate of absorption of water was 2 x 10^{-4} mm/√s. The initial rate of absorption of water increased from 6 x 10^{-4} mm/√s to 9 x 10^{-4} mm/√s on 100% replacement of river sand with coal bottom ash in concrete. This means that bottom ash concrete mixtures took lesser time for rise of water by capillary action and thus bottom ash concrete mixtures were more porous than control concrete. At early curing period of 28 days, both permeable pore space test results and scanning electron micrographs also confirmed more voids in bottom ash concrete mixtures as compared to that in control concrete. The absorption of more water at a faster rate by the porous particles of coal bottom ash and the rise of more water through higher number of capillary voids may be the possible explanation for higher initial water sorptivity of bottom ash concrete mixtures. Sorptivity of water of bottom ash concrete mixtures B_{20}, B_{30}, B_{40}, B_{50}, B_{75} and B_{100} was 12.02, 6.70, 17.34, 20.03, 25.35 and 36.03%, respectively, higher than that of control concrete. As shown in Fig. 4.80, total water sorptivity increased almost linearly with the increase in replacement level of river sand with coal bottom ash. Higher value of coefficient of determination (R^2 = 0.9403) indicates good relevance between the curve and data points.

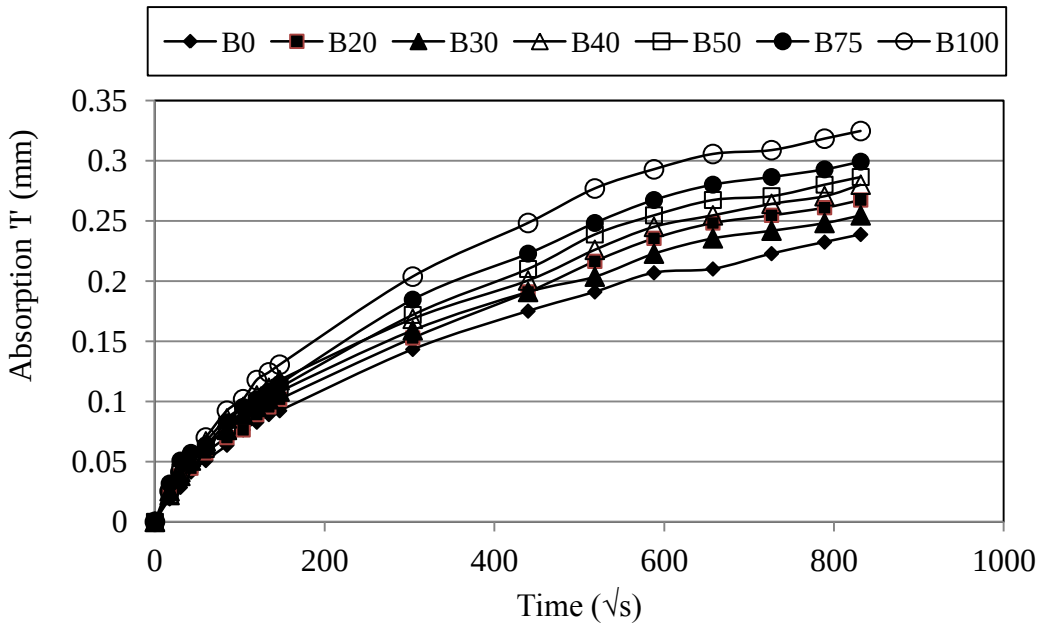

Fig. 4.79: Effect of coal bottom ash on water sorptivity of concrete (Concrete 'B')

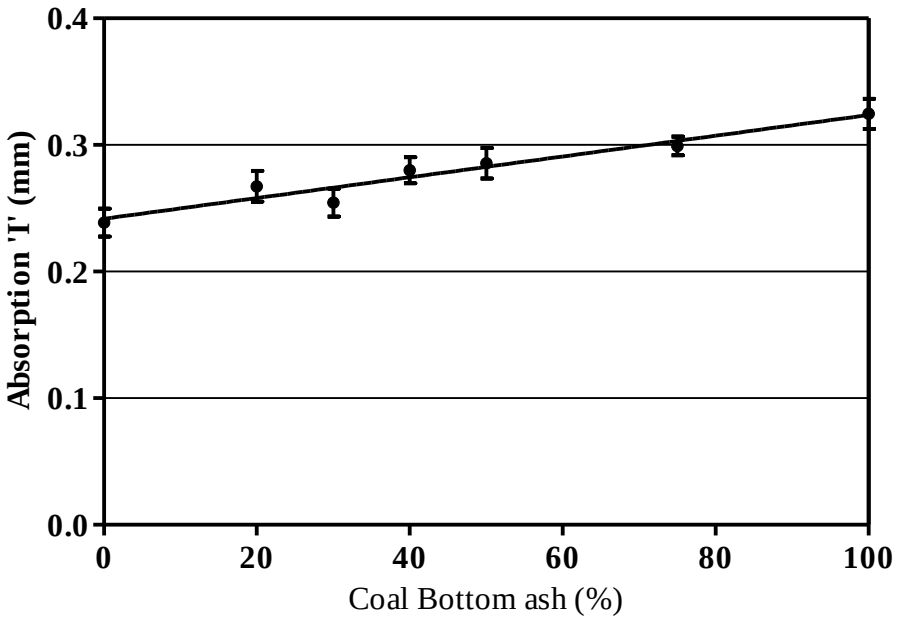

Fig. 4.80: Sorptivity versus coal bottom ash content in concrete (Concrete 'B')

4.4.4.2 Chloride Permeability

Rapid Chloride Penetration Test was used to measure the chloride permeability of concrete specimens. The observed values of charge in coulombs passed through concrete specimens are presented in Fig. 4.81 and Table 4.20. The test results show that at 28 days of curing

age, resistance to chloride ion penetration decreased on use of coal bottom ash in concrete up to 75% replacement of sand. However, on 100% replacement of sand with coal bottom ash in concrete, resistance to chloride ion penetration increased. The total charge passed through bottom ash concrete mixtures $B_{20,}$ $B_{30,}$ $B_{40,}$ B_{50}, B_{75} and B_{100} over a period of 6 hrs was 2523 , 2632, 2513, 2347, 2310 and 2047 coulombs, respectively, as compared to 2276 coulombs passed through control concrete. The total charge passed during the test duration decreased by 10.06% on 100% replacement of sand with coal bottom ash. With the progress of age, the resistance to chloride ion penetration increased with increase in coal bottom ash content in concrete. After 90 days of curing age, the total charge passed through bottom ash concrete specimens was lower than that through control concrete. After 28 days of curing age, the pozzolanic activity of coal bottom ash resulted in consumption of calcium hydroxide and formation of CSH gel. The CSH gel thus formed filled the voids and interrupted the continuity of pores in the bottom ash concrete mixtures. The start of pozzolanic activity of coal bottom ash after 28 days of curing age was evident from SEM image shown in Figs 4.100 to 4.101. The other reason for higher resistance to penetration of chloride ions was that the finer particles of coal bottom ash filled the inter particles voids in concrete. At 90 days of curing age, total charge passed through bottom ash concrete specimens B_{20}, B_{30}, B_{40}, B_{50}, $B_{75,}$ and B_{100} was lower by 2.23, 19.68, 21.39, 19.26, 19.80 and 21.44%, respectively, than that through the control concrete. At 180 days of curing age, these margins increased to 7.22, 28.66, 21.19, 34.57, 65.79 and 70.0%, respectively.

Table 4.20 Charge passed through concrete specimens. (Concrete 'B')

Mix	**Total charge (coulombs) passed through concrete at curing age (days)**			
	28	**90**	**180**	**365**
Control concrete (B_0)	2276	1931	1675	1062
B_{20}	2523	1888	1554	912
B_{30}	2632	1551	1195	824
B_{40}	2513	1518	1320	885
B_{50}	2288	1559	1096	875
B_{75}	2393	1567	573	585
B_{100}	2047	1517	502	417

At 365 days of curing age, total charge passed through bottom ash concrete mixture containing 100% coal bottom ash as fine aggregate was 417 coulombs as compared 1062 coulombs of charge passed through control concrete. Whereas permeable pore space in this bottom ash concrete mixture was 9.73% as compared to 8.85% in control concrete. There are two possible reasons for low charge passed through bottom ash concrete mixture: 1) voids in bottom ash concrete mixture includes voids in coal bottom ash as a result the net interconnected voids in bottom ash concrete mixture were less; 2) alkalinity of pore solution of bottom ash concrete mixture was lower. Inclusion of coal bottom ash lowers the alkalinity of the pore solution. The results of the present study are in good agreement with the results reported in previous studies (Aramraks, 2006; Kou and Poon, 2009).

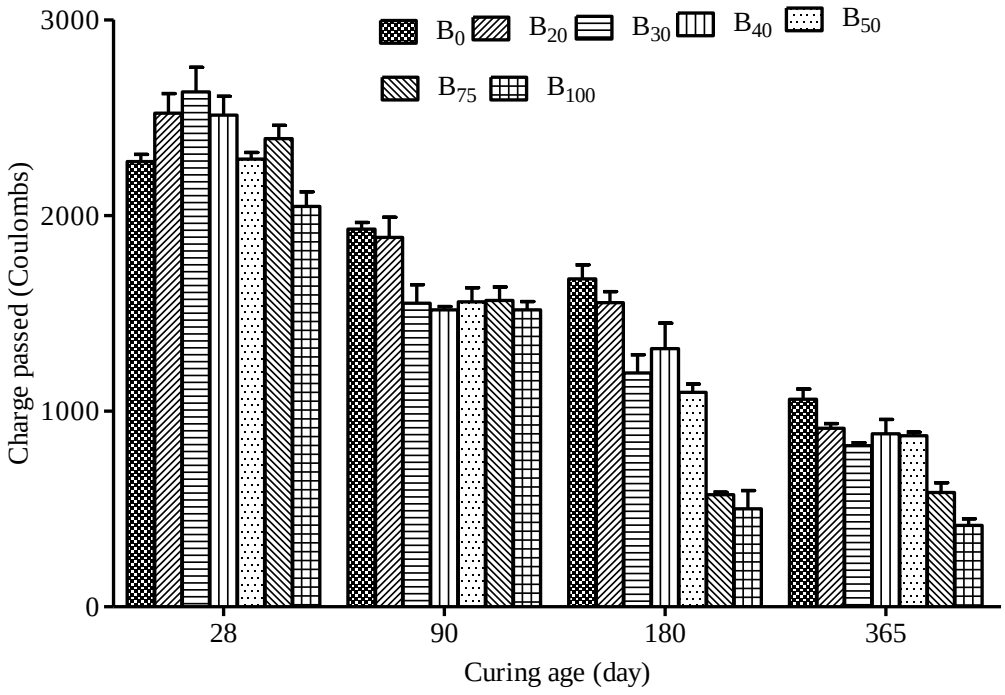

Fig. 4.81: Effect of coal bottom ash on chloride ion penetration in concrete (Concrete 'B')

4.4.4.3 Acid Resistance

Sulphuric acid reacts with calcium hydroxide and produces calcium sulfate ($CaSO_4$). The reaction of sulphuric acid with calcium silicate hydrate also results in forming of silicate oxide in aqueous state. Weight loss and compressive strength loss of the test specimens versus immersion time in sulphuric acid solutions are shown in Figs. 4.82 and 4.83 respectively. Compressive strength and loss of weight are an average of three specimens of

the same concrete mixture. The data for the individual specimens varied between less than 5 percent of the average values.

Mass Loss

The resistance to external acid attack was measured in terms of weight loss of concrete specimens. The weight loss of concrete specimens after external attack of sulphuric acid is illustrated in Fig. 4.82. It was observed that bottom ash concrete specimens performed slightly poorer than control concrete, when immersed in 3% sulphuric acid solution. After 28 days of immersion period, the weight loss of bottom ash concrete mixtures B_{20}, B_{30}, B_{20}, B_{50}, B_{75} and B_{100} was 2.61, 3.07, 3.17, 3.64, 3.41 and 3.02%, respectively, as compared to 2.7% weight loss of the control concrete. Weight loss of all concrete specimens increased with increase in immersion period. At 56 days period of immersion, weight loss of bottom ash concrete mixtures $B_{20,}$ $B_{30,}$ $B_{40,}$ $B_{50,}$ B_{75} and B_{100} increased to 5.21, 5.35, 5.37, 5.96, 5.83 and 5.01%, respectively. Whereas loss of weight of control concrete specimen during the same period was 4.94%. The weight loss of bottom ash concrete specimens after immersion in sulphuric acid solution increased with the increase in coal bottom ash content.

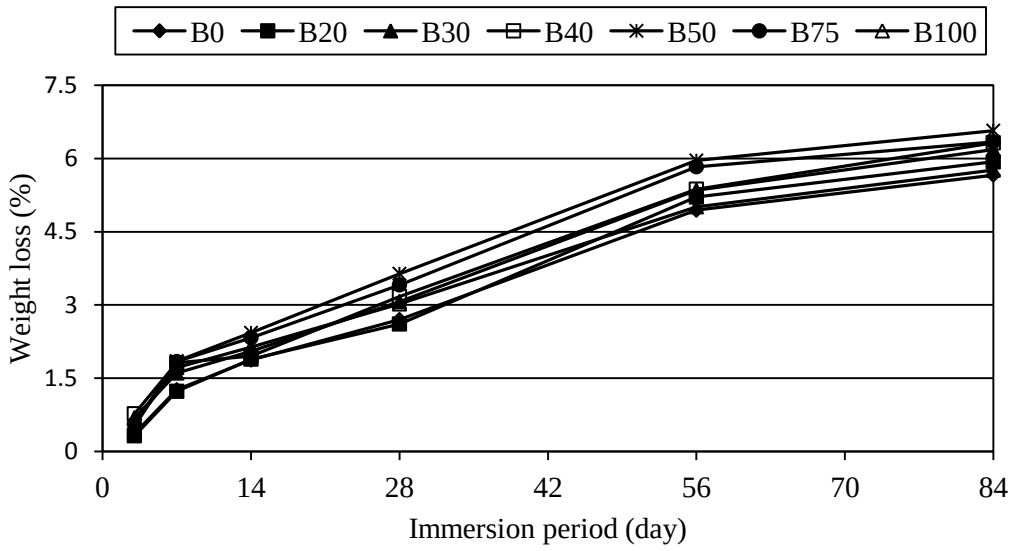

Fig. 4.82: Weight loss of concrete after immersion in 3% sulphuric acid solution (Concrete 'B')

However, on 100% incorporation of coal bottom ash in concrete, the weight loss was comparable to that of control concrete. At the end of test, percentage loss of weight of bottom ash concrete specimens was higher that of control concrete. After 84 days of

immersion in a 3% solution of sulphuric acid, bottom ash concrete mixtures $B_{20,}$ B_{30}, B_{40}, B_{50}, B_{75} and B_{100} experienced 4.77, 9.19, 11.66, 16.1, 12.01 and 1.77%, respectively, higher percentage weight loss than that by control concrete.

Loss in Compressive Strength

Fig. 4.83 shows the compressive strength of concrete specimens after immersion in 3% sulphuric acid solution. After 7 days of immersion in sulphuric acid solution, 28-day compressive strength of bottom ash concrete mixtures $B_{20,}$ $B_{30,}$ B_{40}, B_{50}, B_{75} and B_{100} decreased by 5.91, 7.91, 11.14, 9.59, 9.68 and 11.29%, respectively, as compared to 12.07% decrease in 28-day compressive strength of control concrete. After 7 days of immersion period, 28-day compressive strength of control concrete and bottom ash concrete mix incorporating 100% coal bottom ash as fine aggregate decreased from 34.04 N/mm^2 to 29.93 N/mm^2 and from 26.85 N/mm^2 to 23.82 N/mm^2, respectively. After 28 days of immersion period, the loss in 28-day compressive strength of concrete mixtures $B_{0,}$ $B_{20,}$ $B_{30,}$ B_{40}, B_{50}, B_{75} and B_{100} was 17.95, 18.05, 19.12, 25.18, 26.86, 24.17 and 35.03%, respectively.

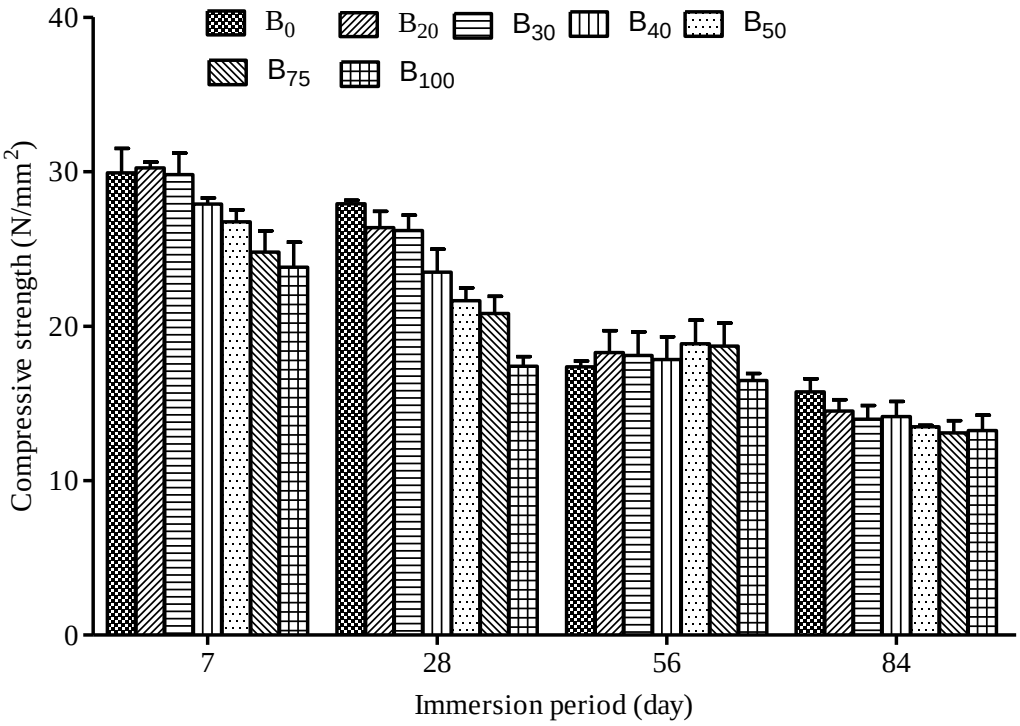

Fig. 4.83: Compressive strength of concrete after immersion in sulphuric acid solution (Concrete 'B')

After 56 days of immersion period, 28-day compressive strength of all specimens decreased drastically. After 84 days of immersion period, loss in 28-day compressive strength of the control concrete $B_{0,}$ bottom ash concrete mixtures $B_{20,}$ $B_{30,}$ B_{40}, B_{50}, B_{75} and B_{100} increased to 53.73, 54.90, 56.83, 54.95, 54.46, 52.31 and 50.65%, respectively. The percentage loss of 28-day compressive strength of bottom ash concrete mixtures was almost identical to that of control concrete. Weakening of concrete matrix, loss of cement paste and reduction in size of specimens due to sulphuric acid attack resulted into reduction in compressive strength of concrete.

4.4.4.4 Sulfate Resistance

Sulfate can enter in concrete solution form the external environment. Sulfates react with cement compounds and form expansive products such as ettringites and gypsum. Sulfate salt ionizes in water and attack calcium hydroxide, calcium aluminates hydrate and calcium silicate hydrate. The formation of ettringites and gypsum due to sulfate reactions result in expansion of concrete, loss in compressive strength, loss in weight, scaling and micro cracking. The assessment of expansion alone does not reflect the extent of deterioration. Susceptibility to sulfate attack can be interpreted through strength loss. Determination of loss of compressive strength provides the supplementary data to assess the extent of damage caused by sulfate attack. On the other side, the increase in strength of concrete may be attributed to continuous hydration and filling of pores with compounds formed by reaction of sulfate**.** Increases in strength do not provide any information about sulfate resistance. Such results show that the cement continues to hydrate in sulfate solution over the test period.

The concrete specimens were immersed in a 10% solution of magnesium sulfate after an initial water curing period of 28 days. The initial length of specimens was recorded before immersion in magnesium sulfate solution. The expansions of bottom ash concrete and control concrete specimens after immersion in magnesium sulfate solution are illustrated in Fig. 4.84. The response of bottom ash concrete specimens to external sulfate attack was almost identical to that of control concrete. The expansion of bottom ash concrete and control concrete increased with the increase in immersion period. During the entire duration of the test, no cracks and insignificant mass loss were observed in all the test specimens. The formation of ettringites in the confined voids might be the possible

explanation of continued expansions and no cracks and no mass loss of the concrete specimens (Ghafoori and Cai, 1998).

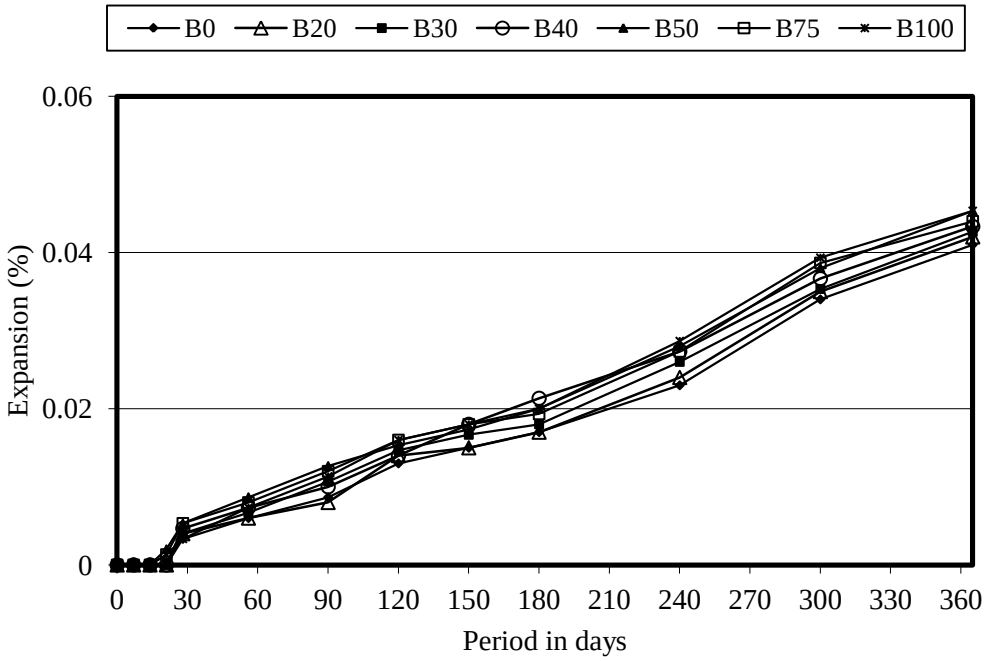

Fig. 4.84: Expansion of bottom ash concrete and control concrete specimens due to external sulphate attack (Concrete 'B')

The formation of ettringites might have interrupted the continuity of voids and retarded the penetration of sulfate solution. The continued hydration of concrete also played an important role in slowing the diffusion of sulfate ions. After 90 days of immersion period, expansions of bottom ash concrete mixture B_{30}, B_{50}, B_{75} and B_{100} were 106.67 x 10^{-4}, 126.67 x 10^{-4},120.00 x 10^{-4} and 113.33 x 10^{-4}%, respectively, as compared to 86.67 x 10^{-4}% expansion of control concrete. After 150 days of immersion period, the expansion of bottom ash concrete mixtures B_{30}, B_{50}, B_{75} and B_{100} was 11.33, 15.55, 20.0 and 20%, respectively, higher than that of control concrete. At 180 days of immersion period, expansions of bottom ash concrete mixture B_{30}, B_{50}, B_{75} and B_{100} were 180 x 10^{-4}, 200 x 10^{-4}, 193.33 x 10^{-4} and 200 x 10^{-4}%, respectively, as compared to 170 x 10^{-4}% expansion of control concrete. After 240 days of immersion in sulphate solution, the total expansion of bottom as a concrete mixture incorporating 30, 50, 75 and 100% coal bottom ash was 260 x 10^{-6}, 280 x 10^{-6}, 273.33 x 10^{-6} and 286.67 x 10^{-6}, respectively, as compared to 230 x 10^{-6} that of control concrete. At the end of test i.e. 365 days, total expansion of bottom ash concrete mixtures $B_{20,}$ $B_{30,}$ $B_{40,}$ $B_{50,}$ B_{75} and B_{100} was 420 x 10^{-6}, 426.67 x10^{-6}, 433.33 x10^{-6}, 453.33 x10^{-6}, 440 x $10^{-6}$and 453.67 x10^{-6}, respectively, as compared to 410 x10^{-6} of

control concrete. Total expansion of bottom ash concrete mixture containing 100% coal bottom ash concrete was 10.65% more than that of control concrete. The results obtained in the present study are comparable to that reported in published research work (Ghafoori and Bucholc, 1996, 1997). Ghafoori and Cai (1998) reported that the roller compacted bottom ash concrete showed excellent resistance to sulfate attack.

Mass Loss

No cracks and spalling were observed in all the concrete specimens during the entire duration of test. Even after 240 days of immersion in 10% magnesium sulphate solution, no loss in mass of all the concrete specimens was observed. However, signs of white deposit were noticed after 210 days of immersion period. After 365 days of immersion in 10% magnesium sulphate solution, mass loss of bottom ash concrete specimens $B_{20,}$ $B_{30,}$ $B_{40,}$ $B_{50,}$ B_{75} and B_{100} was 0.39, 0.61, 0.45, 0.40, 0.32 and 0.0.36%, respectively, as compared to 0.30% of control concrete.

Change in Compressive Strength

Test results of compressive strength after immersion in 10% magnesium sulphate solution are presented in Fig 4.85. The test results show that no reduction in compressive strength was observed after immersion in 10% magnesium sulphate solution, rather it continued to increase during the test period. The increase in compressive strength of concrete mixtures over their 28-day compressive strength, after immersion in magnesium sulphate solution is illustrated in Fig. 4.86.

After 28 days of immersion period, percentage increase in 28-day compressive strength of bottom ash concrete mixtures except B_{75} and B_{100} was lower than that of control concrete. Concrete mixtures B_{75} and B_{100} displayed 15.54 and 15.72%, respectively, increase in 28-day compressive strength. However, after 90 days of immersion period, increase in 28-day compressive strength of bottom ash mixtures was higher than that of control concrete. After 180 days of immersion period, the increase in 28-day compressive strength of bottom ash concrete mixtures $B_{20,}$ $B_{30,}$ B_{40}, B_{50}, B_{75} and B_{100} was 18.51, 24.15, 23.05, 37.6, 37.13 and 24.69%, respectively, as compared to 18.48%, increase in 28-day compressive strength of control concrete. This indicates that the cement continued to hydrate in magnesium sulphate solution over the test period. The increase in compressive strength of concrete may be attributed to continuous hydration and the filling of pores with compounds formed by the reaction of sulphate. The reason for insignificant mass loss and

no reduction in 28-day compressive strength and continued expansions may be the formation ettringites within the confined voids. The continued hydration of concrete specimens and formation of ettringites interrupted the continuity of pores, which resulted in further reduction in its permeability. The reduced continuity of voids prevented the penetration of sulphate ions into the concrete. Low permeability of bottom ash concrete specimens may also be the reason for the better performance against sulphate attack.

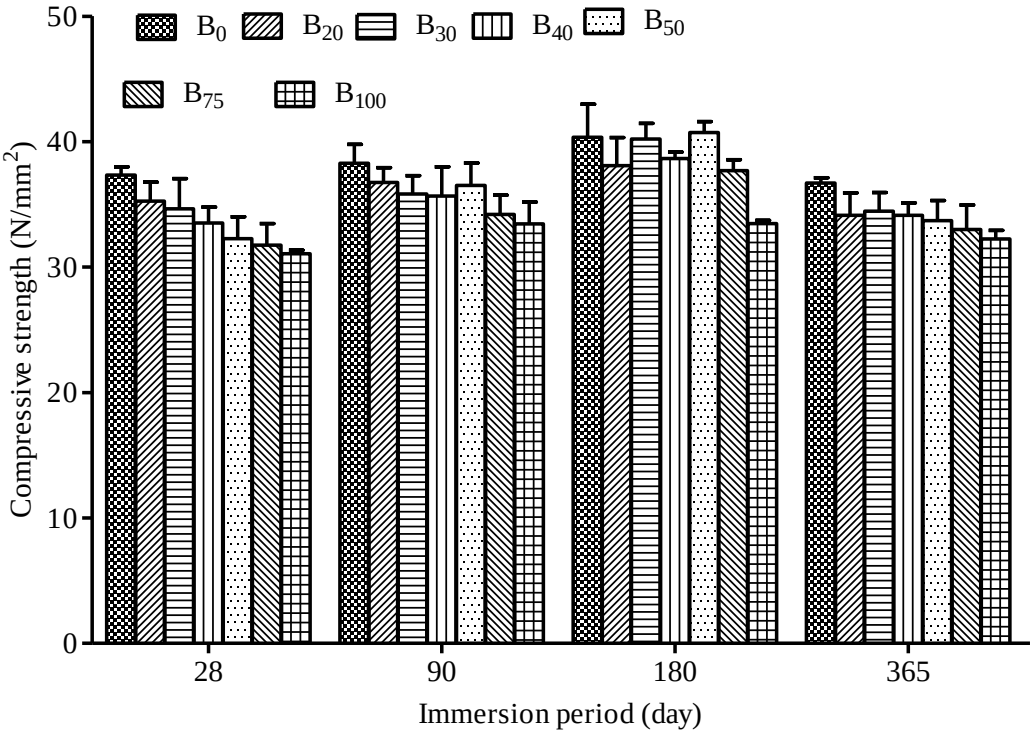

Fig. 4.85 Compressive strength of concrete after immersion in 10% magnesium sulphate solution (Concrete 'B')

Table 4.21 Compressive strength of concrete at 28 days of water curing (Concrete 'B')

Mix	B_0	B_{20}	B_{30}	B_{40}	B_{50}	B_{75}	B_{100}
Compressive strength (N/mm^2)	34.04	32.15	32.38	31.41	29.6	27.47	26.85

After 365 days of immersion period, the increase in 28-day compressive strength of bottom ash concrete mixtures $B_{20,}$ $B_{30,}$ B_{40}, B_{50}, B_{75} and B_{100} dropped to 6.16, 6.46, 8.70,

13.84, 20.13 and 20.07%, respectively, as compared to 7.93%, increase in 28-day compressive strength of control concrete.

Irassar et al. (1996) reported that the compressive strength of concrete containing 40% fly ash as cement replacement increased by 86 % and 144% over their 28-day compressive strength after 1 and 5 year of immersion period, respectively. Brown (1981) reported that the compressive strength of mortars increased initially after the immersion in a sulphate solution. After reaching a certain limit of expansion strain, the compressive strength started decreasing. The beginning of loss of compressive strength of mortars corresponds to 0.1% expansion (Ouyang et al., 1988; Ouyang, 1989). In the present study, the expansion strains of all bottom ash concrete mixtures remained well below than 0.1% even after 365 days of immersion period.

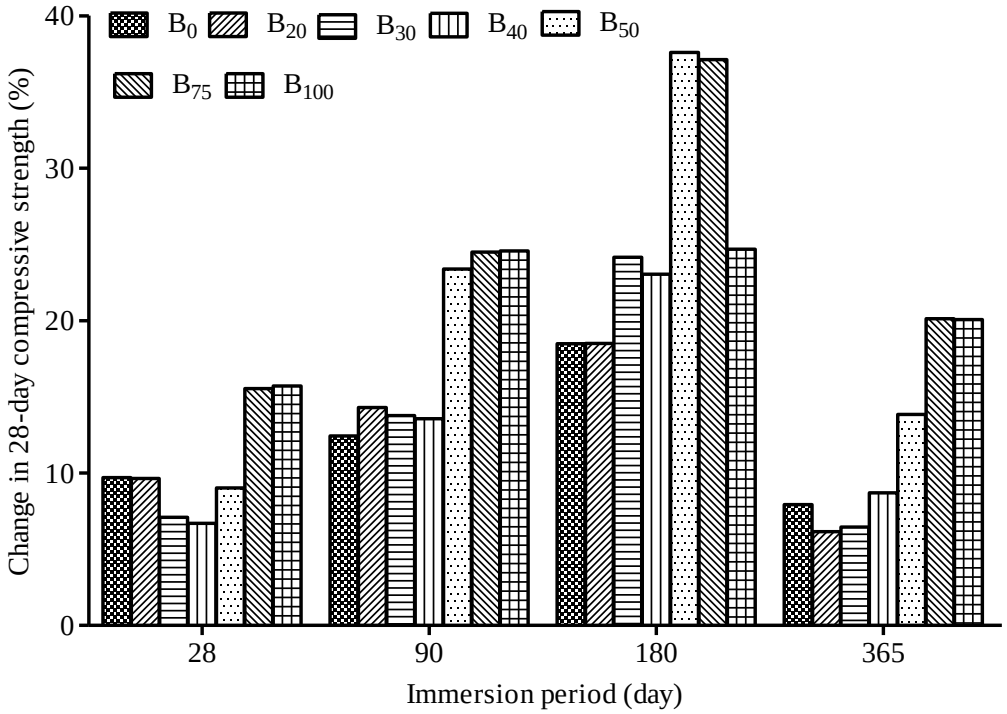

Fig. 4.86: Change in 28-day compressive strength after immersion in sulphate solution (Concrete 'B')

Microstructure

Scanning electron micrographs (SEM) of concrete mixtures after 180 days of immersion in 10% magnesium sulphate solution are shown in Figs. 4.87 to 4.89. In this study, fractured pieces of concrete were mounted on the SEM stub and images were obtained using secondary electron (SE) image mode.

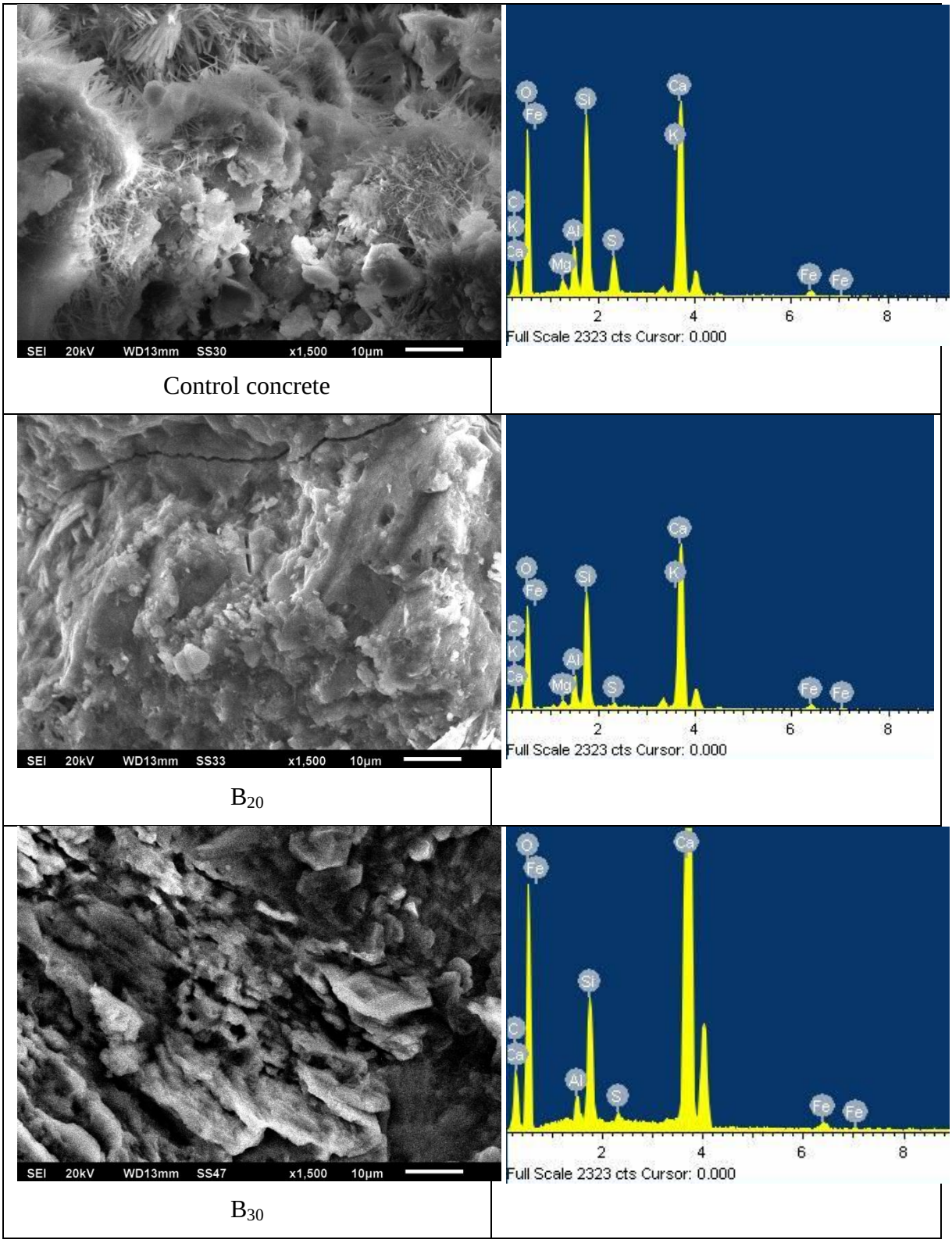

Fig. 4.87: Scanning electron micrograph and EDS spectrum of control concrete (Concrete 'B') and bottom ash concrete ($B_{20,}$ B_{30}) after 180 days of immersion period in magnesium sulfate solution

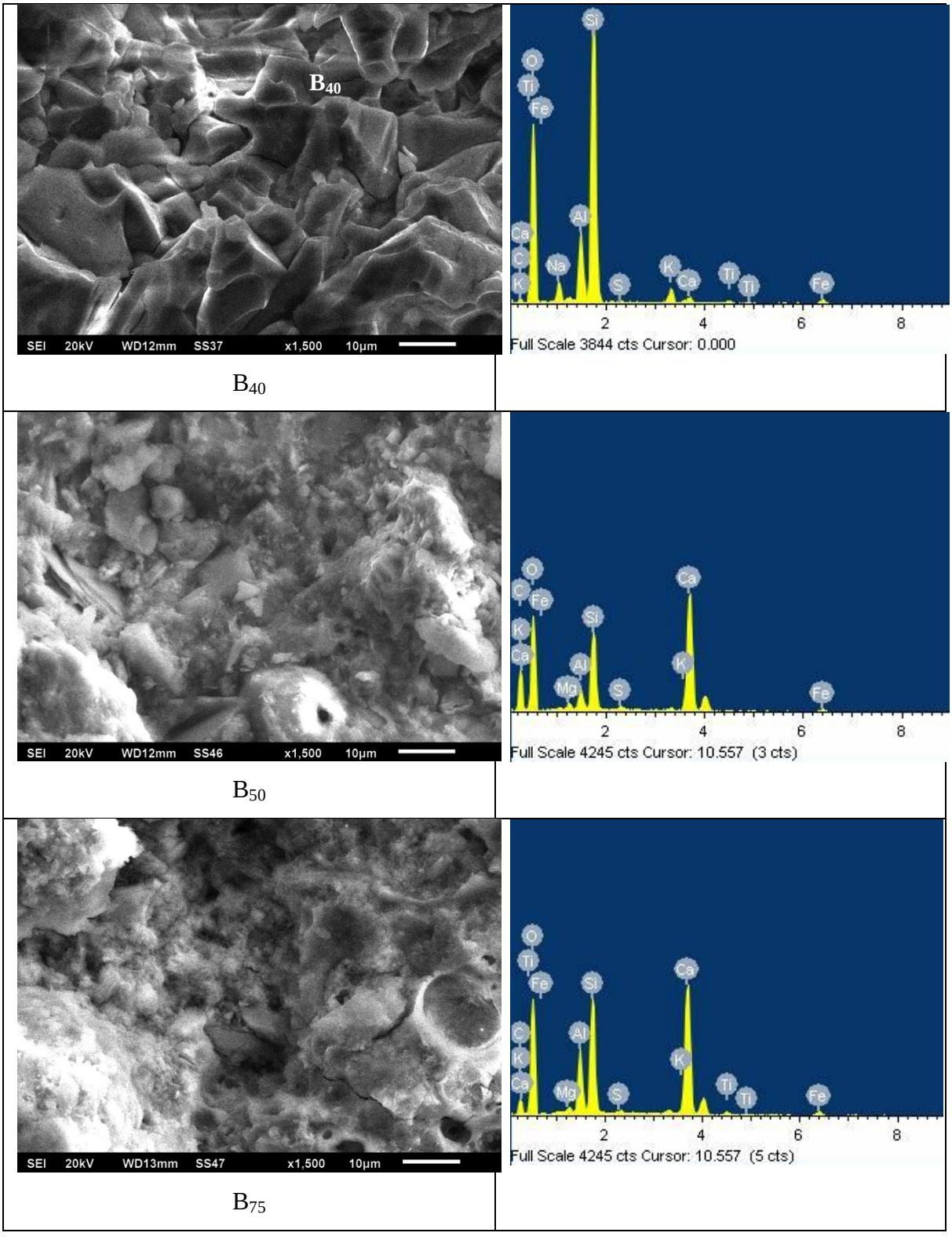

Fig. 4.88: Scanning electron micrograph and EDS spectrum of bottom ash concrete (B_{40}, B_{50} and B_{75}) after 180 days of immersion period in magnesium sulfate solution

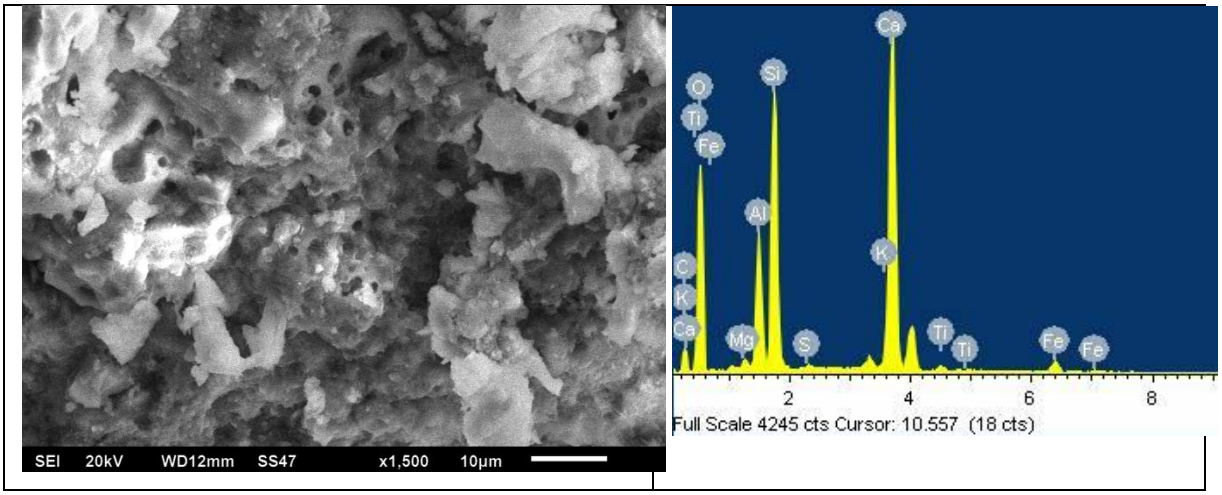

Fig. 4.89: Scanning electron micrograph and EDS spectrum of bottom ash concrete (B_{100}) after 180 days of immersion period in magnesium sulfate solution

Table 4.22 Chemical composition of concrete after immersion in 10% magnesium sulfate solution for 180 days (Concrete 'B')

Element	**Weight (%) in concrete mixtures**						
	Control concrete	**B_{20}**	**B_{30}**	**B_{40}**	**B_{50}**	**B_{75}**	**B_{100}**
Ca	17.20	22.32	32.97	0.77	16.86	17.80	21.39
Si	10.12	9.93	3.18	25.47	7.03	10.03	11.31
Al	2.54	2.63	0.70	5.82	1.72	5.45	5.37
K	0.57	1.09	-	1.89	0.28	0.47	0.56
Mg	0.84	0.72	-	-	0.68	0.43	0.45
C	7.29	3.11	7.98	3.34	16.82	5.23	4.18
O	56.90	57.90	54.25	57.72	55.34	58.23	54.30
S	2.61	0.44	0.26	0.14	0.33	0.34	0.14
Fe	1.42	1.87	0.66	1.53	0.92	1.25	1.85
Ti	-	-	-	0.55	-	0.57	0.47
Na	-	-	-	2.84	-	-	-

The concrete specimens were coated with thin layer of gold to make them electrically conductive before placing on the scanning electron microscopy (SEM) stem. It is apparent from the SEM images that sulphate ion diffusion did not take place even to a depth near to the surface. No signs of gypsum and monosulfate morphologies, which can indicate the attack by sulphate, were observed in either of the concrete mixtures. At higher resolution, very small ettringite needles in few voids were observed in the concrete mixtures. All the SEM images show dense and evenly spread calcium silicate hydrate gel.

Energy dispersive spectrometry (EDS) analysis results are presented in Table 4.22. The small fraction of sulphur content in the concrete mixtures observed in EDS analysis might have due to sulphur trioxide present in cement or coal bottom ash.

XRD Phase Identification

XRD spectrums of concrete mixtures after 180 days of immersion in 10% magnesium sulphate solution are shown in Figs. 4.90 to 4.92. The cement pastes were separated from the concrete samples and were sieved through 90 μm sieve. The XRD investigations were performed for diffraction angle 2θ ranged between 5° and 80° in steps of 2θ = 0.017°. The diffraction pattern, list of d-spacing and relative intensities of diffraction peaks was prepared and was compared with the standard peaks of compounds in the diffraction database released by International Centre for Diffraction Data (ICDD). The XRD and SEM analysis indicate the concrete specimens were not damaged by the external attack of sulphate. The increase in 28-day compressive strength of concrete also supports that sulphate ions could not penetrate and deteriorate the concrete specimens up to the age of the test. After 180 days of immersion in a 10% solution of magnesium sulphate, no change in phase composition of concrete was observed in XRD spectrums. Analysis of XRD spectrums indicates that the absolute intensity of portlandite peaks of bottom ash concrete mixtures except M1 mixture was lower than that in control concrete. The total intensity of portlandite (d = 4.90 °A and 2.62 °A) in bottom ash mixtures B_{20}, B_{30}, B_{40}, B_{50}, B_{75}, and B_{100} was 1168, 1160, 2297, 989, 1103 and 749 counts, respectively, as compared to 1491 counts in control concrete. Assuming total intensity of a phase is connected with the amount of that phase present in the concrete mixture, the lower intensities of portlandite indicate that the influence of coal bottom ash is significant in case of portlandite phase.

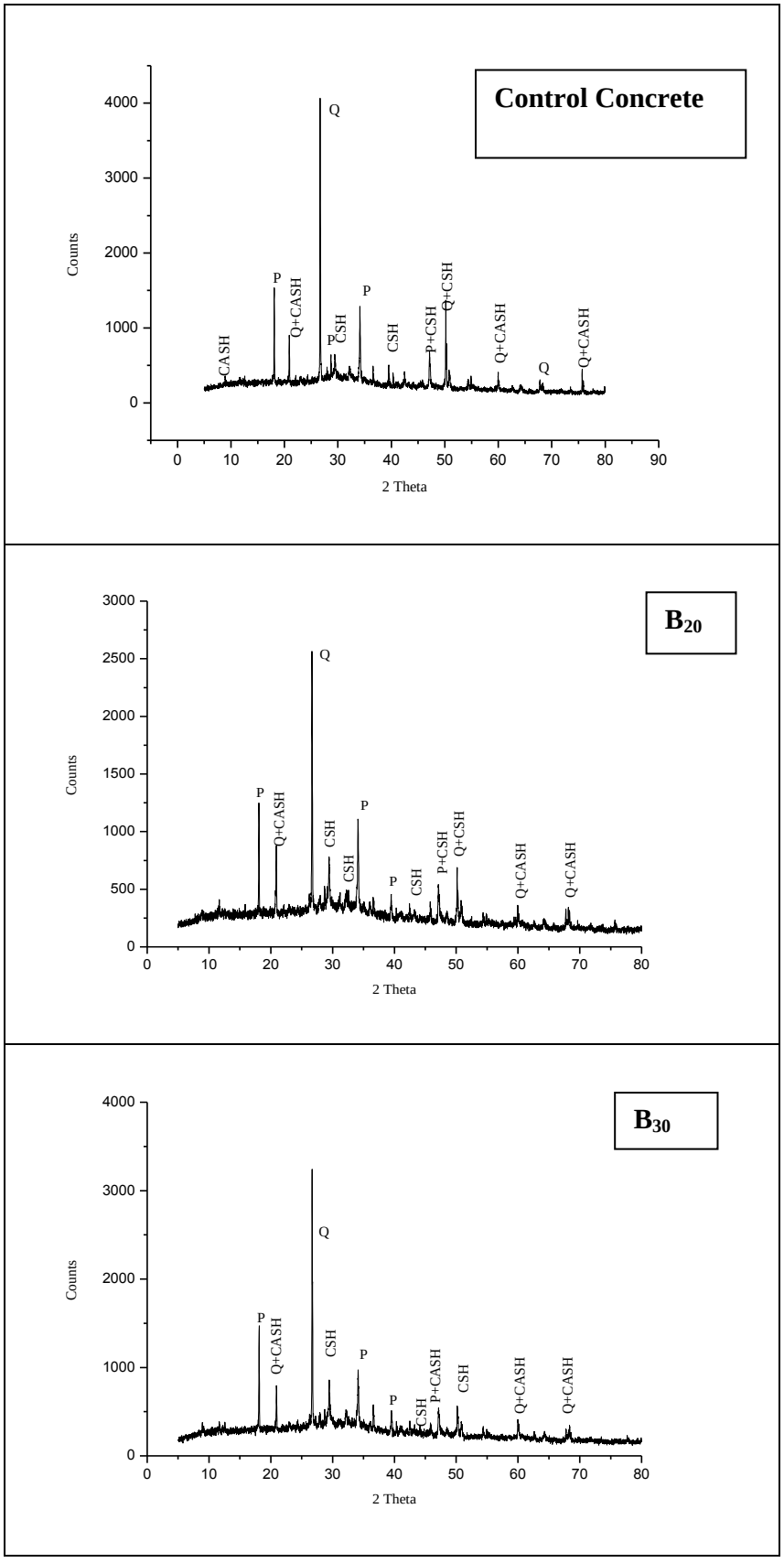

Fig. 4.90: XRD spectrum of control concrete (Concrete 'B') and bottom ash concrete (B_{20} and B_{30}) after 180 days of immersion period in magnesium sulfate solution (CASH = Calcium alumino silicate hydrate; CS = Calcium silicate; CSH = Calcium silicate hydrate; E = Ettringite; P = Portlandite; Q = Quartz)

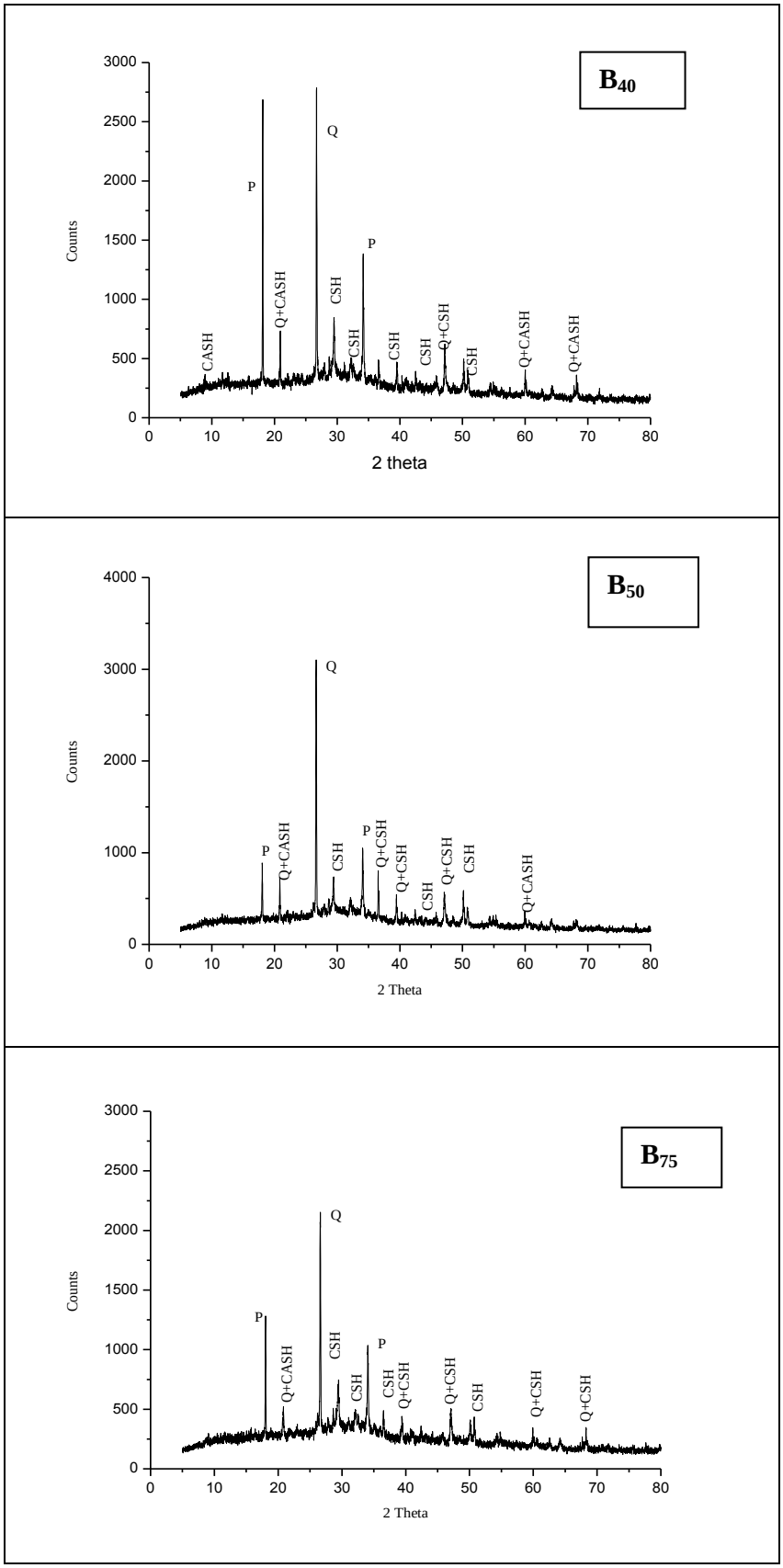

Fig. 4.91: XRD spectrum of bottom ash concrete (B_{40}, B_{50}, and B_{75}) after 180 days of immersion period in magnesium sulfate solution (CASH = Calcium alumino silicate hydrate; CS = Calcium silicate; CSH = Calcium silicate hydrate; E = Ettringite; P = Portlandite; Q = Quartz)

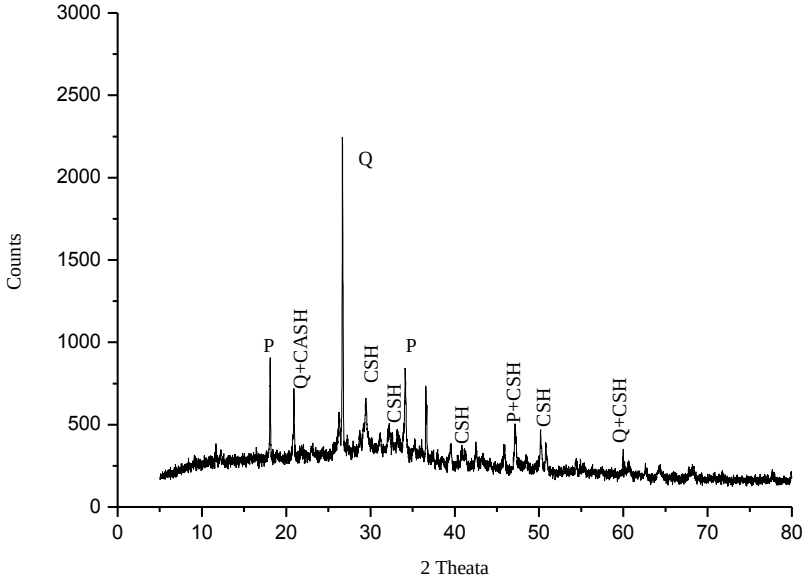

Fig. 4.92: XRD spectrum of bottom ash concrete (B_{100}) after 180 days of immersion period in magnesium sulfate solution (CASH = Calcium alumino silicate hydrate; CS = Calcium silicate; CSH = Calcium silicate hydrate; E = Ettringite; P = Portlandite; Q = Quartz)

4.4.3.5 Drying Shrinkage

Hardened concrete stored in unsaturated air experience shrinkage called drying shrinkage. Withdrawal of water from the hardened concrete on air-drying causes shrinkage. Absorption of water by the cement paste in concrete causes expansion called swelling. In other words, it is the movement of water, which causes expansion, or shrinkage of hardened concrete. Fig. 4.93 presents the drying shrinkage behaviour of bottom ash concrete and control concrete. Shrinkage strains decreased with the increase in coal bottom ash content in concrete. At 90 days of drying period, the shrinkage strains of bottom ash concrete mixtures $B_{20,}$ $B_{30,}$ $B_{40,}$ $B_{50,}$ B_{75} and B_{100} were $^{486.67}$ x 10^{-6}, 460 x $10^{-}6$, 440 x 10^{-6}, 466.67 x 10^{-6}, 413.33 x 10^{-6} and 400 x 10^{-6}, respectively. However, during the same period, shrinkage strain of control concrete was 500 x 10^{-6}. At 180 days of drying period, bottom ash concrete mixtures $B_{30,}$ $B_{40,}$ $B_{50,}$ B_{75} and B_{100} experienced 5.20, 8.33, 10.42, 13.55, and 13.55%, respectively, less shrinkage strain as compared to that of control concrete. However, the bottom ash concrete mixture B_{20} containing 20% coal bottom ash as fine aggregate experienced 2.08% higher drying shrinkage strain than that of the control concrete. The shrinkage strain values of bottom ash concrete specimens except B_{20}

specimen were lower than that of control concrete during the entire drying period of the test.

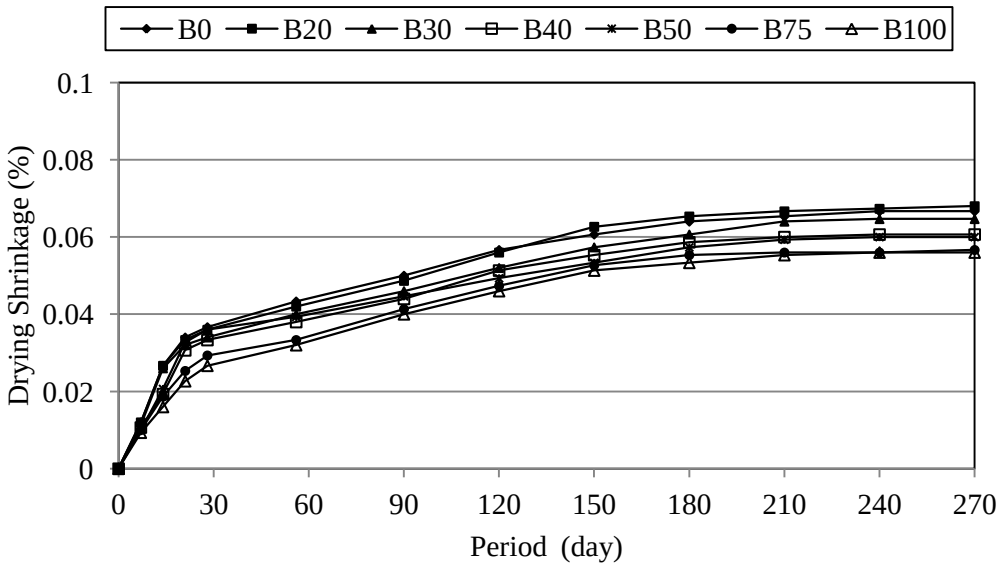

Fig. 4.93: Effect of coal bottom ash on drying shrinkage of concrete (Concrete 'B')

At 270 days of drying period, the shrinkage strains of bottom ash concrete mixtures $B_{20,}$ $B_{30,}$ $B_{40,}$ $B_{50,}$ B_{75} and B_{100} were 680 x $10^{-}6$, 646.67 x 10^{-6}, 606.67 x 10^{-6}, 600 x 10^{-6}, 566.67 x 10^{-6} and 560 x 10^{-6}, respectively, as compared to 666.67 x 10^{-6} of control concrete. The reduced shrinkage strain exhibited by bottom ash concrete mixtures was probably due to lower free water-cement ratio. The porous particles of dry coal bottom ash absorbed part of water internally during the mixing process. It is also believed that, the porous coal bottom ash particles released the water during drying of specimens. This resulted in lesser shrinkage strains on drying of bottom ash concrete mixtures.

The drying shrinkage results of the present study compare well with the work done by Bai et al. (2005) and Ghafoori and Bucholc (1996, 1997). They have also observed that concrete containing coal bottom ash exhibited greater dimensional stability as compared to conventional concrete. Ghafoori and Cai (1998) has also observed lower shrinkage strains of roller compacted concrete made with coal bottom ash.

4.4.4.6 Abrasion Resistance

Figs. 4.94 to 4.98 show the resistance to abrasion of bottom ash concrete and control concrete. The wear tests were performed at the ages of 28, 90, 180 and 365 days for all concrete mixtures. Bottom ash concrete displayed lower wear resistance at all the ages. At

28 days of curing age, depth of wear after 15 min of wear of bottom ash concrete mixtures B_{20}, B_{30}, B_{40}, B_{50}, B_{75} and B_{100} was 0.752, 0.75, 0.8578, 0.94, 1.02 and 1.23 mm, respectively, as compared to 0.67 mm for control concrete. At 90 days of curing age, the depth of wear for concrete mixtures $B_{20,}$ B_{30}, B_{40}, B_{50}, B_{75} and B_{100} was 0.72, 0.72, 0.80, 0.82, 0.91 and 0.94 mm, respectively, as compared to 0.65 mm for control concrete. The test results show that depth of wear for bottom ash concrete mixtures decreased significantly with increase in curing age, which means that wear resistance of these bottom ash concrete mixtures increased with age.

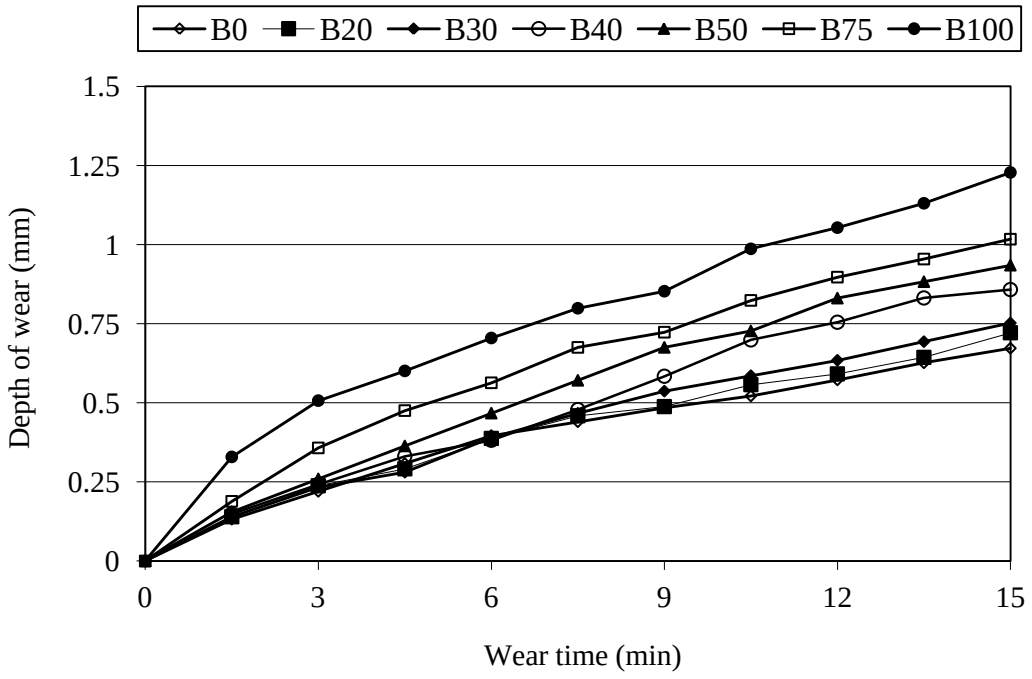

Fig. 4.94: Variation in depth of wear with coal bottom ash content in concrete at 28 days of curing age (Concrete 'B')

This is possibly due to the increase in compressive strength resulting from increased maturity and densification of the concrete matrix. At 365 days, the average depth of wear of bottom ash concrete mixtures B_{20}, $B_{30,}$ B_{40}, B_{50}, B_{75} and B_{100} was 0.549, 0.551, 0.581, 0.579, 0.648 and 0.722 mm, respectively, as compared to 0.526 mm of control concrete The average depth of wear of bottom ash concrete mixture incorporating 100% coal bottom ash as fine aggregate at 28, 90, 180 and 365 days curing age was 82.66, 43.88, 44.25 and 37.26%, respectively, higher than that of control concrete. As seen in Fig. 4.123, abrasion resistance of bottom ash concrete mixtures increased with increase in compressive strength.

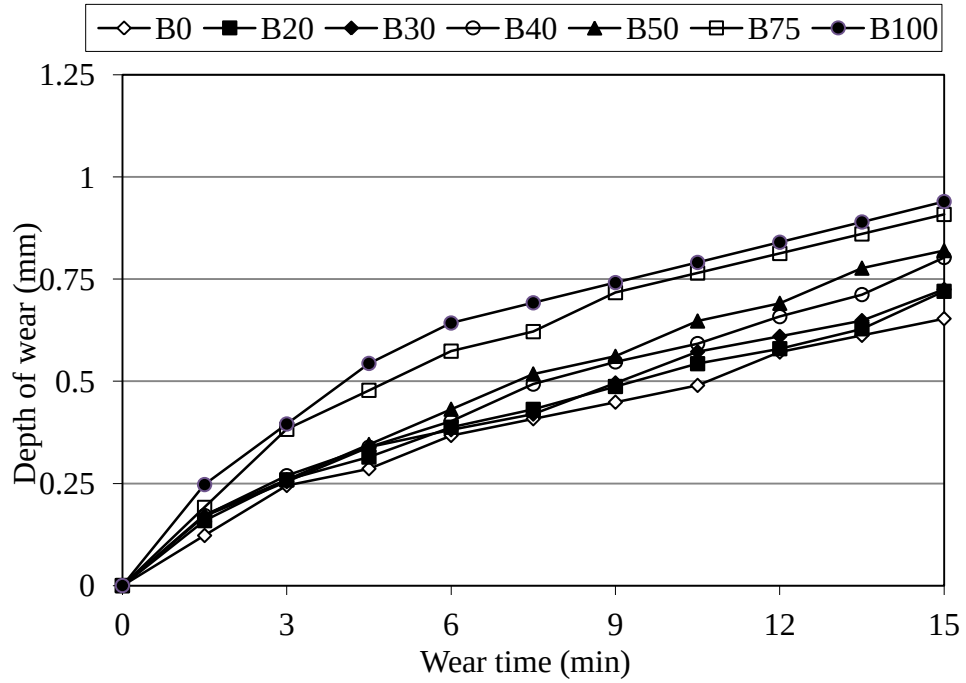

Fig. 4.95: Variation in depth of wear with coal bottom ash content in concrete at 90 days of curing age (Concrete 'B')

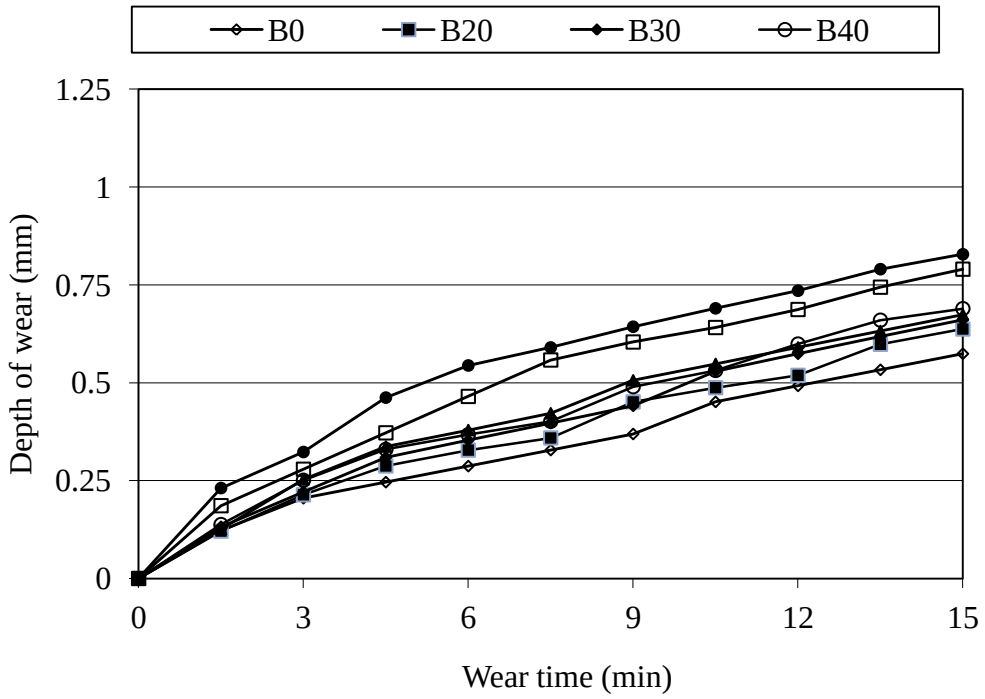

Fig. 4.96: Variation in depth of wear with coal bottom ash content in concrete at 180 days of curing age (Concrete 'B')

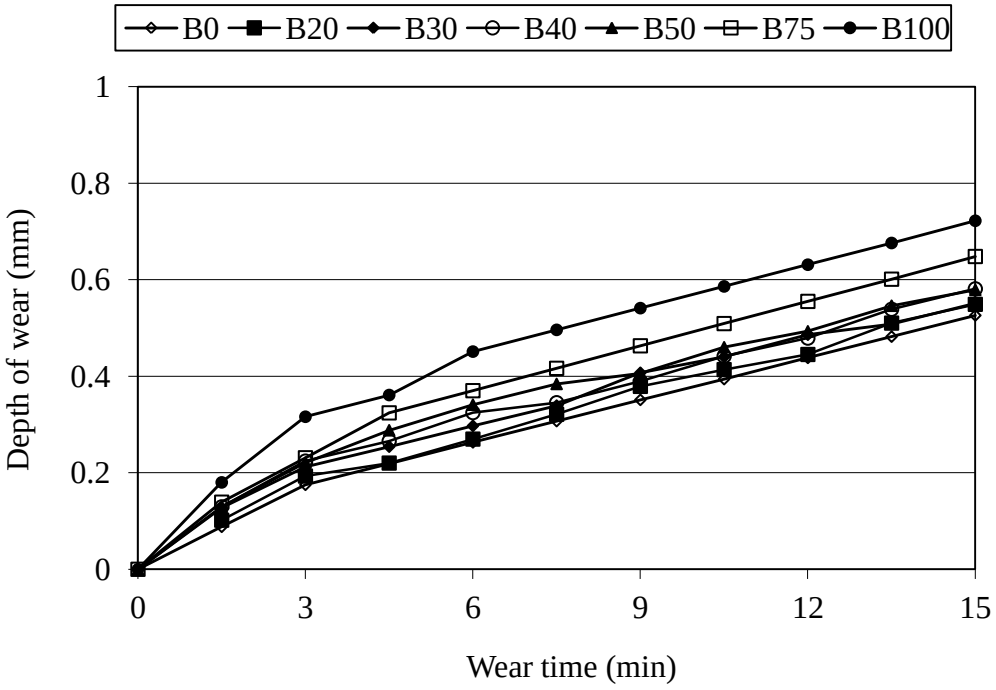

Fig. 4.97: Variation in depth of wear with coal bottom ash content in concrete at 365 days of curing age (Concrete 'B')

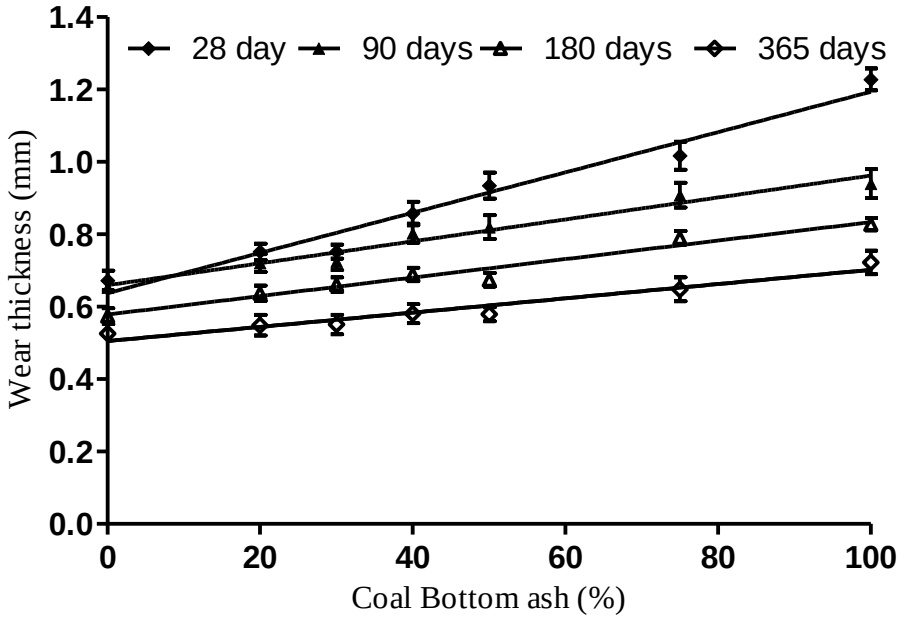

Fig. 4.98: Variation in abrasion resistance of concrete with coal bottom ash content (Concrete 'B')

4.4.5 Micro-structural Properties of Concrete

The application of Scanning electron microscopy enhances the ability to characterize the concrete microstructure and helps in ascertaining the factors affecting the mechanical properties and durability of concrete. The concrete microstructure is integrated system consisting of CSH gel, calcium hydroxide, calcium sulfoaluminate hydrate (ettringite and monosulfate), coarse and fine aggregate and interfacial transition zone between aggregate and cement hydration products. Scanning electron microscopy helps to great extent in resolving the concrete microstructure. Morphology structure of CSH varies from common fibrous type to irregular grains forming a reticular network. At the early age of cement hydration, prominent morphology structure of CSH is fibrous type but reticular network also occurs occasionally. Equant grain morphology of CSH appears as the hydration of cement proceeds. Another type of morphology of CSH has a dimpled appearance with either regular pores or closely packed equant grains. The calcium hydroxide appears in many shapes such as massive, platy crystals, large thin elongated crystals and blocky masses to finely disseminated crystals. Calcium sulfoaluminate hydrates have two morphologies that are ettringites and monosulfate. Ettringites appears as needle like crystals whereas monosulfate appears as hexagonal platy crystals.

The fractured pieces of bottom ash concrete generated from compressive strength test were used for observing the scanning electron micrographs. Scanning electron micrographs of concrete specimens were taken at the curing age of 28 and 90 days. The concrete specimens were coated with thin layer of gold to make them electrically conductive before pacing on the scanning electron microscopy (SEM) stem. The SEM images of concrete specimens were taken in the secondary electron (SE) mode. SEM images of coal bottom ash concrete mixtures $B_{20,}$ B_{30}, B_{40}, B_{50} B_{75} and B_{100} and that of control concrete at 28 and 90 days of curing age are shown in Figs. 4.99 to 4.101.

As shown in Fig 4.100, CSH gel spread over the entire image, needles of ettringites near the spherical particle of coal bottom ash and fraction of calcium hydroxide crystals near the crack are seen in the SEM image of bottom ash concrete incorporating 50% coal bottom ash as fine aggregate at 28 days of curing age. Coal bottom ash particle has started reacting with the portlandite, which indicates that pozzolanic activity of coal bottom has started. As revealed in Fig 4.100, at 90 days of curing age, the CSH gel became denser and monolithic and portlandite crystals decreased.

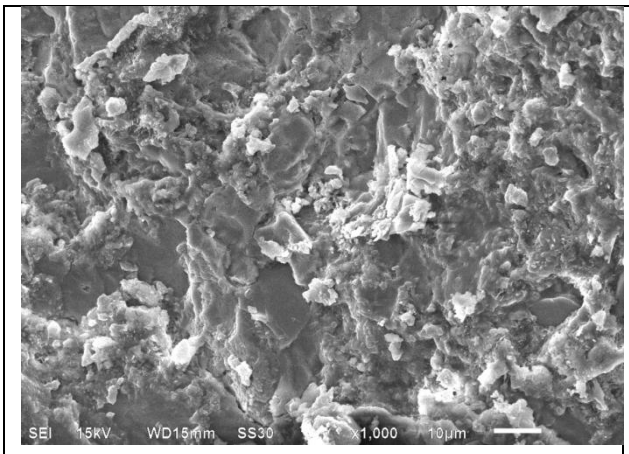

Control concrete at 28 days

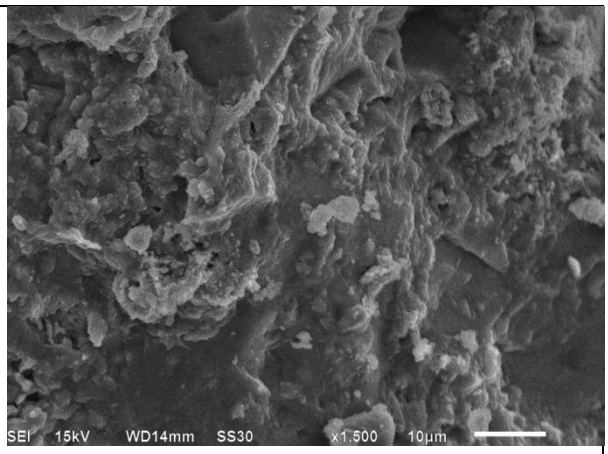

Control concrete at 90 days

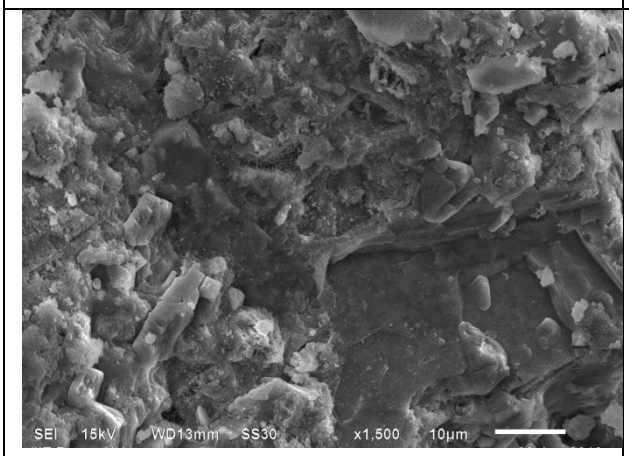

Bottom ash concrete B_{20} at 28 days

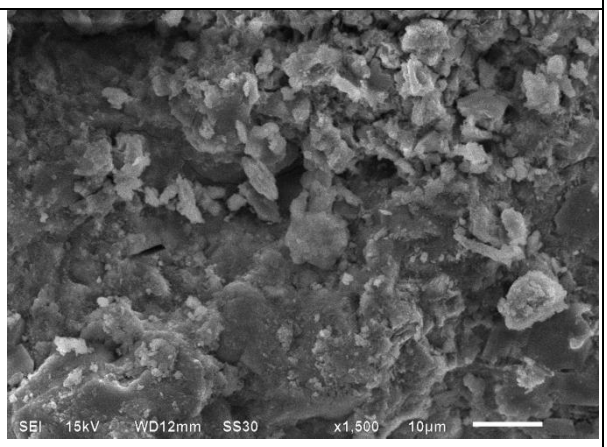

Bottom ash concrete B_{20} at 90 days

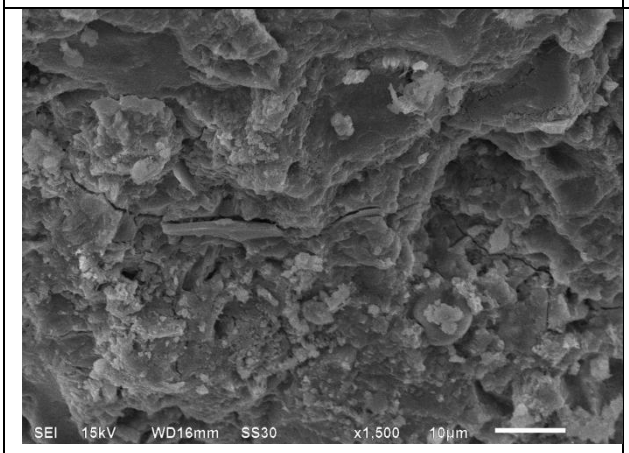

Bottom ash concrete B_{30} at 28 days

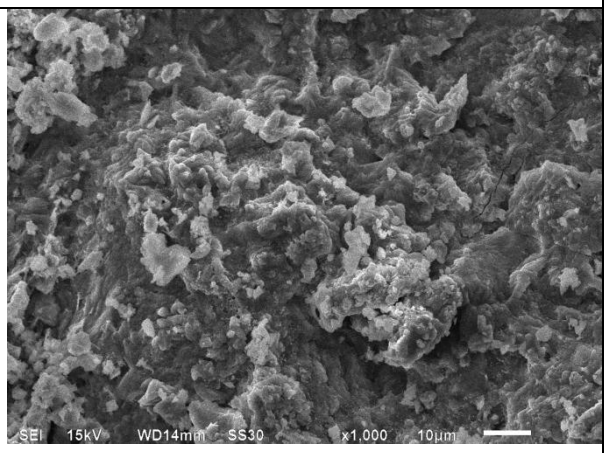

Bottom ash concrete B_{30} at 90 days

Fig. 4.99: Scanning electron micrograph of control concrete (Concrete 'B') and bottom ash concrete (B_{20} and B_{30}) at 28 and 90 days of curing age

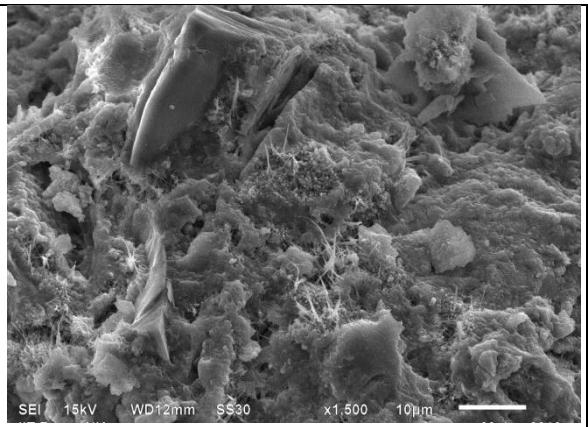

Bottom ash concrete B_{40} at 28 days

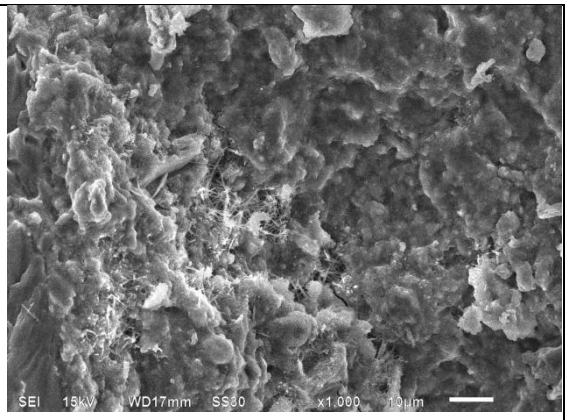

Bottom ash concrete B_{40} at 90 days

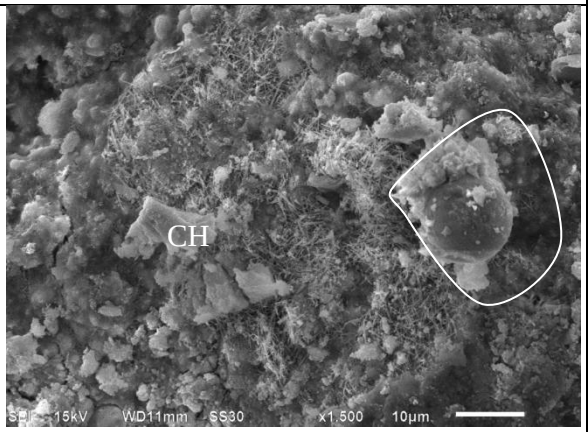

Bottom ash concrete B_{50} at 28 days

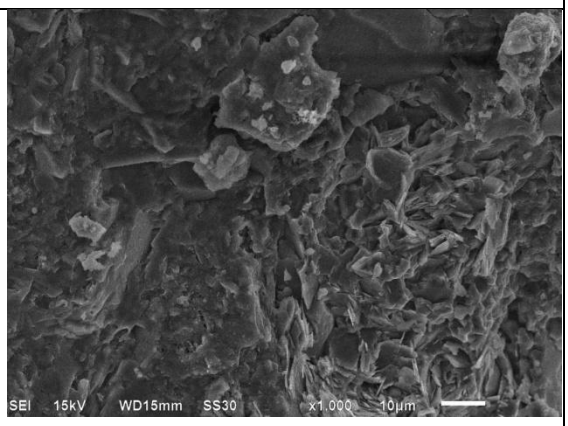

Bottom ash concrete B_{50} at 90 days

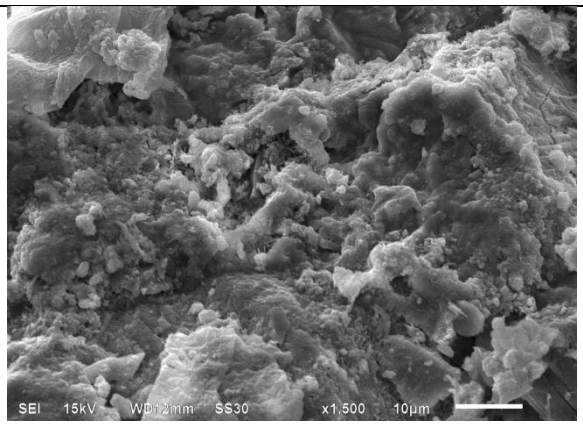

Bottom ash concrete B_{75} at 28 days

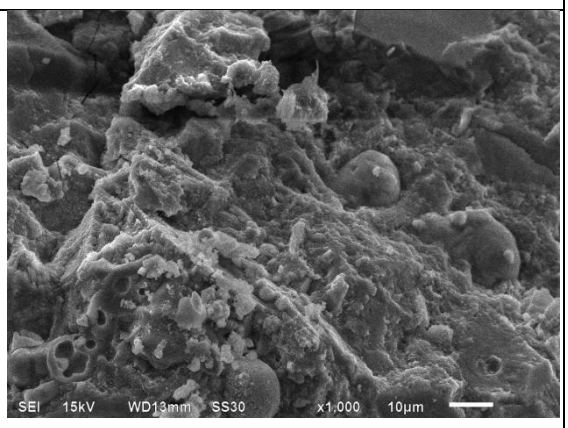

Bottom ash concrete B_{75} at 90 days

Fig. 4.100: Scanning electron micrograph of bottom ash concrete mixtures ($B_{40,}$ B_{50} and B_{75}) at 28 and 90 days of curing age

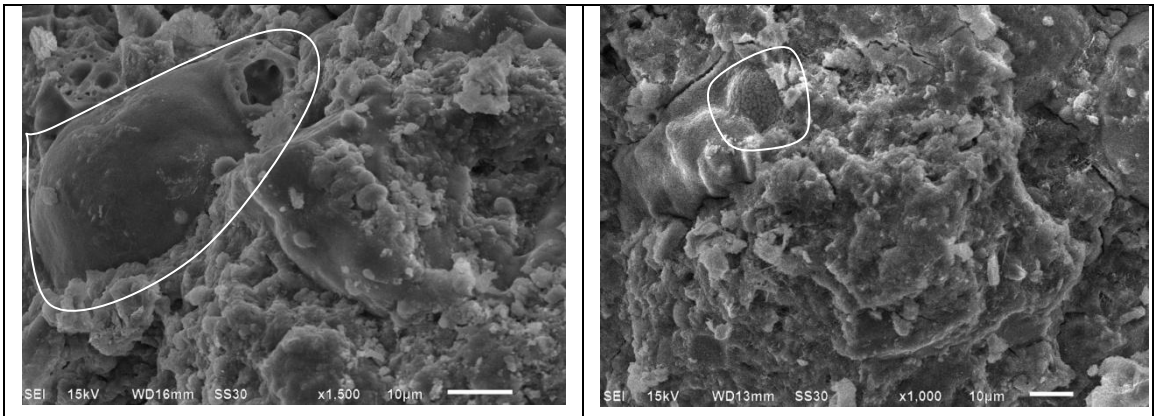

Fig. 4.101: Scanning electron micrograph of bottom ash concrete mixtures (B_{100}) at 28 and 90 days of curing age

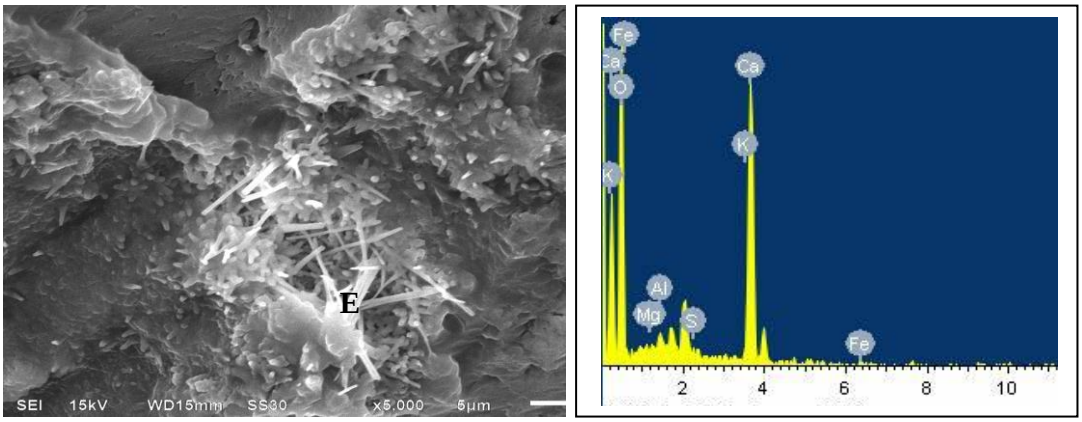

Fig. 4.102: Scanning electron micrograph and EDS spectrum of control concrete (concrete 'B') at 28 days curing age (Ettringites 'E')

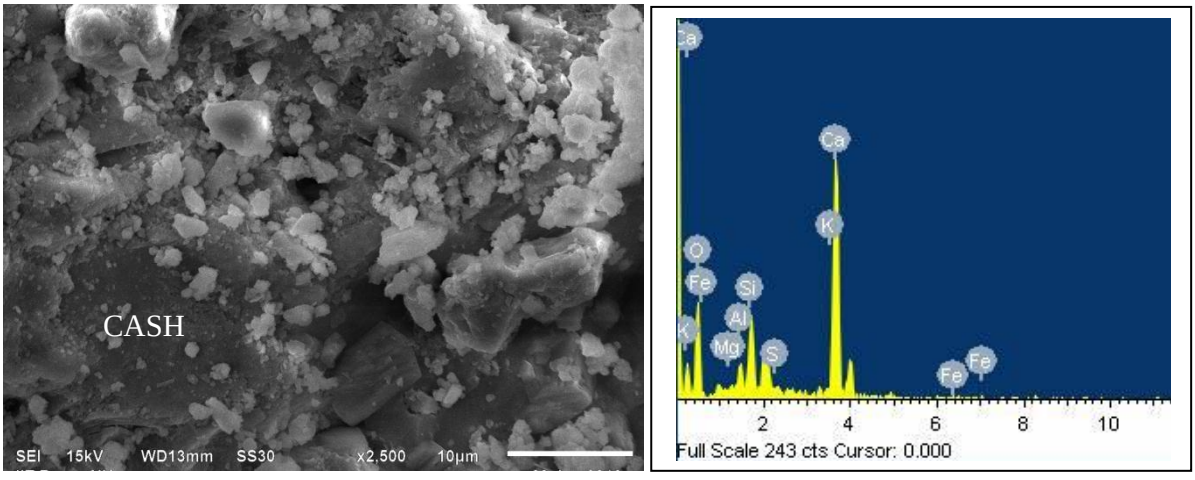

Fig. 4.103: Scanning electron micrograph and EDS spectrum of bottom ash concrete (B_{20}) at 28 days of curing age (Calcium alumino silicate hydrate 'CASH')

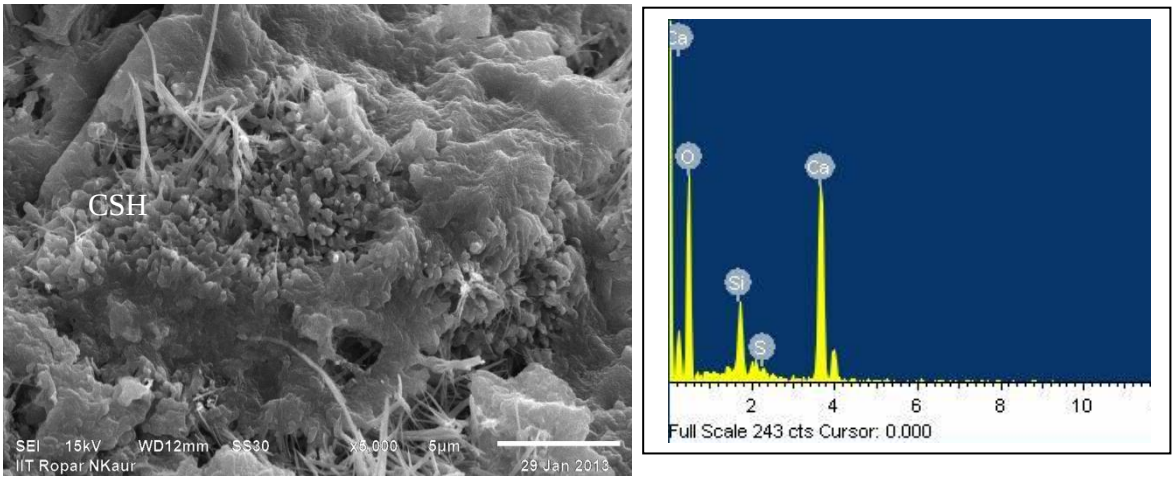

Fig. 4.104: Scanning electron micrograph and EDS spectrum of bottom ash concrete (B_{40}) at 28 days of curing age (Calcium silicate hydrate marked 'CSH')

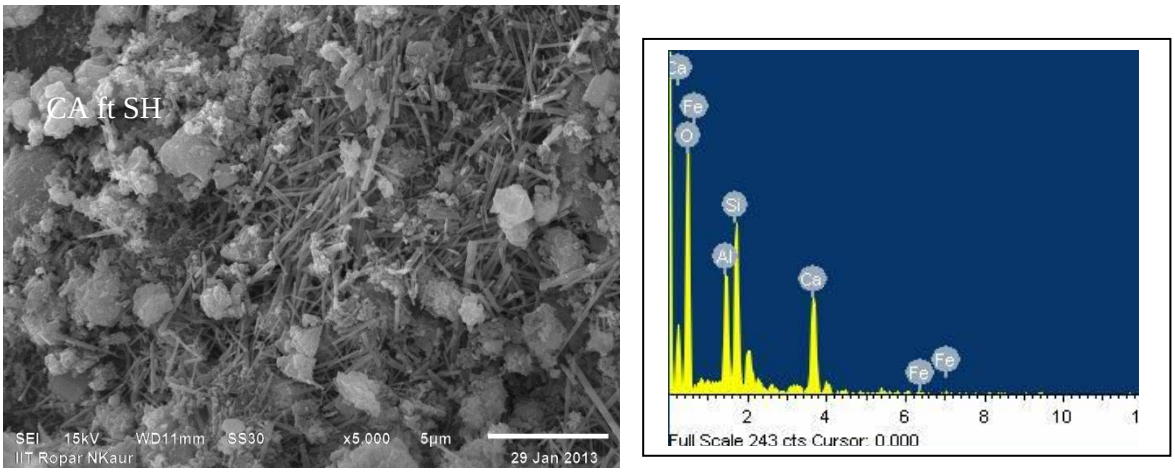

Fig. 4.105: Scanning electron micrograph and EDS spectrum of bottom ash concrete (B_{50}) at 28 days of curing age (calcium alumino-ferrite silicate hydrate marked 'CAftSH')

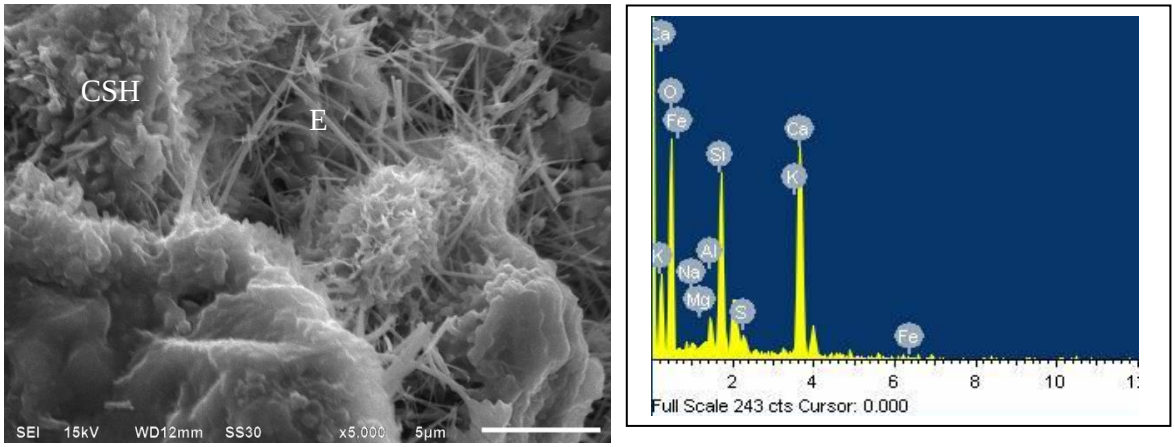

Fig. 4.106: Scanning electron micrograph and EDS spectrum of bottom ash concrete (B_{75}) at 28 days of curing age (Calcium silicate hydrate 'CSH')

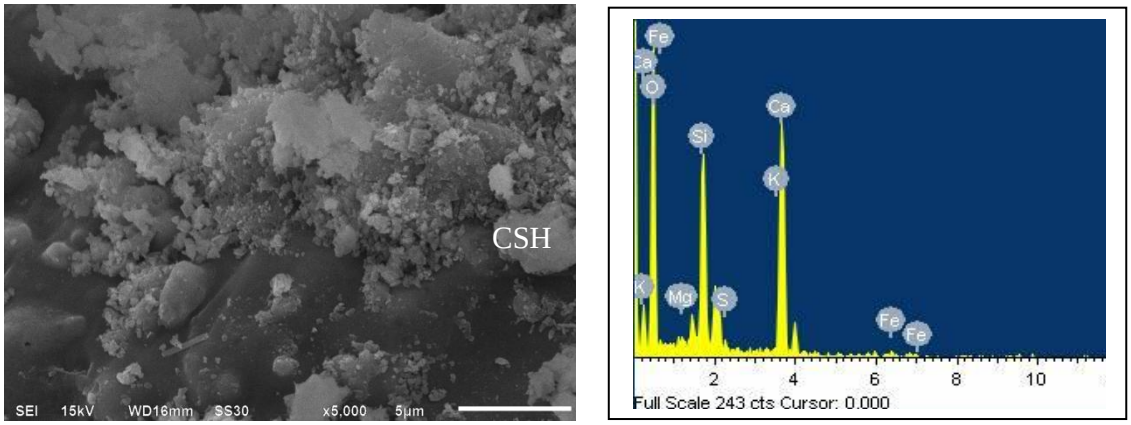

Fig. 4.107: Scanning electron micrograph and EDS spectrum of bottom ash concrete (B_{100}) at 28 days of curing age (Calcium silicate hydrate marked 'CSH')

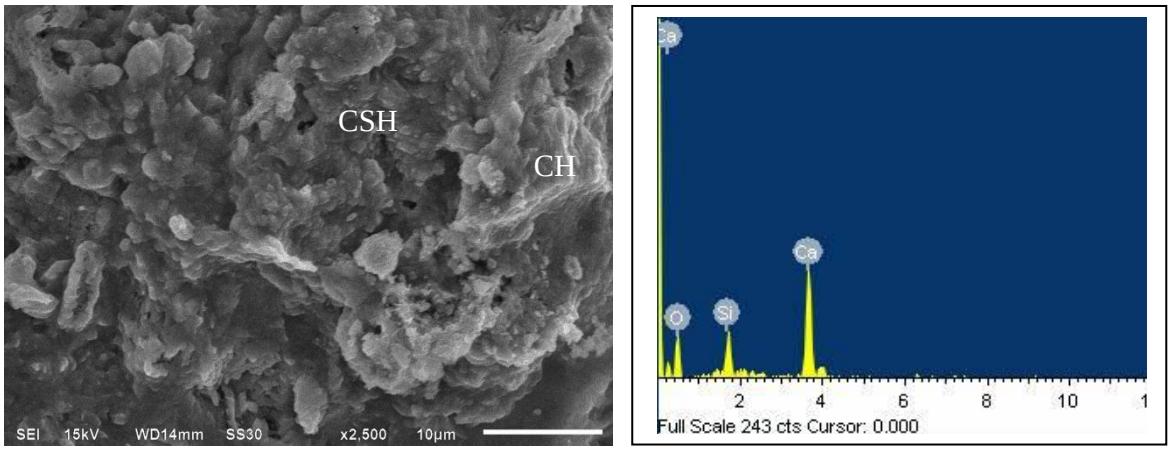

Fig. 4.108: Scanning electron micrograph and EDS spectrum of control concrete (concrete 'B') at 90 days of curing age (Calcium silicate hydrate marked 'CSH')

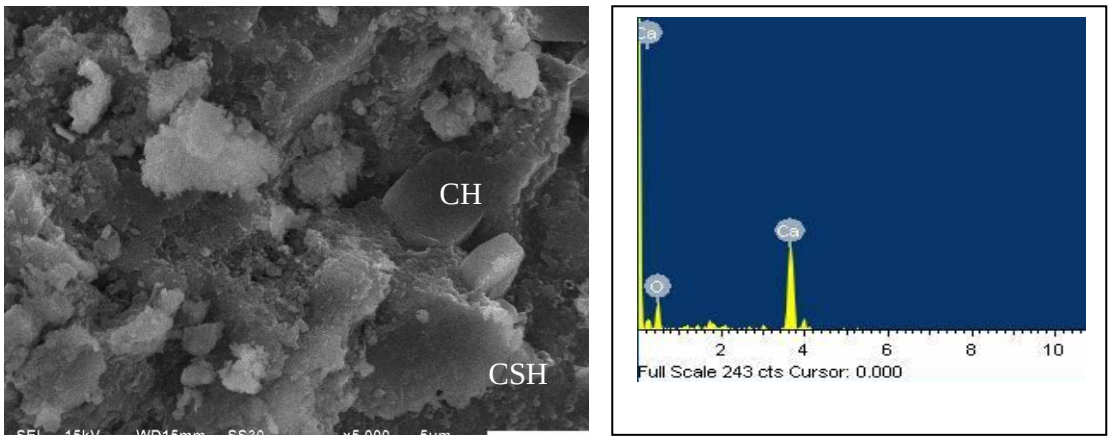

Fig. 4.109: Scanning electron micrograph and EDS spectrum of bottom ash concrete (B_{50}) at 90 days of curing age (Calcium hydroxide marked 'CH')

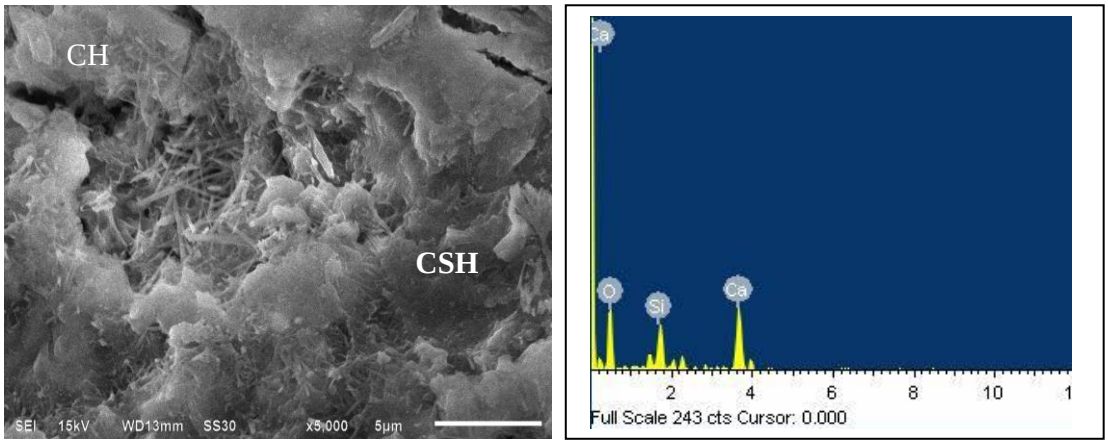

Fig. 4.110: Scanning electron micrograph and EDS spectrum of bottom ash concrete (B_{100}) at 90 days of curing age (Calcium silicate hydroxide marked 'CSH')

At higher resolution, fibrous as well as discrete grain type CSH gel was seen in micrograph of bottom ash concrete containing 75% coal bottom as fine aggregate. The porous particle and un-reacted particle of coal bottom ash in bottom ash concrete containing 100% coal bottom ash seen in the Fig 4.101 indicate that pozzolanic activity has yet not started at 28 days of curing age. However, at 90 days of curing age, as seen at the top left corner of SEM image of bottom ash concrete mixture B_{100}, the particles of coal bottom ash has started reacting with calcium hydroxide. The CSH gel is evenly spread over the entire images and ettringites are present. Also the pozzolanic activity of coal bottom ash was observed at 90 days of curing age in bottom ash concrete mixture B_{75}. It shows that above 50% replacement of sand with coal bottom ash in concrete, the pozzolanic activity is delayed with the increase in coal bottom ash content.

At the age of 90 days, Fig 4.100 shows compact, monolithic and crippled sheet type CSH gel evenly spread over the entire image of bottom ash concrete mixture containing 50% coal bottom ash. Similarly, at the age of 90 days, SEM image of control concrete shows that CSH gel is compact and monolithic and spread over the entire image. From the study of microstructure of the bottom ash concrete mixtures, it is clear that pozzolanic activity is slow at the age 28 days and after that, the bottom ash particles started reacting with calcium hydroxide resulting in formation of CSH gel. As such at the age of 90 days, the compressive strength of bottom ash concrete mixtures was comparable to that of control concrete. Figs. 4.102 to 4.110 show the SEM morphology and EDS analysis of calcium silicate hydrates, calcium hydroxide, calcium aluminio silicate hydrate, ettringites and calcium aluminium ferrite silicate hydrate.

4.4.6 XRD Phase Analysis

The X-ray diffraction technique was used for the identification of phases present in the concrete. XRD spectrums of powdered concrete mixtures at 28 and 90 days of curing age are presented in Figs. 4.111 to 4.116. The main phases present in the concrete are calcium hydroxide (P), calcium silicate hydrate (CSH), calcium aluminium silicate hydrate (CASH) and calcium silicate (CS). The remnants of aggregate and coal bottom ash in the form of quartz were also observed in the XRD spectrums of powdered concrete paste. The phase composition did not changed qualitatively on use of coal bottom ash in concrete. However, the change in proportions of phases in concrete mixtures was observed on incorporation of coal bottom ash in concrete. The effect of coal bottom ash on portlandite composition was significant. There was no evidence of late ettringite formation with the use of coal bottom ash in concrete.

Table 4.23 Intensity of calcium hydroxide peaks (Concrete 'B')

Mix	**Total Intensity (Counts) of portlandite at curing age (days)**							
	28				**90**			
	d = 4.90°A	**d = 2.62°A**	**Total**	**Composition (%)**	**d = 4.90°A**	**d = 2.62°A**	**Total**	**Composition (%)**
Control concrete	2376	1875	4251	100	2601	2532	5133	100
B_{20}	3247	2372	5619	132	5020	2854	7874	153
B_{30}	2673	2627	5300	125	2484	2879	5363	104
B_{40}	4147	1663	5810	137	5548	2349	7879	153
B_{50}	2569	1903	4472	105	3555	2868	6423	125
B_{75}	1595	2329	3924	92	2902	2259	5161	100
B_{100}	3521	2095	5616	132	2679	2329	5008	98

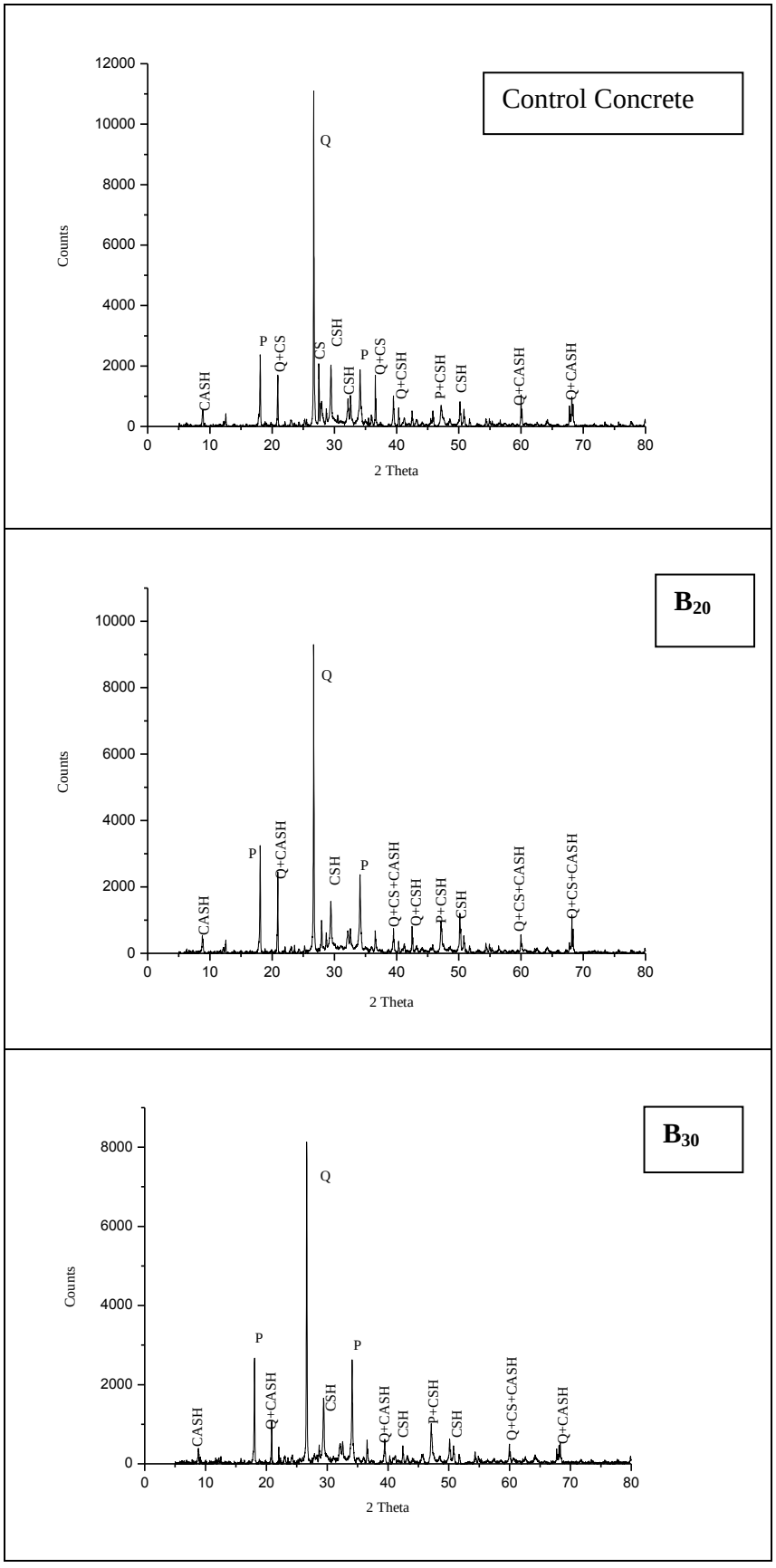

Fig. 4.111: XRD spectrum of control concrete and bottom ash concrete (B_{20} and B_{30}) at 28 days (CASH = Calcium alumino silicate hydrate; CS = Calcium silicate; CSH = Calcium silicate hydrate; E = Ettringite; P = Portlandite; Q = Quartz)

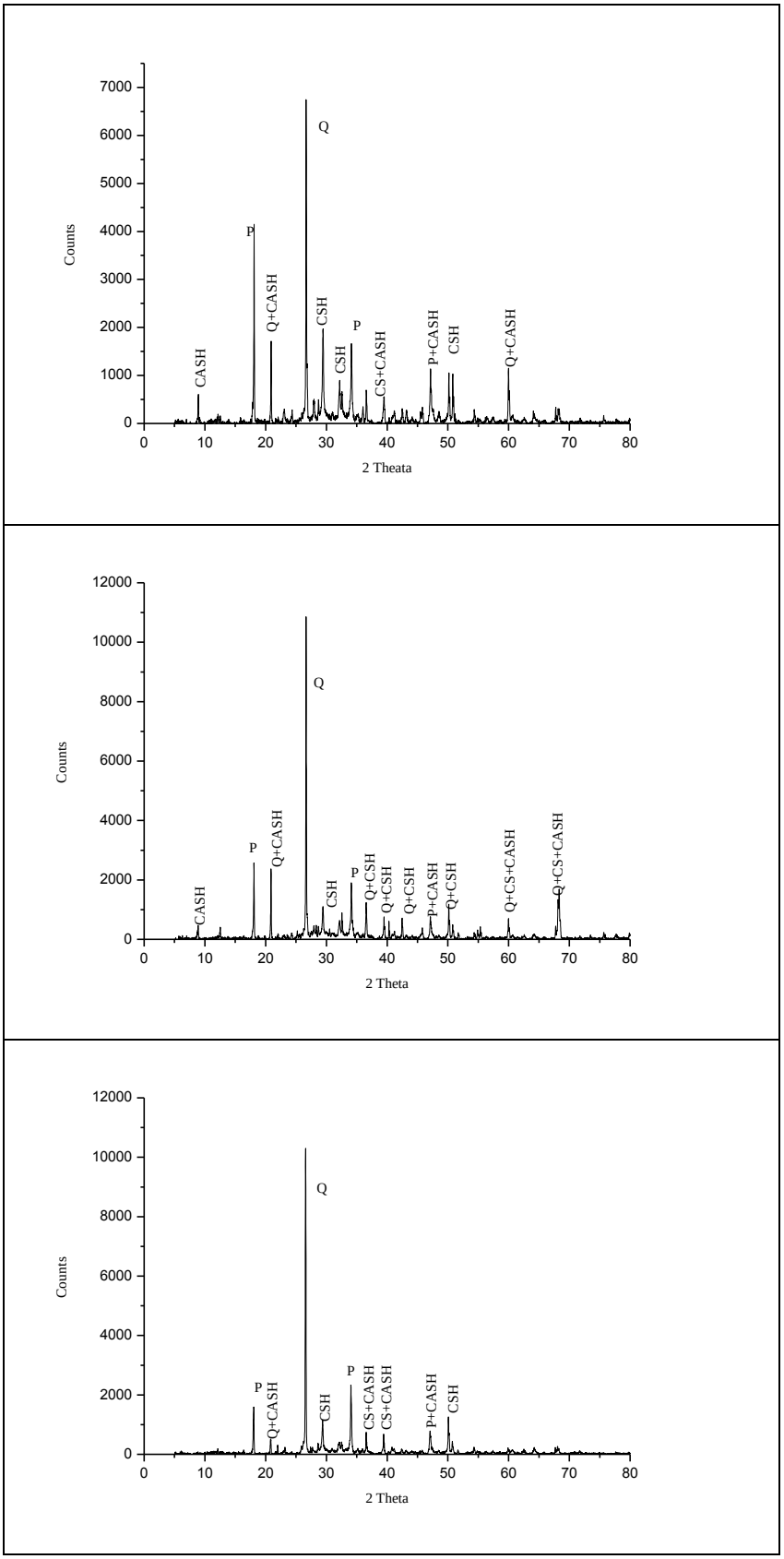

Fig. 4.112: XRD spectrum of bottom ash concrete (B_{40}, B_{50} and B_{75}) at 28 days (CASH = Calcium alumino silicate hydrate; CS = Calcium silicate; CSH = Calcium silicate hydrate; E = Ettringite; P = Portlandite; Q = Quartz)

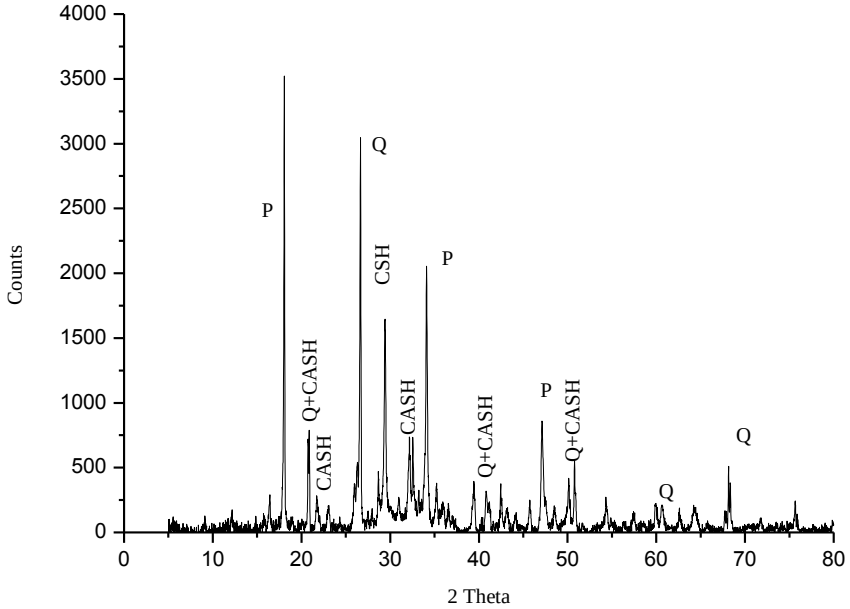

Fig. 4.113: XRD spectrum of bottom ash concrete (B_{100}) at 28 days (CASH = Calcium alumino silicate hydrate; CS = Calcium silicate; CSH = Calcium silicate hydrate; E = Ettringite; P = Portlandite; Q = Quartz)

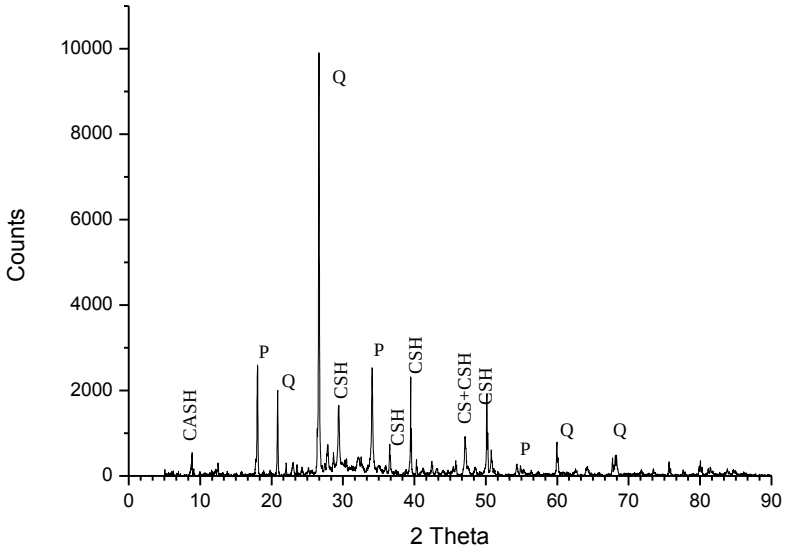

Fig. 4.114: XRD spectrum of control concrete (Concrete 'B') at 90 days (CASH = Calcium alumino silicate hydrate; CS = Calcium silicate; CSH = Calcium silicate hydrate; E = Ettringite; P = Portlandite; Q = Quartz)

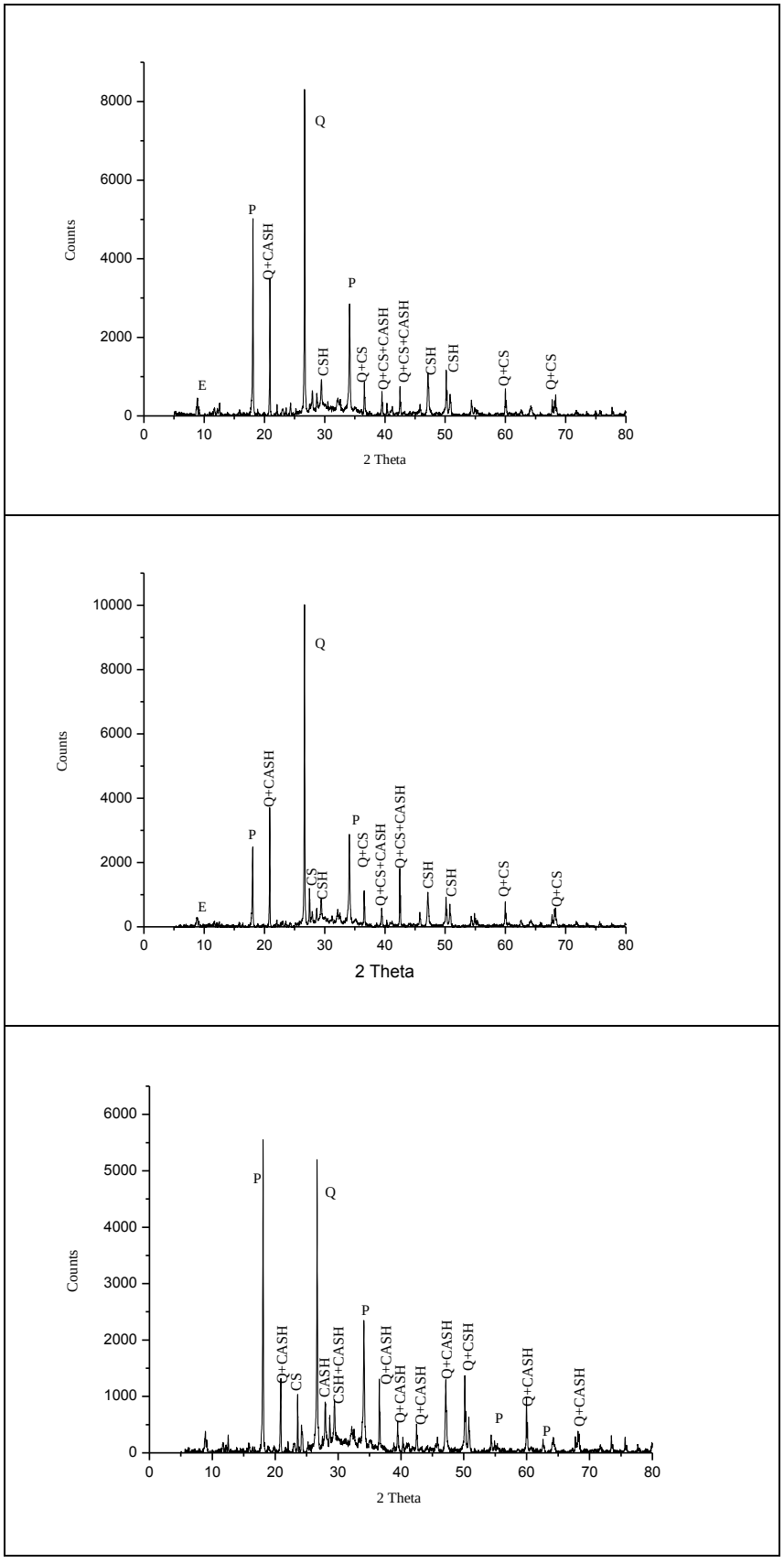

Fig. 4.115: XRD spectrum of bottom ash concrete B_{20}, B_{30} and B_{40} at 90 days (CASH = Calcium alumino silicate hydrate; CS = Calcium silicate; CSH = Calcium silicate hydrate; E = Ettringite; P = Portlandite; Q = Quartz)

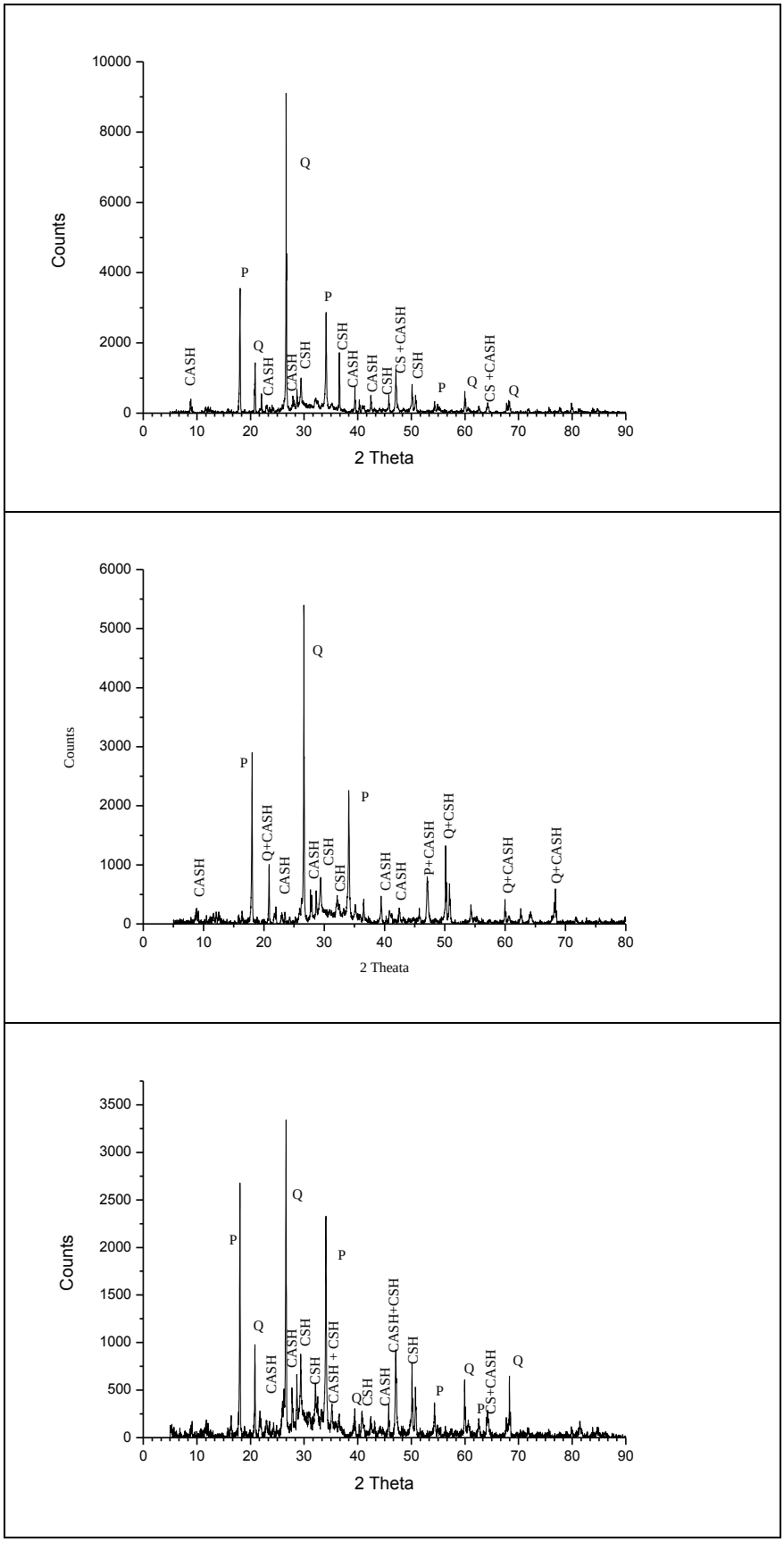

Fig. 4.116: XRD spectrum of bottom ash concrete B_{50}, B_{75} and B_{100} at 90 days (CASH = Calcium alumino silicate hydrate; CS = Calcium silicate; CSH = Calcium silicate hydrate; E = Ettringite; P = Portlandite; Q = Quartz)

At 28 days of curing age, the evaluation of XRD spectrums intensities revealed that the total intensity of portlandite (d = 4.90 °A, 2.62 °A) in coal bottom ash concrete mixtures with the exception of concrete mixture B_{75} was higher than that in control concrete. The total intensity of portlandite (d = 4.90 °A, 2.62 °A) in concrete mixtures$B_{20,}$ $B_{30,}$ $B_{40,}$ B_{50} and B_{100} was 32.18, 24.7, 36.67, 5.2 and 31.1%, respectively, higher than that in control concrete. At 90 days of curing age, the total intensity of portlandite (d = 4.90 °A, 2.62 °A) in all bottom ash concrete mixtures with the exception of concrete mixture B_{20}, $B_{30,}$ B_{50} was almost comparable to that in control concrete. Total intensity of calcium hydroxide for bottom ash mixtures B_{20}, $B_{30,}$ B_{50} was 53, 53, and 25%, respectively, higher than that in control concrete. The total intensity of portlandite (d = 4.90 °A, 2.62 °A) in bottom ash concrete mixtures B_{20}, $B_{30,}$ $B_{40,}$ B_{50}, B_{75} and B_{100} was 7874, 5263, 7879, 6433, 5161 and 5008 counts, respectively, as compared to 5132 counts in control concrete. At early curing age, the relative difference in intensities of calcium silicate hydrate and portlandite in the bottom ash concrete mixtures was more as compared to that in control concrete.

4.4.7 Statistical Analysis of Results

4.4.7.1 Relationship between Compressive Strength and Splitting Tensile Strength

Fig. 4.117 demonstrates the relation between splitting tensile strength and compressive strength of bottom ash concrete. The relationships between compressive strength and splitting tensile strength together with the coefficients of determination R^2 derived from test results of present study is given below.

$f_t = 0.0817\ (\sigma)^{0.9888}$ $R^2 = 0.9627$

Kockal and Ozturan (2011) proposed similar equation for light weight concrete

$ft = 0.1109(\sigma)^{0.9389}$ $R^2 = 0.9912$

where

f_t = Splitting tensile strength of concrete in N/mm^2,

σ = Compressive strength of cube specimen of concrete in N/mm^2

The regression analysis performed showed strong relation between compressive strength and splitting tensile strength of bottom ash concrete. The value of coefficient of determination R^2 indicates the good relation between regression curve and data points. The comparison of splitting tensile strength values calculated as per relation given in CEB-FIP is given in Table 4.24.

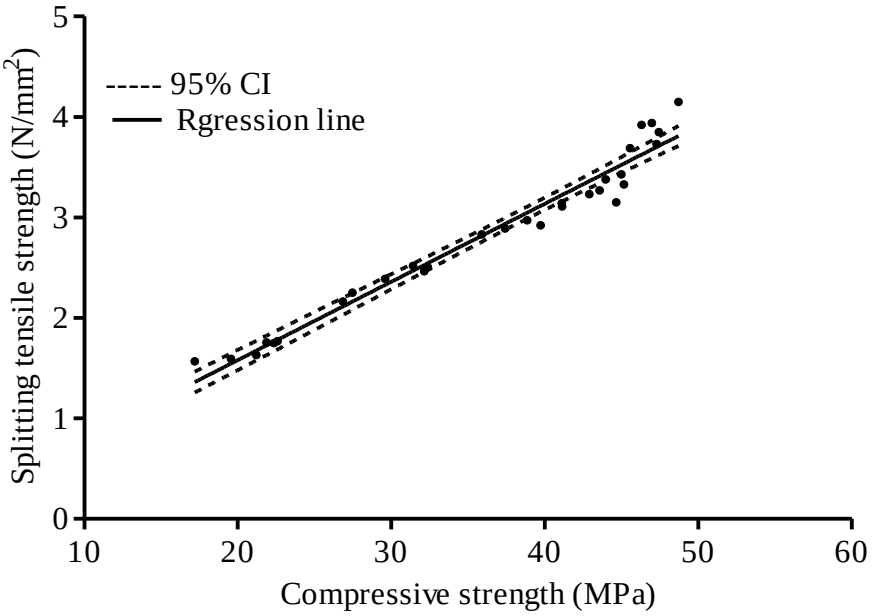

Fig. 4.117: Relation between compressive strength and splitting tensile strength of concrete (Concrete 'B')

Table 4.24 Comparison of relation given in CEB-FIP and derived from present study (Concrete 'B')

Cube Compressive strength (N/mm^2)	**Splitting tensile strength (N/mm^2) as per**		**Actual splitting tensile strength (N/mm^2)**
	$f_t = 0.3(f_{cyl})^{2/3}$	**$f_t = 0.0817\ (f_{cu})^{0.9888}$**	
17.19	1.72	1.36	1.57
26.65	2.31	2.10	2.16
32.88	2.65	2.58	2.83
36.85	2.86	2.89	2.70
42.90	3.17	3.36	3.23
46.17	3.33	3.61	3.43

4.4.7.2 Relationship between Compressive Strength, Dry Bulk Density and Modulus of Elasticity

Fig. 4.118 shows the relationship between compressive strength, dry bulk density and modulus of elasticity of concrete obtained from the present study. The equation showing the relationships between compressive strength, dry bulk density and modulus of elasticity together with the coefficients of determination R^2 derived is given below. The empirical

parameters of the equation obtained from the present study are almost similar to that given in BS: 8110 (Part 2)-1985. Higher value of coefficient of determination indicates good relevance between the data points and regression curve. Dry bulk density of bottom ash concrete mixtures varied between 2363 kg/m^3 and 2161 kg/m^3.

$E = 1.01 \rho^2 \sigma^{0.33} + 8.132$ $R^2 = 0.8050$ (Author)

$E = 1.7 \rho^2 \sigma^{0.33}$ BS: 8110 (Part 2):1985

where,

σ = Cube compressive strength of concrete in N/mm^2

E = Modulus of elasticity of concrete in GPa

ρ = Dry bulk density of concrete in kg/m^3

The coefficient of determination value ($R^2 = 0.805$) indicates that 80.5% data is explained by the derived relation and 19.5% data remained unexplained.

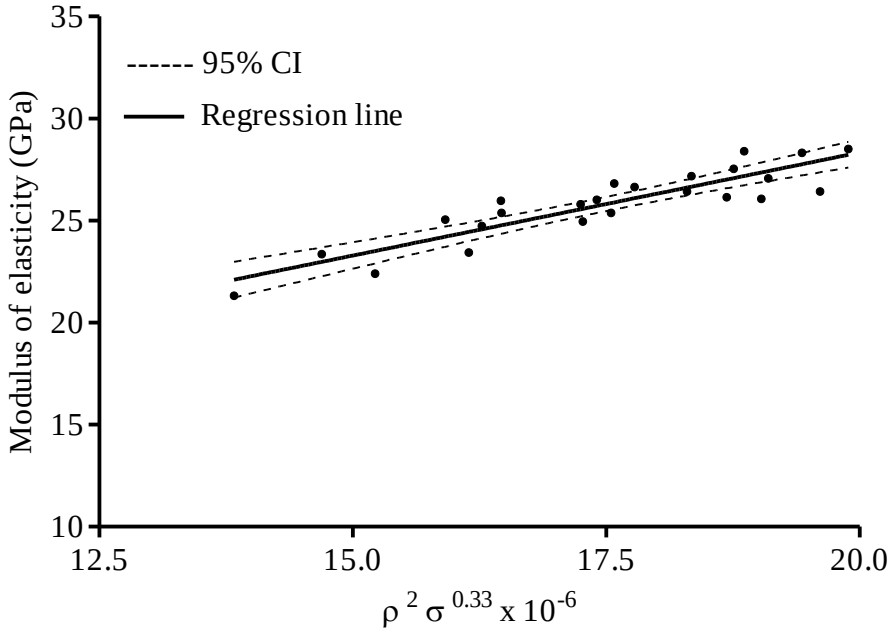

Fig. 4.118: Relationship between compressive strength, dry bulk density and modulus of elasticity (Concrete 'B')

4.4.7.3 Relationship between Compressive Strength and Pulse Velocity

Fig. 4.119 shows the relationship between pulse velocity and compressive strength of concrete obtained from the test results of the present study..

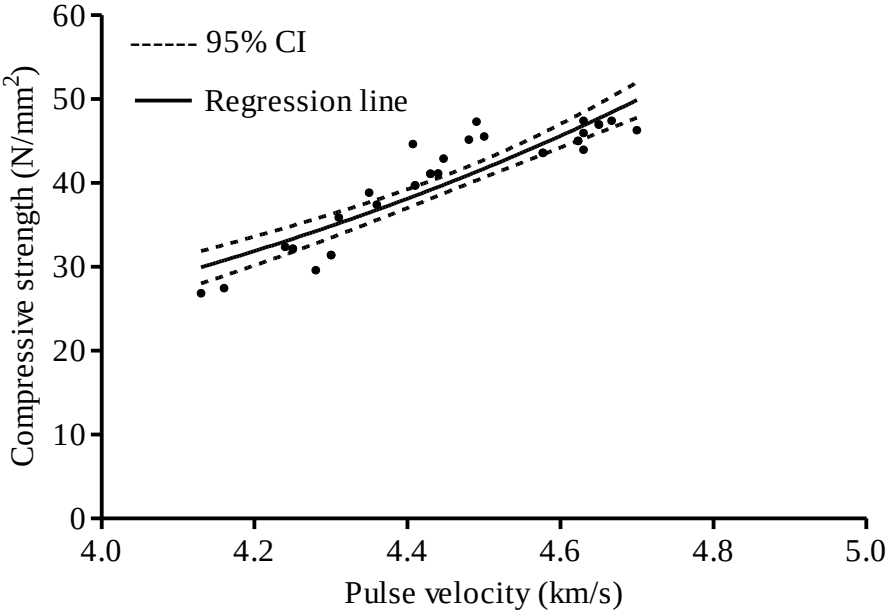

Fig. 4.119: Relationship between compressive strength and pulse velocity (Concrete 'B')

The equation expressing the relationships between compressive strength σ and the pulse velocity of longitudinal waves V, together with the coefficients of determination R^2 derived is given below

$$\sigma = 0.7432 \exp(0.8950V) \qquad R^2 = 0.8184$$

where

σ = Compressive strength of cube specimen of concrete in N/mm^2

V = Pulse velocity through concrete in km/s

Higher value of coefficient of determination indicates good relevance between the data points and regression curve.

Verification of Proposed Relation between Compressive Strength and Pulse Velocity

To verify the above relation between compressive strength and pulse velocity, 10 cube specimens of concrete incorporating different proportions of coal bottom ash as fine aggregate were cast. The specimens were tested at the curing age of 365 days for compressive strength and pulse velocity. The actual compressive strength and predicted compressive strength from above equation are given in Table 4.25.

Table 4.25 Verification of relation between pulse velocity and compressive strength (Concrete 'B')

Sample	Pulse velocity (m/s)	Predicted compressive strength (N/mm^2)	Actual Compressive strength (N/mm^2)	Variation
1	4640	47.28	44.58	+6.06%
2	4750	52.17	50.13	+4.06%
3	4440	39.53	40.36	-2.06%
4	4670	48.56	44.05	+10.24%
5	4550	43.62	44.62	-2.25%
6	4820	55.54	53.38	+4.05%
7	4600	45.61	44.93	1.52%
8	4670	48.56	51.86	-6.36%
9	4720	50.79	49.11	+3.41%
10	4850	57.05	56.22	+1.48%

All the predicted values of compressive strength are within +10.24 % and –6.36% variations from the actual compressive strength of concrete specimens. This verifies the proposed relation for estimation of compressive strength from measured pulse velocity through concrete.

4.4.7.4 Relationship between Chloride Permeability and Pulse Velocity

The relationship between pulse velocity and chloride permeability of bottom ash concrete derived from the test results of the present study is presented in Fig 4.120. The equation expressing the relationships between chloride permeability (total charge passed through bottom ash concrete specimens) and the pulse velocity of longitudinal waves V, together with the coefficients of determination R^2 derived is given below

$$Q = -3245.2V + 15820 \qquad R^2 = 0.5709$$

where

Q = Total charge passed through the specimen in Coulombs

V = Pulse velocity through concrete in km/s

The low value of R^2 indicates that weaker relationship between charges passed and pulse velocity through concrete exits. Panzera et al. (2008) reported a decrease in pulse velocity

with increase in porosity and oxygen permeability of concrete. The voids present in concrete leads to a reduction in pulse velocity.

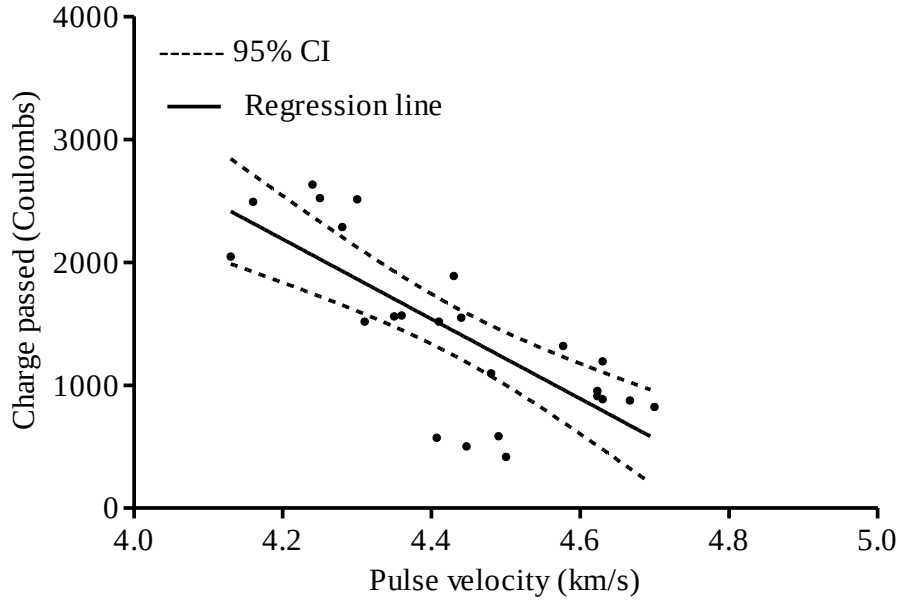

Fig. 4.120: Relation between pulse velocity and chloride permeability of bottom ash concrete (Concrete 'B')

4.4.7.5 Relationship between Compressive Strength and Chloride Permeability

Fig. 4.121 depicts the relationship between chloride permeability and compressive strength of concrete obtained from the present study. The equation expressing the relationships between compressive strength σ and the total charge passed Q in coulombs, together with the coefficients of determination R^2 derived is given below.

$$\sigma = -0.008521Q + 52.10 \qquad R^2 = 0.795$$

where

σ = Compressive strength of cube specimen of concrete in N/mm^2

Q = Total charge passed through the specimen in coulombs

Higher value of coefficient of determination, R^2 indicates good relevance between the data points and regression curve. Compressive strength and resistance to chloride ion penetration of concrete are linked to its pore structure. The denser is the concrete, higher is compressive strength and lower is the chloride permeability. It is evident from the above equation that the higher is the total charge passed through the concrete, lower is the compressive strength.

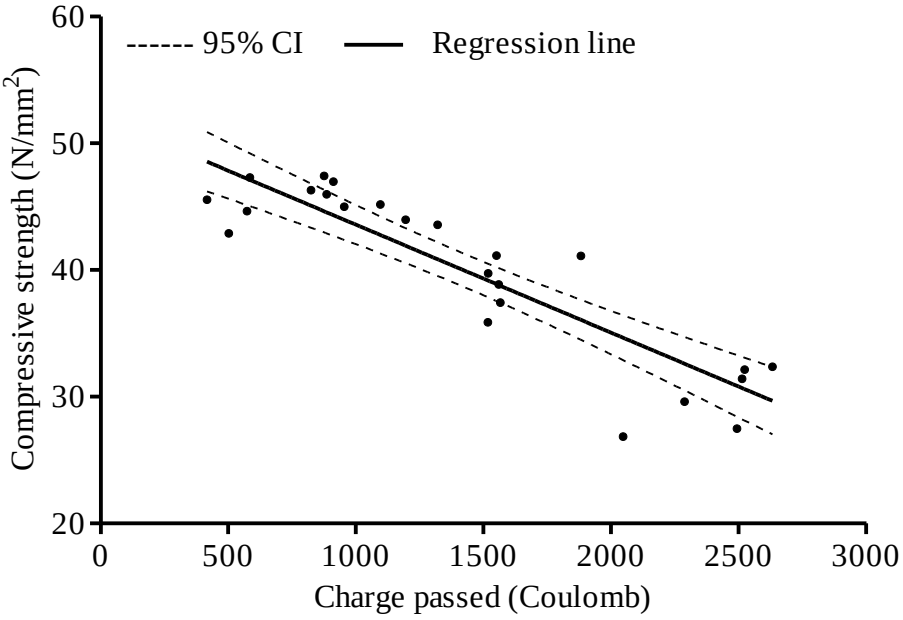

Fig. 4.121: Relation between compressive strength and chloride permeability of bottom ash concrete (Concrete 'B')

4.4.7.6 Relation between Percentage Loss in Weight and Reduction in 28-day Compressive Strength

The relationship between reduction in 28-day compressive strength of concrete specimens and their weight loss due to immersion in 3% sulphuric acid solutions is shown in Fig. 4.122. The higher value of coefficient of determination R^2 indicates the good relevance between the data points and the regression curve. The loss in compressive strength increased approximately linearly with the increase in mass loss of concrete specimens.

The equation of relationship between mass loss and compressive strength loss of concrete due to external sulphuric acid attack is given as under

$$\Delta\sigma = 8.6749\Delta m - 5.041 \qquad R^2 = 0.8945$$

where

$\Delta\sigma$ = percentage loss in 28 day compressive strength of concrete

Δm = percentage loss in mass of concrete specimen

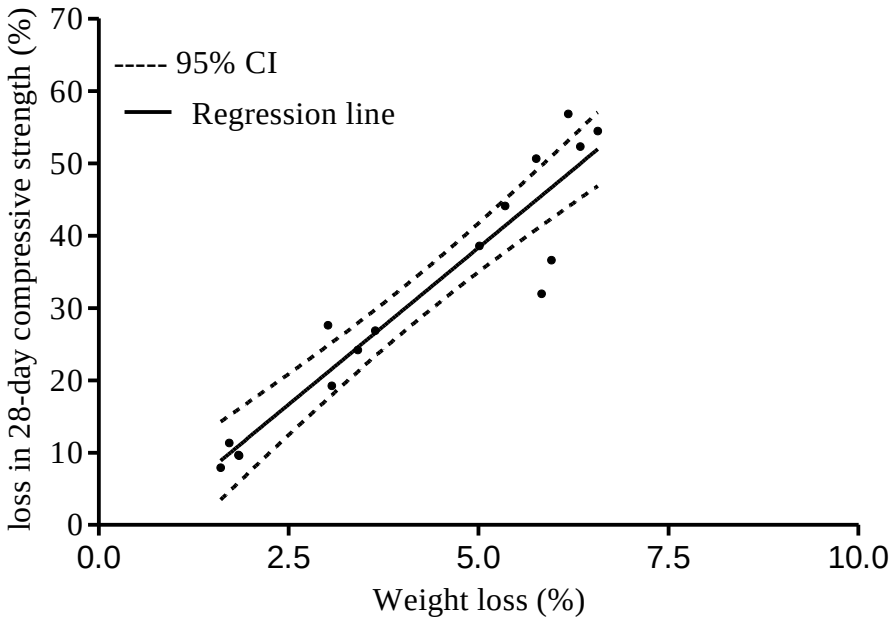

Fig. 4.122: Relation between loss in 28-day compressive strength and weight loss after immersion in 3% sulphuric acid solution (Concrete 'B')

4.4.7.7 Relationship between Compressive Strength and Abrasion Resistance

Fig. 4.123 shows the relationship between compressive strength and average depth of wear of concrete obtained from the present study. The equation showing the relationships between compressive strength (σ) and the average depth of wear (d) against abrasion of concrete, together with the coefficient of determination (R^2) derived is given below. The empirical parameters of the equation obtained from the present study are almost similar to that reported by Naik et al. (1995) for high strength concrete made with C type fly ash as replacement of cement. Higher value of coefficient of determination indicates good relevance between the data points and regression curve. Siddique (2013) observed that the abrasion resistance of self compacting concrete mixes is related with its compressive strength and increases with increase in compressive strength. Siddique (2010) observed that depth of wear of fly ash concrete against abrasion has very good correlation with compressive strength.

d	=	-0.0207σ + 1.6218	R^2 = 0.7227 (R = 0.85)	for 15 min abrasion (Author)
d	=	-0.03951σ + 4.0444	R^2 = 0.6724 (R = 0.82)	for 60 min abrasion (Naik et al., 1995)

d = -1.5992Ln(x) + 7.7283 R^2 = 0.9044 (R = 0.97) for 60 min abrasion (Siddique, 2010)

where

d = Average depth of wear in mm

σ = Compressive strength of cube specimen of concrete in N/mm^2

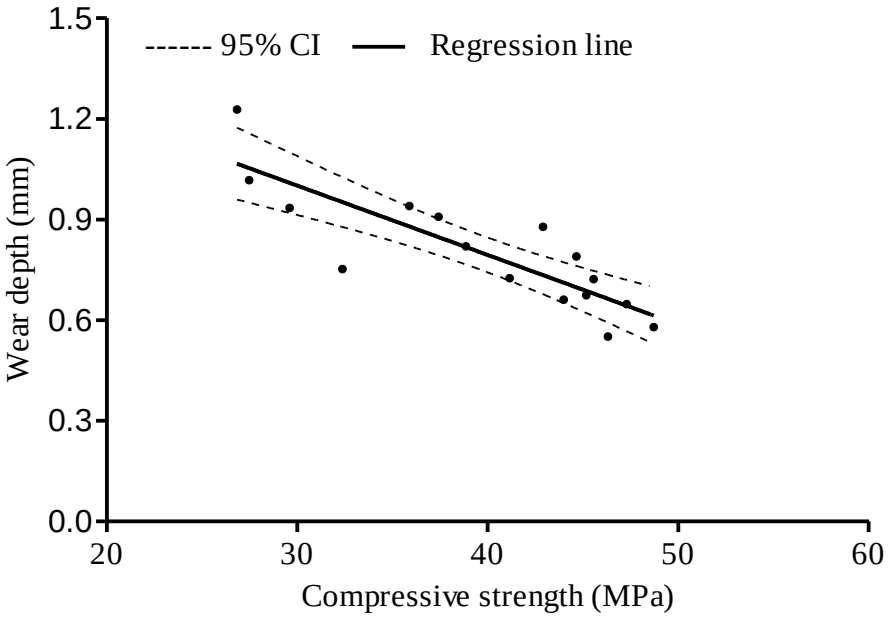

Fig. 4.123: Relationship between compressive strength and average depth of wear of concrete (Concrete 'B')

4.5 COMPARISON BETWEEN PROPERTIES OF CONCRETES MADE WITH SANDS HAVING DIFFERENT FINENESS MODULUS

4.5.1 Workability

Comparison of effect of coal bottom ash on slump values of bottom ash concrete mixtures of concrete ‘A’ and concrete ‘B’ evaluated on percentage decease over that of control concrete is illustrated in Fig. 4.124. Slump of control concrete was 70 mm for concrete ‘A’ (A_0) and 125 mm for concrete ‘B’ (B_0). Percentage decrease in slump values of bottom ash concrete mixtures of both concretes ‘A’ and ‘B’ increased with increase in coal bottom ash content.

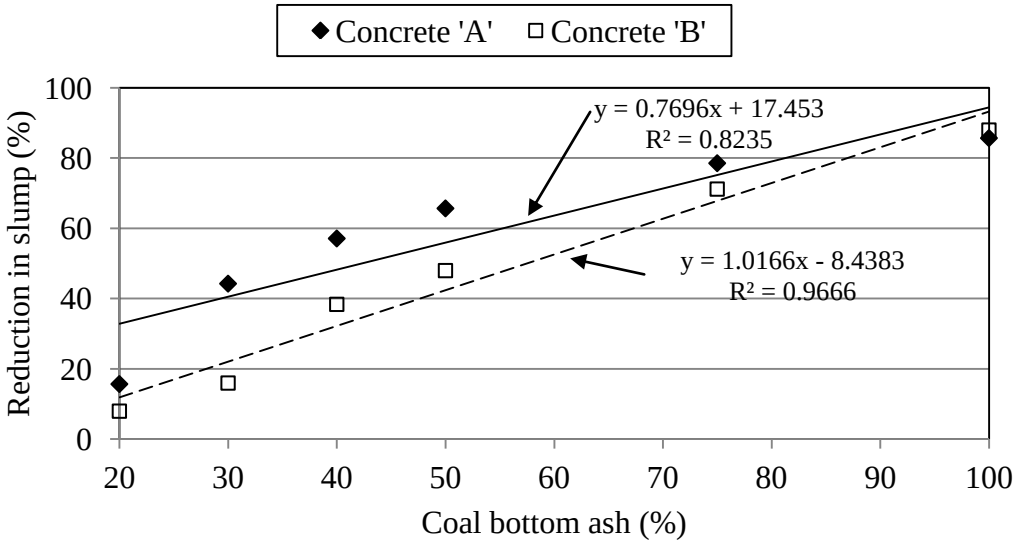

Fig. 4.124: Reduction in slump versus coal bottom ash content in concrete

The decrease in slump of bottom ash concrete mixtures over their respective control concrete mixture was almost linear with increase in coal bottom ash content. Up to 50% replacement level, bottom ash concrete mixtures of concrete ‘A’ showed more decrease in slump values as compared to that of bottom ash concrete mixtures of concrete ‘B’. However, bottom ash concrete mixtures containing 75 and 100% coal bottom ash of both concretes ‘A’ and ‘B’ displayed almost identical decrease in slump values. Bottom ash concrete mixtures containing 75% coal bottom ash displayed 78% for concrete ‘A’ and 71% for concrete ‘B’ decrease in slump values. On incorporation of 100% coal bottom ash as fine aggregate in concrete, slump decreased by 86% for concrete ‘A’ and 88% for concrete ‘B’. For replacement up to 50%, higher water cement ratio, less cement content and use of superplasticizer may be the possible reason for lesser decrease in slump of bottom ash concrete mixtures of concrete ‘B’. Esteves et al. (2010) observed that fine

aggregate particles in size range of 75 and 1000 μm in the concrete acts as water fixation point. In the present work, contents of fine aggregate particles finer than 1000 μm were more in concrete mixtures of concrete 'A' than those in concrete mixtures of concrete 'B'. Bottom ash concrete mixture A_{50} containing 50% coal bottom ash has 84.5% fine aggregate particles finer than 1000 μm as compared to 73.75% in bottom ash concrete mixture B_{50}. Up to 50% replacement level, higher percentage of fine aggregate particles finer than 1000 μm in bottom ash concrete mixtures of concrete 'A' caused more decrease in slump values as compared to that of bottom ash concrete mixtures of concrete 'B'. At 75% replacement level, fine aggregate particles finer than 1000 μm was 88% in bottom ash concrete mixture A_{75} and 81% in bottom ash concrete mixtures B_{75}. Increase in fine aggregate particles finer than 1000 μm on incorporation of bottom ash in concrete resulted in increase in surface area which caused decrease in slump values. Higher water absorption by the coal bottom ash particles was also the reason for decrease in slump of bottom ash concrete. Dry and porous particles of coal bottom ash absorbed water internally which resulted in reduction in free water for lubrication of particles. Esteves et al. (2010) also noted that frictional force may be the governing factor for resistance to flow of concrete containing fine aggregate particles coarser than 1000 μm. Interlocking characteristics, angular shape and rough texture of coal bottom ash particles resulted in increase in frictional forces which retarded the flow of fresh concrete.

4.5.2 Bleeding

Comparison of effect of coal bottom ash on water loss through bleeding in bottom ash concrete mixtures of concrete 'A' and concrete 'B' evaluated on the basis of percentage decrease over that in control concrete is illustrated in Fig. 4.125. Bottom ash concrete mixtures of concrete 'B' displayed higher reduction in bleeding as compared to bottom ash concrete mixtures of concrete 'A' on use of coal bottom ash as fine aggregate. Water loss through bleeding was 3.14% for A_0 and 8.45% for B_0. Slump of control concrete mixture B_0 was more than that of control concrete mixture A_0. Since more free water was present in the inter particle voids in control concrete mixture B_0 as compared to that in control concrete mixture A_0. As such concrete mixture of concrete 'B' displayed higher water loss through bleeding. Water loss through bleeding of bottom ash concrete mixture containing 100% coal bottom ash was 1.66% for concrete mixture A_{100} and 1.68% for concrete mixture B_{100}. Volume of bleeding water per unit exposed area decreased from 0.2017 to 0.11 g/cm^2 for concrete 'A' and from 0.5134 to 0.1039 g/cm^2 for concrete 'B' on

incorporation of 100% coal bottom ash in concrete. Percentage decrease in water loss through bleeding gradually increased with the increase in coal bottom ash content in bottom ash concrete mixtures of concrete 'B'. However, percentage decrease in bleeding in bottom ash concrete mixtures of concrete 'A' increased up to 50% increase in coal bottom ash content and for 50, 75 and 100% replacement of sand with coal bottom ash, water loss through bleeding was almost identical. Bottom ash concrete mixtures of concrete 'B' displayed higher reduction in bleeding as compared to bottom ash concrete mixtures of concrete 'A' on use of coal bottom ash as fine aggregate. Bottom ash concrete mixtures containing 50, 75 and 100% coal bottom ash displayed 44, 45 and 47% for concrete 'A' and 53, 61 and 80% for concrete 'B' reduction in bleeding. Bottom ash concrete mixture A_{100} contained 37% particles finer than 1000 micron as compared to 35% in bottom ash concrete mixture B_{100}. Comparing the quantities of water added and slump values both bottom ash concrete mixtures A_{100} and B_{100}, the quantity of free water in inter particle voids was almost equal in both the concrete mixtures. As a result both concrete mixtures A_{100} and B_{100} displayed almost identical bleeding percentage and volume of water loss per unit exposed surface area. Since water loss through bleeding of concrete mixture B_0 was much higher than that of $A_{0,}$ thus bottom ash concrete mixture B_{100} displayed higher percentage decrease in bleeding as compared to that of $A_{100.}$

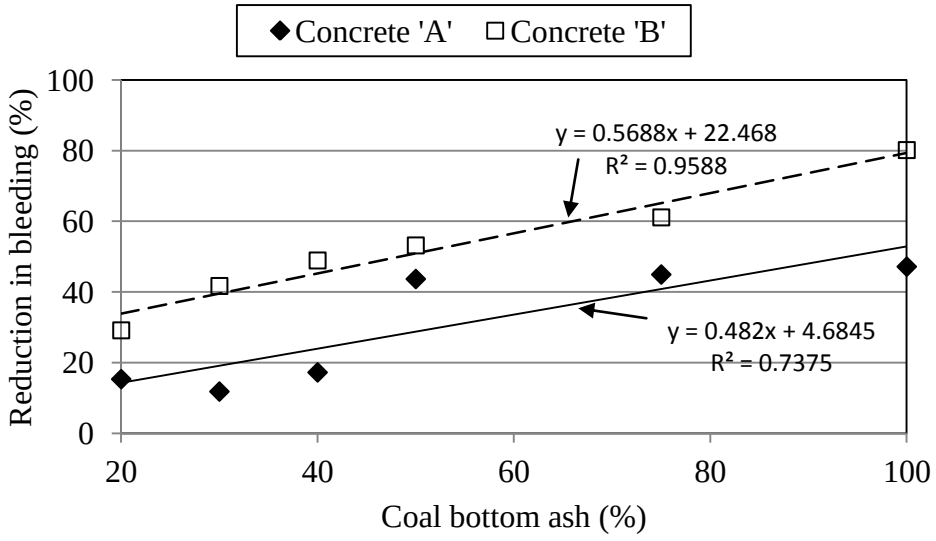

Fig. 4.125: Bleeding variation versus coal bottom ash content in concrete

4.5.3 Density

Comparison of effect of coal bottom ash on density of bottom ash concrete mixtures of concrete 'A' and concrete 'B' is illustrated in Fig 4.120. One-day density of control concrete mixtures was 2404 kg/m^3 for concrete 'A' and 2396 kg/m^3 for concrete 'B'. The

variations of dry bulk densities of bottom ash concrete mixtures over that of control concrete varied between -1.76% and -9.97% for concrete ‘A’ and between -1.38% and 9.84% for concrete ‘B’ depending upon the coal bottom ash content in concrete. Density of bottom ash concrete mixtures of both concretes ‘A’ and ‘B’ decreased almost equally on use of coal bottom ash. Low specific gravity of coal bottom ash was the reason for decrease in density of bottom ash concrete mixtures. In both concretes ‘A’ and ‘B’, the decrease in density of bottom ash concrete mixtures was equal to difference in weight of sand and coal bottom ash in concrete. Densities of bottom ash concrete mixtures incorporating 100% coal bottom ash as fine aggregate reduced by 9.97% for concrete ‘A’ and 9.84% for concrete ‘B’.

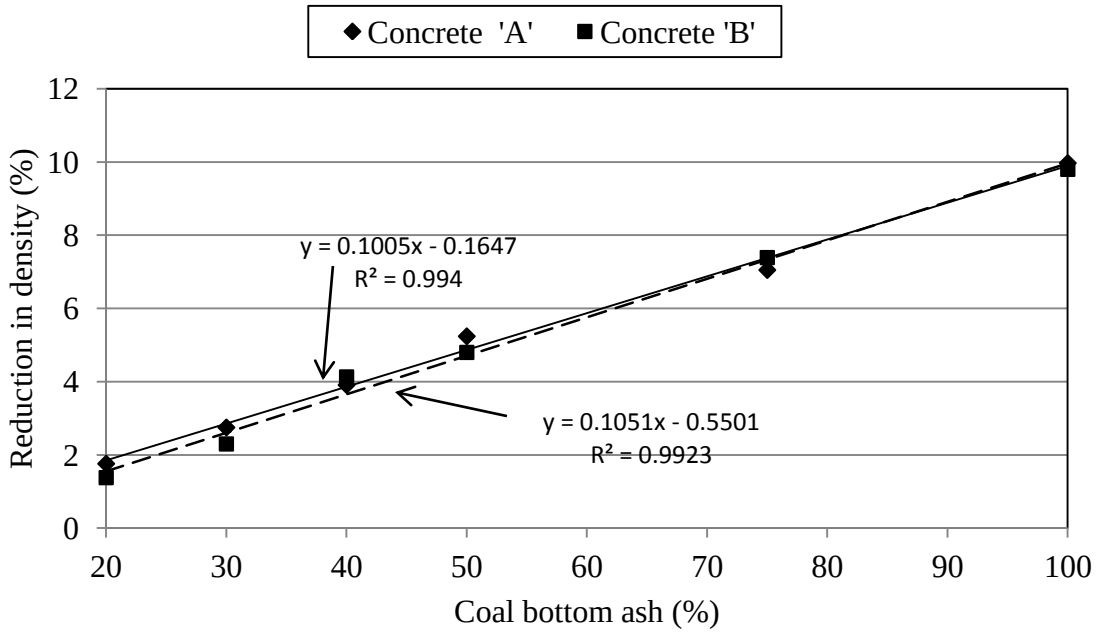

Fig. 4.126: Reduction in dry bulk density versus coal bottom ash content in concrete

4.5.4 Compressive Strength

Variation in compressive strength of concrete on use of coal bottom ash as fine aggregate with respect to respective control concrete is illustrated in Fig. 4.127. At 28 days of curing age, decrease in compressive strength of concrete on incorporation of coal bottom ash varied between 4.53% and 8.45% for bottom ash concrete mixtures of concrete ‘A’ and between 5.55% and 21.12% for bottom ash concrete mixtures of concrete ‘B’. The delay in hydration on use of coal bottom ash as fine aggregate in concrete may be possible explanation for significant decrease in compressive strength of bottom ash concrete mixtures of concrete ‘B’. It was observed that pozzolanic activity of coal bottom ash was

also not started at the 28 days of curing age. The SEM images of bottom ash concrete mixtures of concrete ‘B’ showed that particles of coal bottom ash started reacting after 90 days of curing period. At 90 days of curing age, bottom ash concrete mixtures of concrete ‘A’ gained higher compressive strength than the control concrete and the increase in compressive strength was between 2.06% and 10.38%.

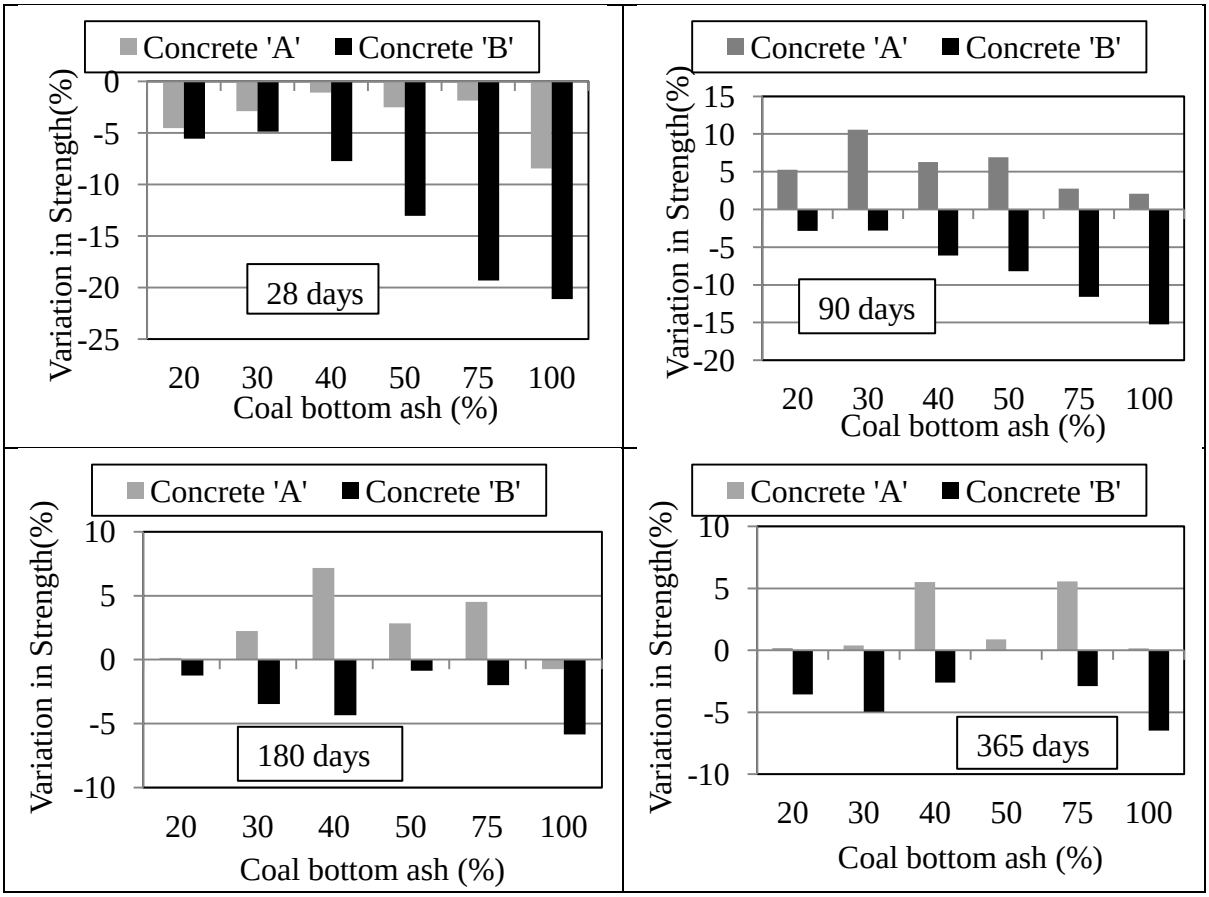

Fig. 4.127: Compressive strength variation versus coal bottom ash content in concrete

However, compressive strength of bottom ash concrete mixtures of concrete ‘B’ still remained lower than that of control concrete and the decrease in compressive strength was between 2.79% and 15.22% depending upon the coal bottom ash content. At 180 days of curing age, compressive strength of bottom ash concrete mixtures of concrete ‘B’ improved significantly and the decrease in compressive strength was between 0.86% and 5.84%. Whereas, at the same curing age, bottom ash concrete mixtures of concrete ‘A’ showed increase in compressive strength between -0.75% and 7.16%. At 365 days of curing age, bottom ash concrete mixtures of concrete ‘A’ displayed compressive strength comparable to that of reference concrete and variation in compressive strength of bottom ash concrete mixtures was between 0.16% and 5.51%. Compressive strength of bottom

ash concrete mixtures of concrete ‘B’ was almost comparable to that of control concrete. Compressive strength of concrete mixture B_{100} was lower by 6.47% than that of control concrete. Bottom ash concrete mixture containing 50% coal bottom ash showed variation in compressive strength as -2.51% for concrete ‘A’ and -13.04% for concrete ‘B’ at 28days; 6.93% for concrete ‘A’ and -8.2% for concrete ‘B’ at 90 days; 2.83% for concrete ‘A’ and -0.86% for concrete ‘B’ at 180 days; and 0.88% for concrete ‘A’ and 0% for concrete ‘B’ at 365 days. Higher cement content may be the possible explanation of increase in compressive strength of bottom ash concrete mixtures of concrete ‘A’. Ghafoori and Bucholc (1997) also observed that concrete mixtures incorporating high-calcium coal bottom ash as fine aggregate and high cement content displayed comparable compressive strength and bottom ash concrete mixtures with low cement content attained lower compressive strength than that of reference concrete mixtures Another study also revealed that there was no significant effect of coal bottom ash on compressive strength of concrete with high binding content (Kim and Lee, 2011)..

4.5.5 Splitting Tensile Strength

The effect of coal bottom ash on splitting tensile strength of bottom ash concrete mixtures evaluated on the basis of percentage increase/decrease over that of control concrete is illustrated in Fig. 4.128. At 28 days of curing age, bottom ash concrete mixtures of concrete ‘A’ displayed increase in splitting tensile strength over control concrete between 1.76% and 11.01%. Bottom ash concrete mixture containing 50% coal bottom ash showed maximum increase of 11.01% in strength. However, bottom ash concrete mixtures of concrete ‘B’ showed decrease in splitting tensile strength between 2.02% and 15.74% depending on the coal bottom ash content in concrete mixture. Bottom ash concrete mixture B_{100} attained 15.74% lower splitting tensile strength at 28 days of curing age. At 90 days of curing age, increase in splitting tensile strength of bottom ash concrete mixtures varied between 3.46% and 7.08% for concrete ‘A’ and between -6.42% and 3.84% for concrete ‘B’. Bottom ash concrete mixture containing 50% coal bottom ash displayed highest increase of 7.08% for concrete ‘A’ and lowest decrease of 1.79% for concrete ‘B’. At 180 days of curing age, bottom ash concrete mixture (B_{50}) containing 50% coal bottom ash attained 3.03% higher splitting tensile strength than that of control concrete. At 365 days of curing age, increase in strength varied between 0.53% and 2.63% for concrete ‘A’ and -10.22% and 0.97% for concrete ‘B’. Bottom ash concrete mixture B_{100} showed maximum decrease in splitting tensile strength of 10.22% at 365 days. Bottom ash concrete

mixtures of concrete ‘B’ displayed either lower or equal splitting tensile strength than control concrete at all the curing ages. However bottom concrete mixtures of concrete ‘A’ displayed either equal or higher splitting tensile strength than that of control concrete at all curing ages.

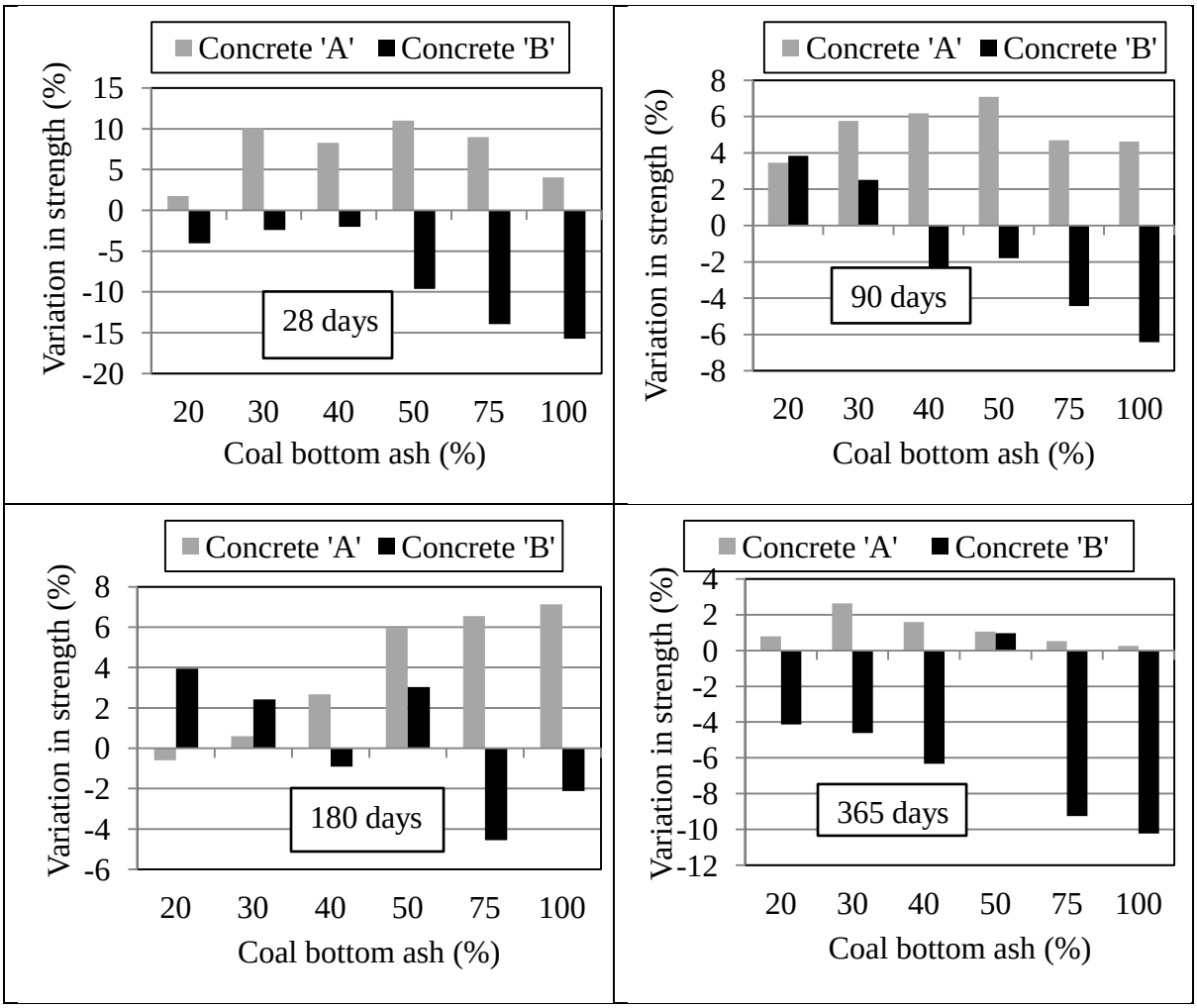

Fig. 4.128: Splitting tensile strength variation versus coal bottom ash content in concrete

Higher cement content resulted in better quality of paste in concrete which may be the possible explanation of increase in splitting tensile strength of bottom ash concrete mixtures of concrete ‘A’. Up to 50% replacement of sand with coal bottom ash in concrete, there was no significant effect of coal bottom ash on splitting tensile strength of bottom ash concrete mixtures of both concretes ‘A’ and ‘B’. Similar study on use of high-calcium coal bottom ash as fine aggregate in concrete also revealed that concrete mixture with high cement content attained either equal or higher splitting tensile strength than that of control concrete (Ghafoori and Bucholc, 1997).

4.5.6 Modulus of Elasticity

The effect of coal bottom ash on modulus of elasticity of bottom ash concrete mixtures evaluated on the basis of percentage increase/decrease over that of control concrete is illustrated in Fig. 4.129. All the bottom ash concrete mixtures of both concretes ‘A’ and ‘B’ displayed lower modulus of elasticity than that of conventional concrete. The decrease in 28 day modulus of elasticity of bottom ash concrete mixtures varied between 5.24% and 20.7% for concrete ‘A’ and 0.04% and 16.03% for concrete ‘B’. Up to 50% replacement of sand with coal bottom ash in concrete mixtures of concrete ‘B’, modulus of elasticity of bottom ash concrete mixtures was comparable to that of control concrete and for replacement more than 50%, modulus of elasticity of bottom ash concrete mixtures decreased significantly.

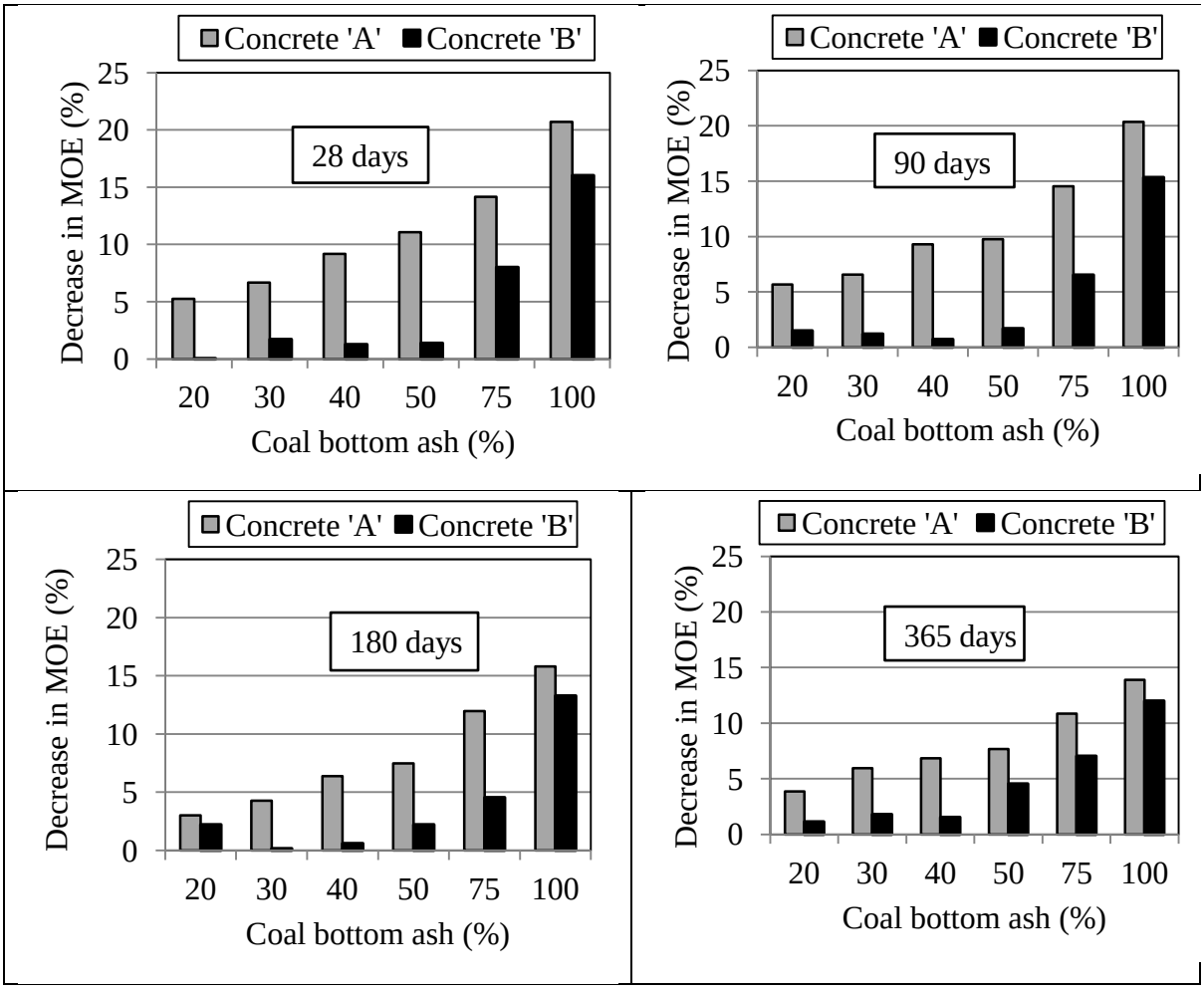

Fig. 4.129: Modulus of elasticity variation versus coal bottom ash content in concrete

Modulus of elasticity of bottom ash concrete mixtures B_{100} was 16% lower than that of control concrete. Although modulus of elasticity of bottom ash concrete mixtures increased

with age but the difference in modulus of elasticity of bottom ash concrete mixtures and control concrete remained the same at 90 days of curing ages. At 180 and 365 days of curing ages, both bottom ash concrete mixtures A_{100} and B_{100} displayed almost equal decrease in modulus of elasticity with respect to modulus of elasticity of respective control concrete mixtures. At 365 days of curing age, decrease in modulus of elasticity of bottom ash concrete mixtures over that of control concrete ranged between 3.85% to 13.9% for concrete 'A' and 1.14% to 12% for concrete 'B'. Control concrete of concrete 'A' contained 55% coarse aggregate as compared to 56.6% coarse aggregate in control concrete of concrete 'B'. Higher quantity of coarse aggregate in bottom ash concrete mixtures of concrete 'B' may be the reason for lower decrease in modulus of elasticity than that in bottom ash concrete mixtures of concrete 'A'.

4.5.7 Sorptivity

Comparison of effect of coal bottom ash on sorptivity of water of bottom ash concrete mixtures of concrete 'A' and concrete 'B' is illustrated in Fig. 4.130. Coal bottom ash displayed similar effect on total sorptivity of water of both concretes 'A' and 'B'. Increase in sorptivity of water of bottom ash concrete mixtures over that of control concrete varied between 6.03 and 38.79% for concrete 'A' and between 6.7 and 36.03% for concrete 'B' depending upon the coal bottom ash content. The increase in sorptivity of water of bottom ash concrete mixtures was almost linear with the increase in coal bottom ash content for both concretes 'A' and 'B'. Bottom ash concrete mixtures containing 100% coal bottom ash as fine aggregate in both concretes 'A' and 'B' displayed highest sorptivity of water. Initial rate of absorption of water of bottom ash concrete mixtures increased from 13×10^{-4} to 19×10^{-4} mm/√s for concrete 'A' and from 6×10^{-4} to 9×10^{-4} mm/√s for concrete 'B' on incorporation of 100% coal bottom ash as fine aggregate. However, for both concretes 'A' and 'B', the secondary rate of absorption of water were 2×10^{-4} mm/√s for all bottom ash concrete and control concrete mixtures. The absorption of more water at a faster rate by the porous particles of coal bottom ash and the rise of more water through higher number of capillary voids may be the possible explanation for higher initial water sorptivity of bottom ash concrete mixtures. These results are in line with water absorption results.

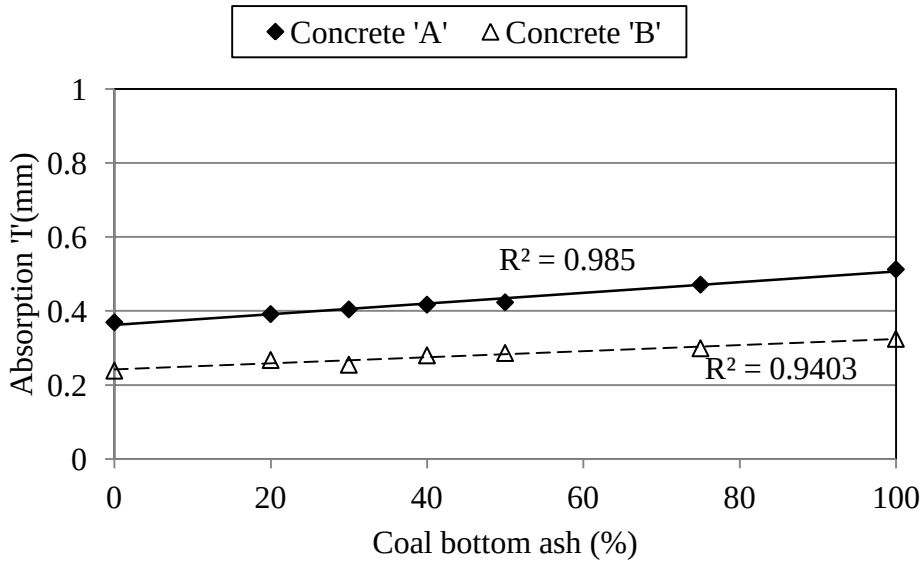

Fig. 4.130: Sorptivity variation versus coal bottom ash content in concrete

4.5.8 Abrasion Resistance

Variation in abrasion resistance of bottom ash concrete mixtures of concrete 'A' and concrete 'B' evaluated on the basis of percentage increase/decrease over that of control concrete is illustrated in Fig. 4.131. At 28 days of curing age, increase in average depth of wear of bottom ash concrete mixtures over that of control concrete varied between 10.03 and 42.59% for concrete 'A' and between 7.39 and 82.66% for concrete 'B' depending upon the coal bottom ash content. Depth of wear increased with increase in coal bottom ash content in concrete mixtures of both concrete 'A' and 'B'. Low compressive strength of bottom ash concrete mixture B_{100} may be the possible explanation for higher wear depth than that of control concrete. Bottom ash concrete mixtures of both concretes 'A' and 'B' demonstrated lower depth of wear with age. At 90 days of curing age, increase in average depth of wear of bottom ash concrete mixtures varied between 4.24 and 31.64% for concrete 'A' and between 10.26 and 43.88% for concrete 'B'. Densification of matrix due to continuous hydration and pozzolanic activity of coal bottom ash is the reason for lower wear depth with age. At 365 day of curing age, compressive strength of bottom ash concrete mixtures of both concretes 'A' and 'B' containing 75 and 100% coal bottom ash was almost identical and as such, they displayed almost similar abrasion resistance. It shows that abrasion resistance is closely related to compressive strength of bottom ash concrete. Average depth of wear after 15 min of wear time of bottom ash concrete mixture reduced from 1.14 mm at 28 days to 0.7 mm at 365 days for A_{100} and from 1.23 mm at 28 days to 0.722 mm at 365 days for B_{100}. Bottom ash concrete mixture containing 50% coal

bottom ash was worse by 27.52% for concrete ‘A’ and 39.05% for concrete ‘B’ at 28 days; 16.57% for concrete ‘A’ and 25.52% for concrete ‘B’ at 90 days; and 20.96% for concrete ‘A’ and 10.08% for concrete ‘B’ at 365 days than control concrete. However, the depth of wear of all bottom ash concrete mixtures after 7.5 min of wear time was much less than 2 mm specified in Indian Standard BIS: 1237 -2012 for heavy duty tiles.

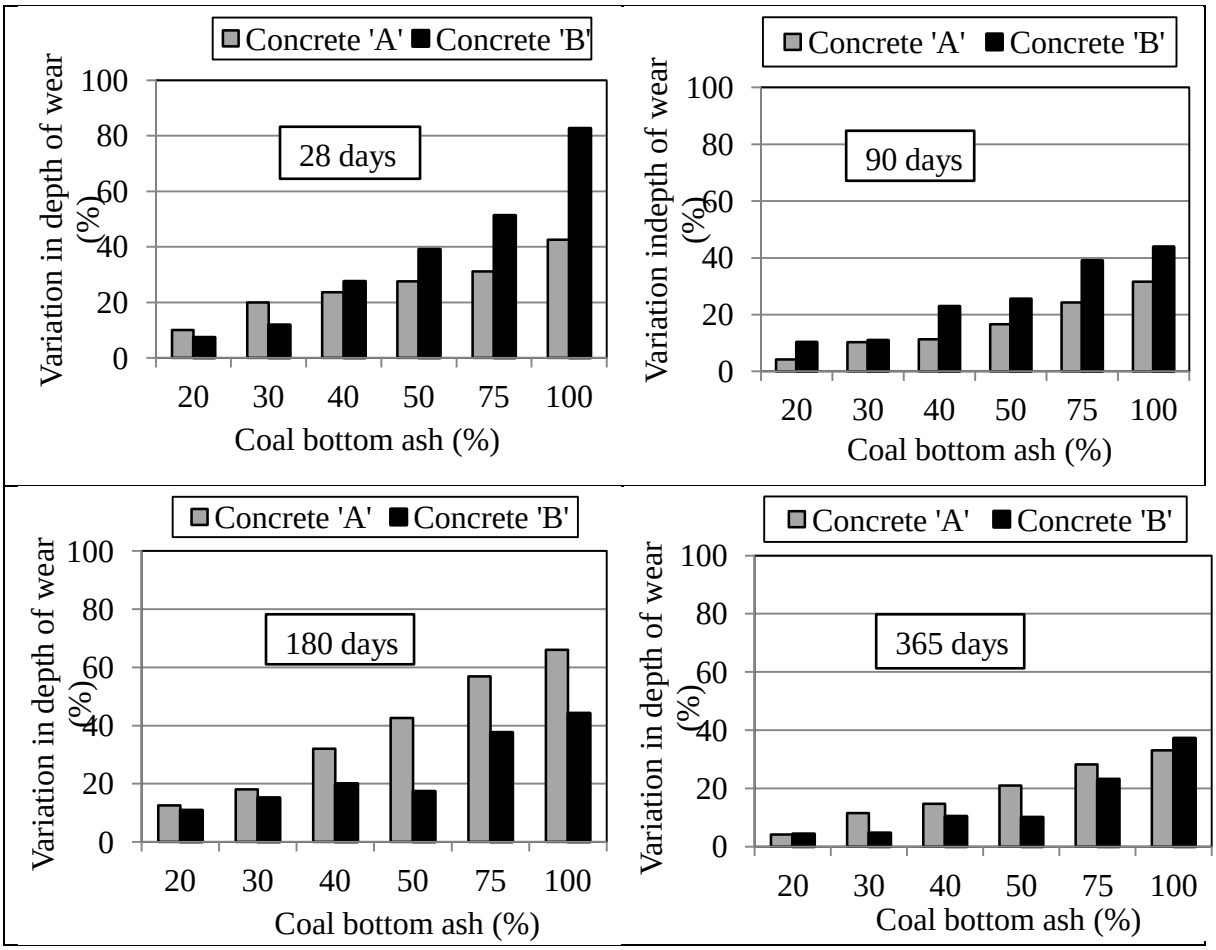

Fig. 4.131: Abrasion resistance variation versus coal bottom ash content in concrete

4.5.9 Acid Resistance

Effect of coal bottom ash on resistance to external acid attack of bottom ash concrete mixtures of concrete ‘A’ and concrete ‘B’ evaluated in terms of variation in loss of weight and compressive strength is illustrated in Fig. 4.132 and Fig.4.133, respectively. After 84 days of immersion in 3% sulphuric acid solution, mass loss of bottom ash concrete mixtures of concrete ‘A’ varied between 11.65% and 12.59 % against 13.01% mass loss of control concrete. For bottom ash concrete mixtures of concrete ‘B’, during the same period mass loss was between 5.76 and 6.57% as compared to 5.56% mass loss of control concrete.

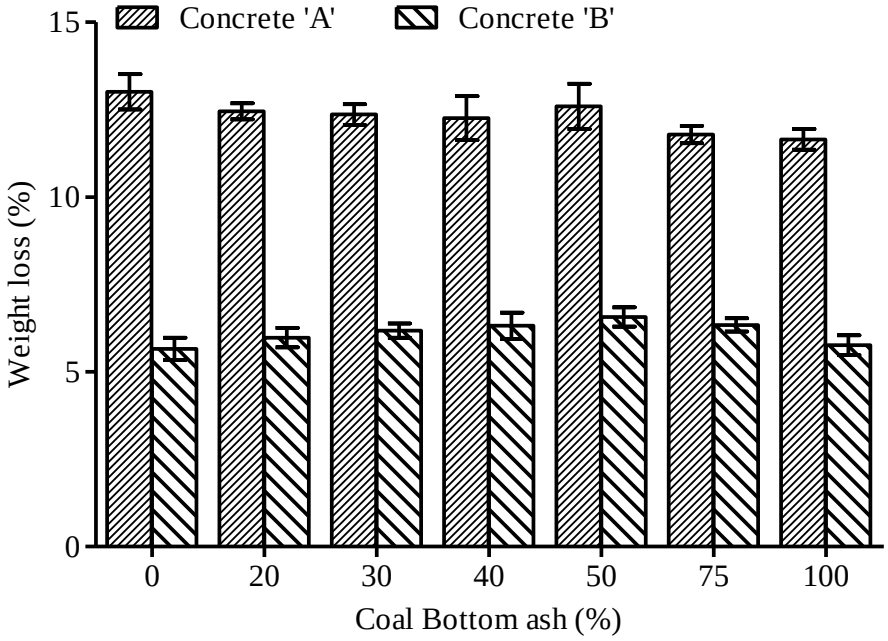

Fig. 4.132: Weight loss variation under acid attack after 84 days versus coal bottom ash in concrete

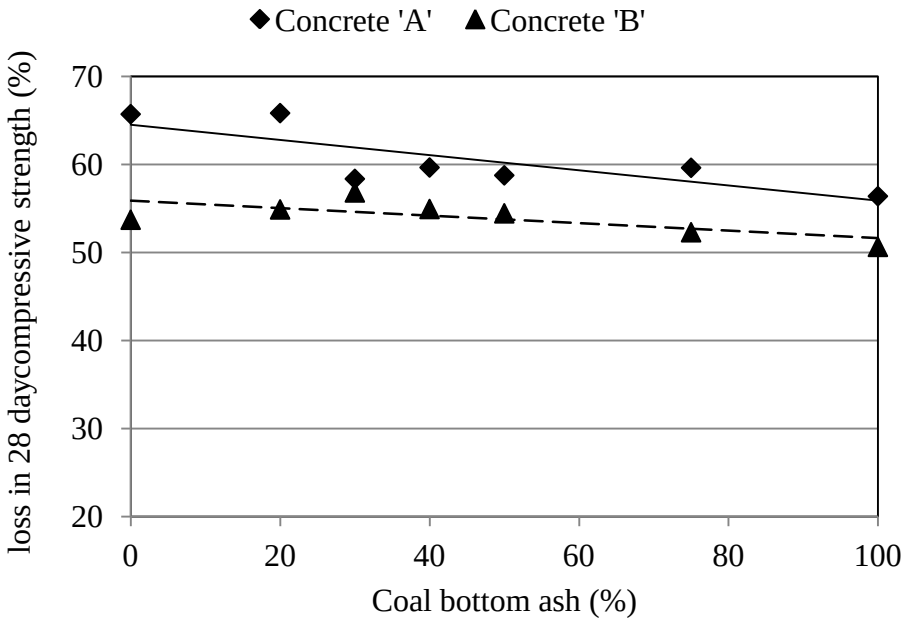

Fig. 4.133: Variation in loss in 28-day compressive strength of bottom ash concrete mixtures after 84 days of immersion in 3% sulphuric acid solution

However, bottom ash concrete mixture of both concretes ‘A’ and ‘B’ containing 50% coal bottom ash displayed higher weight loss as compared to other bottom ash concrete mixtures. Mass loss of bottom ash concrete mixtures over that of control concrete varied between -3.23 and -10.45% for concrete ‘A’ and between 1.77 and 16.08% for concrete

'B'. At the end of test, the loss in 28-day compressive strength of bottom ash concrete mixtures of concrete 'A' was 56.40 and 65.84% as compared to 65.72% of control concrete. For concrete 'B', loss in 28-day compressive strength of bottom ash concrete mixtures was between 50.65 and 56.83% in comparison to 53.72% loss in 28-day compressive strength of control concrete. Loss in 28-day compressive strength decreased with increase in coal bottom ash content in concrete for both concretes 'A' and 'B'.

4.5.10 Sulfate Resistance

Comparison of effect of coal bottom ash on resistance to external sulfate attack of bottom ash concrete mixtures of concrete 'A' and concrete 'B' evaluated in terms of variation in expansion and compressive strength over that of respective control concrete is illustrated in Figs.4.134 to 4.136. After 365 days of immersion in 10% magnesium sulfate solution, total expansion of control concrete mixtures of concrete 'A' and concrete 'B' was 333.33 $x10^{-6}$ and 410 x 10^{-6}, respectively. The increase in expansion values of bottom ash concrete mixtures over that of control concrete varied between 5.01 and 31.02% for concrete 'A' and between 2.44 and 10.57% for concrete 'B'. Total expansion of bottom ash concrete mixtures of both concretes 'A' and 'B' containing 100% coal bottom ash as fine aggregate was almost identical. Increase in percentage of expansion of bottom ash concrete mixtures of both concretes 'A' and 'B' over that of respective control concrete was almost linear with the increase in coal bottom ash content.

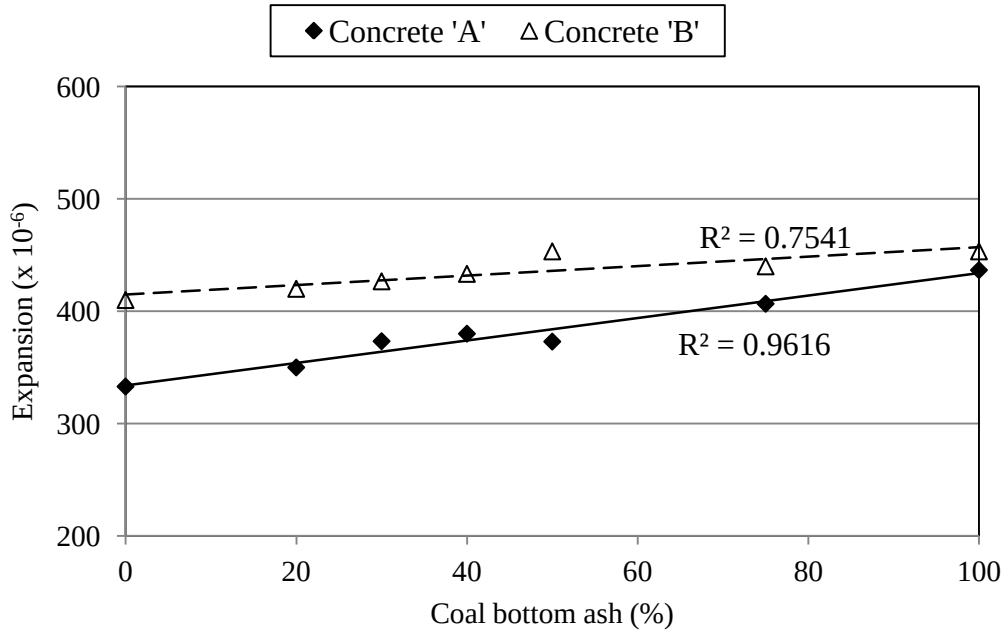

Fig. 4.134: Expansion variations under sulfate attack versus coal bottom ash in concrete

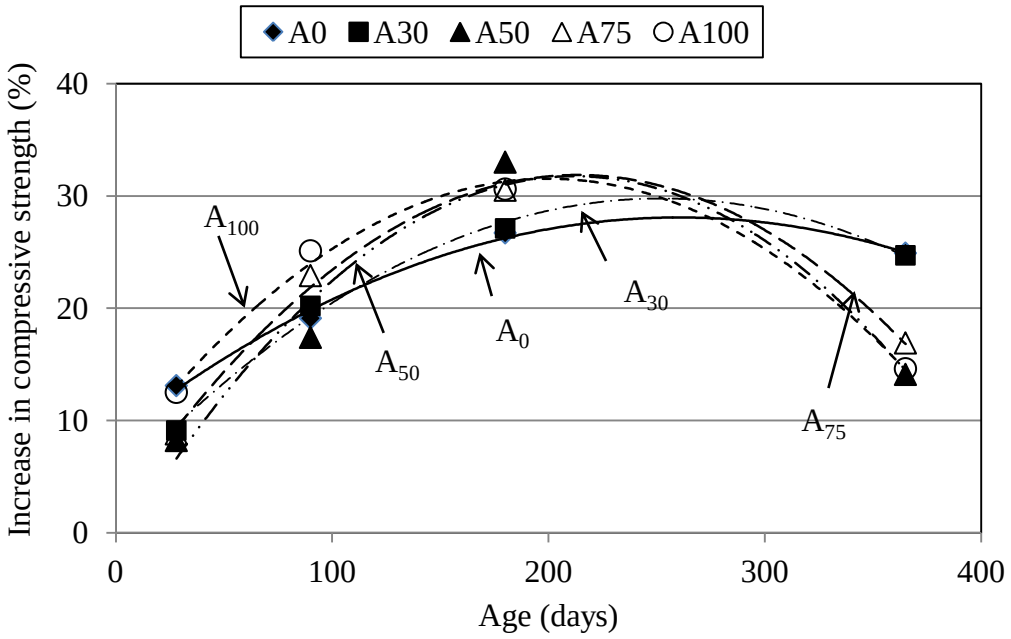

Fig. 4.135: Compressive strength of bottom ash concrete under sulfate attack (Concrete 'A')

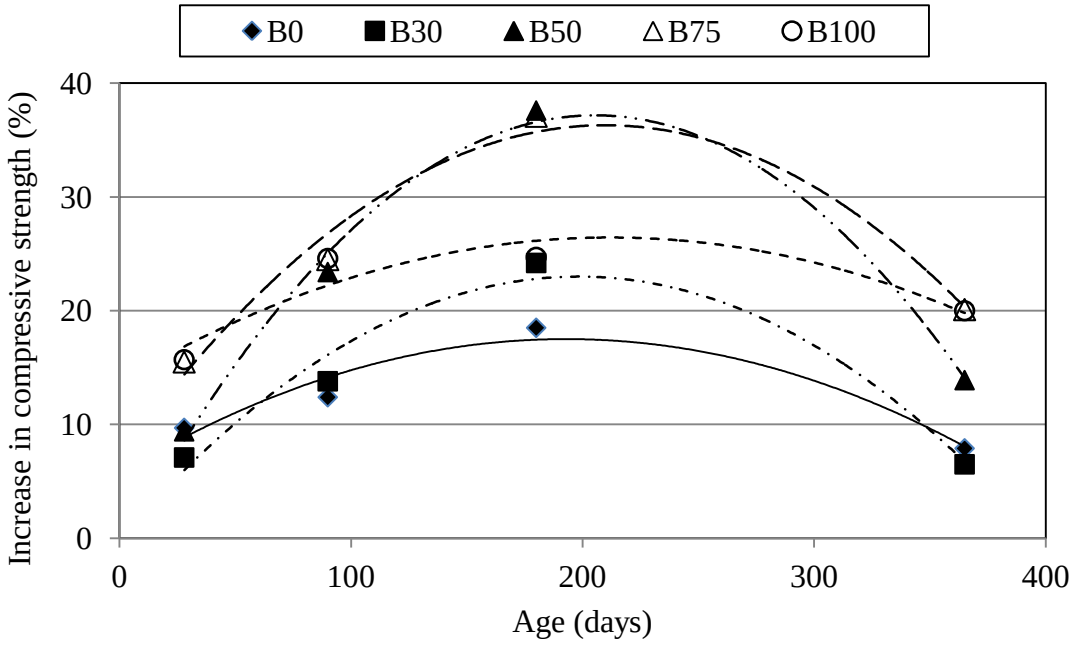

Fig. 4.136: Compressive strength of bottom ash concrete under sulfate attack (Concrete 'B')

For concrete 'A', after 365 days of immersion period, mass loss decreased from 0.72 to 0.24% on incorporation of 100% coal bottom ash in concrete. During the same period,

mass loss of bottom ash concrete mixture of concrete B containing 100% coal bottom ash was 0.36% as compared to 0.30% of control concrete. At the end of test, bottom ash concrete mixtures of both concretes 'A' and 'B' displayed higher compressive strength than their 28 day compressive strength. At 365 days of immersion period, the increase in compressive strength over 28-day compressive strength of bottom ash concrete mixtures of concrete 'A' containing 50, 75 and 100% coal bottom ash was 14.1, 16.8 and 14.6%, respectively, For concrete 'B', after 365 days of immersion increase over 28-day compressive strength of bottom ash concrete mixtures containing 50, 75 and 100% coal bottom ash was 13.9, 20.1 and 23.8%, respectively. Bottom ash concrete mixtures of both concretes 'A' and 'B' showed maximum increase in compressive strength up to 180 days of immersion period. Thereafter decrease in compressive strength started decreasing.

4.5.11 **Drying Shrinkag**e

Effect of coal bottom ash on drying shrinkage of bottom ash concrete mixtures of concrete 'A' and concrete 'B' evaluated in terms of variation in length change is illustrated in Fig. 4.137. Concrete mixtures made coal bottom ash as replacement of sands of both concretes 'A' and 'B' displayed better dimensional stability as compared to respective control concretes. Drying shrinkage of bottom ash concrete mixtures of both concretes 'A' and 'B' decreased with increase in coal bottom ash content. At 90 days of drying period, shrinkage for bottom ash concrete mixtures containing 50, 75, and 100% coal bottom ash was 366.67 x 10^{-6}, 320 x 10^{-6} and 300 x 10^{-6}, respectively, for concrete 'A' and was 466.67 x 10^{-6}, 413.33 x 10^{-6} and 400 x 10^{-6}, respectively, for concrete 'B'. At 270 days, drying shrinkage of these bottom ash concrete mixtures increased to 426.67 x 10^{-6}, 366.67 x 10^{-6} and 360 x 10^{-6}, respectively, for concrete 'A' and to 600 x 10^{-6}, 566.67 x 10^{-6} and 560 x 10^{-6}, respectively, for concrete 'B'. Shrinkage of control concrete mixtures during this period was 533.33 x 10^{-6} for concrete 'A' and 666.67 x 10^{-6} for concrete 'B'. Decrease in drying shrinkage of bottom ash concrete mixtures over that of control concrete varied between 11.25% and 32.5% for concrete 'A' and between 3% and 16% for concrete 'B'. Higher water cement ratio may be attributed to higher drying shrinkage of control concrete of concrete 'B'. As shown in Fig. 4.137, the trend of decrease in drying shrinkage was similar in bottom ash concrete mixtures of both concretes 'A' and 'B'. It is believed that water absorbed by coal bottom ash internally during mixing process helped in reducing the drying shrinkage of concrete mixtures made with coal bottom ash as fine aggregate.

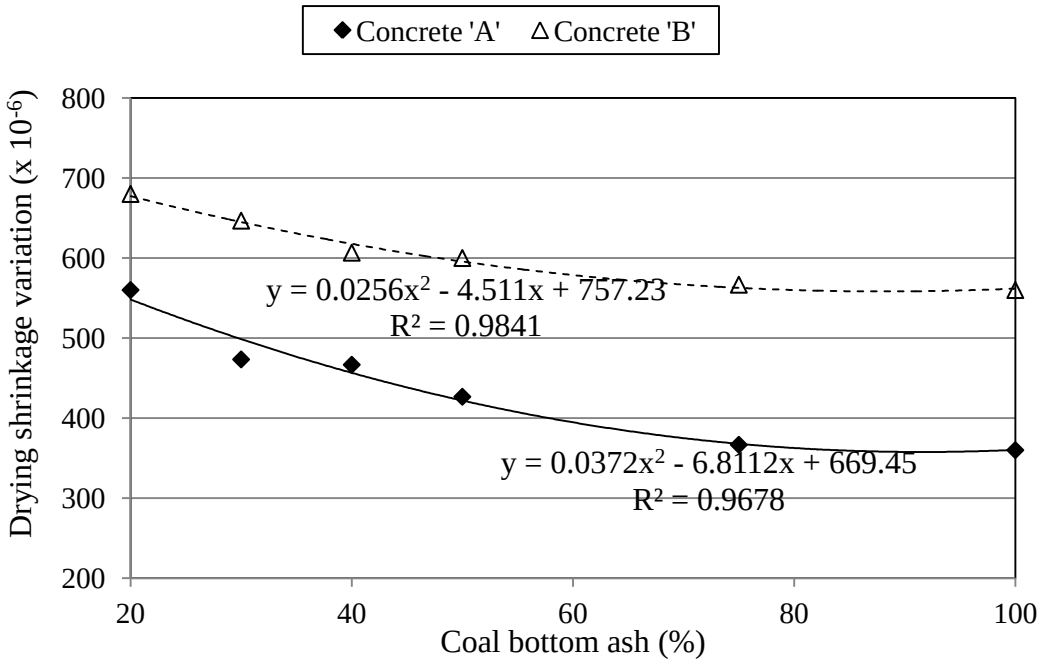

Fig. 4.137: Drying shrinkage variation versus coal bottom ash in concrete

4.5.12 Pulse Velocity

Effect of coal bottom ash on pulse velocity through bottom ash concrete mixtures of concrete 'A' and concrete 'B' evaluated on the basis of percentage increase/decrease over that of respective control concrete is illustrated in Fig. 4.138. At 28 days of curing age, variation in pulse velocity through bottom ash concrete mixtures of concrete 'A' over that of control concrete was between 1% and -1.27%, whereas for concrete 'B', the pulse velocity through bottom ash concrete mixtures varied between -1.83% and -5.71%. Pulse velocity of bottom ash concrete mixtures increased with age but decreased with increase in coal bottom ash content. Comparing the pulse velocity of bottom ash concrete mixtures obtained in this study with those given in BIS 13311–1997, the quality of concrete made with coal bottom ash as fine aggregate can be graded as good. At 365 days of curing age, decrease in pulse velocity through bottom ash concrete mixtures on incorporation of coal bottom ash was between 0.44 and 1.15% for concrete 'A' and 1.67 and 6.21% for concrete 'B'. For both concretes 'A' and 'B', the variations in pulse velocities through bottom ash concrete mixtures and control concrete were not significant. The effect of coal bottom ash as fine aggregate in concrete on pulse velocity was similar in both concretes 'A' and 'B'.

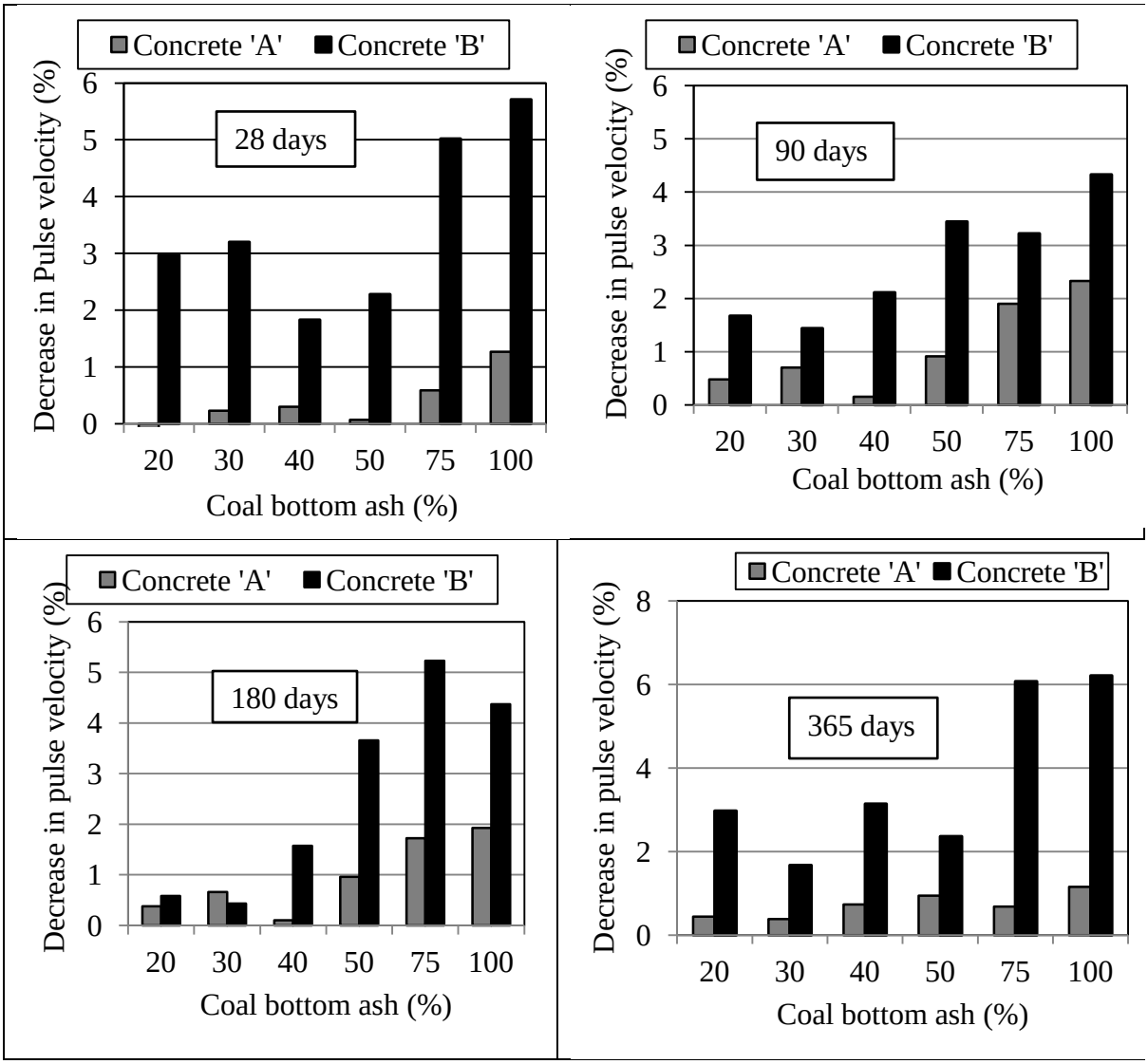

Fig. 4.138: Pulse velocity variation versus coal bottom ash content in concrete

4.5.13 Chloride Permeability

Effect of coal bottom ash on chloride permeability of bottom ash concrete mixtures of concrete ‘A’ and concrete ‘B’ evaluated in terms of variation of charge passed over that of control concrete is illustrated in Fig. 4.139. At 28 days of curing age, bottom ash mixtures of concrete ‘A’ displayed lower chloride permeability than the control concrete. Percentage variation of total charge passed through bottom ash concrete specimens with respect to control concrete varied between -8.30 and -16.91%. For concrete ‘B’, percentage variation of total charge passed through bottom ash concrete over that of control concrete was between -10.06 and 15.64%. Total charge passed through all bottom ash concrete mixtures except concrete mixture containing 100% coal bottom ash were more than that through control concrete. With age, the resistance to chloride ion penetration increased with the

increase in coal bottom ash content in bottom ash concrete mixtures of both concretes ‘A’ and ‘B’. It is evident from the test results that after 28 days curing age, compressive strength and resistance to chloride ion penetration increased significantly due to pozzolanic action of coal bottom ash. Total charge passed through bottom ash concrete mixtures containing 100% coal bottom ash as fine aggregate was lower by 28.69% at 90 days, 64.14% at 180 days and 54.37% at 365 days than that through control concrete for concrete ‘A’ and was lower by 21.44% at 90 days, 70.03% at 180 days and 60.73% at 365 days than that through control concrete for concrete ‘B’. Bottom ash concrete mixtures of both concretes ‘A’ and ‘B’ showed identical resistance to chloride ion penetration.

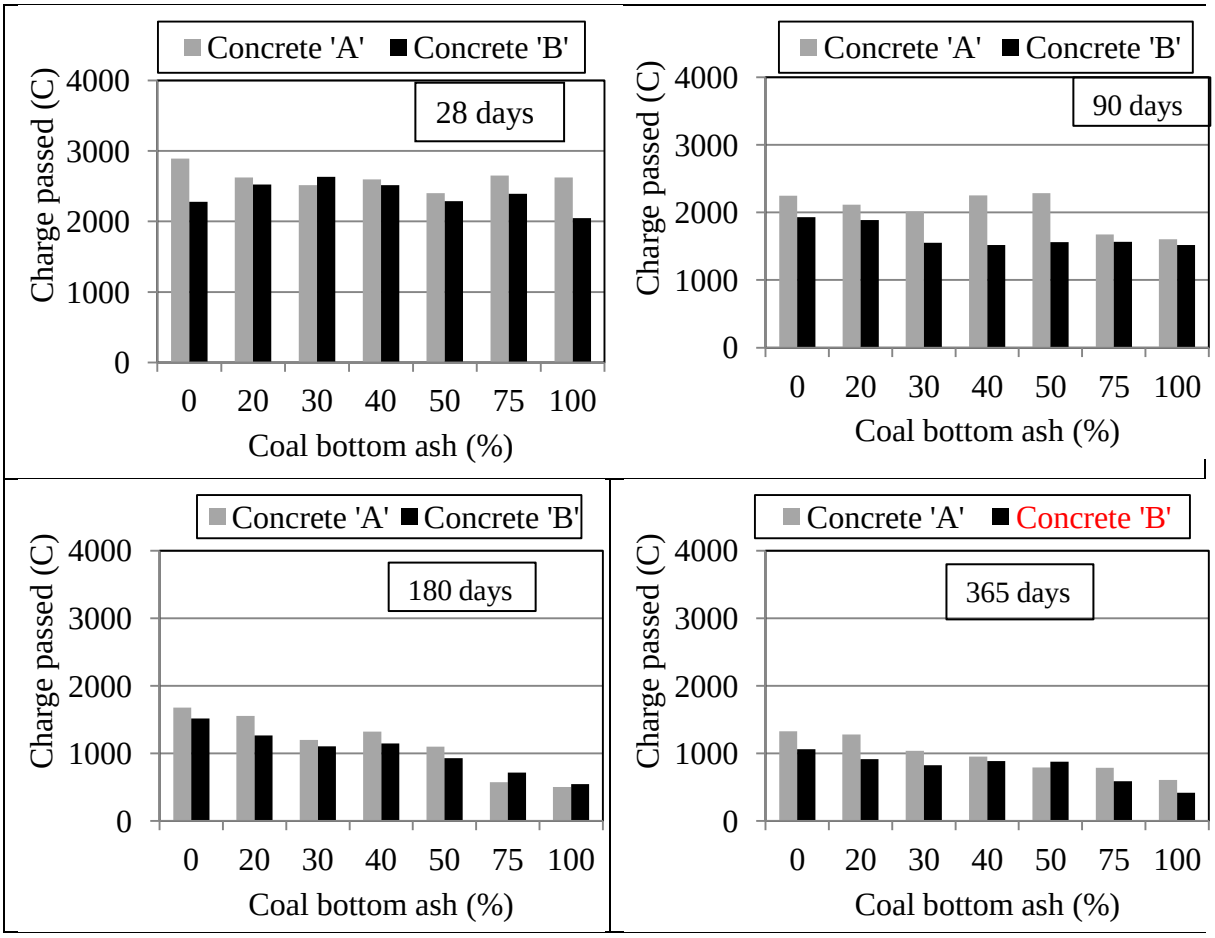

Fig. 4.139: Variations in charge passed versus coal bottom ash content in concrete

4.5.14 Permeable Pore Space

Fig 4.140 shows variation in permeable pore pace in bottom ash concrete mixtures of concrete ‘A’ and concrete ‘B’. Permeable pore space in bottom ash concrete mixtures of both concretes ‘A’ and ‘B’ increased on use of coal bottom ash as fine aggregate. On

incorporation of 100% coal bottom ash as fine aggregate in concrete, permeable pore space in bottom ash mixtures increased from 10.82 to 11.99% for concrete ‘A’ and from 10.39 to 11.58% for concrete ‘B’.

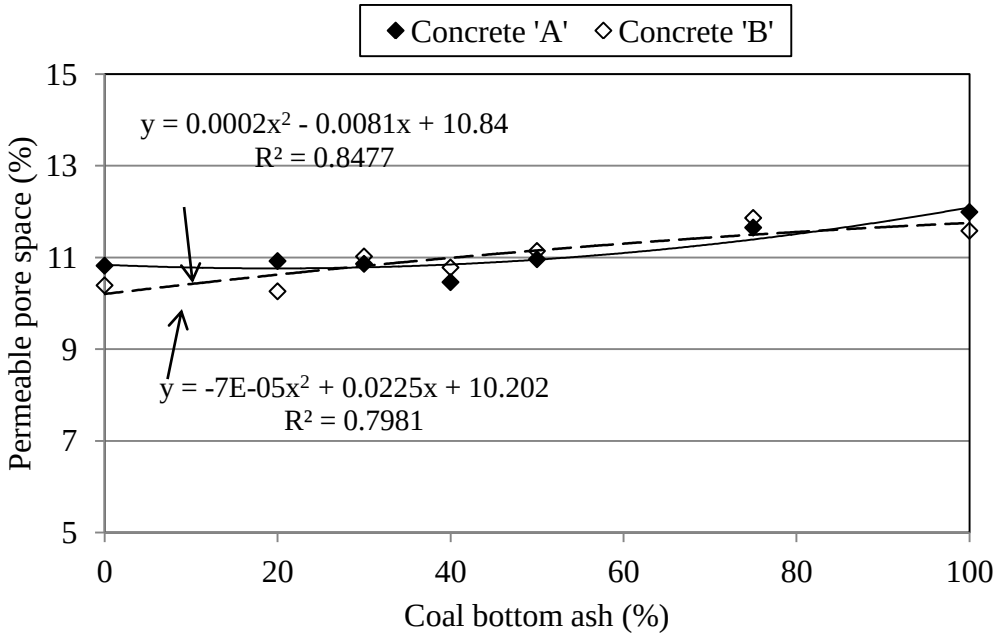

Fig. 4.140: Permeable pore space versus coal bottom ash in concrete

With age, permeable pore space in bottom ash concrete mixtures of both concretes ‘A’ and ‘B’ reduced significantly. The effect of coal bottom ash on permeable pore space in concrete was almost identical in both the mixes.

4.5.15 Water Absorption

Fig 4.141 shows variation in water absorption of bottom ash concrete mixtures of concrete ‘A’ and concrete ‘B’. Water absorption of bottom ash concrete mixtures of both concretes ‘A’ and ‘B’ increased on use of coal bottom ash as fine aggregate. On incorporation of 100% coal bottom ash as fine aggregate in concrete, water absorption of bottom ash mixtures increased from 4.68 to 5.56% for concrete ‘A’ and from 4.22 to 5.04% for concrete ‘B’. With age, water absorption of bottom ash concrete mixtures of both concretes ‘A’ and ‘B’ reduced significantly. The effect of coal bottom ash on water absorption of concrete was almost identical in both the mixes.

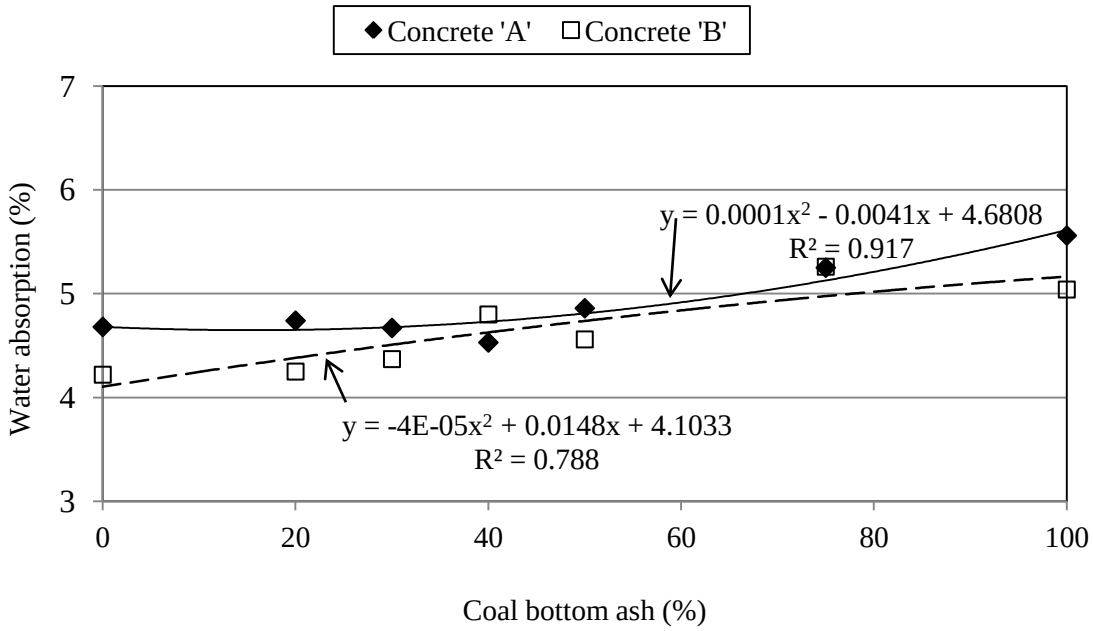

Fig. 4.141: Water absorption versus coal bottom ash in concrete

4.5.16 Statistical Analysis of Combined Results of Both Concretes

4.5.16.1 Relationship between compressive strength and splitting tensile strength

The relationship between compressive strength and splitting tensile strength of bottom ash concrete mixtures is shown in Fig 4.142 and Fig 4.143. The equation derived from the test results of this study and reported in published literature along with coefficient of determination is given in table 4.26.

The regression analysis performed showed strong relation between compressive strength and splitting tensile strength of bottom ash concrete. The higher values of coefficient of determination (R^2 = 0.96 and 0.98) verifies the goodness of fit of the regression line. The data which can not be explained by this equation is only 4% for concrete mixture containing 20 to 100% and 2% for concrete made with 100% coal bottom ash as fine aggregate. Also the probability value ($p < 0.0001$) shows high significance of the regression model. It is found that splitting tensile strength of concrete containing 20 to 100 and 100% coal bottom ash as fine aggregate followed a power relationship with the compressive strength.

Table 4.26 Compressive strength and splitting tensile strength relationships

Report	Equation	Coefficients of determination (R^2)	Remarks
Author's	$ft = 0.1162\sigma^{0.8912}$	0.9571	For concrete containing 20 to 100% coal bottom ash as sand replacement
Author's	$ft = 0.1276\sigma^{0.8717}$	0.9840	For concrete containing 100% coal bottom ash as sand replacement
Kockal and Ozturan (2011)	$ft = 0.171\sigma^{0.8269}$	0.9781	for light weight and normal weight concrete in 28 and 56 days
Kockal and Ozturan (2011)	$ft = 0.1109\sigma^{0.9389}$	0.9912	for light weight concrete in 28 and 56 days
Khan and Lynsdale (2002)	$ft = 0.14\sigma^{0.85}$	0.95	
BS 8007	$ft = 0.12\sigma^{0.7}$	-	British Code of Practice

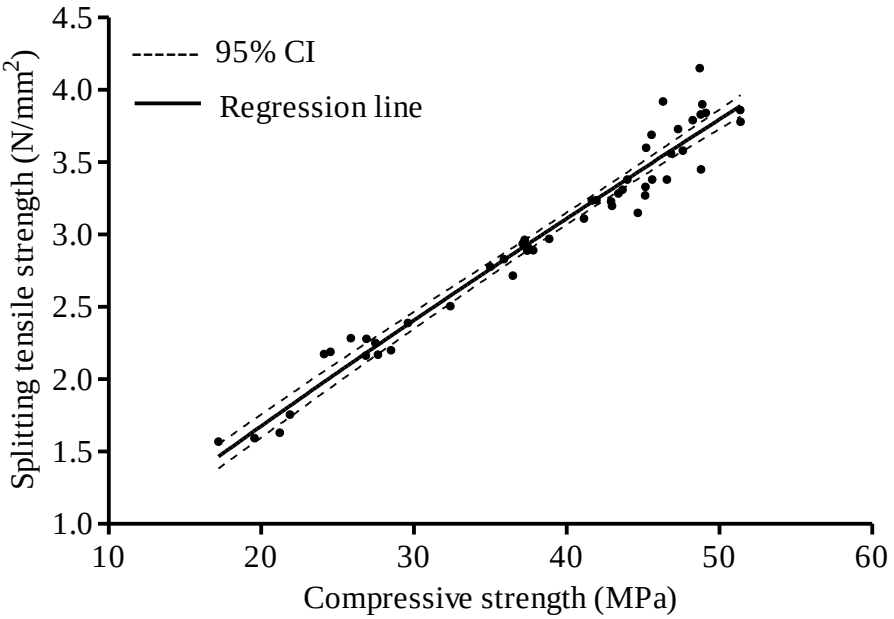

Fig 4.142: Relationship between compressive strength and splitting tensile strength of bottom ash concrete containing 20 to 100% coal bottom ash

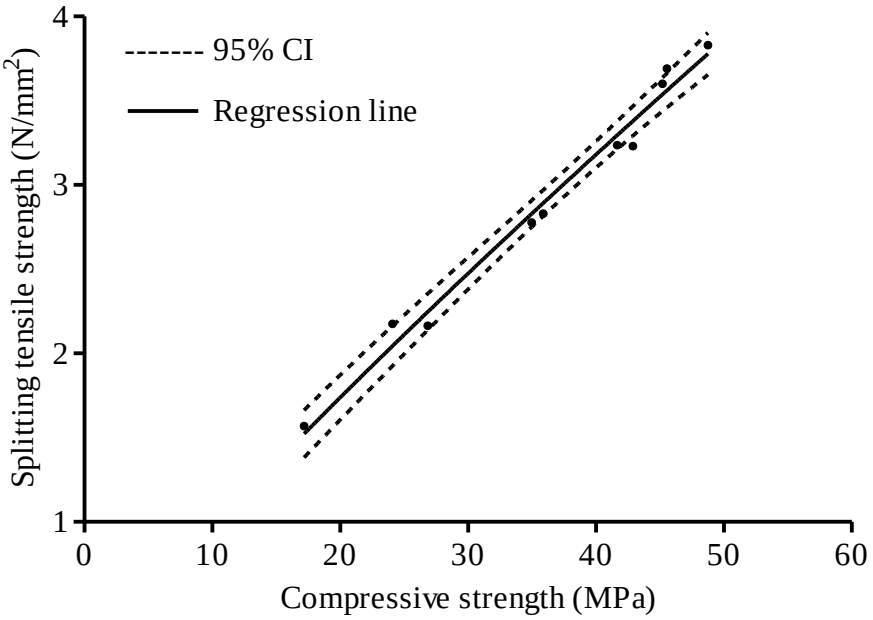

Fig 4.143: Relation between compressive strength and splitting tensile strength of concrete containing 100% coal bottom ash

4.5.16.2 Relationship between compressive strength, density and modulus of elasticity

Fig. 4.144 shows the relationship between compressive strength, dry bulk density and modulus of elasticity of concrete containing 20 to 100% coal bottom ash as fine aggregate, obtained from the present study. The equation together with the coefficients of determination R^2 derived is given below.

$E = 1.4541\ \rho^2\ \sigma^{0.33} + 2.0196$ $\quad R^2 = 0.7626$ (Author)

$E = 1.7\ \rho^2\ \sigma^{0.33}$ $\quad$ BS: 8110 (Part 2):1985

where,

σ = Cube compressive strength of concrete in N/mm^2

E = Modulus of elasticity of concrete in GPa

ρ = Dry bulk density of concrete in kg/m^3

Coefficient of correlation value (R = 0.87) indicates good relation between data and regression line. Coefficient of determination (R^2 = 0.763) shows that 76.3% data is explained by the derived relationship between compressive strength, density and modulus of elasticity of concrete. The remaining 23.7% data is not explained by the derived equation. It is found that modulus of elasticity of concrete containing 20 to 100% coal bottom ash as fine aggregate was almost directly proportional to the variable $\rho^2\ \sigma^{0.33}$, following a linear relationship.

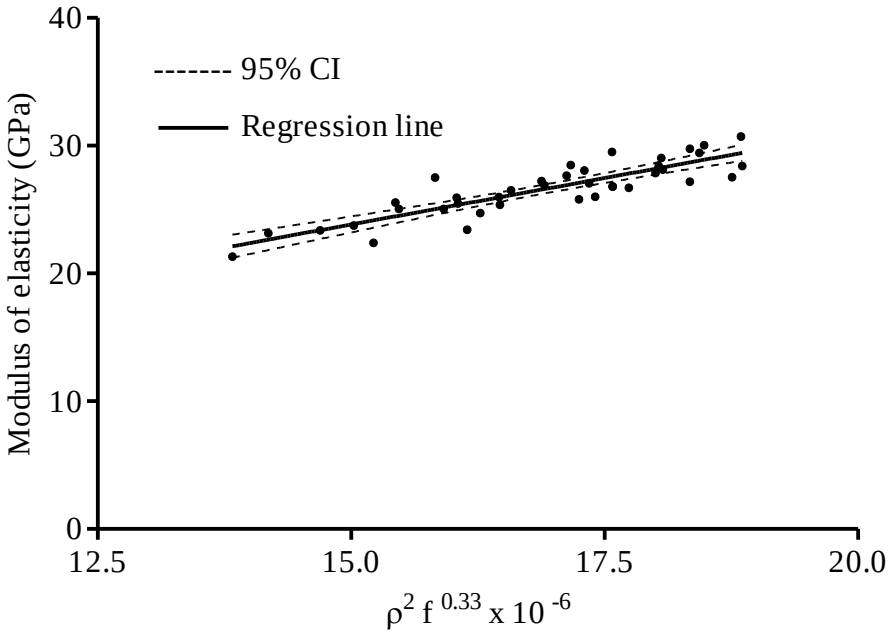

Fig 4.144: Relationship between compressive strength, density and modulus of elasticity of bottom ash concrete

4.5.16.3 Relationship between compressive strength and modulus of elasticity

The relationship between compressive strength and modulus of elasticity of concrete derived from the test results is shown in Fig. 4.145. The equations along with coefficient of determination (R^2) for bottom ash concrete containing 20 to 100% and 100% coal bottom ash as fine aggregate are given as under:

For concrete containing 20 to 100% coal bottom ash as replacement of sand

$E = 7.027\rho^{0.3568}$ $R^2 = 0.5333$ (Author)

For concrete containing 100% coal bottom ash as replacement of sand

$E = 5.594\rho^{0.3958}$ $R^2 = 0.7959$ (Author)

Lower value of coefficient of determination ($R^2 = 0.5333$) for concrete containing 20 to 100% coal bottom ash as partial or total replacement of sand indicates that 53.33% data around the regression line is explained by the equation and 46.67% data remained unexplained. As such, for concrete containing 20 to 100% coal bottom ash as replacement of sand, no clear relationship could be established between the compressive strength and modulus of elasticity. However, for concrete containing 100% coal bottom ash as replacement of sand, higher value of coefficient of determination ($R^2 = 0.796$) indicate that modulus of elasticity of concrete followed power relationship with compressive strength.

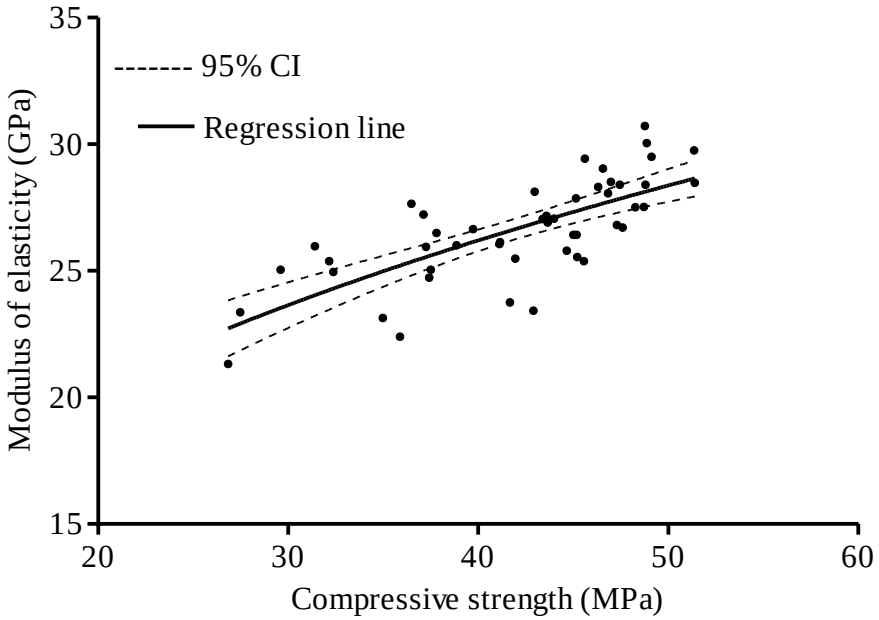

Fig.4.145 Relationship between compressive strength and modulus of elasticity of concrete containing 20 to 100% coal bottom ash

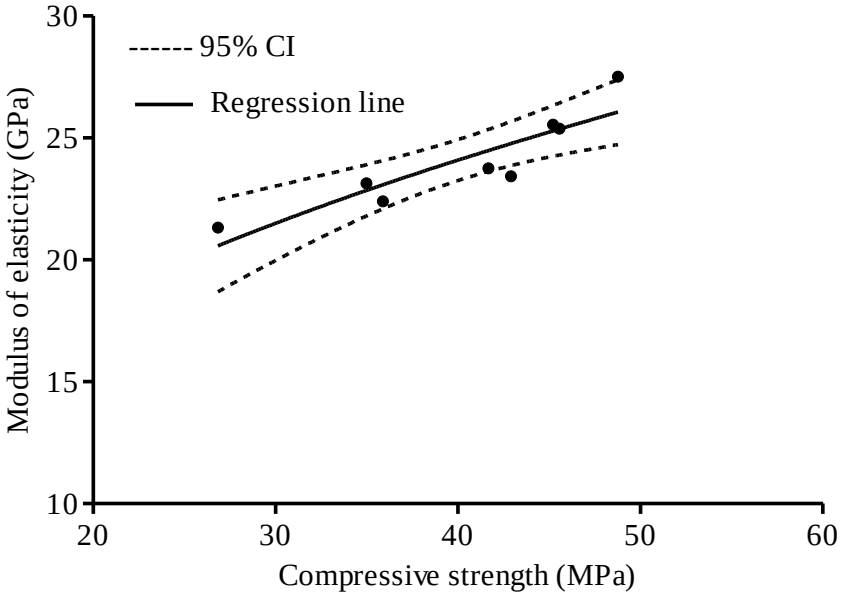

Fig.4.146 Relationship between compressive strength and modulus of elasticity of concrete containing 100% coal bottom ash

The similar equations for relationship between compressive strength and modulus of elasticity of light weight and normal weight concrete reported in the published literature are given as under:

For light weight concrete

$E = 0.6258\sigma^{0.9185}$ $R^2 = 0.9114$ (Kockal and Ozturan, 2011)

For light weight and normal weight concrete

$E = 0.1155\sigma^{1.3558}$ $R^2 = 0.8237$ (Kockal and Ozturan, 2011)

$E = 22\ [\sigma /10]^{0.3}$ (BS EN 1992-1-1)

where,

σ = Cube compressive strength of concrete in N/mm^2

E = Modulus of elasticity of concrete in GPa

4.5.16.4 Relationship between compressive strength and pulse velocity

The relationship between compressive strength and pulse velocity of concrete made with coal bottom ash as partial or total replacement of sand is shown in Fig. 4.147. The equation obtained from this study and those reported in literature are given as under:

$\sigma = 1.024 \exp(0.8222V)$ $R^2 = 0.8588$ (Author)

Similar equations reported in published literature for normal concrete and rice husk ash concrete are given as under:

$\sigma = 1.146 \exp(0.77V)$ $R^2 = 0.80$ (Turgut, 2004)

$\sigma = 1.19 \exp(0.715V)$ $R^2 = 0.59$ (Nash't et al., 2005)

$\sigma = 13.49V - 30.30$ $R^2 = 0.681$ for rice husk ash concrete (Umoh, 2012)

where

σ = compressive strength of concrete in N/mm^2

V = Pulse velocity through concrete in km/s

The regression analysis performed show strong relation between compressive strength and pulse velocity values. Concrete being a heterogeneous material, it is believed that coefficient of determination more than 0.7 indicates the strong relationship and more than 0.9 shows excellent relation between independent and dependent variables (Yang et al., 2015; Al-Amoudi et al., 2009; Mačiulaitis and Malaiškien, 2009; and Ghrieb et al., 2014). In the present case, coefficient of correlation value (R= 0.93) and very narrow 95% confidence band, indicate the strong relation between the regression line and the data. The coefficient of determination value (R^2 = 0.8588) means that 85.88% data around the

regression line is explained by the equation and 14.12% residual data remains unexplained. It is found that increase in compressive strength of concrete containing 20 to 100% coal bottom ash as fine aggregate increased exponentially with the increase in pulse velocity, following exponential relationship.

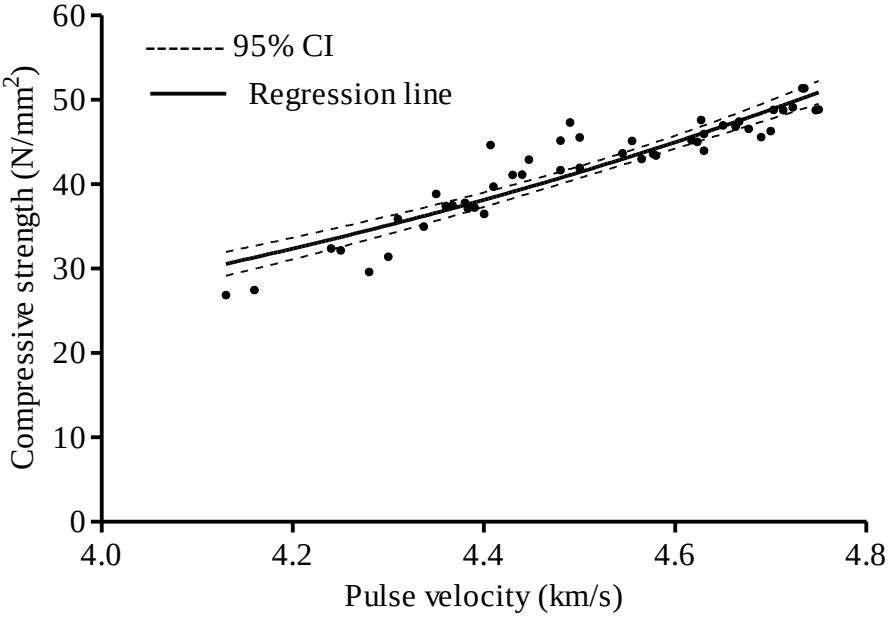

Fig 4.147: Relation between pulse velocity and compressive strength of bottom ash concrete

4.5.16.5 Relationship between compressive strength and wear depth

The relationship between compressive strength and depth of wear under abrasion obtained from the test results is shown in Fig. 4.148. Coefficient of correlation value (R = 0.79) and narrow 95% confidence band shows good relation between the data and regression line. Statistical analysis of data indicates that compressive strength has significant effect on the depth of wear under abrasion. The relation obtained between compressive strength and wear depth shows that 62% data is explained by the equation and 38% data remained unexplained. As such, no clear relationship could be established between compressive strength and depth of wear of concrete containing 20 to 100% coal bottom ash as fine aggregate.

For concrete containing 20 to 100% coal bottom ash as fine aggregate

$d = -0.0219\sigma + 1.7284$ $R^2 = 0.6204$ (R = 0.79) for 15 min abrasion (Author)

Similar equations reported in published literatures for fly ash concrete are given as under:

$d = -0.03951\sigma + 4.0444$ $R^2 = 0.6724$ (R = 0.82) for 60 min abrasion (Naik et al., 1995)

d = -1.5992Ln(x) + 7.7283 R^2 = 0.9044 (R = 0.97) for 60 min abrasion (Siddique, 2010)

where

d = Average depth of wear in mm

σ = Compressive strength of concrete in N/mm^2

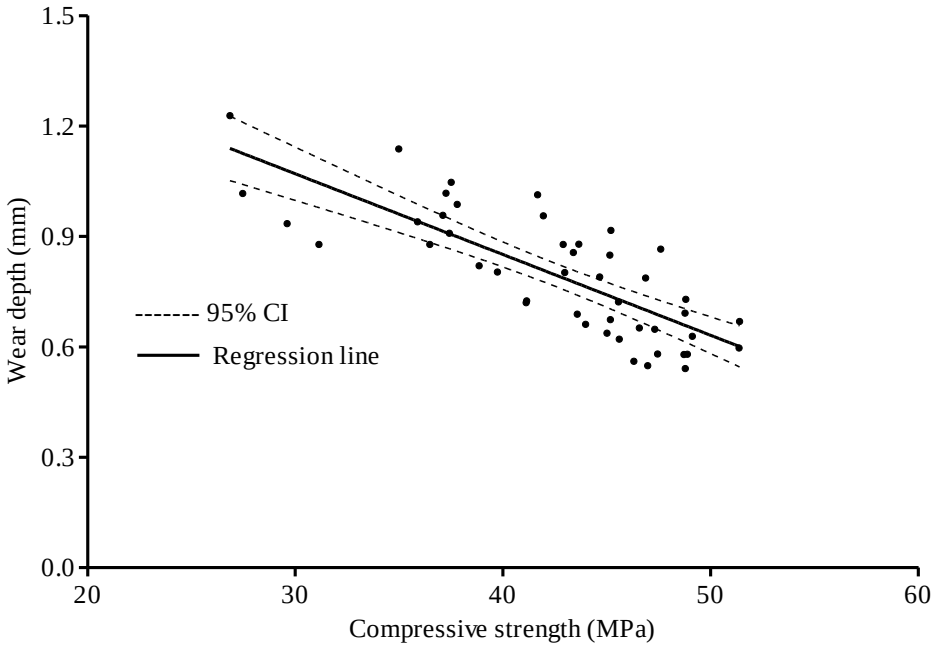

Fig 4.148: Relation between compressive strength and abrasion resistance of bottom ash concrete

4.5.16.6 Relation between weight loss and loss in 28-day compressive strength of bottom ash concrete after external sulphuric acid attack

The relationship between reduction in 28-day compressive strength of concrete specimens and their weight loss due to immersion in 3% sulphuric acid solutions is shown in Fig. 4.150. The equation along with coefficient of determination (R^2) derived from the test data is given as under:

Δσ = 4.088Δm + 10.64 R^2 = 0.8224 (Author)

Hewayde et al., 2007 reported that the decline in compressive strength of concrete specimens subjected to H_2SO_4 attack was directly proportional to their mass loss, following a linear relationship. The equation proposed by them is given as under:

Δσ = 2.3352Δm + 7.2081 R^2 = 0.92 (Hewayde et al., 2007)

where

Δσ = percentage loss in 28-day compressive strength of concrete

Δm = percentage loss in mass of concrete specimen

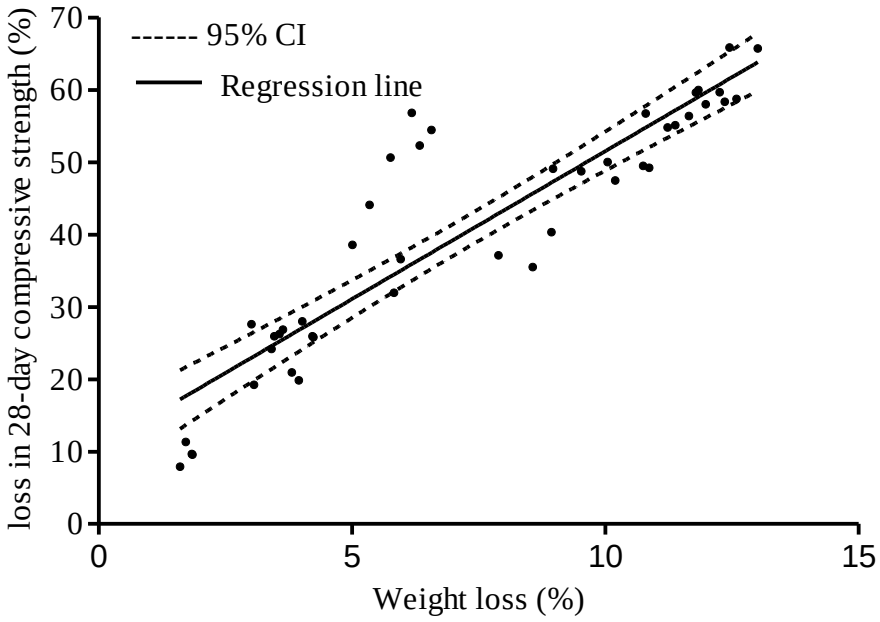

Fig 4.149: Relation between weight loss and loss in 28-day compressive strength of bottom ash concrete after external sulphuric acid attack

The higher value of coefficient of determination R^2 indicates the good relevance between the data points and the regression curve. The loss in compressive strength increased approximately linearly with the increase in mass loss of concrete specimens. The linear regression line obtained in the present study suggests that percentage loss in 28-day compressive strength of bottom ash concrete mixtures is approximately 4.088 times the percentage loss in their mass.

4.5.16.7 Relationship between chloride permeability and pulse velocity

The relationship between pulse velocity and chloride permeability of bottom ash concrete containing 20 to 100% coal bottom ash as fine aggregate, derived from the test results of the present study is presented in Fig 4.151. The equations expressing the relationship between chloride permeability (total charge passed through bottom ash concrete specimens) and the pulse velocity of longitudinal waves V, together with the coefficients of determination R^2 derived for concrete containing 20 to 100% and 100% coal bottom ash are given below.

For concrete containing 20 to 100% coal bottom ash

$Q = -2910\ V + 14620 \qquad R^2 = 0.4584$

For concrete containing 100% coal bottom ash

Q = -3419 V +16380 $R^2 = 0.6303$

where

Q = Total charge passed through the specimen in Coulombs

V = Pulse velocity through concrete in km/s

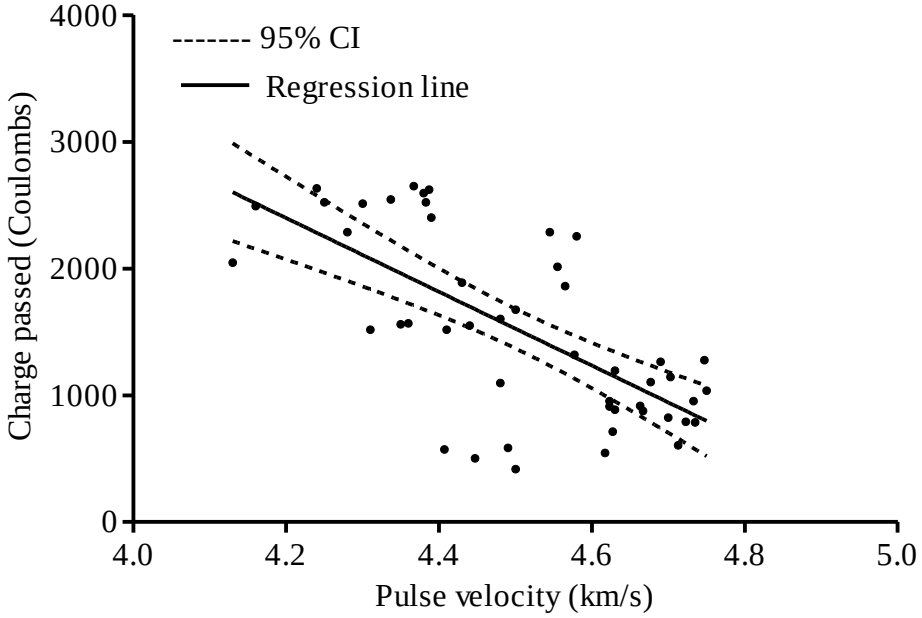

Fig. 4.150: Relationship between pulse velocity and charge passed through concrete containing 20 to 100% coal bottom ash

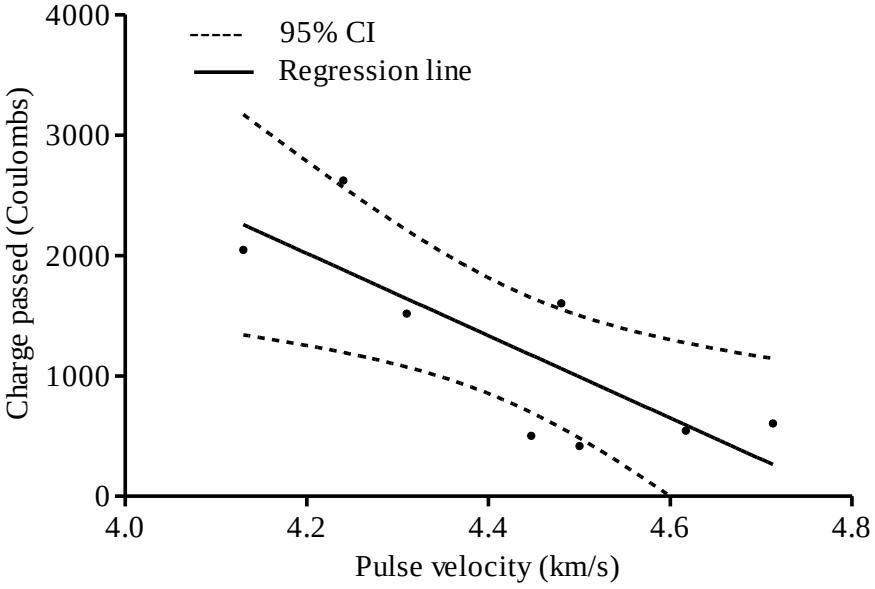

Fig. 4.151: Relationship between pulse velocity and charge passed through concrete containing 20 to 100% coal bottom ash

For concrete containing 20 to 100% coal bottom ash, lower value of coefficient of determination (R^2=0.46) indicate that no clear relationship could be established between charges passed and pulse velocity through concrete. For concrete containing 100% coal bottom ash, the wider 95% confidence band suggests that lower accuracy of the regression line. Panzera et al. (2008) reported a decrease in pulse velocity with increase in porosity and oxygen permeability of concrete. The voids present in concrete leads to a reduction in pulse velocity.

4.5.16.7 Relationship between chloride permeability and compressive strength

Fig. 4.152 depicts the relationship between chloride permeability and compressive strength of concrete obtained from the present study. The equation expressing the relationships between compressive strength (σ) and the total charge passed (Q) in coulombs, together with the coefficients of determination R^2 derived is given below.

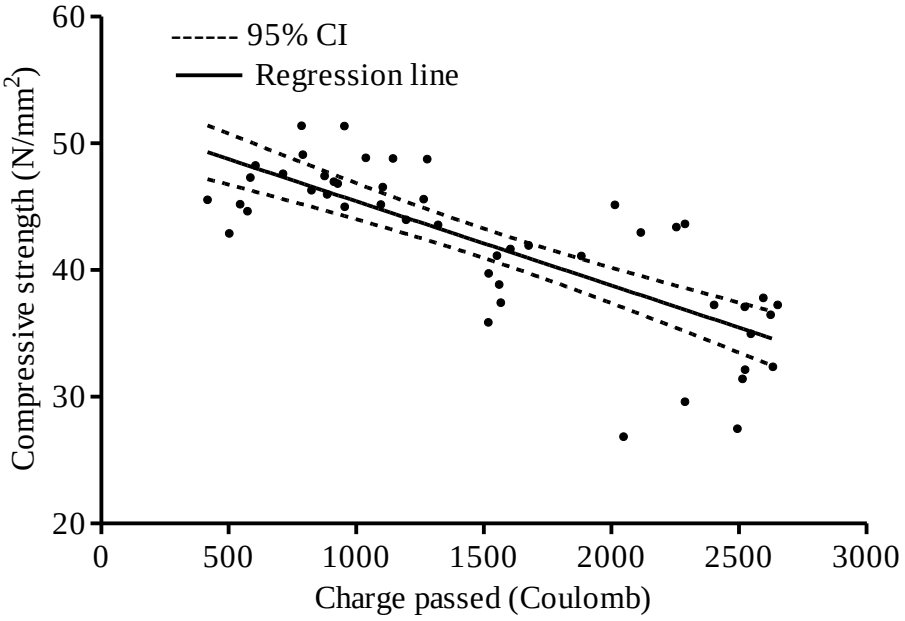

Fig. 4.152: Relationship between charge passed and compressive strength of concrete

σ =- 0.006646 Q + 52.08 R^2 = 0.5977

where

σ = Compressive strength of cube specimen of concrete in N/mm^2

Q = Total charge passed through the specimen in coulombs

The coefficient of determination value (R^2 = 0.60) indicates that 60% around the regression line is explained by the equation and 40% data remained unexplained. Coefficient of correlation value (R = 0.77) indicates that weaker relationship between charge passed and compressive strength of concrete exits and clear relationship could be established by including the other variables which affects the charge passed through concrete.

CHAPTER-5
CONCLUSIONS

In this research work, the effect of low-calcium coal bottom ash as partial or total replacement of two types of sands having different fineness modulus on properties of fresh concrete, strength and durability properties of concrete has been studied. The properties of concrete studied include workability, air content, water loss through bleeding, unit density, compressive strength, splitting tensile strength, pulse velocity, permeable pore space, water absorption, drying shrinkage, sorptivity, abrasion resistance, chloride permeability, sulfate resistance, acid resistance. The microstructure and XRD analysis of concrete have also been carried out in this work.

Test results indicate that low-calcium coal bottom ash is a suitable material to be used as fine aggregates either in partial or total replacement of river sand in production of concrete. Based on the analysis of test results and discussion following conclusions can be drawn.

5.1 PROPERTIES OF FRESH CONCRETE

In addition to properties such as workability and water loss through bleeding, air content in fresh concrete incorporating low-calcium coal bottom ash which has not been reported so far, has been studied in this work

5.1.1 Workability

- Workability of concrete decreased on addition of coal bottom ash as partial or total replacement of sand. The absorption of more water internally by the coal bottom ash during the mixing process lead to decrease in free water for lubrication of particles of mixture. At fixed water-cement ratio, both slump and compaction factor values of concrete decreased almost linearly with the increase in coal bottom ash content.

- More the replacement of sand with coal bottom ash in concrete, greater was the effect.

5.1.2 Air Content

- The entrapped air content in concrete mixtures containing up to 30% coal bottom ash as replacement of sand did not changed significantly. More than 30% replacements resulted in significant increase in entrapped air content in bottom ash concretes.

5.1.3 Bleeding

- At fixed water-cement ratio, bottom ash concrete mixtures exhibited lower bleeding as compared to control concretes. The less quantity of free water leads to lower bleeding in bottom ash concrete mixtures.

5.2 STRENGTH PROPERTIES OF HARDENED CONCRETE

In addition to unit density, compressive strength and splitting tensile strength which have been reported in the literature, the strength properties such as modulus of elasticity, pulse velocity, permeable pore space, water absorption, *microstructure and XRD analysis of concrete incorporating low-calcium coal bottom ash as fine aggregate which have not been reported so far, have been studied in this research work*

5.2.1 Unit Density

- Unit density concrete decreased linearly as the replacement of sand with coal bottom ash increased. The decrease in dry bulk density of bottom ash concrete mixtures was equivalent to the difference in weight of coal bottom ash and sand.

5.2.2 Compressive Strength

- Compressive strength of bottom ash concrete mixtures developed in a comparable manner to that of control concrete. Addition of coal bottom ash as fine aggregate in concrete resulted in lower compressive strength as compared to that of control concrete at an early age of 7 days. At 28 days, compressive strength of bottom ash concrete mixtures incorporating up 50% coal bottom ash was comparable to that of control concrete.

- With age, compressive strength of bottom ash concrete mixtures increased at faster rate than that of control concrete. The pozzolanic activity of coal bottom ash which started after 28 days of curing age contributed significantly in improving the compressive strength of bottom ash concrete mixtures.

5.2.4 Splitting Tensile Strength

- At 28 day, bottom ash concrete mixtures incorporating up to 50% coal bottom ash achieved splitting tensile strength comparable to that of control concrete. After 90 days, splitting tensile strength of bottom ash concretes mixtures of was either equal or more than that of respective control concrete mixtures.

- At early curing age of 7 days, inclusion of coal bottom ash as fine aggregate in concrete has significant effect on splitting tensile strength and compressive strength ratio. With age, the effect of replacement of sand with coal bottom ash in concrete on splitting tensile strength and compressive strength ratio was not so predominant.
- Similar to sand concrete, with age, the compressive strength of bottom ash concrete mixtures improved at a faster rate than the splitting tensile strength.

5.2.5 Modulus of Elasticity

- Modulus of elasticity of bottom ash concrete mixtures decreased on inclusion of coal bottom ash as replacement of sand. Up 40% replacement level, the decrease in Modulus of elasticity of bottom ash concrete mixtures was within 10%.

- The modulus of elasticity values of bottom ash concrete incorporating 100% coal bottom ash as fine aggregate obtained in this work falls within the typical range of 20 GPa to 32 GPa of static modulus of elasticity for M30 grade concrete given in BS 8110: (Part 2)-1985

5.2.6 Pulse Velocity

- Pulse velocities through bottom ash concrete mixtures were not significantly affected on inclusion of coal bottom ash. Comparing the pulse velocity values given in BIS: 13311-1992 (Part–I) and pulse velocity values obtained in this study it is concluded that good quality of concrete can be made with coal bottom ash as partial or total replacement of sand.

5.2.7 Permeable Pore Space and Water Absorption

- Water absorption and permeable pore space in bottom ash concrete mixtures increased with increase in coal bottom ash content. With age, water absorption and voids in bottom ash concrete mixtures reduced significantly as compared to that in control concrete. Bottom ash concrete mixtures had lower water absorption characteristics.

5.2.8 Microstructure

- The microstructure of the bottom ash concrete shows that pozzolanic activity is slow at 28 days and thereafter bottom ash particles started reacting with calcium hydroxide resulting in the formation of CSH gel.

- When the sand replacement level was increased from 50 to 100%, compact CSH structure of equant grains was observed in bottom ash concrete samples but the CSH gel structure was slightly less monolithic than that of control concrete.

- The compressive strength test results confirm the contribution of pozzolanic activity of coal bottom ash.

5.2.9 XRD Phase Analysis

- Phase composition of powder concrete paste did not change qualitatively, however, change in phase proportions was observed on use of coal bottom ash in concrete.

- XRD analysis showed the peaks of portlandite (CH), calcium silicate hydrate (CSH), calcium silicate (CS), calcium alumino silicate hydrate (CASH), calcium alumino-ferrite silicate hydrate (CAftSH) and Ettringite (E).

5.3. DURABILITY PROPERTIES OF CONCRETE

In addition to drying shrinkage, the durability properties such as sorptivity, chloride permeability, abrasion resistance, acid resistance and sulfate resistance of concrete incorporating low-calcium coal bottom ash as fine aggregate which have not been investigated so far have been reported in this work.

5.3.1 Sorptivity

- Initial rate of absorption (sorptivity) of bottom ash concrete mixtures increased on inclusion of coal bottom ash. No change in secondary rate of absorption of bottom ash concrete mixtures was observed on inclusion of coal bottom ash.

- Cumulative absorption of water increased almost linearly with increase in coal bottom ash content in concrete. Bottom ash concrete mixtures containing 100% coal bottom ash displayed 36 to 39%, higher commutative capillary water absorption than control concrete mixtures.

5.3.2 Abrasion Resistance

- Bottom ash concrete mixtures demonstrated lower abrasion resistance than control concrete mixtures. Average wear depth of bottom ash concrete mixtures was much below than 2 mm for 7.5 minutes of wear time specified in BIS: 1237-2012 for heavy duty tiles.

- Abrasion resistance of bottom ash concretes increased with age. Compressive strength strongly affected the abrasion resistance of concrete. Average depth of wear decreased almost linearly with increase in compressive strength of bottom ash concrete.

5.3.3 Chloride Permeability

- At 28 days, the addition of coal bottom ash as fine aggregate in concrete has no significant affect on the resistance to chloride ion penetration. With age, bottom ash concrete mixtures showed better resistance to chloride ion penetration. At 365 days, total charged passed through bottom ash concrete mixtures containing 100% coal bottom ash was 55 to 60% lower than that passed through control concrete.

5.3.4 Drying Shrinkage

- Concrete mixtures incorporating coal bottom ash as fine aggregate exhibited better dimensional stability. Drying shrinkage of bottom ash concrete mixtures decreased with the increase in coal bottom ash content.

5.3.5 Acid Resistance

- The performance of bottom ash concrete mixtures under external sulphuric acid attack in terms of mass loss and loss in 28-day compressive strength was almost identical to that of control concrete.

5.3.6 Sulfate Resistance

- Bottom ash concrete mixtures experienced slightly higher expansion strains when exposed to external sulphate attack. The expansion strains of all concrete mixtures observed after 365 days of immersion period were much less than 0.1%.

- After 365 days of immersion in sulfate solution, compressive strength of bottom ash concrete mixtures except concrete mixture A_{100} was comparable to respective control concrete.

5.4 Further Research

The inclusion of coal bottom ash as fine aggregate decreases an early age compressive strength of concrete. As such, further research to explore the possible ways to enhance the early age strength of bottom ash concrete is needed.

REFERENCES

Abd elaty, M. a. a., (2014). "Compressive strength prediction of Portland cement concrete with age using a new model." Housing and Building National Research Center (HBRC) Journal; 10: 145-155

Aggarwal P., Aggarwal Y. and Gupta S.M. (2007), "Effect of bottom ash as replacement of fine aggregates in concrete." Asian Journal of Civil Engineering (Building and Housing); 8: 49-62

Al-Amoudi, O.S.B., Al-Kutti, W. A., Ahmad, S. and Maslehuddin, M., (2009). "Correlation between compressive strength and certain durability indices of plain and blended cement concretes" Cement & Concrete Composites; 31: 672–676

American Coal Ash Association (ACAA). 2006 coal combustion product (CCP) production and use. Aurora, CO: American Coal Ash Association; 2007.

Andrade L.B., Rocka J.C.and Cheriaf M. (2007), "Aspects of moisture kinetics of coal bottom ash in concrete." Cement and Concrete Research; 37: 231-241

Andrade L.B., Rocka J.C. and Cheriaf M (2009), "Influence of coal bottom ash as fine aggregate on fresh properties of concrete." Construction and Building Materials; 23: 609-614

Aramraks T. (2006), "Experimental study of concrete mix with bottom ash as fine aggregate in Thailand" Symposium on Infrastructure Development and the Environment, 1-5

Arumugam K., Ilangovan R. and James M. D. (2011), "A study on characterization and use of pond ash as fine aggregate in concrete" International Journal of Civil and Structural Engineering, 2: 466-474

ASTM C 597-02, "Standard test methods for pulse velocity through concrete." ASTM International, West Conshohocken, USA, 2002

ASTM C 642-97, "Standard test method for density, absorption, and voids in hardened concrete." ASTM International, West Conshohocken, USA, 1997

ASTM C 1585-04, "Standard test methods for Measurement of Rate of Absorption of Water by Hydraulic - Cement Concretes." ASTM International, West Conshohocken, USA. 2004

ASTM C 157-03, "Standard test methods for Length Change of Hardened Hydraulic-Cement Mortar and Concrete." ASTM International, West Conshohocken, USA.

ASTM C 1202-10, "Standard test methods for Electrical Indication of Concrete's Ability to Resist Chloride Ion Penetration." ASTM International, West Conshohocken, USA.

ASTM C1012-10, “Standard test methods for Length Change of Hydraulic-Cement Mortars Exposed to a Sulphate Solution.” ASTM International, West Conshohocken, USA.

ASTM C 267-01, “Standard Test Methods for chemical resistance of mortars, grouts and monolithic surfacing and polymer concretes.” ASTM International, West Conshohocken, USA.

ASTM C 232-09, Standard test methods for bleeding, ASTM International, West Conshohocken, USA.

Bai Y., Darcy F. and Basheer P.A.M. (2005), "Strength and Drying shrinkage properties of concrete containing furnace bottom ash as fine aggregate." Construction and Building Materials, 19: 691-697

Barnes I. and Sear L. (2004), “Ash utilization from coal based power plants.”Report No COAL R274 DTI/ Pub. URN 04/1915

BIS: 8112-1989, “Indian standard 43 Grade ordinary Portland cement – specification.” Bureau of Indian Standards, New Delhi, India.

BIS: 383-1970, “Indian standard Specification for coarse and fine aggregates from natural sources for concrete.” Bureau of Indian Standards, New Delhi, India.

BIS: 10262-1982, “Recommended guidelines for concrete mix design.” Bureau of Indian Standards, New Delhi, India.

BIS: 1199-1959, “Indian standard methods of sampling and analysis of concrete.” Bureau of Indian Standards, New Delhi, India.

BIS: 516-1959, “Indian standard methods of test for strength of concrete.” Bureau of Indian Standards, New Delhi, India.

BIS: 5816-1999, “Indian standard Splitting tensile strength of concrete- Test method.” Bureau of Indian Standards, New Delhi, India.

BIS: 1237-2012, “Indian standard Specification for cement concrete flooring tiles.” Bureau of Indian Standards, New Delhi, India.

BIS: 11331-1992, “Indian standard Specification for Non-destructive testing of concrete: Part 1 Ultrasonic pulse velocity.” Bureau of Indian Standards, New Delhi, India.

Behim M., Cyr M., and Clastres P., (2011), “Physical and chemical effects of El Hadjar slag used as an additive in cement-based materials.” European Journal of Environmental and Civil Engineering; 15(10): 1413-32

Brown PW. (1981), “An evaluation of the sulphate resistance of cements in a controlled environment.” Cement and Concrete Research; 11:719–27.

Cachim P., Velosa AL, and Ferraz E. (2014), "Substitution Materials for sustainable concrete production in Portugal." KSCE Journal of Civil Engineering; 18(1): 60-66

Cachim, P. B. (2009), "Mechanical properties of brick aggregate concrete." Construction and Building Materials; 23 (3): 1292-1297.

CEA (2014), Report on fly ash generation at coal/lignite based thermal power stations and its utilization in the country for the year 2013-14.

CEA (2012), Power Scenario at a glance, Central Electricity Authority, India.

Chan SYN, and Ji X. (1998), "Water sorptivity and chloride diffusivity of oil shale ash concrete." Construction and Building Materials; 12(4):177–83

Charkradhara Rao M., Bhattacharyya S. K. and Barai S. V. (2011), "Influence of field recycled coarse aggregate on properties of concrete." Journal of Materials and Structures; 205-20

Charkradhara Rao M., Bhattacharyya S. K. and Barai S. V. (2011), "Behaviour of recycled aggregate concrete under drop weight impact load." Construction and Building Material; 25(1): 69-80

Cheriaf M., Rocka J.C. and Pera J. (1999), "Pozzolanic properties of pulverized coal combustion bottom ash." Cement and Concrete Research, 29:1387-1391

Chun L.B., Sung K. J., Sang K. T. and Chae S.T. (2008), "A study on the fundamental properties of concrete incorporating pond-ash in Korea." The 3rd ACF International Conference-ACF/VCA, 401-408

Cwrizen A., Penttala V. and Vornanen C. (2008), "Reactive powder based concretes: Mechanical properties, durability and hybrid use with OPC." Cement and concrete Research; 38:1217-26

Cwrizen A. and Penttala V. (2005), "Aggregate-cement paste transition zone properties affecting the salt–frost Damage of high- performance concretes." Cement and Concrete Research; 35(4): 671-79

Cyr M., Aubert JE., Husson B., and Clastres P. (2006), "Management of mineral wastes in cement- based materials." Revue Europeenne de Genie Civil, 10(3):323-37

Cyr M., Coutand M., and Clastres P. (2007), "Technological and Environmental behaviour of sewerage sludge ash (SSA) in cement based materials." Cement and concrete Research; 37:1278-89

Cyr M., and Ludmann C. (2005), "Low risk meat and bone meal (MBM) bottom ash in mortars as sand replacement." Cement and Concrete Research; 36(3) : 469-480.

Dustan M. R. H. (1983), "Development of high fly ash content concrete." Proceedings of Institution of Civil Engineers Part 1; 74: 495-513

Esteves L. P., Cachim P.B., Ferreira V.M. (2010), "Effect of fine aggregate on the rheology properties of high performance cement-silica systems." Construction and Building Materials; 24: 640-649

Evangelista L and Brito JD, (2007), "Mechanical behaviour of concrete made with fine recycled aggregate." Cement and Concrete Research; 29:397-401

Figueiredo C. P., Santos F. B., Cascudo O., Carasek H., Cachim P. and Velosa A. (2014), "The role of metakaolin in the protection of concrete against the deleterious action of chlorides." IBRACON Structures and Materials Journal; 7(4): 685-708

Fernandez-Turiel J.L., Georgakopoulos A., Gimeno D., Papastergios G. and Kolovos N. (2004), "Ash Deposition in a Pulverized Coal-Fired Power Plant after High-Calcium Lignite Combustion." Energy and Fuels; 18:1512-1518

Folagbade, Samuel Olufemi (2012), "Effect of fly ash and silica fume on the sorptivity of concrete." International Journal of Engineering Science and Technology (IJEST); 4(9):4238-46

Folagbade, Samuel Olufemi (2012), "Sorptivity of Cement Combination Concretes Containing Portland Cement, Fly Ash And Metakaolin." International Journal of Engineering Research and Applications (IJERA); 2(5):1953-59

Ghafoori N. and Bucholc J. (1996), "Investigation of Lignite Based Bottom Ash for Structural concrete." Journal of Materials in Civil Engineering; 8(3):128-137

Ghafoori N. and Bucholc J. (1997), "Properties of High-Calcium Dry Bottom Ash concrete." ACI Materials Journal; 94(2): 90-101

Ghafoori N. and Cai Y. (1998 a), "Laboratory-Made Roller Compacted Concretes Containing Dry Bottom Ash: Part-I-Mechanical Properties." ACI Material Journal; 95(2):121-130.

Ghafoori N. and Cai Y. (1998 b), "Laboratory - Made Roller Compacted concretes containing Dry Bottom Ash : Part II–Long Term Durability." ACI Materials Journal; 95(3):244-251

Gunny Y., Sari YD, Yalcin M., Tuncan A. and Donme S. (2010), "Reusage of waste foundry sand in high strength concrete." Waste Management; 30:1705-13

Gupta S. M., Aggarwal P. and Aggarwal Y. (2006), "Shrinkage of high strength concrete." Asian Journal of Civil Engineering (Building and Housing); 7(2): 183-194

Hemalatha, T., Ramaswamy, A. and Kishen, J. M. C. (2014a), "Simplified Mix Design for production of self compacting concrete." ACI Materials Journal; DOI: 10.14359/51687102

Hemalatha, T., Ramaswamy, A. and Kishen, J. M. C. (2014b), "Micromechanical Analysis of self compacting concrete." Materials and Structures; DOI: 10.1617/s11527-014-0435-z

Hewayde E, Nehdi ML, Allouche E, Nakhla G. (2007), "Using concrete admixtures for sulphuric acid resistance." Proceedings of the institution of civil engineers construction materials; 160: 25–35.

Irassar EF, Maio ADi, Batic OR. (1996), "Sulphate attack on concrete with mineral admixtures." Cement Concrete Research; 26(1):113–23

Jaturapitakkul C. and Cheerarot R. (2003), "Development of Bottom ash as Pozzolanic Material." Journal of Materials in Civil Engineering; 15(1):48-53

Kurama H. and Kaya M. (2008), "Usage of coal combustion bottom ash in concrete mixture." Construction and Building Materials; 22:1922-1928

Kasemchaisiri R. and Tangetermsirikul S. (2007), "A method of determine water retainability of porous fine aggregate for design and quality control of fresh concrete." Construction and Building Materials; 21:1322-1334

Kim H.K. and Lee H.K. (2011), "Use of Power Plant bottom ash as fine and coarse aggregate in high-strength concrete." Construction and Building Materials; 25:1115-1122.

Khan MI and Lynsdale CJ (2002), "Strength, permeability and carbonation of high performance concrete." Cement and Concrete Research; 32:123-131

Khan MI, (2003), "Permeation of High Performance Concrete." Journal of Materials in Civil Engineering; 15 (1): 84-92

Khatib JM and Clay RM (2004), "Absorption characteristics of metakaolin concrete." Cement and Concrete Research; 34(1):19–29.

Khatib JM and Hibbert JJ (2005), "Selected engineering properties of concrete incorporating slag and metakaolin." Construction and Building Materials; 19:460-472

Khatib JM, Negim EM, Yeligbayeva G. ZH, and Mun G. A. (2014), "Strength characteristics of mortar containing high volume metakaolin as cement replacement." Research and Reviews in Materials Science and Chemistry; 3(1): 85-95

Khatib JM, Negim EM and E Gjonbalaj (2012), "High Volume metakaolin as Cement Replacement in Mortar." World Journal of Chemistry; 7 (1): 07-10

Khatib JM (2008), "Performance of self compacting concrete containing fly ash." Construction and Building Materials; 22:1963-71

Khatib JM (2005), "Properties of concrete incorporating fine recycled aggregate." Cement and Concrete Research; 35:763-69

Khatib JM and Ellis DJ (2001), "Mechanical properties of concrete containing foundry sand." ACI Special Publication; SP-200:733-748

Khatib JM and Mangat PS (1995), "Absorption characteristics of concrete as a function of location relative to casting position." Cement and Concrete Research; 25(5):999–1010.

Kantiranis N., Georgakopoulos A., Filippidis A. and Drakoulis A. (2004), "Mineralogy and organic matter content of bottom ash samples from Agios Dimitrios power plant, Greece." Bulletin of the Geological Society of Greece vol. XXXVI, Proceedings of the 10th International Congress, Thessaloniki, April 2004.

Kockal, N. U. and Ozturan, T. (2011), "Strength and elastic properties of structural lightweight concretes." Materials and Design; 32: 2396–2403

Kosior-Kazberuk M. (2011), "Applications of SSA as partial replacement of aggregate in concrete." Journal of Environment studies; 20(2): 365-70.

Menadi B., Kenai S., Khatib J. and Ait-Mokhtar A. (2009), "Strength and durability of concrete incorporating crushed limestone sand." Construction and Building Materials; 23: 625–633

Mishra S, Yamamoto A, Tsutsumi T and Motohashi K. (1994), "Application of rapid chloride permeability test to quality control of concrete." Special publication ACI; 145:487-502

Muhardi, Marto A., Kassim K.A., Makhtar A.M., Wei L.F. and Lim Y.S. (2010), "Engineering Characteristics of Tanjung Bin Coal Ash." EJGE, 15:1117-1129

Mačiulaitis R. and Malaiškien J. (2009). "The regulation of structural parameters of ceramics depending on the drying regime" Journal of Civil Engineering and Management; 15(2): 197–204

McCarter W. J., Ezirim H and Emerson M. (1992), "Absorption of water and chloride into concrete." Magazine of Concrete Research; 44(158):31–7.

McCarter W. J. (1993), "Influence of Surface Finish on Sorptivity on Concrete." Journal of Materials in Civil Engineering; 5(1): 130-136.

Naik T. R., Kraus R.N., Chun Y. M. and Nageotte S. O. (2007), "Coal-Combustion bottom ash for reducing shrinkage of concrete made with Portland cement and sulfoaluminate cement." Report No CBU-2006-22 REP-621, 1-13

Naik T. R., Singh S. S. and Hossain M. M. (1995), "Abrasion resistance of high–strength concrete made with class C fly ash." ACI Material Journal; 92(6):649-59

Nash't I. H., A'bour S. H. and Sadoon A. A. (2005), "Finding an united relationship between crushing strength of concrete and non-destructive tests." Proceedings of Middle East Non destructive Testing Conference and Exhibition, Bahrain.

Oluokun FA, Burdette EG and Deatherage JH. (1991), "Splitting tensile strength and compressive strength relationships at early ages." ACI Materials Journal;88(2):115–21.

Ouyang C, Naani A. and Chang WF. (1988), "Internal and external sources of sulphate ions in Portland cement mortar: two types of chemical attack." Cement and Concrete Research;18: 699–709.

Ouyang C. A. (1989), "Damage model for sulphate attack of cement mortars." Cement Concrete Aggregate, CCAGDP;11 (2):92–9.

Paiva H., Velosa A., Cachim P., Ferreira V.M (2012), "Effect of metakaolin dispersion on the fresh and hardened state properties of concrete." Cement and Concrete Research 42: 607–12

Price, Walter H. (1951), "Factors influencing concrete strength." Journal ACI, Proceedings; 47: 417–32.

Prince M. J. R. and Bhupinder Singh (2014 a), "Investigation of bond behaviour between recycled aggregate concrete and deformed steel bars" Structural Concrete; 15(2): 154-68

Prince M. J. R. and Bhupinder Singh (2014 b), "Bond strength of deformed steel bars in high-strength recycled aggregate concrete." Materials and Structures; DOI 10.1617/s11527-014-0452-y

Rakshvir M. and Barai S. V. (2006), "Studies of recycled aggregate based concrete." Waste Management Research; 24(3): 225-34

Ramachandran V. S. (1995), "Concrete admixture handbook." Noyes Publications Park Ridge, New Jersey, USA.

Rao A, Jha K and Misra S. (2007), "Use of aggregate from recycled construction and demolition waste in concrete." Resource, Conservation and Recycling; 50(1): 71-81

Razak HA., Chai HK., Wong HS. (2004), “Near surface characteristics of concrete containing supplementary cementing materials.” Cement and Concrete Composites; 26: 883–89.

Regev, Lior, Ronald L. Merksy, and Ayalon, Ofira (2014), "Economic Feasibility of Waste Separation at Source: Case Study of Neighborhoods in Haifa, Israel." Presentation at the Proceedings of the Twenty-Ninth International Conference on Solid Waste Technology and Management. Philadelphia, PA, March 30–April 2, 2014

Sahu AK, Kumar S and Sachan AK, (2003), “Crushed stone waste as fine aggregate for concrete”. The Indian concrete journal; 1: 845-48

Sani M.S.H.M., Muftah F. and Muda Z. (2010), “The Properties of Special Concrete Using Washed Bottom Ash (WBA) as partial Sand Replacement.” International Journal of Sustainable Construction Engineering and Technology; 1(2):65-76.

Scott R. and Singh SP (2011), “High performance silica fume concrete and some applications in India.” Proceeding of the International UKIERI concrete congress – New Developments in concrete construction, 8-10 March, pp. 217-238, IIT Delhi.

Shi-Cong Kou and Chi-Sun Poon (2009), “Properties of concrete prepared with crushed fine stone, furnace bottom ash and fine recycled aggregate as fine aggregate.” Construction and Building Materials; 23: 2877-2886.

Siddique R., (2003a), “Effect of fine aggregate replacement with class F fly ash on the mechanical properties of concrete.” Cement and Concrete Research; 33(4):539-47

Siddique R., (2003b), “Effect of fine aggregate replacement with class F fly ash on the abrasion resistance of concrete.” Cement and Concrete Research; 33(11):877-81

Siddique R., (2004), “Performance characteristics of concrete containing high volumes class F fly ash.” Cement and Concrete Research; 34(3):487-93

Siddique R., Schutter G., and Noumowe A., (2009), “Effect of used foundry sand on the mechanical properties of concrete.” Construction and Building Materials; 23: 976-80

Siddique R., (2010), “Wear Resistance of High-Volume Fly Ash Concrete.” Leonardo Journal of Sciences; 17: 21-36

Siddique R. (2013), “Compressive strength, water absorption, sorptivity, abrasion resistance and permeability of self-compacting concrete containing coal bottom ash.’ Construction and Building Materials; 47: 1444–50

Tikalsky P. J., Carrasquillo P. M. and Carrasquillo R. L. (1988), “Strength and durability considerations affecting mix proportioning of concrete containing fly.” ACI Materials Journal; : 505-11

Topcu I. B. and Bilir T. (2010), "Effect of Bottom Ash as Fine Aggregate on Shrinkage Cracking of Mortars." ACI Materials Journal; 107(1):48-56.

Tripathy D K and Barai S V (2006), "Partial replacement using crushed stone dust." Divisional Journal of Civil Engineering; 87:44-46

Turgut P. (2004), "Evaluation of the ultrasonic pulse velocity data." Proceedings of Fourth International Conference on NDE in Relation to Structural Integrity for Nuclear and Pressurised Components, London.

Tasdemir C. (2003), "Combined effects of mineral admixtures and curing conditions on the sorptivity coefficient of concrete." Cement and Concrete Research; 33(10):1637–42

Umoh, A. A., (2012), "Relationship between Compressive Strength and Pulse Velocity of medium Grade Concrete incorporating Rice Husk Ash." International Journal of Engineering Research & Technology; 1(5): 1-9

Wild S., J. M. Khatib and A. Jones (1996), "Relative strength pozzolanic activity and cement hydration in superplasticised MK concrete." Cement and Concrete Research; 26:1537-1544

Yang, K., Basheer, P. A. M., Magee, B., Bai, Y. and Long, A. E., (2015). "Repeatability and Reliability of new Air and Water Permeability Tests for Assessing the Durability of High-Performance Concretes." Journal of Materials in Civil Engineering (ASCE), DOI: 10.1061/(ASCE)MT.1943-5533.0001262

Younsi A., Turcry Ph., Aït-Mokhtar A., Staquet S. (2013), "Accelerated carbonation of concrete with high content of mineral additions: Effect of interactions between hydration and drying." Cement and Concrete Research 43: 25–33

Yuksel I. and Genc A. (2007), "Properties of concrete containing Non-ground ash and Slag as fine Aggregate." ACI Materials Journal; 104(4):397-403.

Yuksel I., Omer Ozkan and Bilir T. (2006), "Use of granulated blast-furnace slag in concrete as fine aggregate." ACI Materials Journal; 103(3):203-208.

Yuksel I., Bilir T. and Omer Ozkan (2007), "Durability of concrete incorporating non-ground blast furnace slag and bottom ash as fine aggregate" Building and Environment; 42(7): 2651-9.

Yuksel I. and Bilir T. (2007), "Usage of industrial by-products to produce plain concrete elements." Construction and Building Materials; 21(3): 686-94

www.thehindu.com/todays-paper/tp-national/tp-andhrapradesh/slurry-from-ntpc-ash-pond-affects-horticulture-crops/article483533.ece

www.sourcewatch.org/index.php/File:SPILL2.JPG

www.caer.uky.edu/kyasheducation/bottomash.html